"The Holsteinian interglacial (MIS 11c) as a palaeoclimatic analogue to the Holocene: Comparison of climate and ecosystem variability"

Dissertation for attaining the PhD degree
of Natural Sciences

submitted to the Faculty of Geosciences and Geography
of the Goethe University Frankfurt

by Andreas Koutsodendris
from Athens (Greece)

Frankfurt am Main,
March 2011

accepted by the Faculty of Geosciences and Geography

of the Goethe University Frankfurt as a dissertation.

Dean: Prof. Dr. Robert Pütz

Expert assessors: Prof. Dr. Jörg Pross
                         Dr. habil. Ulrich C. Müller

Examination board: Prof. Dr. Achim Brauer
                         Prof. Dr. André F. Lotter
                         Dr. habil. Ulrich C. Müller
                         Prof. Dr. Jörg Pross

Date of the disputation:

Table of contents

<u>List of figures</u>

List of tables

Abbreviations

asl	above sea level
AP	arboreal pollen
BP	before present
Corg	organic carbon
ENSO	El Niño - Southern Oscillation
FP	forest phase
H1	Heinrich 1 event
ka	thousand years
LPAZ	local pollen zone
LVI	low variability interval
MAT	modern analogue technique
mbs	meters below surface
Meso.	mesocratic forest phase
MTM	multi-taper method
MIS	Marine Isotope Stage
MP_{year}	mean annual precipitation
MT_{year}	mean annual temperature
NADW	North Atlantic Deep Water
NAO	North Atlantic Oscillation
NAP	non-arboreal pollen
NSAP	non-saccate arboreal pollen
OHO	Older Holsteinian Oscillation
Olig.	oligocratic forest phase
PAR	pollen accumulation rates
PZ	pollen zone
QBO	Quasi-Biennial Oscillation
S1	Sapropel 1
SEM	scanning electron microscope
SEP	steppe element pollen
SST	sea surface temperature
Teloc.	telocratic forest phase
TN	total Nitrogen
TOC	total Organic Carbon
VPDB	Vienna PeeDee Belemnite
YD	Younger Dryas
YHO	Younger Holsteinian Oscillation
µ-XRF	micro X-Ray Fluorescence

<u>Acknowledgements</u>

It was just a couple of weeks after arriving to Frankfurt for a short DAAD-sponsored visit when Jörg Pross, Uli Müller and Bas van de Schootbrugge convinced me to quit what I was working on in Greece, move to Germany and start a new PhD project on a field totally new to me…Three years later I feel deeply indebted to all three of them for this true opportunity, their full support and the great experience working within their "Paleoenvironmental Dynamics Group". I could not have made a better choice.

Jörg has always advised me with patience on how to most efficiently manage my time, set priorities and move forward. I really appreciate that you have been giving me directions and support even when you were on the most remote part of this planet – straightening out, for example, some of my most unfortunate writing attempts while sailing off Antarctica! But apart from making sure that my deliverables are of high standard, you also taught me how fulfilling it is to establish collaborations and promote my work. Thanks Jörg for being the driving force of my PhD project!

Uli has offered me to work on a very exciting project that he had very carefully and successfully outlined. I am grateful to him for his introduction and invaluable guidance in the fields of vegetation dynamics and the role of orbital parameters on climate change. Thanks a lot Uli for giving me some great ideas on the interpretation of the results and the preparation of the manuscripts!

Bas was not scientifically involved in this study; however, his precious and to-the-point comments made me see physical processes from different angles, broadening my way of thinking far beyond the scope of this project. Bas, thanks for your friendly advice in many aspects regarding this project, but also for the hilarious moments we shared after work!

I am grateful to two external advisors – Achim Brauer and Andy Lotter – who have influenced this work by most positive means. Hosting me several times in Potsdam and Utrecht, respectively, they showed me new perspectives in palaeoclimatology and generously offered me their support in data interpretation.

I am also indebted to Ulrich Kotthoff for introducing me to pollen counting and for the long discussions on palaeoclimate, particularly for the Aegean region. Thanks, Kotti, for sharing office routine, ideas and scientific interests, and also for translating a summary of this thesis into German.

I would also like to deeply thank Will Fletcher and Heiko Pälike, whom I have both routinely bothered with questions, for their constructive comments and overall contribution to two of the manuscripts comprising this thesis.

Insightful discussions with colleagues within the Paleontology Section and beyond, such as André Bahr, Jens Fiebig, Oliver Friedrich, Eberhard Gischler, Sabine Gollner, Jens Herrle, Clara Mangili, Wolfgang Oschmann, Justin Parker, Willy Püttmann, and Silke Voigt, have greatly inspired and motivated me to move on.

Abstract

Owing to long-term similarities with regard to orbital climate forcing (i.e., low eccentricity and a dampened influence of precession), Marine Isotope Stage (MIS) 11 represents one of the closest astronomical analogues for present and future climate. Hence, insights into the climate variability of MIS 11 can contribute to a better understanding of the climatic evolution of the present (Holocene) interglacial as it would occur without human interference. In order to elucidate the natural climate variability during MIS 11, this study examines predominantly annually laminated lake sediments of Holsteinian age from Dethlingen, northern Germany. The Holsteinian interglacial is widely accepted to be the terrestrial equivalent of MIS 11c in central Europe and can be biostratigraphically correlated with the Hoxnian, Mazovian and Praclaux interglacials on the British Isles, in Poland and in France, respectively. These correlations yield the potential to cross-check the results from individual sites on a regional scale. This study is based on a multi-proxy approach including palynological, micropaleontological, sedimentological, geochemical and time series analyses within a well-constrained chronological framework that has been established through varve counting and regional bio-stratigraphic correlations with other annually laminated archives of Holsteinian age. In particular, the here-presented study aims at (i) fingerprinting the long-term (centennial- to millennial-scale) and short-term (sub-decadal- to decadal-scale) climate variability during the Holsteinian interglacial, (ii) deciphering the nature, tempo and trigger mechanisms of abrupt climate change under interglacial boundary conditions, and (iii) assessing its impact on terrestrial ecosystems.

With regard to long-term climate variability, the vegetation succession at Dethlingen as inferred from pollen data provides insights into the mesocratic to telocratic forest phases of a glacial-interglacial cycle spanning ~11500 (± 1000) years of the 15-16-ka-long Holsteinian interglacial. The development of temperate mixed forests suggests a general prevalence of mild climatic conditions during the Holsteinian. The older parts of the interglacial are characterised by the strong presence of boreal tree taxa (e.g., *Picea*), whereas the younger parts of the interglacial are marked by the expansion of sub-Atlantic to Atlantic forest elements (e.g., *Abies*, *Buxus*, *Ilex*, *Quercus*) and the decline of boreal tree taxa. This vegetation succession suggests a general warming trend and decreasing seasonality over the course of the Holsteinian interglacial. Based on the maximum pollen abundances of indicator tree taxa (e.g., *Buxus* and *Quercus*), peak warmth was reached during the later stages of the interglacial; it was accompanied by high humidity. The forest succession of the Holsteinian interglacial was punctuated by abrupt and gradual changes in the abundances of temperate plant taxa. These vegetation changes indicate considerable intra-interglacial climate variability. In particular, two marked declines of temperate taxa leading to the transient development of boreal and sub-boreal forests were triggered by centennial-scale climate oscillations, here termed Older and Younger Holsteinian Oscillations (OHO and YHO). These oscillations occurred ~6000 and ~9000 years after the onset of the interglacial pioneer forestation in central Europe, respectively.

To assess the impact of abrupt climate change on terrestrial ecosystems during the Holsteinian and to investigate the underlying driving mechanisms, the intervals spanning the OHO and the YHO at Dethlingen were subjected to decadal-scale palynological and sedimentological analyses. Based on these data, the OHO comprises a 90-year-long decline of temperate taxa associated with expansion of *Pinus* and non-arboreal pollen, and a subsequent 130-year-long recovery of temperate taxa marked by the pioneer expansion of *Betula* and *Alnus*. Owing to its highly characteristic imprint on vegetation dynamics, the OHO can be identified in pollen records from the central European lowlands north of 50º latitude, from the British Isles to Poland. A close inspection of individual pollen records from that region reveals the prevalence of colder winters during the OHO, with a gradient of decreasing temperature and moisture availability, and increased continentality towards eastern Europe. This climate pattern points to a weakened influence of the westerlies and/or stronger influence of the Siberian High connected to the OHO.

The vegetation dynamics during the YHO are characterised by a decline of temperate taxa (particularly of *Carpinus*) and the expansion of pioneer trees (mainly *Betula*). In contrast to the OHO, frost-sensitive taxa (e.g., *Ilex*, *Buxus* and *Hedera*) continued to thrive. This suggests that mean winter temperatures remained relatively high (>0 ºC) during the YHO pointing to a decrease of summer warmth related to the climatic deterioration. The YHO, which has a duration on the order of 300 years, is centered within a long-term (~1500-year) decline and subsequent, millennial-scale recovery of temperate taxa.

Because the impact of the OHO and the YHO on the vegetation at Dethlingen was markedly different, both short-term climate oscillations may have been caused by different trigger mechanisms. For the OHO, the inferred regional-scale winter cooling over central Europe lasting for several decades points to a decrease in ocean heat transport, most likely related to a transient slowdown in North Atlantic Deep Water formation. This view is supported by the strong resemblance of the OHO to the 8.2 ka event of the Holocene with regard to the duration, imprint on terrestrial ecosystems, spatial pattern of the climatic impact, timing within the respective interglacial, and prevailing interglacial boundary conditions. In contrast, the presence of frost-sensitive taxa during the YHO appears to exclude a reduction in oceanic heat transport as postulated for the OHO. Instead, the long-lasting, gradual changes in the abundances of temperate taxa suggest a connection to orbital forcing, with the triggering mechanism causing the centennial-scale vegetation setback itself remaining unclear.

The characteristics of short-term climate variability were investigated based on microfacies and time series analyses of a ~3200-year-long, annually laminated window of the Dethlingen record. The annual laminations at Dethlingen comprise biogenic varves consisting of two discrete sub-layers. The light layers, which are controlled by the intensity of diatoms blooms during spring/summer, reflect changes in the productivity of the Dethlingen palaeolake. In contrast, the dark layers, which consist predominantly of amorphous organic matter and fragmented diatom frustules, represent sediment deposition during autumn/winter. Spectral analyses of the thicknesses of the light and dark layers have revealed several peaks exceeding the 95% and 99% confidence levels that are near-identical to those known from

modern instrumental data and Holocene records. Decadal-scale signals at periods of 90, 25, and 10.5 years are likely associated with the 88-, 22- and 11-year solar cycles; hence, solar activity appears to have been a forcing agent in productivity changes of the Dethlingen palaeolake. Sub-decadal-scale signals at periods between 3 and 5 years and ~6 years may reflect an influence of the El Niño-Southern Oscillation (ENSO) and the North Atlantic Oscillation (NAO) on varve formation during winter.

Chapter 1. Introduction

1.1 Motivation and aims of research

With the drastically mounting evidence of anthropogenic forcing on the Earth's climate, understanding the mechanisms and effects of abrupt climate change is crucial in order to extend the lead time for mitigation and adaptation (e.g., Alley et al., 2003; IPCC, 2007). In this context, the climate variability and the climate-induced environmental changes during Quaternary interglacials represent the closest analogy to the climate and ecosystem change as witnessed today.

Based on this notion, past interglacials of the Quaternary can provide valuable insights not only into the range and tempo of natural climate variability, but also into the environmental consequences of climatic forcing. Because these past interglacials – unlike the Holocene – were unaffected by human interferences, their analysis can contribute towards elucidating the future evolution of the present interglacial (e.g., Shackleton, 1969; Woillard, 1979; Kukla et al., 1997, 2002; Tzedakis et al., 2004a, 2009; Müller et al., 2005; Brauer et al., 2007a).

The palaeoclimatic record of the Quaternary exhibits a large diversity between individual interglacials in terms of their intensity, duration and internal variability (e.g., Winograd et al., 1997; McManus et al., 1999; Petit et al., 1999; EPICA, 2004; Jouzel et al., 2007; Tzedakis et al., 2009; Masson-Delmotte et al., 2010). This poses the question which past interglacial serves as a close analogue to the present Holocene interglacial. Because astronomical forcing is the pacemaker of Quaternary glacial-interglacial cycles (e.g., Hays et al., 1976; Kukla et al., 1981; Imbrie et al., 1984), any such analogue should exhibit an orbital configuration that is close to that of the Holocene. In this context, the most recent interglacial period that evolved under orbital boundary conditions as they characterize the Holocene (i.e., low eccentricity and dampened influence of precession) was Marine Isotope Stage (MIS) 11 (e.g., Berger and Loutre, 2002; Loutre and Berger, 2003); in particular, the astronomically driven insolation of the present and near future (5 ka BP to 60 ka AP) closely mimics the insolation of MIS 11 between 405 and 340 ka BP (Fig. 1.1; Loutre and Berger, 2003).

During the past decade, a number of proxy datasets comprising multiple climatic cycles have provided insights into the climatic evolution of MIS 11 (Fig. 1.2). Marine Isotope Stage 11 marks an extended period of warmth (~30 ka; e.g., McManus et al., 1999, 2003) spanning two insolation peaks (Berger and Loutre, 1991). However, it is commonly accepted that full interglacial conditions were only reached during the second insolation peak (~408 ka), lasting for about 10 ka (Fig. 1.2; e.g., Rohling et al., 2010). This interval is further associated with the highest temperatures during MIS 11 in Antarctic ice cores (Jouzel et al., 2007) and the highest planktic foraminiferal-derived sea-surface temperature (SST) in the northeastern North Atlantic (Kandiano and Bauch, 2007; Helmke et al., 2008). Although MIS 11 has often been considered a stable interglacial (e.g., McManus et al., 2003), oxygen isotope values from several marine records in the North Atlantic have suggested considerable intra-interglacial variability (e.g., Oppo et al., 1998; Poli et al., 2000; Desprat et al., 2005; Martrat

et al., 2007). However, the lack of high-resolution data has yet precluded deeper insights into this variability.
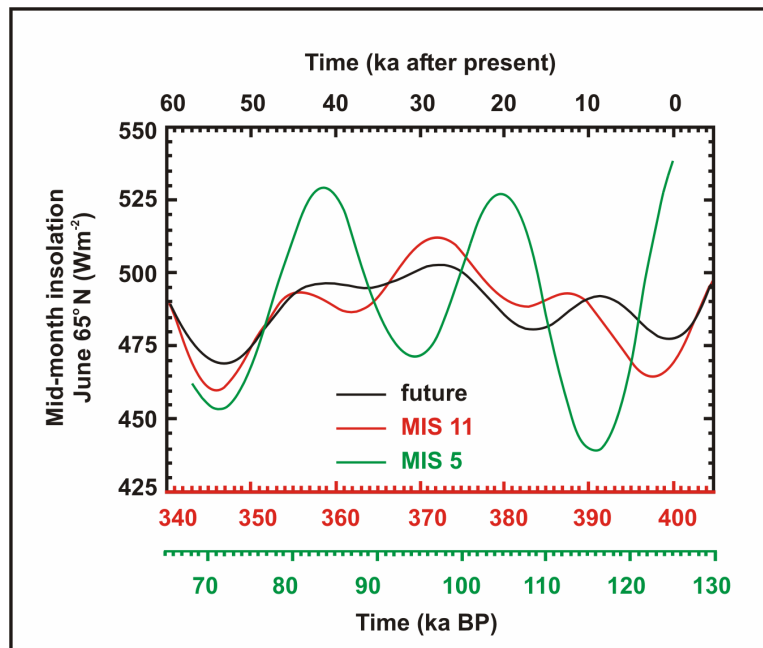
Figure 1.1: *Comparison of June insolation changes (65º N) during MIS 1, MIS 5, MIS 11, and for the upcoming 60 ka (modified after Loutre and Berger, 2003).*
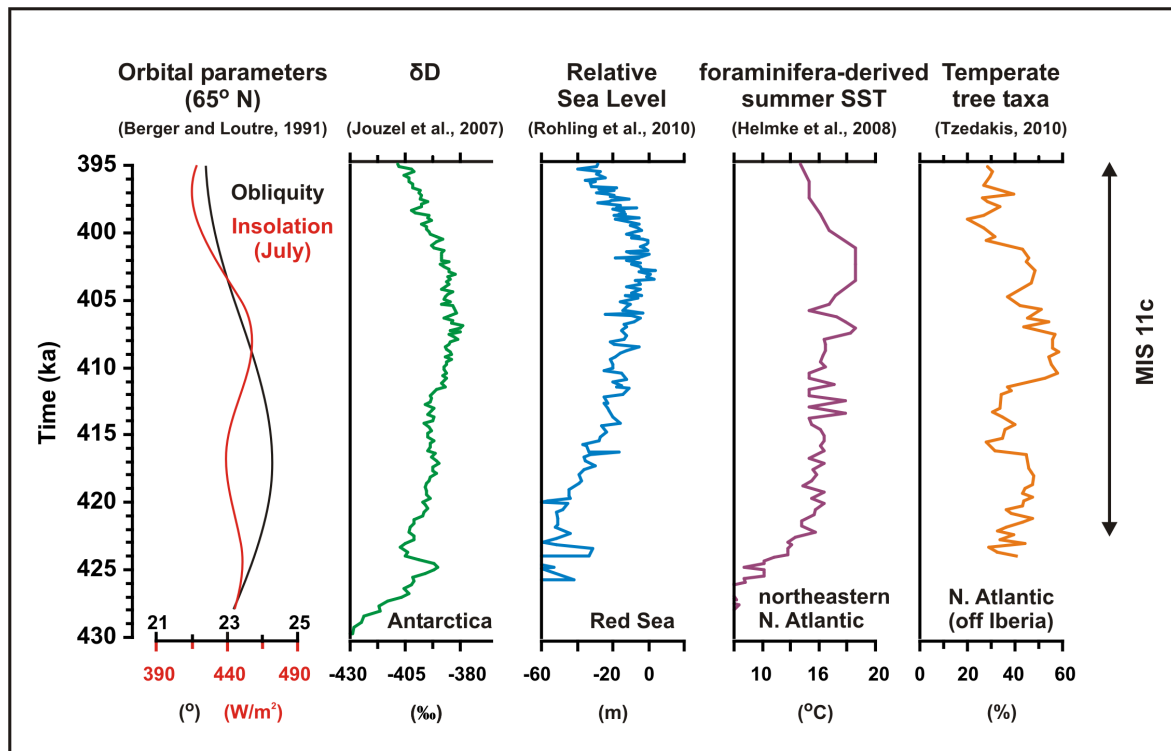
Figure 1.2: *Orbital parameters and multi-proxy climate data from Antarctica, the North Atlantic and the Red Sea spanning MIS 11c.*

In Europe, the terrestrial analogue to MIS 11 has long been a matter of heated debate (see Chapter 2 for a discussion). However, evidence based on a long terrestrial vegetation record from the French Massif Central (Reille et al., 2000) and a direct land-sea correlation off Iberia (Fig. 1.3; Desprat et al., 2005) has led the majority of workers to accept a correlation of MIS 11c with the Holsteinian interglacial (e.g., de Beaulieu et al., 2001; Tzedakis et al., 2001; Kukla, 2003, 2005; Nitychoruk et al., 2005, 2006; Müller and Pross, 2007; Preece et al., 2007). In contrast to most marine records, which typically exhibit relatively low sedimentation rates, terrestrial archives of the Holsteinian have the potential for highly resolved palaeoclimate analyses, with varved records allowing an annual to seasonal resolution and the establishment of a precise floating chronology at the same time.
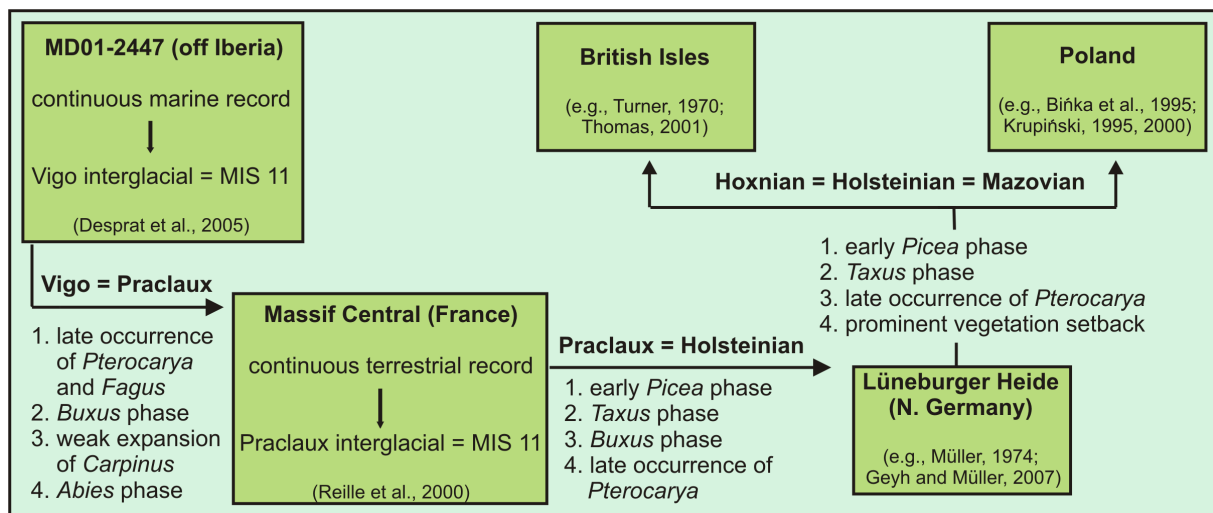
Figure 1.3: *Rationale and principles for a palynostratigraphic correlation of MIS 11c with the Holsteinian interglacial and its terrestrial equivalents in Europe.*

Based on palynological studies on a varved sediment record from Munster-Breloh, Northern Germany (Müller, 1974), it has long been known that the Holsteinian interglacial was marked by climatic instabilities that lasted for several centuries (Fig. 1.4; Müller, 1974; Kukla et al., 2003). However, the limited understanding of the climatic evolution of the Holsteinian interglacial within the context of its correlation to MIS 11 has yet precluded deeper insights into the mechanisms behind these oscillations.

In light of the above, high-resolution (decadal- to centennial-scale), multi-proxy analyses have been carried out on a new core from Holsteinian lake deposits at Dethlingen, Lüneburger Heide, northern Germany, in order to address the following main questions:

1. What is the tempo and mode of Holsteinian intra-interglacial climate variability in central Europe?

2. When did the two prominent climate oscillations take place during the Holsteinian interglacial and MIS 11, respectively?

3. What are the trigger mechanisms for the two prominent climatic oscillations based on their environmental imprint, duration and spatial extent? How can the potential trigger

mechanisms be compared with the forcing mechanisms of abrupt climate change during the onset of the present interglacial?

4. Is the sub-decadal- to decadal-scale climate variability as known from the Holocene (such as the variabilities related to the El Niño/Southern Oscillation [ENSO] and the North Atlantic Oscillation [NAO]) also observed during the Holsteinian?
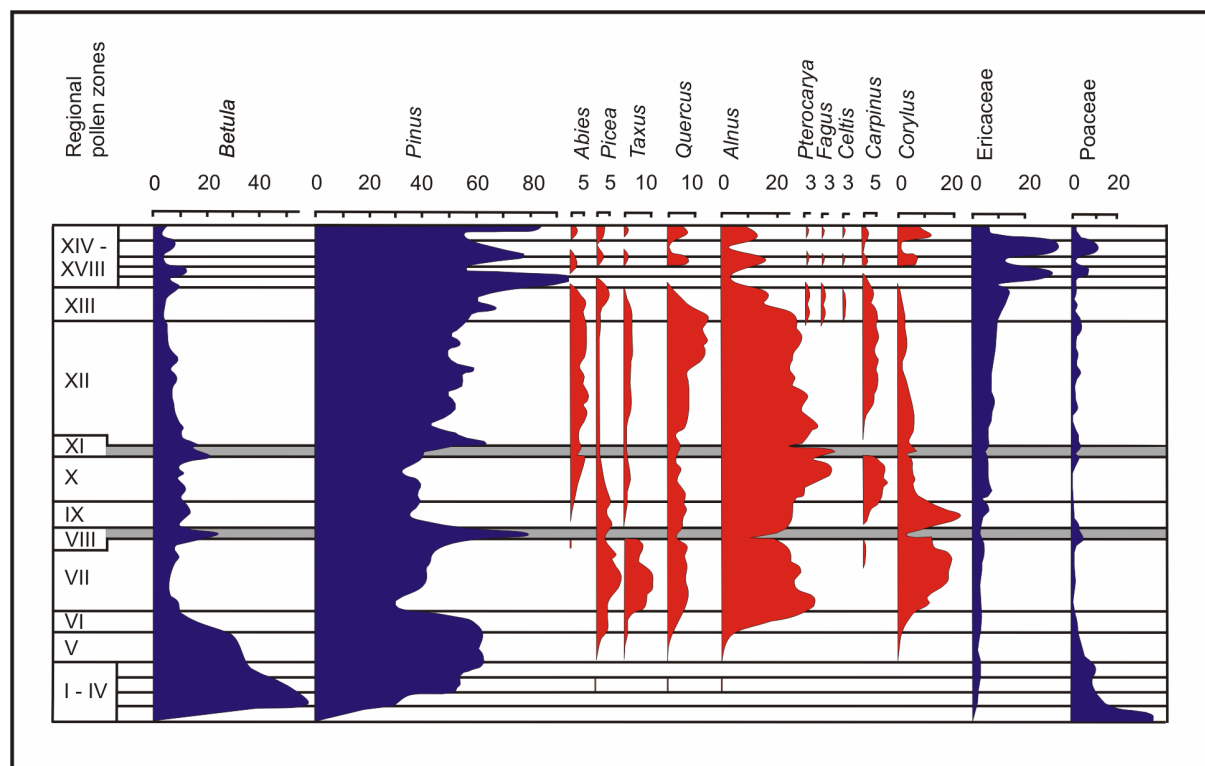
Figure 1.4: *Classical Holsteinian palynological profile from Munster-Breloh and Hetendorf, Lüneburger Heide, northern Germany. Grey bars indicate regressive phases in vegetation development within full interglacial conditions (modified after Müller, 1974 and Kukla, 2003).*

1.2 Study area

The Lüneburger Heide region of Northern Germany is located in a strategic position to study variations in the different components of the higher-latitude climate system (Fig. 1.5). In brief, the central European climate is influenced by a conveyor-like circulation of the ocean system that transports tropical heat northwards in the Atlantic Ocean; as a result, the overlying atmosphere becomes warmer in wintertime over the North Atlantic region and westerlies bring warm maritime air into Europe (e.g., Broecker, 1997; Ganachaud and Wunsch, 2000; Seager et al., 2002). The winter climate, although mild, is influenced by cold air masses originating from the Polar region and Central Asia, the latter being pushed westwards by the Siberian High pressure system (e.g., Cohen et al., 2001).
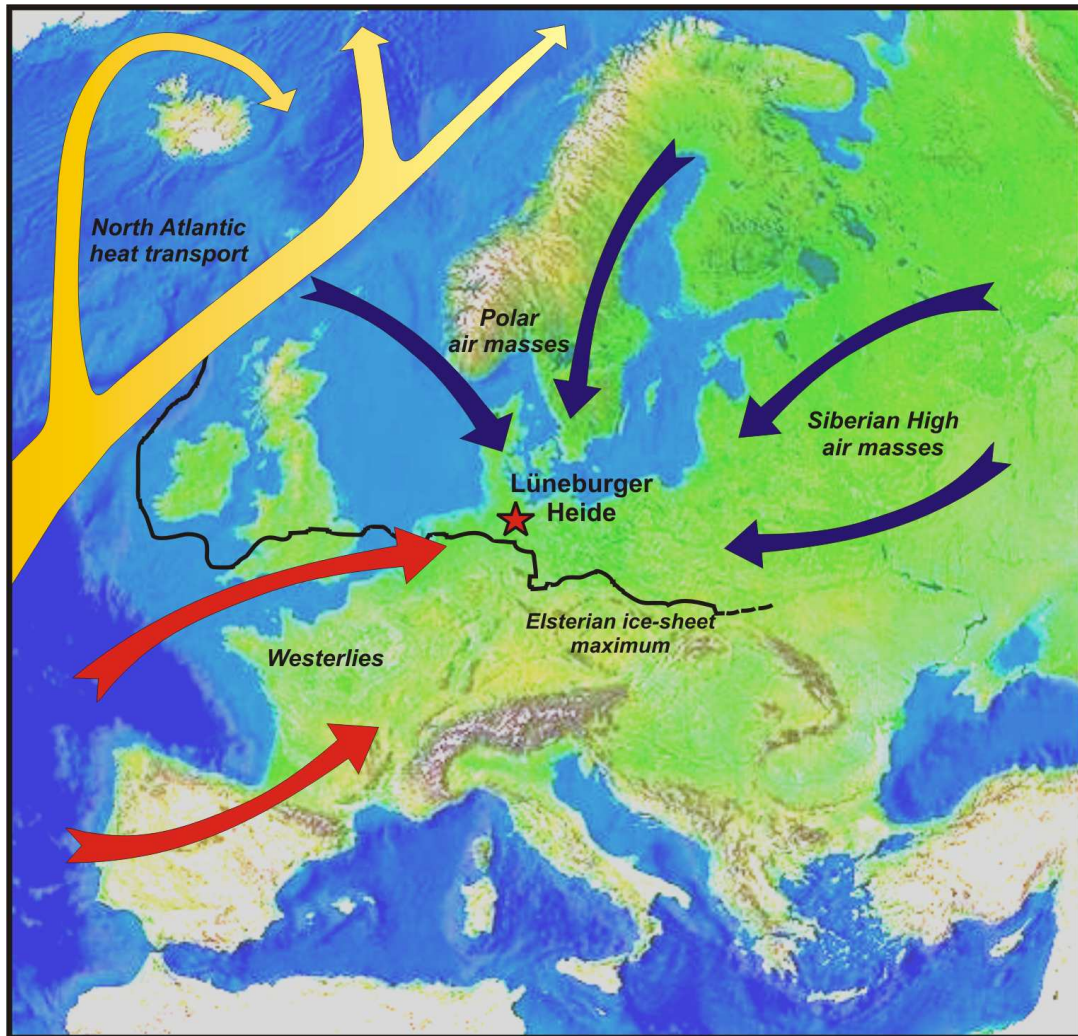
Figure 1.5: *Schematic view of ocean and atmospheric circulation patterns influencing the climate in the Lüneburger Heide region. The maximum extent of the Elsterian ice-sheet is indicated following Ehlers and Gibbard (2004).*

Located in the lowlands of northern Germany, the Lüneburger Heide region is characterized by a temperate, oceanic (atlantic) climate (Fig. 1.5). The modern mean January and July temperatures are between 0 and -1 ºC, and between 16 and 17 ºC, respectively; the annual precipitation is between 600 and 800 mm (Liedtke and Marcinek, 2002).

Owing to the repeated ice-sheet advances during the Middle to Late Pleistocene, the Lüneburger Heide region is dominated by glacial sands and clays, and loess deposits, whereas pre-Quaternary bedrock surfaces only locally (Ehlers and Gibbard, 2004). In particular, the advances of Elsterian glaciers eroded deep channels into poorly consolidated Paleogene and Neogene sediments. Later, during the Elsterian deglaciation, these channels were partially filled by glaciolacustrine sands, tills and clays; other depressions developed into lakes that witnessed the deposition of diatomaceous sediments during the following Holsteinian interglacial (e.g., Benda and Brandes, 1974; Ehlers et al., 1984; Eissmann, 2002). The occurrence of annually laminated diatomites in many of these deposits suggests that the Holsteinian lakes in the Lüneburger Heide region were deep (~5 to more than 20 m),

with anoxic bottom waters allowing the deposition and preservation of varved sediments (Benda and Brandes, 1974).
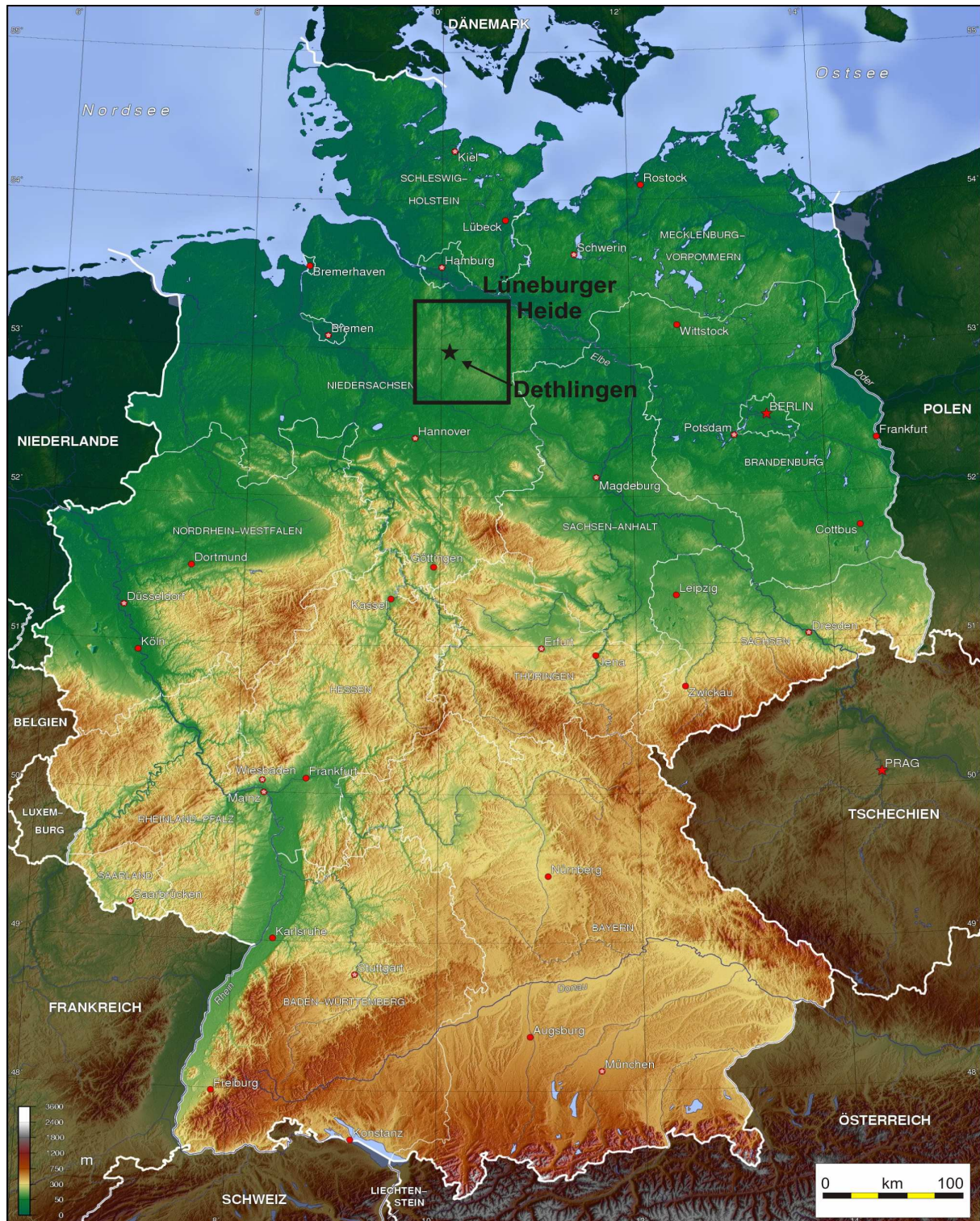
Figure 1.6: *Map of Germany with location of the Lüneburger Heide and the studied site at Dethlingen (from www.mapsorama.com).*

Previous palaeoclimate studies on the Holsteinian of the Lüneburger Heide region were carried out within the framework of coring campaigns aiming at the exploration and exploitation of the economically significant diatomite deposits (Benda, 1974; Meyer, 1974; Müller, 1974). The palynological and diatom investigations at the sites of Munster-Breloh, Hetendorf-Bonstorf, Ober-Ohe and Wiechel in the 1970's have provided the background for any subsequent study of the climate variability during the Holsteinian interglacial in central Europe (Benda, 1974; Benda and Brandes, 1974; Meyer, 1974; Müller, 1974).

For the purposes of this study as outlined above, the Holsteinian deposits around Dethlingen are particularly well suited (Fig. 1.6). Based on drillings in the early 1980's, the spatial extent and thickness of the Holsteinian diatomite are well known (Fig. 1.7; Benda et al., 1984); according to these data, the Dethlingen palaeolake was of rather small size, ~800 m long and ~300-500 m wide as inferred by the extent of the lake deposits. The lake deposits consist of ~20 m of predominantly annually laminated diatomite with intercalated clastic layers (Benda et al., 1984; see Section 1.3.2). The availability of other varved sedimentary records in the vicinity of Dethlingen (i.e., Munster-Breloh – Müller, 1974; Hetendorf-Bonstorf – Meyer, 1974; Wiechel – Benda, 1974; Ober-Ohe – Gistl, 1928; Selle, 1954) yields the possibility to cross-check results on a regional scale.
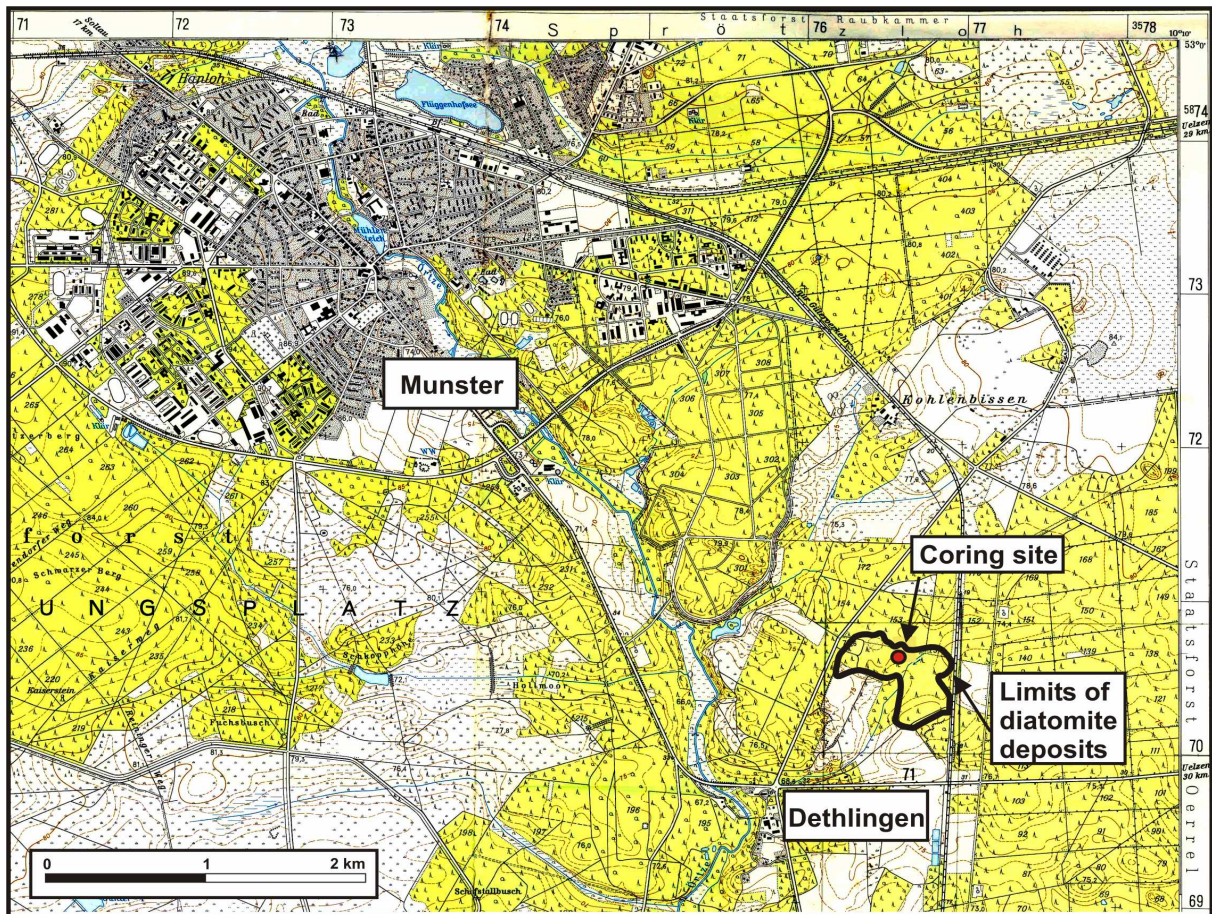
Figure 1.7: *Locality of the coring site near Dethlingen (detail from Sheet 3026, 1:25.000, Niedersächsisches Landesverwaltungsamt – Landesvermessung 1984). The extent of the diatomite deposits at Dethlingen is given following Benda et al. (1984).*

1.3 Material

1.3.1 Coring campaign

To obtain material for the present study, a coring campaign was carried out at Dethlingen in 2004. Drilling operations were handled by the company EURODRILL, using a wireline coring technique (Fig. 1.8). A 20-m-long core was retrieved (23 to 43 meters below surface; mbs) from a site at 52º 57.780' N and 10º 08.367' E, (Fig. 1.7) where the diatomite deposits have their greatest known thickness (Benda et al., 1984). Core recovery was excellent, with core loss being limited to a ~1.7-m-thick interval of coarse sand (lithological unit 7; see Section 1.3.2). The core was cut in 75-cm-long segments in order to facilitate core processing in the laboratory (original segment length 150 cm) and split into two halves that were stored at 4 ºC at the Institute of Geosciences, Goethe University Frankfurt.

Figure 1.8: Drilling operations at the Dethlingen site during the 2004 campaign (photo courtesy of U.C. Müller)

1.3.2 Lithology

The Dethlingen core comprises organic-rich diatomaceous lake sediments between 23 and 43 mbs. From the top to the bottom, the following lithological units occur (Fig. 1.9; see also photographs at Appendix I):

(1) above 23.00 mbs: glacial sands and gravels attributed to the Saalian glaciation (Benda et al., 1984);

(2) 23.00-23.20 mbs: diatomaceous mud with an increase in intercalated sand layers towards the top;

(3) 23.20-24.10 mbs: diatomaceous mud;

(4) 24.10-27.60 mbs: non-laminated diatomite with an increase in intercalated sand layers (~1.5-2 mm thick) towards the bottom;

(5) 27.60-27.93 mbs: laminated diatomite with very poor varve formation;

(6) 27.93-33.68 mbs: laminated diatomite with well-developed dark and light sub-layers of varying thickness (Fig. 1.10); a trend towards poorer formation of varves towards the top;

(7) 33.68-35.40 mbs: sand;

(8) 35.40-36.25: laminated diatomite with well-developed dark and light sub-layers of varying thickness; this lithological unit has erosional contact surfaces with the units 7 and 9, respectively;

(9) 36.25-43.00 mbs: re-deposited mud with intraformational varved clasts and sand.
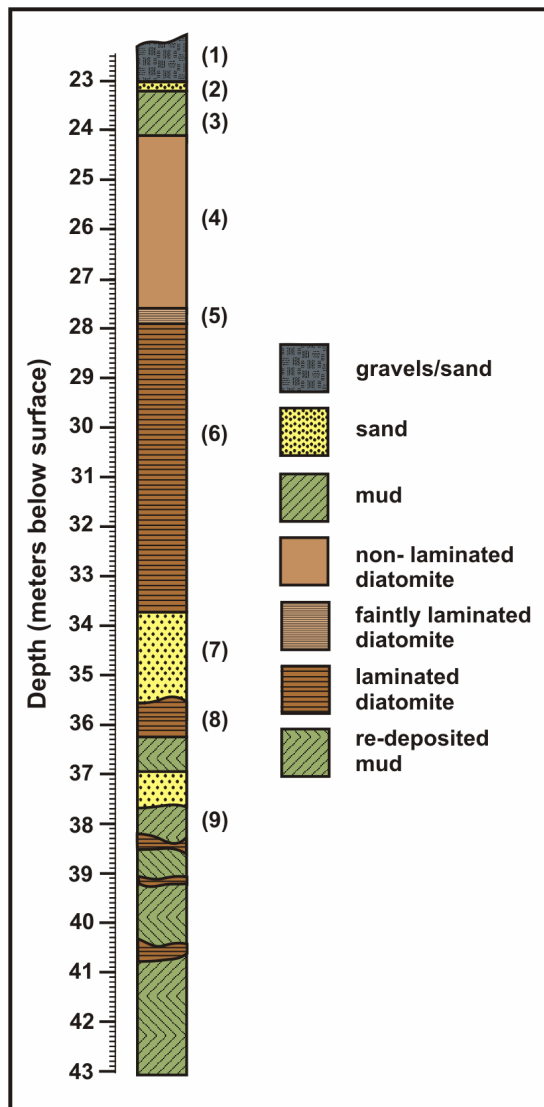
Figure 1.9: *Lithology of the Dethlingen core*
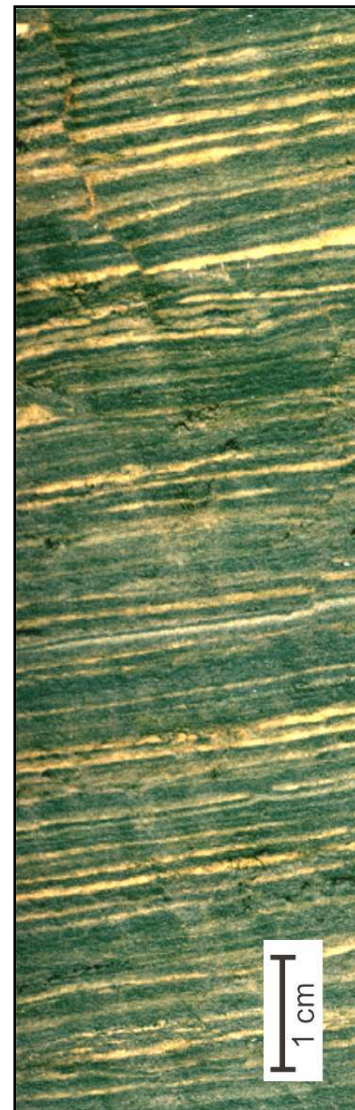
Figure 1.10: *Example for well-developed varves in the Dethlingen core. Shown interval is from lithological unit 6 (compare Fig. 1.9)*

1.4 Methods

A short description of the analyses carried out on the Dethlingen core is given in the following (Fig. 1.11).

1.4.1 Non-destructive analyses

Digital imaging – Lightness: Digital imaging and grey-scale measurements were carried out using a DMT CoreScan II core scanner for the core interval between 23.00 and 33.68 mbs.

Magnetic susceptibility: Magnetic susceptibility measurements were undertaken for the core interval between 23.00 and 33.68 mbs using a Bartington MS2E sensor. The susceptibility readings were carried out in 1 mm steps in order to obtain redundant data such that smoothing is possible without losing resolution. In order to monitor and correct for the sensor's drift, a background reading in air was taken every 10 mm.

μ-XRF: Geochemical measurements were undertaken for the interval from 29.05 to 29.16 mbs with a micro-X-ray fluorescence (μ-XRF) spectrometer EAGLE III XL at different resolutions (step sizes: 50, 100, 200, 500 μm) for Al, Ca, Cl, Fe, K, Mg, Mn, P, S, Si, Sr, and Ti (60 s count time, 0 kV X-ray voltage and 400 μA X-ray current). Measurements were carried out on sediment blocks that had been impregnated with Araldite 2020 epoxy resin.

1.4.2 Sampling series

Pollen: Pollen analysis was carried out for the core interval between 23.00 and 33.68 mbs with sampling intervals of 5 and 10 cm. Critical intervals (25.78-26.18 mbs and 28.73-29.17 mbs) were sampled every 1-2 cm; four additional samples were taken between 35.40 and 36.88 mbs roughly every 50 cm. In total, 208 pollen samples have been analysed. The preparation of pollen samples was undertaken following standard palynological techniques including sediment freeze-drying, weighing, treatment with HCl (10%), NaOH (10%), HF (40%), heavy-liquid separation with $Na_2WO_4 \times 2H_2O$, acetolysis, and slide preparation using glycerine jelly. A defined number of *Lycopodium* marker spores was added to each sample prior to chemical processing in order to calculate pollen accumulation rates (grains cm^{-2} yr^{-1}). The pollen samples were analysed using a Zeiss Axioskop light microscope at 400 x magnification. The minimum counting sum was always above 300 pollen grains per sample (excluding pollen from aquatic plants, spores and algae).

TOC, TN: Total Organic Carbon (TOC) and Total Nitrogen (TN) contents were measured with a LECO EC-12 carbon analyzer and a LECO Truspec N analyzer, respectively, for the same core depths as the pollen samples.

Sediment density: The sediment density was measured with a pycnometer on 50 samples for the core interval between 23.00 and 33.68 mbs, with a general spacing of 30 cm and a spacing of 5-10 cm for critical intervals (25.78-26.18 mbs and 28.73-29.17 mbs).
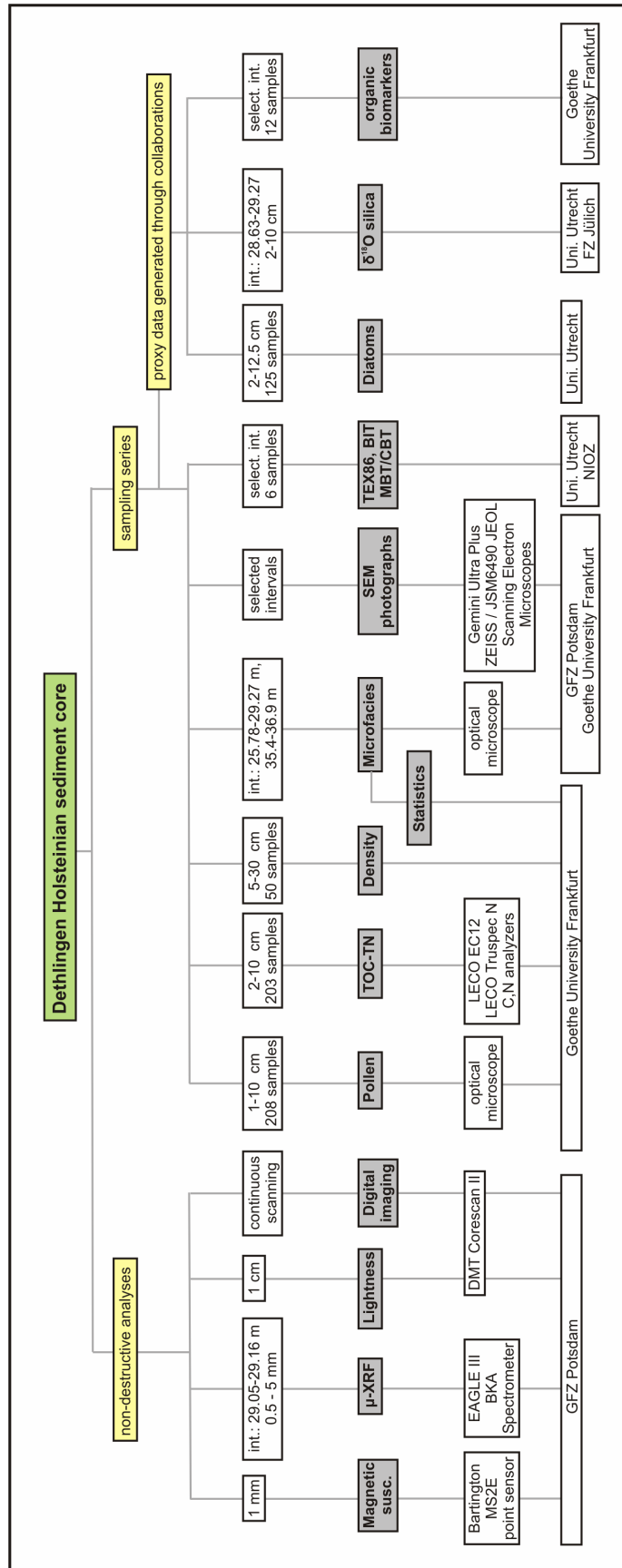
Figure 1.11: *Summary of the methods employed in this study.*

Microfacies: Thin sections (120 x 35 mm) were prepared for the core intervals 25.78-33.68 mbs, 35.88-36.28 mbs and 35.40-36.88 mbs with an overlap of 2 cm between successive sections following standard techniques; these include freeze-drying, impregnation with Araldite 2020 epoxy resin under vacuum, sawing, and grinding of the sediment (Brauer et al., 1999a; Lotter and Lemcke, 1999). Microfacies analyses, varve counting, and varve thickness measurements were undertaken using a petrographic microscope at 100x magnification.

SEM photographs: Sediment photographs from light and dark layers from the varved core intervals were taken with GEMINI Ultra Plus Zeiss and JEOL JSM-6490 scanning electron microscopes.

Organic geochemistry: Six pilot samples from critical intervals (25.78-26.18 mbs and 28.73-29.17 mbs) were investigated for microbially derived glycerol dialkyl glycerol tetraether (GDGT) membrane lipids in order to calculate the TEX_{86} and the MBT/CBT palaeothermometers, and the BIT index. The aim of the analyses was to reconstruct surface-water temperature, mean air temperature estimates of the lake's catchment area, and the amount of soil-derived organic matter relative to the lake organic matter, respectively (Hopmans et al., 2004; Powers et al., 2004; Weijers et al., 2006, 2007).

1.4.3 Statistical analyses

Time-series analyses were applied in order to identify periodic variations in varve thickness time series using MATLAB (e.g., Weedon, 2003). The thicknesses of the seasonal light and dark varve sub-layers were measured on thin sections under a petrographic microscope. Spectral peaks above the significance levels of 95 % and 99 % were determined using the Multi-Taper method (MTM; e.g., Vautard et al., 1992; Mann and Lees, 1996). In addition, wavelet analysis was applied to identify intervals where significant peaks of the non-stationary varve thicknesses time series occur (Torrence and Compo, 1998).

1.4.4 Other proxies

Within the broader scope of this PhD thesis, collaborations have been established in order to employ additional proxies as palaeoclimatic and palaeoenvironmental indicators. In particular, analyses of the diatom assemblages and $\delta^{18}O$ values in diatom silica (in cooperation with A.F. Lotter at Utrecht University and A. Lücke at Forschungszentrum Jülich), and organic biomarkers (in cooperation with W. Püttmann at Goethe University Frankfurt) are currently being carried out for the Dethlingen core. The potential of these studies for palaeoclimatic reconstructions is discussed in Section 6.2 (Outlook).

1.5 Structure of this PhD thesis

This PhD thesis is based on four manuscripts that comprise case studies on climate variability and abrupt climate change during interglacial periods. Two manuscripts have been published in peer-reviewed journals (Chapters 2 and 5) and two are currently under review (Chapters 3 and 4).

The first manuscript (Chapter 2), entitled "Vegetation dynamics and climate variability during the Holsteinian interglacial based on a pollen record from Dethlingen (northern Germany)", outlines the Holsteinian climate variability based on decadal-scale-resolution pollen analysis. An overview of the vegetation dynamics during the mesocratic to telocratic forest phases is given, with a particular focus on the characteristics of two prominent regressive phases. Finally, an effort is made to place the development of the Holsteinian interglacial forests within MIS 11.

The second manuscript (Chapter 3), entitled "Sub-decadal- to decadal-scale climate cyclicity during the Holsteinian interglacial (MIS 11) evidenced in annually laminated sediments", examines the results of microfacies analysis from the Dethlingen core with regard to their palaeoclimatic significance. Spectral and wavelet statistical analyses are carried out on the thicknesses of seasonal light and dark diatomaceous sub-layers in order to investigate the presence and distribution of sub-decadal and decadal-scale climate cyclicity in the Dethlingen record.

The third manuscript (Chapter 4), entitled "A short-term climate oscillation during the Holsteinian interglacial (MIS 11c): An analogy to the 8.2 ka climatic event?", focuses on the characteristics, spatial extent and potential trigger mechanisms of the older regressive phase in vegetation development as identified in Chapter 2. Based on high-resolution pollen analysis and varve counting from the Dethlingen core, a comparison with the 8.2 ka event of the present Holocene interglacial is made with regard to the duration, imprint on terrestrial ecosystems and prevailing boundary conditions. Striking similarities in the spatiotemporal characteristics and environmental impact of the two oscillations suggest that they were triggered by a similar mechanism, i.e., a slowdown in North Atlantic Deep Water formation.

The fourth manuscript (Chapter 5), entitled "Impact of Lateglacial cold events on the northern Aegean region reconstructed from marine and terrestrial proxy data", aims to better understand the response of terrestrial and marine ecosystems to climate perturbations that have been triggered by transient reductions in North Atlantic Deep Water formation. In particular, the study employs centennial-scale-resolution analyses of pollen and dinoflagellate cysts preserved in marine sediments from the Aegean Sea, to provide insights into the environmental impact of well-documented Northern Hemisphere climate perturbations during the Late Pleniglacial to early Holocene with an emphasis on the Heinrich event 1 and the Younger Dryas.

Finally, Chapter 6 presents a summary of the main results and an outlook on future work.

Chapter 2. Vegetation dynamics and climate variability during the Holsteinian interglacial based on a pollen record from Dethlingen (northern Germany)

Andreas Koutsodendris[1], Ulrich C. Müller[1], Jörg Pross[1], Achim Brauer[2], Ulrich Kotthoff[3], André F. Lotter[4]

[1] Paleoenvironmental Dynamics Group, Institute of Geosciences, Goethe University Frankfurt, Altenhöferallee 1, D-60438 Frankfurt, Germany; [2] German Research Centre for Geosciences, Section 5.2 Climate Dynamics and Landscape Evolution, Telegrafenberg, D-14473 Potsdam, Germany; [3] Geological-Paleontological Institute, University of Hamburg, Bundesstraße 55, D-20146 Hamburg, Germany; [4] Institute of Environmental Biology, Palaeoecology, Laboratory of Palaeobotany and Palynology, Utrecht University, Budapestlaan 4, 3584 CD Utrecht, The Netherlands

Abstract: *To better understand the environmental variability during the Holsteinian interglacial, we have palynologically analyzed a new core from Dethlingen, northern Germany, at a decadal resolution. Our data provide insights into the vegetation dynamics and thus also climate variability during the meso- to telocratic forest phases of the interglacial. Temperate mixed forests dominated the regional landscape throughout the Holsteinian. However, changes in the forest composition during the younger stages of the interglacial suggest a climatic transition towards milder conditions in winter. The strong presence of boreal floral elements during the older stages of the Holsteinian interglacial suggests a high seasonality. In contrast, during the younger stages the development of sub-atlantic and atlantic floral elements suggests increasingly warm and humid climatic conditions. Peak warming during the younger stage of the Holsteinian is marked by the maximum pollen abundances of* Buxus, Abies, *and* Quercus. *Although the vegetation dynamics suggest a general warming trend throughout the Holsteinian interglacial, abrupt as well as gradual changes in the relative abundances of temperate plants indicate considerable climatic variability. In particular, two marked declines in temperate taxa leading to the transient development of boreal and sub-temperate forests indicate short-term climatic oscillations that occurred within full interglacial conditions. The palynological signatures of these two regressive phases in vegetation development differ with regard to the expansion of pioneer trees, the abundances and rates of change of temperate taxa, and the presence of frost-sensitive taxa. These differences point to different mechanisms responsible for the individual regressive phases. Assuming a correlation of the interglacial at Dethlingen with Marine Isotope Stage (MIS) 11, our data suggest that temperate forests prevailed in northern Germany during the younger parts of MIS 11c.*

Keywords: *Pollen record; vegetation dynamics; abrupt climate change; Europe; Holsteinian interglacial; Marine Isotope Stage 11.*

2.1 Introduction

The study of past interglacials can significantly contribute to improving the prediction of future climate change and its potential impact on the biotic and abiotic environment (e.g., EPICA, 2004; Tzedakis et al., 2004a, 2009; Müller et al., 2005; Brauer et al., 2007a; Jouzel et al., 2007; Pross et al., 2009). In this context, the Holsteinian interglacial has received considerable attention owing to its presumed correlation to MIS 11 (e.g., Reille et al., 2000; de Beaulieu et al., 2001; Tzedakis et al., 2001), which, with regard to orbital forcing, represents one of the closest palaeoclimatic analogues for the present interglacial (e.g., Loutre and Berger, 2003; Ruddiman, 2005).

Based on the available climate information from continental archives, the Holsteinian represents a long interglacial (~15-16 ka; Müller, 1974) that is characterized by the development of mixed temperate forests in central and northwestern Europe (e.g., Erd; 1970; Turner, 1970; Müller, 1974; Kukla, 2003; Nitychoruk et al., 2005). Pollen-based temperature reconstructions from central European records suggest an overall warming trend. This trend, which is particularly reflected in July temperatures (from 17.5 to 19.7 ºC), resulted in warmer conditions than today during the younger stages of the Holsteinian (Kühl and Litt, 2007). The abovementioned studies indicate long-lasting mild climatic conditions during the Holsteinian. However, earlier palynological studies have suggested the presence of climatic instabilities lasting for several centuries as reflected by two intervals with abrupt shifts in forest composition associated with the development of pioneer vegetation (Müller, 1974; Kukla, 2003). These two phases have been identified at numerous sites in central and northwestern Europe, such as in England (West, 1956; Turner, 1970; Coxon, 1985; Thomas, 2001), Germany (Müller, 1974; Diehl and Sirocko, 2007), and Poland (Krupiński, 1995; Bińka and Nitychoruk, 1995, 1996; Bińka et al., 1997; Nitychoruk et al., 2005). However, the lack of high-resolution data has yet precluded deeper insights into the vegetation and climate dynamics of these phases. As a consequence, the mechanisms responsible for the regressive phases in vegetation development have remained unclear (Kukla, 2003).

Owing to the formation of numerous lakes after the melting of the Elsterian ice-sheet (Ehlers et al., 1984), the region of Lüneburger Heide in northern Germany is characterized by a number of partially annually laminated sedimentary archives of Holsteinian age (Benda and Brandes, 1974). Sedimentological investigations for mining purposes have been carried out on several diatomite deposits of the Lüneburger Heide region (Benda and Brandes, 1974), including Dethlingen (Benda et al., 1984). In this context, palaeoclimate studies were carried out on the sites of Munster-Breloh (Müller, 1974), Hetendorf (Meyer, 1974), Ober-Ohe (Gistl, 1928; Selle, 1954), and Wiechel (Benda, 1974). The potential for annual time-control, the good preservation of palynomorphs, and the possibility to crosscheck results on a regional scale make these archives well suited for the analysis of short-term climate and vegetation variability during the Holsteinian interglacial.

In light of the above, we describe the vegetation dynamics during the Holsteinian interglacial based on a decadal-scale-resolution record of terrestrial palynomorphs from a new core retrieved at Dethlingen, northern Germany.

2.2 Materials and methods

The Dethlingen site is located in the Lüneburger Heide region within the lowlands of northern Germany (10° 08' E, 52° 57' N, 65 m a.s.l., see Fig . 2.1). Dethlingen is surrounded by several basins that contain Holsteinian lacustrine deposits, such as Munster-Breloh, Hetendorf, Wiechel, and Ober-Ohe (Benda and Brandes, 1974).
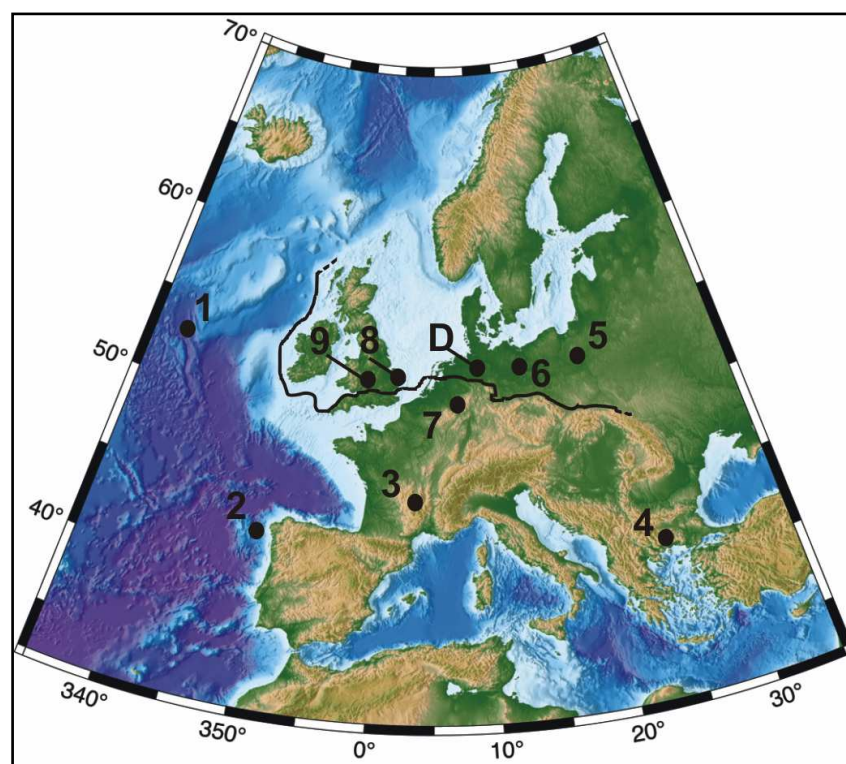
Figure 2.1: *Map indicating the location of Dethlingen and other sites mentioned in the text. The black line indicates the southern limit of the Elsterian ice sheet (after Ehlers and Gibbard, 2004). (D) Dethlingen; (1) core M23414; (2) core MD01-2447; (3) Praclaux; (4) Tenaghi Philippon; (5) Biała Podlaska; (6) Gröbern-Schmerz; (7) Döttingen; (8) Hoxne and Marks Tey; (9) Quinton.*

The Dethlingen core was retrieved in 2004 and comprises organic-rich lake sediments between 37 and 23 m depth below the present-day soil surface (mbs; Fig. 2.2). The lower part of the core (37 to 27.80 mbs) consists of a laminated diatomite with an intercalated, c. 2 m thick sand layer between 35.90 and 33.68 mbs. This interval is overlain by non-laminated diatomaceous sediments (27.80 to 24.10 mbs) and diatomaceous mud with increasing sand content (24.10 to 23 mbs). The lake sediments are topped by glacial gravel and sand that have been attributed to the Saalian glaciation (Benda et al., 1984). In this study, we exclusively focus on the interval between 33.68 and 23 mbs in order to avoid potential sediment unconformities and reworking that may have resulted from the deposition of the 2-m-thick sand layer (Fig. 2.2).
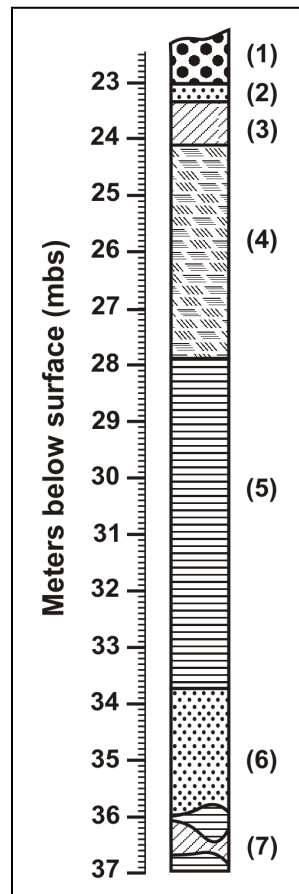
Figure 2.2: *Lithology of the Dethlingen core. (1) Gravels and sand; (2) Sand; (3) Diatomaceous mud; (4) Non-laminated diatomite; (5) Laminated diatomite; (6) Sand; (7) Re-deposited diatomite, partially laminated.*

Pollen samples were taken at intervals of between 5 and 10 cm; subsequently, dynamic phases in vegetation development were sampled every 1 to 2 cm. The thickness of individual samples varied between 0.5 cm for the non-laminated part of the core and the dynamic intervals, and 1 cm for the laminated part of the core. Based on varve counting of the Dethlingen core the sample spacing yields a decadal-scale resolution, i.e., c. 40-60 years between samples for the laminated diatomite, a mean of c. 75 years (min. 45 years; max. 130 years) for the non-laminated diatomite, and 10-15 years for the dynamic intervals. Each sample integrates c. 5-10 years for the dynamic intervals and c. 10-15 years for the rest of the core.

The preparation of pollen samples followed standard palynological techniques including sediment freeze-drying, weighing, treatment with HCl (10 %), NaOH (10 %), HF (40 %), heavy-liquid separation with Na_2WO_4 x $2H_2O$, acetolysis, and slide preparation using glycerine jelly. In total, 196 samples were analysed using a Zeiss Axioskop light microscope at 400 x magnification. An average of 407 pollen grains (excluding pollen from aquatics, spores, and algae) were counted per sample; the minimum counting sum was always above 300 pollen grains per sample. The percentages of aquatics, spores, and algae were calculated relative to the pollen sum of terrestrial taxa.

2.3 Results

2.3.1 Biostratigraphic age assignment

The Dethlingen pollen record (Fig. 2.3) exhibits an early, prominent *Taxus* phase accompanied by *Picea* and a subsequent *Carpinus-Abies* phase associated with the occurrence of *Buxus*, *Pterocarya,* and *Fagus*. This succession of taxa is characteristic for Holsteinian pollen records from central and northwestern Europe (Erd, 1970; Turner, 1970; Müller, 1974; Linke and Hallik, 1993; Bińka and Nitychoruk, 1995, 1996; Geyh and Müller, 2005; Diehl and Sirocko, 2007). Hence, based on this biostratigraphy, the Dethlingen record can be firmly assigned to the Holsteinian interglacial.

2.3.2 Palynostratigraphy of the Dethlingen record

The palynoflora at Dethlingen as depicted in Fig. 2.3 is dominated by *Alnus* and *Pinus,* which together account for more than 60 % of the terrestrial pollen sum throughout the record. In association with the prominent occurrence of *Carpinus* and the virtual absence of *Fagus* (Fig. 2.3), this pattern is characteristic for the lowland vegetation during the Holsteinian in central Europe (Erd, 1970; Linke and Hallik, 1993; de Beaulieu et al., 2001). The vegetation succession shows a high degree of similarity to that of the nearby site of Munster-Breloh (Müller, 1974). Therefore, the pollen zonation from Munster-Breloh as developed by Müller (1974) has been adopted with minor modifications (Fig. 2.3). The pollen zones (PZ) VII to XIV of Müller (1974), which cover most of the Holsteinian interglacial, are recorded at Dethlingen. Pollen zones I to VI, reflecting the onset of the Holsteinian (Meyer, 1974), are obscured by sediment reworking below 33.68 mbs that resulted from the deposition of the sand layer (see Section 2.2). The development of the palynoflora during the pollen zones identified at Dethlingen (Fig. 2.3) is briefly described below, whereas a summary of the characteristics of each pollen zone is given in Table 2.1.

PZ VII (33.68-29.15 mbs): The lowermost part of the record from Dethlingen can be correlated to PZ VII from Munster-Breloh. This zone is characterised by a strong increase in *Taxus* from ~2 % to an average of ~10 % (with maximum percentages as high as ~20 %). *Picea* and *Corylus* are also characteristic taxa, accounting for 3-5 % and 10 %, respectively. *Betula* (up to 10 %), *Quercus* (up to 5 %), and Ericaceae (3-5 %) are also abundant. *Carpinus*, mixed oak forest elements such as *Fraxinus*, *Ulmus,* and *Tilia,* as well as Poaceae and *Rumex* are present in this zone, albeit in low abundances.

PZ VIII (29.15-28.73 mbs): The onset of PZ VIII is clearly marked by the abrupt decline in pollen of temperate taxa and the increase in pollen of pioneer trees (*Pinus* and *Betula*), grasses, and herbs. The decline of temperate taxa is clearly reflected in the curves of *Taxus*, *Corylus,* and *Quercus* (Fig. 2.3). The abundance of *Picea*, *Alnus,* and Ericaceae pollen also declines. This zone has been described as the older regressive phase in vegetation development at Munster-Breloh, with peak abundances of *Pinus* and *Betula* (Müller, 1974).

PZ IX (28.73-27.28 mbs): This zone is characterised by the increase in percentages of *Corylus*, *Quercus*, *Picea*, and Ericaceae pollen to levels attained prior to the regressive

vegetation phase of PZ VIII. *Taxus*, however, remains at much lower percentages throughout the remainder of the Dethlingen record. *Alnus*, which is the dominant tree pollen of PZ IX, shows a slight increase towards the top of the zone, whereas relative *Pinus* pollen abundances gradually decline. The zone shows an increase of *Carpinus* percentages, the regular presence of *Abies* and the sporadic occurrence of *Ilex* and *Hedera* pollen.

PZ X (27.28-26.18 mbs): During this zone, *Corylus* and *Picea*, which are both characteristic for PZ VII to IX, decline to very low pollen percentages (<3 and ~1 %, respectively). *Carpinus* reaches peak values and *Abies* exhibits an increase with maximum abundances occurring in the upper part of the zone. Pollen grains from *Ilex* are almost permanently present. *Alnus* percentages reach their maximum, and *Betula* percentages increase towards the top of the zone. Pollen Zone X also marks the upper limit for the regular presence of *Tilia*; higher up in the record, pollen of this taxon occur only sporadically. In contrast, pollen of herbs, such as *Rumex*, increase in abundance during this zone and are subsequently frequently recorded until the end of the Holsteinian interglacial.

PZ XI (26.18-25.78 mbs): This pollen zone comprises the younger regressive phase in vegetation development as described at Munster-Breloh (Müller, 1974). The onset of PZ XI is marked by the abrupt decline in *Carpinus*. Smaller declines in *Abies* and *Alnus* can be also observed; the latter, however, reaches an abundance peak during the middle part of the zone. *Betula* pollen percentages increase (max. 18 %), whereas *Pinus* percentages remain nearly stable and even exhibit a transient decline during the lower part of PZ XI (Fig. 2.3). As in PZ X, *Corylus*, *Quercus*, *Taxus*, and *Picea* remain at low levels. Remarkably, the evergreen taxa *Ilex*, *Buxus,* and *Hedera* are not affected during this regressive phase. The abundances of Ericaceae, Poaceae, and *Rumex* pollen as well as of a variety of herb taxa increase, leading to non-arboreal pollen (NAP) percentages as high as 16 % (Fig. 2.4).

PZ XII (25.78-23.78 mbs): This zone is marked by the increase in *Quercus* pollen percentages to peak values throughout the Dethlingen record; *Abies* percentages reach 5%. The percentages of *Carpinus* pollen also increase, but do not reach the level attained prior to the regressive phase of PZ XI. *Buxus* is recorded frequently, whereas *Ilex* pollen occurs only sporadically. Finally, *Pinus*, Ericaceae, and a variety of NAP exhibit a slight increasing trend throughout PZ XII, while *Alnus* gradually declines (Fig. 2.3).

PZ XIII (23.78-23.38 mbs): This zone shows the first occurrence of *Pterocarya*, *Fagus,* and *Celtis*. *Buxus* pollen remains frequent. However, the abundances of pollen of other temperate trees such as *Quercus, Abies*, but also *Alnus*, decline strongly. *Pinus* and *Betula* pollen increase towards the end of the zone, whereas Poaceae percentages increase only gradually.

PZ XIV (23.38-23.03 mbs): The percentages of Ericaceae and Poaceae pollen increase strongly, reaching up to 10 % and 18 %, respectively. Conifer taxa such as *Abies* and *Taxus,* most of the deciduous trees (including *Alnus*, *Carpinus,* and *Quercus*), and evergreen taxa (*Ilex*, *Buxus,* and *Hedera*) decline to minimum values during PZ XIV, whereas *Pinus* pollen remains dominant and *Betula* further increases, reaching values of up to 15 %.

2.4 Discussion

2.4.1 Vegetation dynamics and climate variability

The Dethlingen pollen record reflects a mixed temperate forest that was temporarily replaced by boreal (during PZ VIII) and sub-temperate forests (during PZ XI) (see Table 2.1). These two short phases, described as older and younger regressive phases in vegetation development, are discussed in detail in Section 2.4.2.

The forest in the lower and middle part of the record (i.e., PZ VII to IX) is marked by constant abundances of temperate trees and shrubs (~20-25 %; Fig. 2.4), such as *Taxus*, *Corylus*, *Quercus,* and *Carpinus* (Fig. 2.3), suggesting temperate climatic conditions (Dahl, 1998). However, the occurrence of *Picea* (Fig. 2.3), which has a competitional advantage when growing in climates with a rapid transition between winter and summer (Dahl, 1998), suggests increased seasonality during the older stages of the Holsteinian. The temperate fern *Osmunda* is present especially in the upper parts of PZ VII to IX (Fig. 2.3). Based on the distribution and ecology of *Osmunda regalis* during the present interglacial in Europe (e.g., Birks and Paus, 1991; Dahl, 1998; Landi and Angiolini, 2008), we may assume that this interval was characterised by high humidity and soil moisture, and a mean temperature of the coldest month above -4 ⁰C. During the younger stages of the Holsteinian interglacial (i.e., PZ X to XIII), sub-atlantic and atlantic taxa reached the surroundings of the Dethlingen palaeolake and became part of the mixed temperate forest. This interval is characterised by the development of the *Carpinus-Abies* phase after the decline of *Picea* (Fig. 2.3) and the expansion of evergreen taxa (Fig. 2.4). Such vegetation changes point to a climatic transition towards warm or mild winter conditions with increased humidity (Turner, 1970) and higher precipitation (e.g., Zagwijn, 1996). During this interval (PZ X to XIII), the mixed temperate forest is characterized by considerable variability in vegetation dynamics in comparison to the older stages of the Holsteinian interglacial. Forest openings gradually expand after PZ X, as reflected by an increase of NAP from 8 to 15 % (Fig. 2.4). Furthermore, variability in the abundances of the temperate taxa is indicated by gradual changing trends (Fig. 2.4). At first, during PZ X, a declining phase of the temperate taxa is concurrent with an increase in *Betula* and *Alnus* (Fig. 2.3). This trend reaches a minimum in the abundances of temperate taxa during the prominent younger regressive phase in vegetation development (PZ XI; Fig. 2.4). After this regressive phase, the temperate taxa exhibit an increase during PZ XII that is associated with maximum percentages of *Quercus*, *Abies,* and *Buxus* (Fig. 2.3). *Buxus* has present-day thermal limits of 0 ⁰C in January and 17 ⁰C in July, and requires, similarly to *Abies*, high precipitation rates to grow (Zagwijn, 1996). Therefore, the increase in these temperate taxa suggests that the warmest conditions were reached during the later stages of the Holsteinian, with the peak warmth being accompanied by very high humidity.
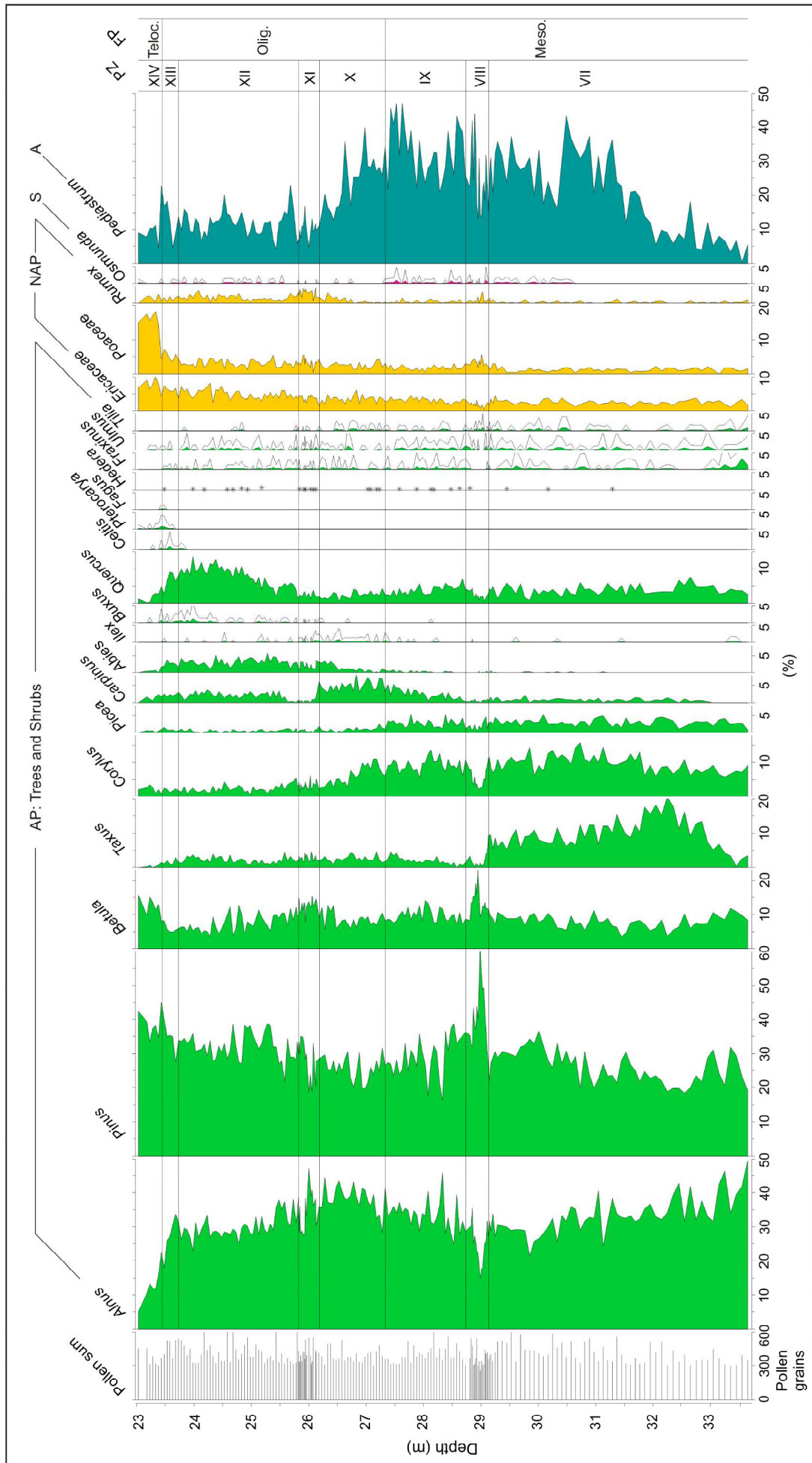
Figure 2.3: *Pollen record of the Holsteinian interglacial at Dethlingen. Percentages of selected tree, shrub, and herb taxa plotted against core depth (meters below the present-day soil surface). The total number of pollen grains per sample (excluding aquatics and spores) and sample depth are indicated. Percentages of* Osmunda *and* Pediastrum *are calculated relative to the main pollen sum. Pollen zones have been adopted from the Holsteinian pollen stratigraphy of Munster-Breloh following Müller (1974). (AP) Arboreal Pollen; (NAP) Non-arboreal pollen; (S) Spores; (A) Algae; (PZ) Pollen Zone; (FP) Forest phase; (Meso.) Mesocratic phase; (Olig.) Oligocratic phase; (Teloc.) Telocratic phase.*

In the upper part of PZ XII the temperate taxa decline as they also do during PZ XIII. Finally, the mixed temperate forest is replaced by pioneer trees (*Pinus* and *Betula*) growing in open habitats (PZ XIV; Table 2.1). During this uppermost pollen zone the temperate taxa reach minimum values of ~6.5 %, whereas pioneer trees and NAP increase, accounting for ~50-60 % and ~30-35 % of the pollen sum, respectively (Fig. 2.4).

The vegetation succession at Dethlingen as described above reflects the trajectory from the mesocratic, oligocratic, to the telocratic forest phase of a glacial-interglacial cycle (Birks, 1986; Andersen, 1994; Birks and Birks, 2004). The mesocratic phase is characterised by the development of temperate forests, the absence of shade-intolerant species (e.g., *Juniperus*), and productive lakes (Birks, 1986; Andersen, 1994). These characteristics are prominent within PZ VII to IX, which show the highest percentages of temperate taxa (Table 2.1; Fig. 2.4) associated with an expansion of shade-tolerant taxa (e.g., *Corylus*; Fig. 2.3). At the same time, maximum percentages of *Pediastrum* as well as high diatom productivity point to elevated trophic conditions in the Dethlingen palaeolake. The oligocratic phase has been described as a retrogressive interglacial phase characterised by decreasing forest cover, declining biomass and lake productivity (Birks, 1986; Andersen, 1994). This forest phase is represented at Dethlingen by PZ X to XIII coinciding with the *Carpinus-Abies* phase (Table 2.1). During that time, the increased percentages of NAP suggest a slight forest opening around Dethlingen, whereas a decline in lake productivity is mirrored by decreasing *Pediastrum* abundances in PZ X (Fig. 2.3). According to the correlation of the Holsteinian interglacial with the Hoxnian (England) and Mazovian (Poland) interglacials (Geyh and Müller, 2007), the *Carpinus-Abies* phase of the Holsteinian is recognisable across central and northwestern Europe. Comparable slight forest openings occurred during the *Carpinus-Abies* phase of the Hoxnian (local PZ HoIII; e.g., Turner, 1970; Coxon, 1985; Thomas, 2001) and the Mazovian (local PZ 7; e.g., Bińka and Nitychoruk, 1997). Thus, the slight forest opening at Dethlingen does not result from a change in local environmental conditions, but rather represents a supraregional signal marking the forest development during the oligocratic phase.

The causes of vegetation changes during the oligocratic phase have been attributed to impoverishment of soils (Andersen, 1994). It is conceivable that such an impoverishment resulted from an increased limitation of P relative to N often associated with reductions in litter decomposition rates and changes in the microbial assemblages (e.g., Wardle et al., 2004). As the vegetation succession during the oligocratic phase is not climatically driven, the opening of the forest and the decline in arboreal pollen (AP) percentages at Dethlingen

PZ	Characteristics	Vegetation dynamics	Forest type	Forest phase
XIV	(+) Ericaceae, Poaceae, herbs (↑) *Pinus*, *Betula* (↓) *Quercus*, *Alnus*, *Picea*, *Carpinus*, *Abies*	• maximum forest opening (↑) pioneer trees (↓) temperate taxa (↓) evergreen taxa	Transition to open vegetation	Telocratic
XIII	(+) *Pterocarya*, *Fagus*, *Celtis*, *Buxus* (↑) *Pinus*, *Betula*, Ericaceae, herbs (↓) *Quercus*, *Alnus*, *Abies*, *Taxus*	(↓) temperate taxa (↑) pioneer trees	Mixed temperate with atlantic taxa and slight forest opening	Oligocratic
XII	(+) *Quercus*, *Buxus*, *Abies* (↑) Ericaceae, herbs (↓) *Alnus*	(↑) temperate taxa (↑) forest opening	"	"
XI	(+) *Betula*, *Ilex*, *Hedera* (↑) Ericaceae, herbs (↓) *Carpinus*, *Abies*	(↑) pioneer trees (↑) forest opening (↓) temperate taxa	Sub-temperate with forest openings	"
X	(+) *Carpinus*, *Ilex* (↑) *Abies*, herbs (↓) *Corylus*, *Picea*	(↓) temperate taxa (↑) evergreen taxa (↑) pioneer trees	Mixed temperate with atlantic taxa	"
IX	(+) *Corylus*, *Picea*, *Quercus*, Ericaceae (↑) *Carpinus* (↓) *Pinus*	(↑) temperate taxa (↓) pioneer trees	Mixed temperate with boreal taxa	Mesocratic
VIII	(+) *Pinus*, *Betula*, Poaceae (↓) *Taxus*, *Corylus*, *Alnus*, *Picea*, *Quercus*, Ericaceae	(↑) pioneer trees (↑) forest opening (↓) temperate taxa	Boreal with forest openings	"
VII	(+) *Taxus*, *Picea*, *Corylus*, *Quercus*	• maximum of temperate taxa	Mixed temperate with boreal taxa	"

Table 2.1: *Summary of pollen zones (PZ) characteristics, vegetation dynamics, inferred forest types, and forest phases for each individual pollen zone. Pollen zones have been adopted from the Holsteinian pollen stratigraphy of Munster-Breloh (Müller 1974). Symbols: (+) characteristic taxa; (↑) increase; (↓) decrease.*

(Fig. 2.4) can indeed coincide with the warmest temperatures and the very humid conditions as reflected by the peak abundances of *Buxus, Abies,* and *Quercus* (PZ XII; Fig. 2.3). Although *Quercus* is usually a prominent forest element of the mesocratic phase (Birks, 1986), it reaches its maximum abundance during the oligocratic phase of the Holsteinian in central Europe. The tree was able to take advantage of the warm climate in combination with the opening of the forests as it is less shade-tolerant than *Corylus* and also more tolerant than *Carpinus* when growing on poor soils (Birks, 1986; Ellenberg, 1988). Finally, the telocratic phase, which is generally characterised by declining temperatures and increasingly open vegetation during the terminal stage of interglacials (Birks, 1986; Andersen, 1994), is represented in the uppermost part of the Dethlingen record (PZ XIV; Table 2.1), indicating a transition towards glacial conditions.
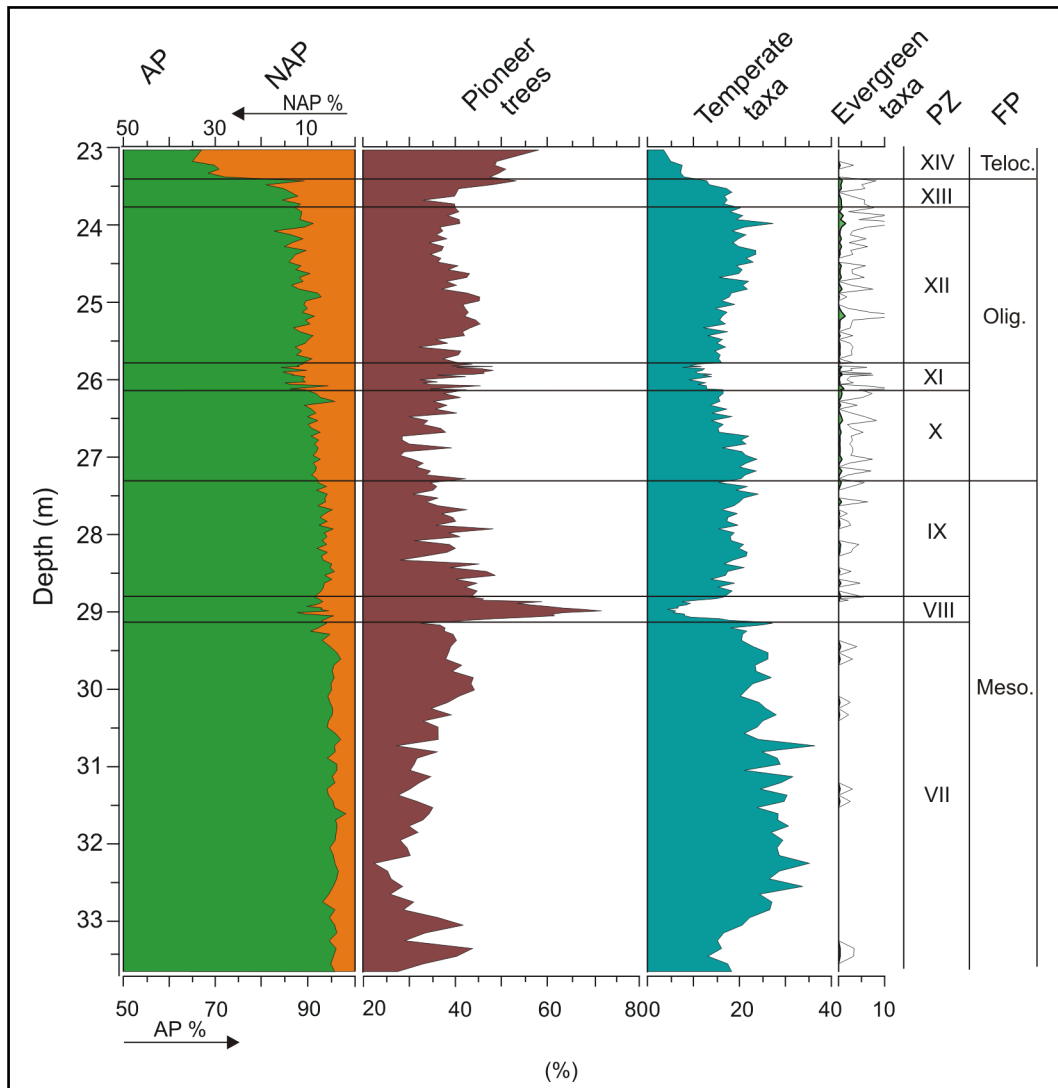
Figure 2.4: *Percentages of selected groups of taxa plotted against depth (meters below the present-day soil surface). (i) Pioneer trees, including* Pinus *and* Betula*; (ii) Evergreen taxa, including* Buxus, Ilex, *and* Hedera*; (iii) Temperate taxa, including the evergreen taxa of group (ii) and* Abies, Acer, Carpinus, Celtis, Corylus, Fagus, Fraxinus, Ostrya, Pterocarya, Quercus, Taxus, Tilia, *and* Ulmus*. Pollen zones have been adopted from the Holsteinian pollen stratigraphy of Munster-Breloh following Müller (1974). (AP) Arboreal Pollen; (NAP) Non-arboreal pollen; (PZ) Pollen Zone; (FP) Forest phase; (Meso.) Mesocratic phase; (Olig.) Oligocratic phase; (Teloc.) Telocratic phase.*

In summary, the overall vegetation composition as reflected by the development of mixed temperate forests at Dethlingen suggests a general prevalence of mild climatic conditions during the Holsteinian. The expansion of sub-atlantic and atlantic floral elements during the younger parts of the interglacial (i.e., PZ X to XIII; Table 2.1) and the decline of boreal elements that characterise the older stages of the interglacial (i.e., PZ VII to IX; Table 2.1) suggest warmer winters and increased humidity. However, both abrupt and gradual changes in the abundances of the temperate plant taxa point to considerable climatic variability during the Holsteinian interglacial.

2.4.2 Short-term regressive phases

The Holsteinian pollen record from Dethlingen exhibits two prominent regressive phases in vegetation development (PZ VIII and XI). Based on varve counts from palaeolake sediments from the Lüneburger Heide region, both the two phases have a duration of c. 300 years. Although they are marked by a short-term forest opening with the expansion of pioneer trees and a decline of temperate taxa (Table 2.1), a close inspection reveals strong differences between the two phases. These differences relate to the magnitude of the expansion of pioneer trees, the occurrence of specific taxa with regard to their frost tolerance, and the rates and intensity of vegetation changes.

2.4.2.1 Older regressive phase (PZ VIII)

The older regressive phase in vegetation development is clearly defined by the abrupt decline in temperate taxa and the pronounced increase in pioneer trees (Fig. 2.4). The percentages of temperate taxa decline to the lowest value (4.5 %) throughout the temperate stage of the interglacial. Pioneer tree abundances reach peak values of 72 % at the expense of the temperate taxa. The declines of *Taxus* and *Corylus* (Fig. 2.3), which are sensitive to severe and prolonged frost (e.g., Tallantire, 2002; Thomas and Polwart, 2003) suggest particularly low winter temperatures during this regressive phase. In addition, considering the coeval decline in *Picea* (Fig. 2.3), which tolerates low winter temperatures, a climatic shift towards drier conditions is also plausible.

A clear distinction of two sub-phases within PZ VIII can be made based on the succession of pioneer trees. *Pinus* peak abundances are recorded during the declining stage of the temperate taxa, whereas the expansion of *Betula* coincides with the onset of the recovery of temperate taxa during the middle part of PZ VIII (Fig. 2.3). This suggests that the expansion of *Pinus* represents the primary vegetation response to the cooling (and possibly drying), whereas the expansion of *Betula* would mark the onset of subsequent warming, with this tree expanding as a pioneer during the forest recovery.

2.4.2.2 Younger regressive phase (PZ XI)

The younger regressive phase in vegetation development punctuates a gradual decline in temperate taxa that started in PZ X (Fig. 2.4). Although this phase is marked by a final abrupt decline and a short recovery, it seems to be centred within a long-term vegetation change that includes the time covered by PZ X to XII. During this interval, the percentages of temperate taxa decrease to ~8 % (Fig. 2.4). The phase is marked by the abrupt decline in *Carpinus* and *Abies* (Fig. 2.3). The expansion of pioneer trees is mainly reflected by an increase in *Betula*; *Pinus*, in contrast, even shows a declining trend. The considerable changes in *Alnus* (Fig. 2.3) suggest fluctuations in the palaeolake level.

With regard to low temperature tolerance, pollen grains of several winter frost-sensitive taxa such as *Ilex, Buxus, Hedera*, and *Abies* occur throughout the younger regressive phase (Fig. 2.3). *Abies* and *Hedera* cannot tolerate mean winter temperatures below -4 ºC and -2 ºC, respectively, whereas *Ilex* and *Buxus* require mean winter temperatures above 0 ºC (Iversen,

1944; Zagwijn, 1996). It is therefore unlikely that the younger regressive phase was related to a substantial decline in mean winter temperatures, particularly given that *Buxus* seems to start immigrating at the onset of PZ XI (Fig. 2.3). The presence of winter frost-sensitive taxa together with the minimum of temperate taxa possibly suggests a lack of summer warmth, although changes in precipitation or other factors cannot be excluded.

2.4.2.3 Comparison of the regressive phases

The two regressive phases in vegetation development (PZ VIII and XI) are both characterised by the replacement of temperate forest by pioneer trees, although this process is much more pronounced during the older regressive phase. The rates of vegetation change and the presence of frost-sensitive taxa provide information on further differences between the two phases. They suggest that an abrupt onset of severe climatic conditions related to low winter temperatures, probably in combination with drier conditions, took place during the older regressive phase. In contrast, the younger regressive phase is possibly part of a long-term gradual trend of decreasing and subsequently increasing summer warmth.

The comparison of Holsteinian pollen records from central and northwestern Europe provides information on the distribution of the two regressive phases. The older phase, identified by increased NAP and pioneer tree abundances before the establishment of the *Carpinus-Abies* phase of the Holsteinian interglacial, is detected in numerous records from central and northwestern Europe, e.g., Munster-Breloh (Müller, 1974) and Döttingen (Diehl and Sirocko, 2007) in Germany; Hoxne (West, 1956; Coxon, 1985), Marks Tey (Turner, 1970), and Quinton (Thomas, 2001) in England; and around Biała Podlaska in Poland (e.g., Krupiński, 1995; Bińka and Nitychoruk, 1995, 1996; Bińka et al., 1997) (Fig. 2.1). The younger regressive phase, however, which is associated with a decline in *Carpinus* and an expansion of pioneer trees within the *Carpinus-Abies* phase, has so far only been clearly evidenced in records from northwestern Germany, e.g., at Munster-Breloh (Müller, 1974), Gröbern-Schmerz (Eissmann, 2002), and Döttingen (Diehl and Sirocko, 2007) (Fig. 2.1). It seems possible that the occurrence of evergreen taxa during the younger regressive phase and the lack of high-resolution Holsteinian pollen data have yet precluded its detection in records from other geographic regions. Therefore, high-resolution pollen analyses are needed to better constrain its distribution in central and northwestern Europe.

Although the two regressive phases have been known for decades, their triggering mechanisms have remained poorly understood. Causes that have been proposed include fire or animal grazing (Turner, 1970) and volcanism (Diehl and Sirocko, 2007). However, given the nature of the vegetation changes and the supraregional distribution of the regressive phases, they may well have resulted from climate oscillations (Müller, 1974; Kukla, 2003). Such a scenario is strongly supported by our data. However, because the Dethlingen record indicates that the two phases exhibit different characteristics, it appears likely that they have been caused by different triggering mechanisms. The signature of the older phase is reminiscent of the imprint of the Holocene 8.2 kyr cold event on the vegetation in central and northern Europe (see e.g., Tinner and Lotter, 2001, 2006; Veski et al., 2004); thus, a

relationship to a meltwater-forced slowdown of the North Atlantic circulation appears possible. However, as the phase took place ~6000 years after the onset of the Holsteinian interglacial (Müller, 1974), it remains to be explained how it could have been triggered within a period of low ice volume. Hence, a decrease in solar activity, as it has also been suggested for the 8.2 kyr and other events in the North Atlantic (Bond et al., 2001; Muscheler et al., 2004), may also be a possible explanation for the older regressive phase.

The younger regressive phase, in contrast, appears to be related to long-term, gradual changes in vegetation dynamics during the younger stages of the Holsteinian (PZ X to XII). Based on the duration of the pollen zones at Munster-Breloh (Müller, 1974), these long-term changes occurred over c. 4000 years. The trend in temperate taxa abundances and the long duration of the gradual changes suggest a connection to orbital forcing. However, the mechanism triggering such a short-term regressive phase under changing orbital boundary conditions remains unclear.

2.4.3 The Holsteinian interglacial and MIS 11

The absence of long, continuous terrestrial records in northwestern Europe and the lack of reliable absolute dates have led to conflicting views on the chronostratigraphic position of the Holsteinian interglacial (e.g., Reille et al., 2000; de Beaulieu et al., 2001; Tzedakis et al., 2001; Geyh and Müller, 2005). There is an ongoing debate as to whether the Holsteinian correlates with MIS 9 (Rowe et al., 1997; Eissmann, 2002; Geyh and Müller, 2005; Degering and Krbetschek, 2007; Meijer and Cleveringa, 2009) or MIS 11c (e.g., Turner, 1998; Rowe et al. 1999; Reille et al., 2000; Grün and Schwarcz, 2000; Tzedakis et al., 2001; Kukla, 2005; Nitychoruk et al., 2005, 2006; Müller and Pross, 2007; Preece et al., 2007; Ashton et al., 2008; Pawley et al., 2009). Moreover, studies on the British Isles of interglacial deposits displaying a Hoxnian/Holsteinian vegetational and faunal development may include stratigraphic units corresponding to sub-stages of both MIS 9 and 11 (Dowling and Coxon, 2001; Scourse, 2006; Roe et al., 2009). Circumventing the complexities connected to the stratigraphic position of terrestrial records for the Holsteinian interglacial, a land-sea correlation off Iberia (Fig. 2.1; Desprat et al., 2005) has provided the opportunity to directly compare the marine isotope record to terrestrial vegetation changes. These data support a correlation of the Holsteinian interglacial to MIS 11c. Given the significance of this direct land-sea correlation, we propose to place the Holsteinian interglacial forest development in central Europe into the chronological frame of MIS 11c (i.e., 423-395 ka BP) as proposed by SPECMAP (Fig. 2.5C; Imbrie et al., 1984).

Data from Antarctic ice cores indicate that peak warmth occurred towards the end of MIS 11c in contrast to more recent interglacials, including MIS 9, for which early peak warmth and continuous cooling are typical (Fig. 2.5D; EPICA, 2004; Jouzel et al., 2007). As already discussed in Section 2.4.1, the Holsteinian vegetation succession indicates peak warmth during the younger part of the interglacial, which is in agreement with the warming trend of MIS 11c rather than MIS 9.

Based on annually laminated sediment records from the Lüneburger Heide region (northern Germany), the Holsteinian interglacial forests in central Europe lasted for ~15-16 ka (Meyer, 1974; Müller, 1974), which is similar to the duration of the Holsteinian climatic optimum at Lake Ossówka (Poland)(Nitychoruk et al., 2005). However, the duration of MIS 11c has been estimated to be roughly twice as long, i.e., ~28 ka (Imbrie et al., 1984). If the spread of Holsteinian forests started with the onset of MIS 11c, the end of the terrestrial interglacial would have been at ~408 ka BP. Such a scenario would, however, be inconsistent with the summer insolation maximum in the northern hemisphere (65º N; Berger and Loutre, 1991) and the climatic optimum of MIS 11c in the North Atlantic, which is centred between 416 and 398 ka BP (de Abreu et al., 2005; Kandiano and Bauch, 2007; Helmke et al., 2008). It therefore seems that in contrast to southern Europe, where Holsteinian forests spread soon after Termination V as documented off Iberia (Desprat et al., 2005), Holsteinian forests in central Europe expanded later, i.e., in the second half of MIS 11c, after 415 ka BP (Fig. 2.5).
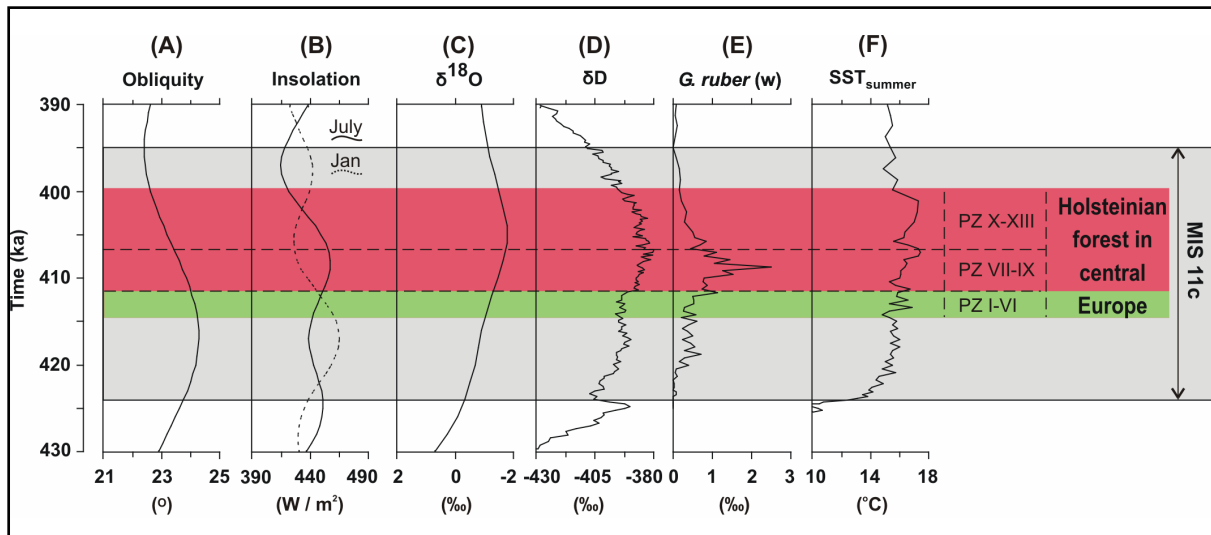
Figure 2.5: *Orbital parameters and climate proxy records plotted against time (ka) for MIS 11. (A) Obliquity and (B) Insolation at 65ºN (Berger and Loutre, 1991); (C) SPECMAP curve (Imbrie et al., 1984) as proxy for global ice volume; (D) Deuterium (δD) composition of ice from EPICA Dome C (Jouzel et al., 2007) as temperature proxy; (E) relative abundance of* G. ruber (w) *and (F) planktic foraminiferal-derived summer SST at Site M23414 (Fig. 1) in the North Atlantic (Kandiano and Bauch, 2007) plotted after the age model of Helmke et al. (2008). Grey area corresponds to MIS 11c according to SPECMAP (Imbrie et al., 1984). Green and red bars mark the suggested intervals of Holsteinian boreal and temperate forests, respectively, in central Europe (see Section 2.4.3 for details); pollen zones have been adopted from the Holsteinian pollen stratigraphy.*

In the following, we attempt to justify this scenario considering that the Atlantic heat transport is a key driving mechanism for European climate (e.g., Broecker, 1997; von Grafenstein et al., 1999). The pioneer boreal forests in central Europe have most probably expanded in response to the strengthening of the oceanic heat transport to the North Atlantic after 415 ka BP (Dickson et al., 2009). This forest phase prevailed for c. 3000 – 4000 ka (PZ I-VI; Meyer, 1974) before it was replaced by a temperate forest (PZ VII – XIII). The prevalence of temperate forests (PZ VII to XIII; Fig. 2.5) was most likely associated with the peak

expansion of warm surface-water advection into the polar North Atlantic notably in the younger stages of MIS 11c (Bauch et al., 2000; Helmke and Bauch, 2003). The mesocratic forest phase (PZ VII to IX) is most probably related to the warming in the North Atlantic between ~411 and 407 ka as inferred by the relative abundance peak of *Globigerinoides ruber* (w) at Site M23414 (Fig. 2.5E; Kandiano and Bauch, 2007; Helmke et al., 2008). Hence, this forest phase coincides with the summer insolation maximum (Fig. 2.5B; Berger and Loutre, 1991), low global ice volume (Fig. 2.5C; Imbrie et al., 1984), and highest temperatures in Antarctica during MIS 11c (Fig. 2.5D; Jouzel et al., 2007). As already mentioned in Section 2.4.1, the oligocratic forest phase (PZ X – XIII) reflects peak warming during the younger Holsteinian. If correct, the maximum expansion of the summer-warmth-requiring trees during this interval, such as *Quercus* and *Buxus* (Fig. 2.3), was related to the continuously increasing summer sea surface temperature (SST) in the North Atlantic (Fig. 2.5F; Kandiano and Bauch, 2007; Helmke et al., 2008). In addition, the maximum expansion of evergreen trees (Fig. 2.4), such as *Buxus* and *Ilex*, was favoured by the decreasing seasonality as inferred by the decline in summer insolation and the increase in winter insolation during that time (Fig. 2.5B; Berger and Loutre, 1991). The decline of the Holsteinian forest (upper PZ XII – XIII) in central Europe should hence be placed after ~401 ka BP when the North Atlantic summer SST declined (Fig. 2.5F; Kandiano and Bauch, 2007; Helmke et al., 2008); the telocratic phase (PZ XIV) should coincide with the summer insolation minimum at ~397 ka BP (Fig. 2.5B) that also terminated the interglacial vegetation successions in Praclaux, France and Tenaghi Philippon, Greece (Müller and Pross, 2007).

2.5 Conclusions

A new high-resolution palynological record from Dethlingen, northern Germany, provides evidence for climatic variability during the Holsteinian interglacial. Our data suggest decreasing seasonality and increasing warmth and precipitation towards the younger stages of the interglacial. The nature and tempo of this climatic change supports a correlation of the Holsteinian interglacial with MIS 11c, as the latter, in contrast to MIS 9, shows peak warmth at the end of the warm period. Considering that the Atlantic heat transport strongly influences vegetation development in central Europe, it is conceivable that the 15-ka-long period of Holsteinian forest development in central Europe is coeval with the second half of MIS 11c.

The temperate stage of the Holsteinian interglacial was interrupted by two short (c. 300 years long) regressive phases of vegetation development characterised by boreal and sub-temperate forests. The decline in temperate taxa and the expansion of pioneer trees during these phases, along with the observation that these phases occur supraregionally across central and northwestern Europe, suggest climatic forcing as the underlying mechanism. With regard to the pollen signatures of the two phases, it seems plausible that they were caused by different triggering mechanisms. For the older phase, a slowdown of the North Atlantic circulation and/or decreasing solar activity are the most likely driving forces.

Our results underscore the need to elucidate the causes of the two vegetation regressive phases in order to better understand the effect of potentially analogous abrupt events during

the present interglacial. The high-resolution Dethlingen pollen record provides a significant contribution in this direction; its interpretation will be further refined through future investigations of additional high-resolution, multi-proxy data and the development of a varve chronology with annual time resolution.

2.6 Acknowledgements

Chapter 3. Sub-decadal- to decadal-scale climate cyclicity during the Holsteinian interglacial (MIS 11) evidenced in annually laminated sediments

Andreas Koutsodendris[1], Achim Brauer[2], Heiko Pälike[3], Jörg Pross[1], Ulrich C. Müller[1], André F. Lotter[4]

[1] Paleoenvironmental Dynamics Group, Institute of Geosciences, Goethe University Frankfurt, Altenhöferallee 1, D-60438 Frankfurt, Germany; [2] German Research Centre for Geosciences, Section 5.2 Climate Dynamics and Landscape Evolution, Telegrafenberg, D-14473 Potsdam, Germany; [3] National Oceanography Centre, Southampton, University of Southampton, Waterfront Campus, European Way, SO14 3ZH Southampton, United Kingdom; [4] Institute of Environmental Biology, Palaeoecology, Laboratory of Palaeobotany and Palynology, Utrecht University, Budapestlaan 4, 3584 CD Utrecht, The Netherlands

Abstract: To unravel the short-term climate variability during Marine Isotope Stage (MIS) 11, which represents a close analogue to the Holocene with regard to orbital boundary conditions, we performed microfacies and time series analyses on a ~3200-year-long window from annually laminated Holsteinian lake sediments from Dethlingen, northern Germany. These biogenic varves comprise two sub-layers: A light layer, which is controlled by spring/summer diatom blooms, and a dark layer consisting mainly of amorphous organic matter and fragmented diatom frustules deposited during autumn/winter. Time series analyses were performed on the thickness of the light and dark layers. Signals exceeding the 95 % and 99 % confidence levels occur at periods that are near-identical to those known from modern instrumental data and Holocene palaeoclimatic records. Spectral peaks at periods of 90, 25, and 10.5 years are likely associated with the 88-, 22- and 11-year solar cycles, respectively. This variability is mainly expressed in the light layer spectra, suggesting solar influence on the palaeoproductivity of the lake. Significant signals at periods between 3 and 5 years and at ~6 years are strongest expressed in the dark layer spectra and may reflect an influence of the El Niño-Southern Oscillation (ENSO) and the North Atlantic Oscillation (NAO) during autumn/winter. Our results suggest that solar forcing and ENSO/NAO-like variability influenced central European climate during MIS 11 similar to the present interglacial, thus demonstrating the comparability of the two interglacial periods at sub-decadal to decadal timescales.

Keywords: Marine Isotope Stage 11; Holsteinian interglacial; biogenic varves; ENSO; NAO; solar cycles.

3.1 Introduction

An understanding of the mechanisms and effects of natural short-term (i.e., decadal- to sub-decadal-scale) climate variability is essential for providing projections of possible climate change for the near future. Short-term climate changes are linked to shifts in the modes of variability of the climate system (e.g., the southern and northern annular modes; Stenseth et al., 2003); therefore, a better representation of such climate-mode shifts in climate models may improve simulations of abrupt climate changes (Alley et al., 2003). Although the instrumental record is becoming more valuable as it is lengthened, it is still insufficient to cover the full range of climatic behavior. Specifically, instrumental datasets do not reach beyond the past ~300 years (Jones and Mann, 2004), which precludes deeper insights into the underlying physical processes and the evolution of decadal- to sub-decadal-scale climate variability on longer (e.g., interglacial) timescales. In this context, high-resolution palaeoclimate records, particularly from past interglacials that unlike the Holocene were unaffected by human interference, can make an important contribution towards elucidating natural short-term climate variability and its future evolution during the present interglacial (e.g., Alley et al., 2003; Brauer et al., 2007a; Müller and Pross, 2007; Tzedakis et al., 2009).

Marine Isotope Stage (MIS) 11 is considered one of the best analogues for present and future climate based on long-term similarities with regard to orbital climate forcing, i.e., low eccentricity and dampened influence of precession (e.g., Berger and Loutre, 2002; Loutre and Berger, 2003; Ruddiman, 2005). A number of proxy datasets have provided insights into the long-term comparability between MIS 11 and the present interglacial (e.g., de Abreu et al., 2003; McManus et al., 2003; Helmke et al., 2008; Rohling et al., 2010; Tzedakis, 2010), but owing to a lack of data with sufficiently high temporal resolution the short-term comparability between the two interglacials has remained ambiguous.

In contrast to most marine records from MIS 11, which typically exhibit relatively low sedimentation rates, varved sequences from lake sediments yield the potential to test whether MIS 11 and MIS 1 exhibit comparable decadal to sub-decadal climate variability. The terrestrial analogue to MIS 11 in central Europe has long been a matter of heated debate (e.g., de Beaulieu et al., 2001; Geyh and Müller, 2005; see also Koutsodendris et al., 2010, for a discussion); however, based on evidence from long terrestrial and marine vegetation records from the Massif Central (France; Reille et al., 2000) and off Iberia (Desprat et al., 2005) there is now a substantial body of research that indicates a land-sea correlation of MIS 11c with the Holsteinian interglacial (e.g., de Beaulieu et al., 2001; Kukla, 2003; Nitychoruk et al., 2005, 2006; Müller and Pross, 2007; Preece et al., 2007).

The variations in the composition and thickness of varves reflect sedimentation processes that are controlled by various climatic and environmental factors at different times of the year (e.g., O'Sullivan, 1983; Lotter, 1989; Anderson, 1992; Lotter and Birks, 1997; Brauer et al., 1999b; Brauer, 2004). Deeper insights into these processes have been gained through the time series analysis of varve thickness datasets; such efforts have successfully linked cyclical patterns in lake sediments with short-term natural periodic climate forcing (e.g., Anderson and Koopmans, 1963; Anderson, 1992; Zolitschka, 1992; Vos et al., 1997;

Rittenour et al., 2000; Livingstone and Hajdas, 2001). To date, although several well-preserved Holsteinian varved archives are known (e.g., Turner, 1970; Müller, 1974; Krupiński, 1995; Nitychoruk et al., 2005), the potential of using varves to better understand the decadal- to sub-decadal-scale climate variability during MIS 11 has been poorly explored (Mangili et al., 2005, 2007; Brauer et al., 2008a).

In light of the above, we here analyze a ~3200-year-long Holsteinian varve succession from the Dethlingen palaeolake, northern Germany. In particular, we have performed (i) a detailed microfacies analysis to understand the season-dependent sedimentological processes controlling varve deposition, and (ii) time series analyses on the varve sub-layer thickness in order to investigate the short-term climate cyclicity during MIS 11 and to compare it with instrumental data and palaeoclimatic records of the Holocene.

3.2 Material and methods

The Dethlingen palaeolake is located in the Lüneburger Heide region within the lowlands of northern Germany (Fig. 3.1). After the disintegration of the Elsterian (MIS 12) ice sheet, several deep lakes formed in the vicinity of Dethlingen that were subject to the deposition of diatomaceous, partially annually laminated sediments during the following Holsteinian interglacial (e.g., Benda and Brandes, 1974; Ehlers et al., 1984; Koutsodendris et al., 2010). Based on the spatial extent and thickness of the Holsteinian diatomite, the size of the Dethlingen palaeolake is estimated to ~800 m in length and 300-500 m in width (Benda et al., 1984). The deposits cored at Dethlingen (10°08.367′ E, 52°57.780′ N, 65 m a.s.l.) that has yielded the material for this study comprises organic-rich, predominantly regularly and finely laminated lake sediments (Koutsodendris et al., 2010). Here we focus on the interval between 27.93 and 33.68 meters below surface (mbs) that comprises annual laminations spanning the mesocratic forest phase of the Holsteinian interglacial in central Europe (~411-408 ka BP), including a prominent centennial-scale climate perturbation, the so-called "Older Holsteinian Oscillation" (OHO; Koutsodendris et al., 2010, subm.).

Varve counting and layer-thickness measurements were carried out at 100x magnification on thin sections (size: 120 x 35 mm) using a petrographic microscope. Thin-section preparation followed standard techniques comprising freeze-drying, impregnation with Araldite 2020 epoxy resin under vacuum, sawing, and grinding of the sediment (Brauer et al., 1999a; Lotter and Lemcke, 1999). To warrant continuity of observation, successive thin sections with an overlap of 2 cm were analyzed.

Geochemical measurements were undertaken with a micro-X-ray fluorescence (μ-XRF) spectrometer EAGLE III XL at different resolutions (step sizes: 50, 100, 200, 500 μm) for Al, Ca, Cl, Fe, K, Mg, Mn, P, S, Si, Sr, and Ti (60 s count time, 0 kV X-ray voltage and 400 μA X-ray current). Measurements were carried out on sediment blocks that had been impregnated with Araldite 2020 epoxy resin.
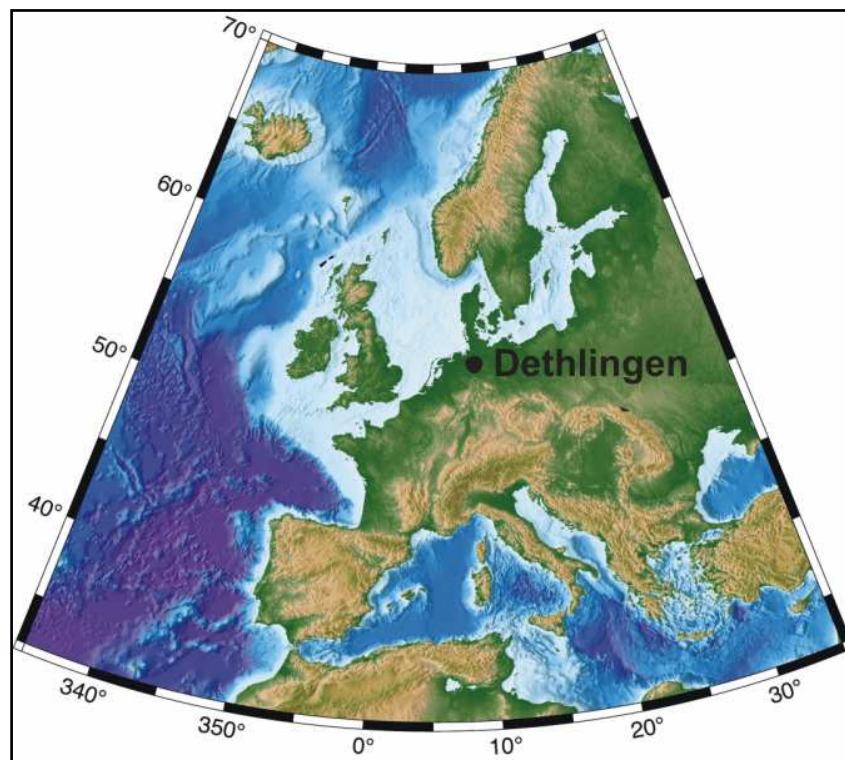
Figure 3.1: *Map indicating the location of the Dethlingen palaeolake.*

Time series analyses were carried out on the thickness measurements of the light and dark layers. Multi-taper spectral analysis (MTM) was used for spectral estimation (bandwidth parameter p=5, and 9 tapers) (e.g., Vautard et al., 1992). The MTM represents an optimal method for producing spectral estimates with high frequency resolution for given degrees of freedom, low bias and a distribution amenable to the location of confidence levels (Mann and Lees, 1996). In addition, wavelet analysis was applied to identify occurrence intervals and related amplitudes of periodic components of the non-stationary sub-layer thickness time series (Torrence and Compo, 1998).

3.3 Results and discussion

3.3.1 Structure of varves and depositional processes

The finely laminated sediments from Dethlingen comprise biogenic varves consisting of two discrete layers, a light and a dark one. The transition from the light layers to the overlaying dark layers is diffuse, whereas the boundary between the dark and the following light layer is sharp (Fig. 3.2A-C).

The composition and thickness of the light layers are predominantly controlled by the annual cycle of diatom blooms, which is dominated by taxa of the genera *Stephanodiscus*, *Ulnaria*, and *Aulacoseira*. In most cases, the light layers are dominated by one of these genera, resulting in an almost monospecific diatomaceous layer. However, a successive deposition of two sub-layers of different genera during the growing season can be also observed. The

47

light layers often contain organic matter that increases in abundance towards the boundary with the dark layers. Small-sized (<10 µm) pyrite framboids are often present (Fig. 3.2D) and occasionally few angular-shaped grains, ranging in size from coarse silt to fine sand, are scattered within the light layers (Fig. 3.2E).

The dark layers are composed predominantly of amorphous organic matter with fragments of diatom frustules. Reworked periphytic diatoms, plant remains, freshwater sponge spicules from the littoral zone, and chrysophycean cysts are common (Figs. 3.2F, 3.3A-B). The dark layers often contain low concentrations of clay particles, in contrast to the light layers where fine-grained minerogenic particles are almost absent.
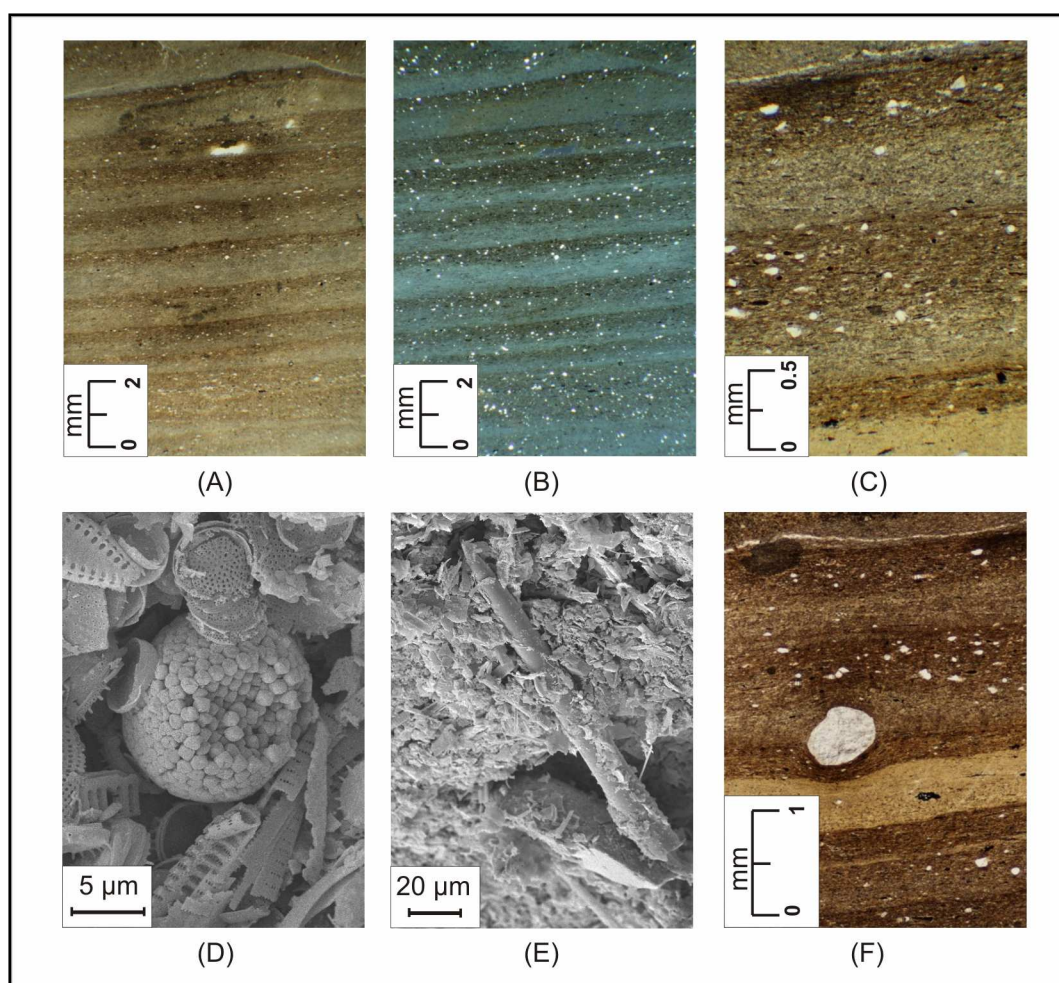
Figure 3.2: *Thin-section and scanning electron microscope photographs of varves from the Dethlingen core: Light and dark layers (A) under parallel-polarized light and (B) under cross-polarized light; (C) diffuse and sharp boundaries between successive dark and light layers; (D) pyrite framboids; (E) sponge spicule; (F) wind-transported fine sand grain.*

The succession and characteristics of the individual varve layers as described above suggest that the diatomaceous light layers were deposited during spring and summer, whereas the organic-detrital dark layers were formed during autumn and winter (e.g., O'Sullivan, 1983; Lotter, 1989; Brauer, 2004). In particular, water circulation and high nutrient availability in

spring and summer promote diatom blooms that lead to the deposition of diatoms frustules at the lake bottom, forming the light layers. Stratification of the water column in summer leads to anoxic bottom lake conditions facilitating the preservation of varves (e.g., O'Sullivan, 1983; Brauer, 2004). The deposition of detritus diatom frustules, organic matter and other material from the littoral zone of the lake suggests the re-establishment of the lake circulation during the deposition of the dark layers. The mixing of the water column can be attributed predominantly to an enhancement of wind and wave activity during autumn and early winter; in addition, the low content of clay particles in the dark layers points to minor runoff from the catchment area into the lake during that time. The sharp boundary between the dark and succeeding light layer suggests a transient break in sediment accumulation, which may be attributed to an ice-cover of the lake during winter; during that time, single wind-transported coarse silt and sand grains were trapped in the ice, being deposited within the lake sediments after ice melting in spring. These dropstone-like sand grains additionally confirm the seasonal interpretation of the sub-layers. The above-mentioned characteristics suggest that the Dethlingen palaeolake was dimictic, being ice-covered and stratified during parts of the year, and experiencing periods of mixing between these two states (e.g., Lewis, 1983).
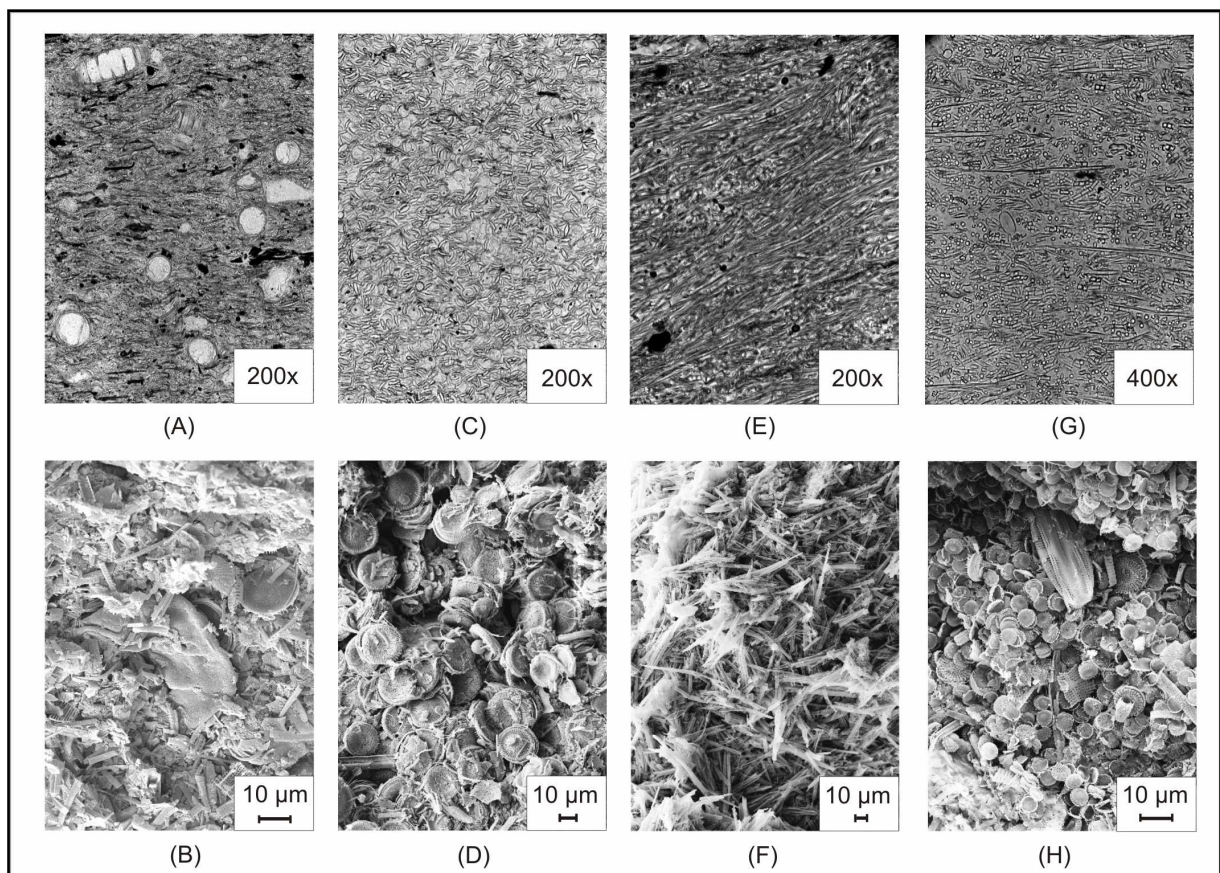
Figure 3.3: Thin-section and scanning electron microscope photographs from different varve layers from Dethlingen: (A, B) dark layer; light layers: (C, D) type A; (E, F) type B; (G, H) type C.

3.3.2 Varve counting and thickness measurements

In total, 2864 varves were counted between 27.93 and 33.68 mbs. For small-scale core intervals where varve preservation was poor or sediment had been disturbed during coring or laboratory processing, interpolations were performed based on the average thickness of 20 varves deposited directly below and above the respective interval. Based on these procedures, the floating chronology for the laminated diatomite at Dethlingen was calculated to comprise 3255 varve years (Koutsodendris et al., subm.).

The average varve thickness is 1.74 mm (Fig. 3.4). The thickness of the light layers varies between 0.05 and 5 mm (average: 0.68 mm), whereas the thickness of the dark layers varies between 0.08 and 5 mm (average: 1.06 mm) (Fig. 3.4). A qualitative distribution of different types of light layers in the examined core interval was established based on the dominant diatom genera observed in the thin sections; Type-A is dominated by diatoms of the genera *Stephanodiscus* with a size >10µm (Figs. 3.3C, D), type-B is dominated by elongated diatoms of the genus *Ulnaria* (Figs. 3.3E, F), and type-C mainly comprises small-sized diatoms (<10µm) of the genera *Aulacoseira* and *Stephanodiscus* (Figs. 3.3G, H). In general, representatives of type-A are thicker (average: 0.87 mm) than those of type-C (0.54 mm) and type-B (0.52 mm), respectively (Fig. 3.4). The distribution of these light layer types within the studied core interval documents a clear succession in diatom assemblages (Fig. 3.4). The light layers from the lower interval of the laminated diatomite (33.68-31.22 mbs) are dominated by large *Stephanodiscus* species (type-A) succeeded by *Ulnaria* species (type-B) in the middle part (31.22-30.20 mbs), whereas the upper laminated interval (30.20-27.93 mbs) is characterised by a prevalence of small *Stephanodiscus* and *Aulacoseira* species (type-C).
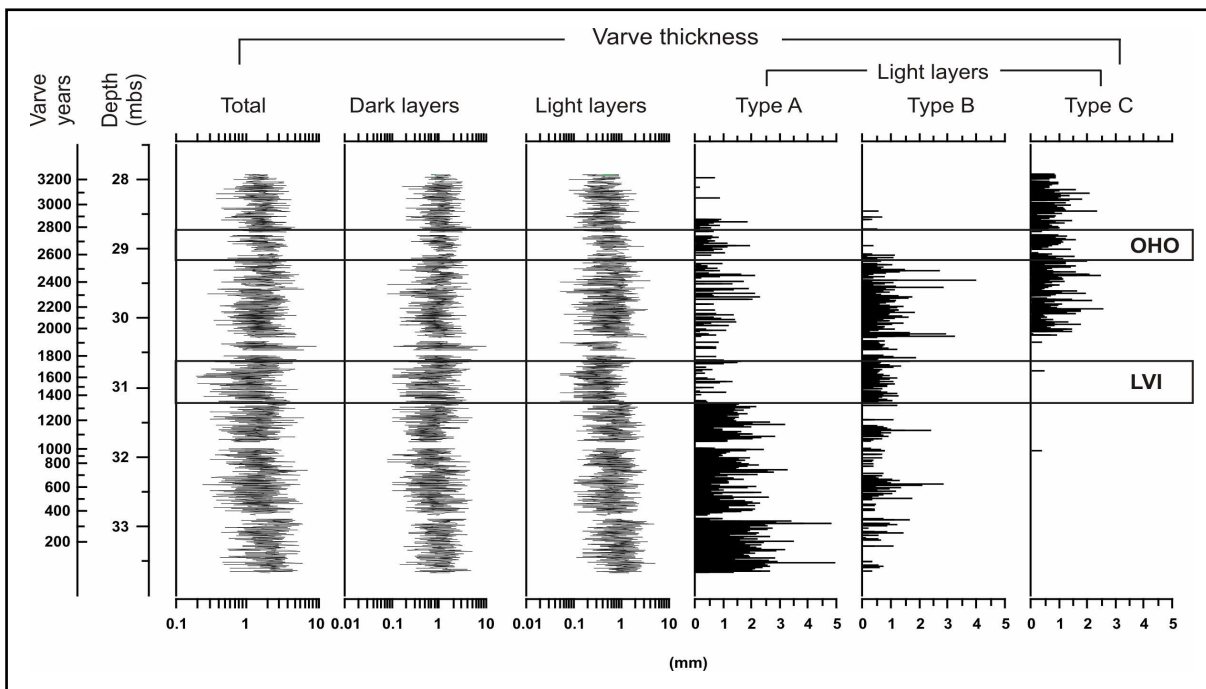
Figure 3.4: *Varve thickness measurements of dark layers and different types of light layers. Positions of the Older Holsteinian Oscillation (OHO) and the Low Variability Interval (LVI) are indicated (see Section 3.3.4).*

3.3.3 Time series analyses

The power spectra of the datasets for the light and dark layers exhibit several peaks that exceed the 95 % and 99 % confidence levels (Fig. 3.5). Significant peaks occur at decadal-scale periods of 90, 25, 15, and 10.5 years, but also at sub-decadal-scale periods of 5.8-6.1, 3-5 and 2-3 years. In addition, the wavelet spectra show a prominent cycle at ~512 years for both the light and dark layers (Fig. 3.6). In the following, we compare these signals to solar cycles and spatio-temporal modes of global climate variability, such as the El Niño-Southern Oscillation (ENSO), the North Atlantic Oscillation (NAO) and the Quasi-Biennial Oscillation (QBO), which are well known from analyses of modern instrumental climate data and the Holocene palaeoclimatic record (e.g., Stuiver and Braziunas, 1993; Hoyt and Schatten, 1997; Mann and Park, 1996; Wanner at al., 2001).

3.3.3.1 Solar-cyclicity-like variability

Four peaks from the Dethlingen varve time series spectra can be correlated to known solar cycles (Fig. 3.5; Table 3.1). The most prominent, at 90 years, can be attributed to the 88-year Gleissberg solar cycle (e.g., Gleissberg, 1944; Stuiver and Braziunas, 1993; Hoyt and Schatten, 1997) that has previously been recorded in several glacial (Anderson and Koopmans, 1963; Vos et al., 1997; Prasad et al., 2004) and interglacial varve time series (Anderson and Koopmans, 1963; Vos et al., 1997; Dean et al., 2002; Brauer et al., 2008a). The 25- and 10.5-year peaks from Dethlingen may correlate to the 22-year Hale and 11-year Schwabe solar cycles, respectively (e.g., Hoyt and Schatten, 1997) that have also been widely found in Quaternary varve time series of glacial (Anderson, 1961; Anderson and Koopmans, 1963; Vos et al., 1997; Rittenour et al., 2000) and interglacial origin (Anderson, 1961; Anderson and Koopmans, 1963; Anderson, 1992; Zolitschka, 1992; Vos et al., 1997; Livingstone and Hajdas, 2001; Dean et al., 2002; Theissen et al., 2008). The statistically significant expression of all three prominent decadal-scale solar cycles makes the Dethlingen varve record unique because most known varve records only contain evidence for one or two of these cycles, probably because of insufficient sensitivity of each individual lake's sedimentological properties to record the solar magnetic modulation (e.g., Solanki, 2004; Muscheler et al., 2005) over certain time periods (e.g., Anderson, 1992).

In addition to these cycles, our record provides evidence for a centennial-scale cycle at ~512 years, which has been rarely detected in varve time series (Prasad et al., 2004; Brauer et al., 2008a). To date, its origin remains unclear; it is considered to be related to either solar forcing (Stuiver et al., 1995; Sarnthein et al., 2003) or changes in the North Atlantic thermohaline circulation (Stuiver and Braziunas, 1993; Chapman and Shackleton, 2000; Damon and Peristykh, 2000; Risebrobakken et al., 2003).

Because the solar-like cycles are evidenced in both light and dark layer spectra, we argue that solar forcing has influenced the lake sedimentation throughout the year. The light layers at Dethlingen, which represent the primary lake productivity (see Section 3.3.1), are characterized by peaks of all three decadal-scale solar cycles (i.e., Gleissberg, Hale and Schwabe cycles) at the 99 % confidence level (Fig. 3.5). This suggests a significant solar

influence on the biological productivity of the lake, most likely by affecting water mixing intensity, temperature, and light and UV radiation that exert a strong control on algal productivity (e.g., Bothwell et al., 1994; Beer et al., 2000; Graham and Wilcox, 2000). The occurrence of solar-like cyclicity in the dark layers, particularly the Gleissberg cycle (Fig. 3.5), points to solar influence on lake circulation during autumn and winter, most likely through atmospheric circulation changes that modulated wind and wave activity (see Section 3.3.1). Possible links between solar irradiance and atmospheric circulation have been attributed to the solar influence on stratospheric temperature that may modify zonal winds and storm tracks (e.g., Haigh, 1996; Carslaw et al., 2002).

Summarizing the above, the time series analysis of the Dethlingen varve record suggests a strong impact of solar cycles on the processes responsible for the seasonal sedimentation by influencing the lake's primary productivity and the atmospheric circulation over the study area.

3.3.3.2 Variability within the ENSO/NAO band

The Dethlingen varve record reveals significant variability at sub-decadal time scales, with signals exceeding the 95 % or 99 % confidence levels grouped into three distinct bands, i.e., 2-2.7 years, 3-5 years, and 5.8-6.1 years (Fig. 3.5; Table 3.1). Most of the significant peaks are recorded in the range of 3 to 5 years within the conventional ENSO bandwidth (Mann and Park, 1994; D'Arrigo et al., 2005). Variability within the ENSO bandwidth has been reported in lateglacial to recent varve sequences from North and South America (Rittenour et al., 2000; Nederbragt and Thurow, 2005; Fagel et al., 2008), but to date has not been clearly witnessed in varves from Europe. The ENSO is a natural mode of oscillation that results from unstable interactions between the tropical Pacific Ocean and the atmosphere, affecting weather and climate worldwide (e.g., Fedorov and Philander, 2000). A teleconnection between the Pacific region and Europe via the stratosphere allows ENSO to influence European climate in late winter and spring (e.g., Brönnimann, 2007; Brönnimann et al., 2007; Ineson and Scaife, 2009). The signal in European climate comprises two modes: during El Niño conditions, when a reduction of coastal upwelling and an increase in sea-surface temperature along the western coast of tropical South America is observed in the equatorial Pacific, the European continent witnesses very low temperatures in NE Europe, increased precipitation in the northern Mediterranean region and decreased precipitation in Norway; reversed conditions are observed in Europe during La Niña conditions, which comprise the opposite mode of El Niño in the equatorial Pacific (e.g., Brönnimann, 2007). The cyclicity observed at Dethlingen is in agreement with modern weather observations from Europe that suggest an ENSO influence on climate every 3.5 years (Rodó et al., 1997). The ENSO-like variability is stronger expressed in the spectrum of the dark layers, pointing to a pronounced ENSO impact on winter atmospheric circulation during the Holsteinian interglacial (Fig. 3.5).
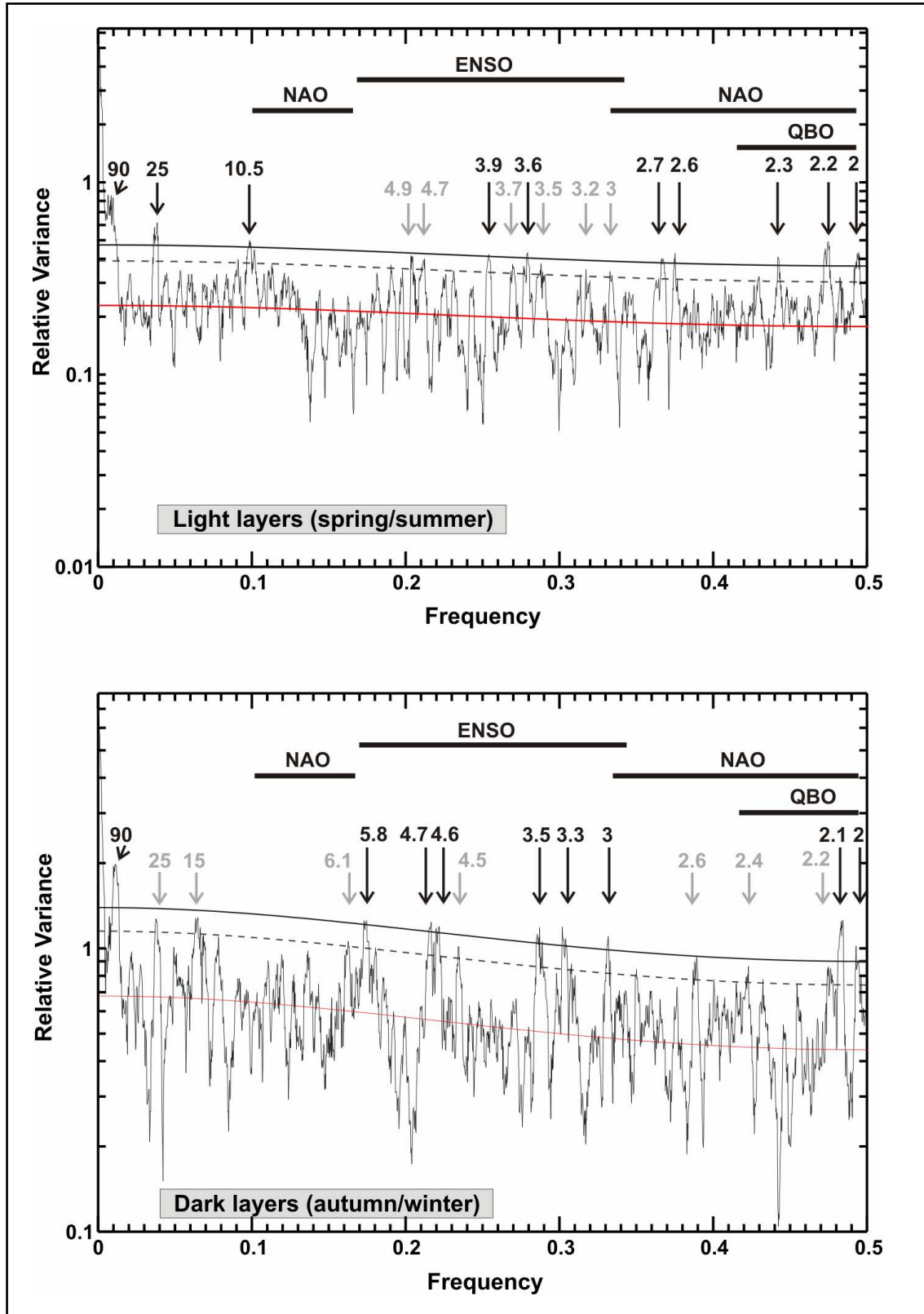
Figure 3.5: *Power spectra of the light and dark layers thickness measurements. The red line indicates the median red noise; the dashed and solid black lines indicate the 95 % and 99 % confidence levels, respectively. El Niño-Southern Oscillation (ENSO), North Atlantic Oscillation (NAO), and Quasi-Biennial Oscillation (QBO) bandwidths are after Mann and Park (1996).*

The Dethlingen varve time series further shows significant variability at the margins of the ENSO bandwidth between 5.8 and 6.1 and between 2.4 and 2.6 years (Fig. 3.5). Although this variability may again represent an ENSO impact on varve formation, modern observational data suggest that these signals are better attributed to the NAO. The NAO, which represents a hemispheric meridional oscillation in atmospheric masses centered near Iceland and the subtropical Atlantic, affects European climate particularly in boreal winter from December through March (e.g., Hurrell, 1995; Visbeck et al., 2001; Wanner et al., 2001). The NAO is characterized by a positive mode related to warmer and wetter than average conditions in north Europe and colder and drier conditions in the Mediterranean region, and a negative mode with reversed characteristics. The NAO variability occurs at bandwidths of 2.5-3 and 6-10 years (e.g., Hurrell and van Loon, 1997; Appenzeller et al., 1998; Pozo-Vásquez et al., 2000). Varve time series from central and western Europe have also reported significant peaks at 6.1-6.2 years during the Holocene (Livingstone and Hajdas, 2001; O'Sullivan et al., 2002), whereas a similar period at 6.6 years has been recorded on oxygen isotope variations of calcite varves from the southern Alps during MIS 11 (Mangili et al., 2010). It therefore seems that the ~6 year signal documented in European varve sequences represents NAO-like variability rather than ENSO-like variability because the latter is generally more pronounced in the 3-5 years bandwidth (Mann and Park, 1994). Further evidence for a NAO-like variability in the Holsteinian record from Dethlingen is provided by the fact that the ~6 year signal is only evident in the spectrum from the dark layers. It therefore reflects sedimentation processes during autumn/winter, which is in good agreement with the present-day seasonal impact of the NAO on European climate (e.g., Hurrell, 1995; Visbeck et al., 2001; Wanner et al., 2001). The variability between 2 and 2.7 years may be attributed to either the NAO or the QBO (Mann and Park, 1996). The QBO is one of the most commonly recorded circulation patterns in modern data, comprising a variability of the equatorial stratosphere expressed by an alternation in the downward propagation of easterly and westerly wind regimes (e.g., Baldwin et al., 2001). Although such periodicities commonly occur in varved sequences, these signals should be interpreted with caution because of their proximity to the 2-year Nyquist frequency of annual sampling (e.g., Weedon, 2003).

Finally, the spectrum for the dark layers exhibits a periodicity of 15 years exceeding the 95 % confidence level (Fig. 3.5). Such a periodicity has been previously noticed in central Europe during the Holocene and MIS 11, although its forcing has remained unclear (Livingstone and Hajdas, 2001; Mangili et al., 2010). We suggest that this 15-year cyclicity may be related to the interdecadal ENSO variability at 15-18 years (Mann and Park, 1994). This interpretation is further corroborated by modern observations from Iberia that demonstrate the existence of an amplified ENSO signal at 14.2 years, i.e., after every four ENSO events (Rodó et al., 1997).

To summarize, the Dethlingen varve time series indicates significant sub-decadal climate variability in European climate during MIS 11, which may be attributed to ENSO- and NAO-like climate modes. The pronounced signals in the spectrum of the dark layers point to a

strong influence of the ENSO/NAO-like variability especially on winter climate, possibly through changes in atmospheric circulation that influenced lake mixing and the duration of ice cover.

Period (years)	Light layers spectra	Dark layers spectra	Forcing
512	95 %	95 %	Solar or ocean circulation
90	99%	99%	Solar (88-year Gleissberg cycle)
25	99%	95%	Solar (22-year Hale cycle)
15	-	95%	ENSO
10.5	99%	-	Solar (11-year Schwabe cycle)
5.8 - 6.1	-	99%	NAO
3 - 5	mainly 95 %	mainly 99 %	ENSO
2 - 2.7	99%	mainly 95 %	NAO / (QBO)

Table 3.1: *Summary of significant spectral peaks of light and dark layer time series of the Dethlingen varves and their possible forcing mechanisms.*

3.3.4 Variability of varve thickness through time

The sub-decadal- and decadal-scale cyclicity as described in Sections 3.3.3.1 and 3.3.3.2 is evidenced in most parts of the Dethlingen record (Fig. 3.6). However, a close inspection of the wavelet spectra for the light and dark layers reveals distinct intervals where this variability appears only in one of the two spectra or is discontinuous in both spectra.

An example for the first case is a 430-year-long interval between 1320 and 1750 varve years (Fig. 3.6). This interval, hereafter named low-variability interval (LVI), is marked by a strong sub-decadal and decadal cyclicity in the dark layer spectrum and a very weak cyclicity in the light layer spectrum. We therefore hypothesize that although the spectrum for the dark layers points to an external cyclical forcing influencing the Dethlingen palaeolake system, changes in the boundary conditions (e.g., nutrients, water level) during spring and summer precluded the recording of this forcing in the light layer spectrum. To test this hypothesis, we take a closer look at the varve microfacies during the LVI. The onset of the LVI coincides with a major change in the spring-blooming diatom assemblages accompanied by a thinning of the light layers (Fig. 3.4). In particular, the diatoms dominating the light layers change from *Stephanodiscus* (>10 µm) to *Ulnaria* species, the latter requiring a higher Si:P ratio and higher temperatures (e.g., Kilham et al., 1986; Cox, 1993). Therefore it appears likely that the compositional change in diatom assemblages during this interval is triggered by modifications in atmospheric circulation patterns. Specifically, atmospheric changes may have caused a weakening of the spring circulation, thereby decreasing the phosphorus transport from the hypolimnion to the photic zone to the benefit of diatoms that require high

Si:P ratio to grow and increasing surface-water temperature. As a result, the boundary conditions of the Dethlingen palaeolake were seasonally modified, precluding the light layers to record external forcing. The sedimentation processes became susceptible to the recording of external forcing again when the lake system returned to conditions that supported a stronger blooming of *Stephanodiscus* species (Fig. 3.4).
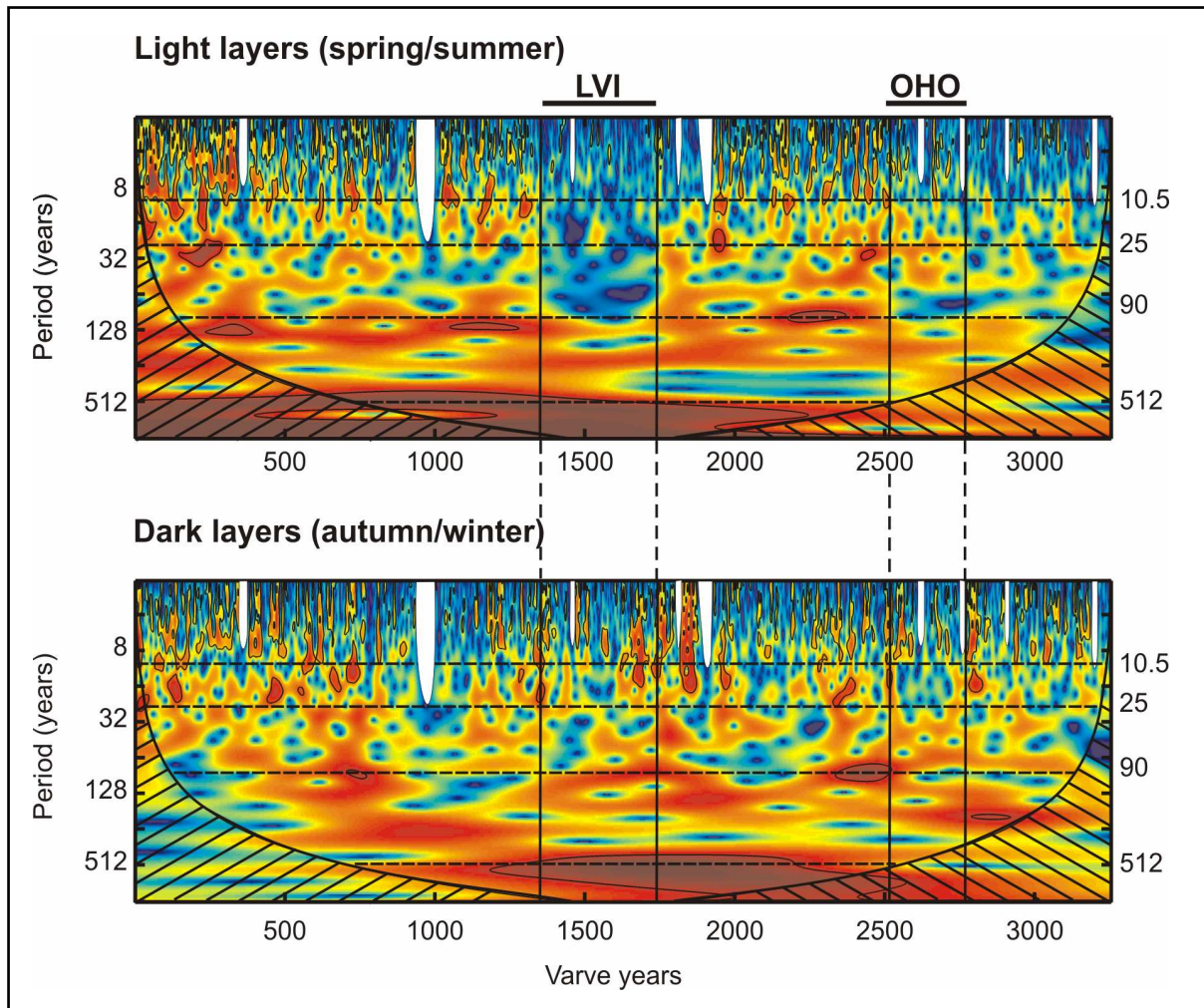
Figure 3.6: *Wavelet spectra of the light and dark layers thickness measurements. Wavelet amplitudes are colour coded from red (high power) to blue (low power). Contoured areas exceed the 95 % confidence levels for a red noise background spectrum. Hatched areas indicate the cone of influence where wavelet analysis is affected by edge effects. Dashed lines mark the solar-like periodicities. White cones indicate intervals with no varve-thickness data. Positions of the Older Holsteinian Oscillation (OHO) and the Low Variability Interval (LVI) are indicated (see Section 3.3.4).*

A good example of the second case, i.e., when the spectra of both the light and dark layers do not show variability, is the interval between 2564 and 2782 varve years (29.15 to 28.73 mbs; Fig. 3.7) that coincides with the prominent OHO event (e.g., Müller, 1974; Kukla, 2003; Koutsodendris et al., 2010). Across the OHO, the wavelet spectra of both the light and dark layers do not show any statistically significant indication for the 11-year Schwabe cycle; moreover, there is a strong weakening of the 22- and 88-year solar cycles (Fig. 3.7). In

addition, the ENSO/NAO-like sub-decadal variability almost ceases with the onset of the OHO and only recovers again after the end of the event (Fig. 3.7). Following a similar concept as for the LVI, the absence of short-term variability during the OHO may be explained by seasonal changes in the boundary conditions of the Dethlingen palaeolake.
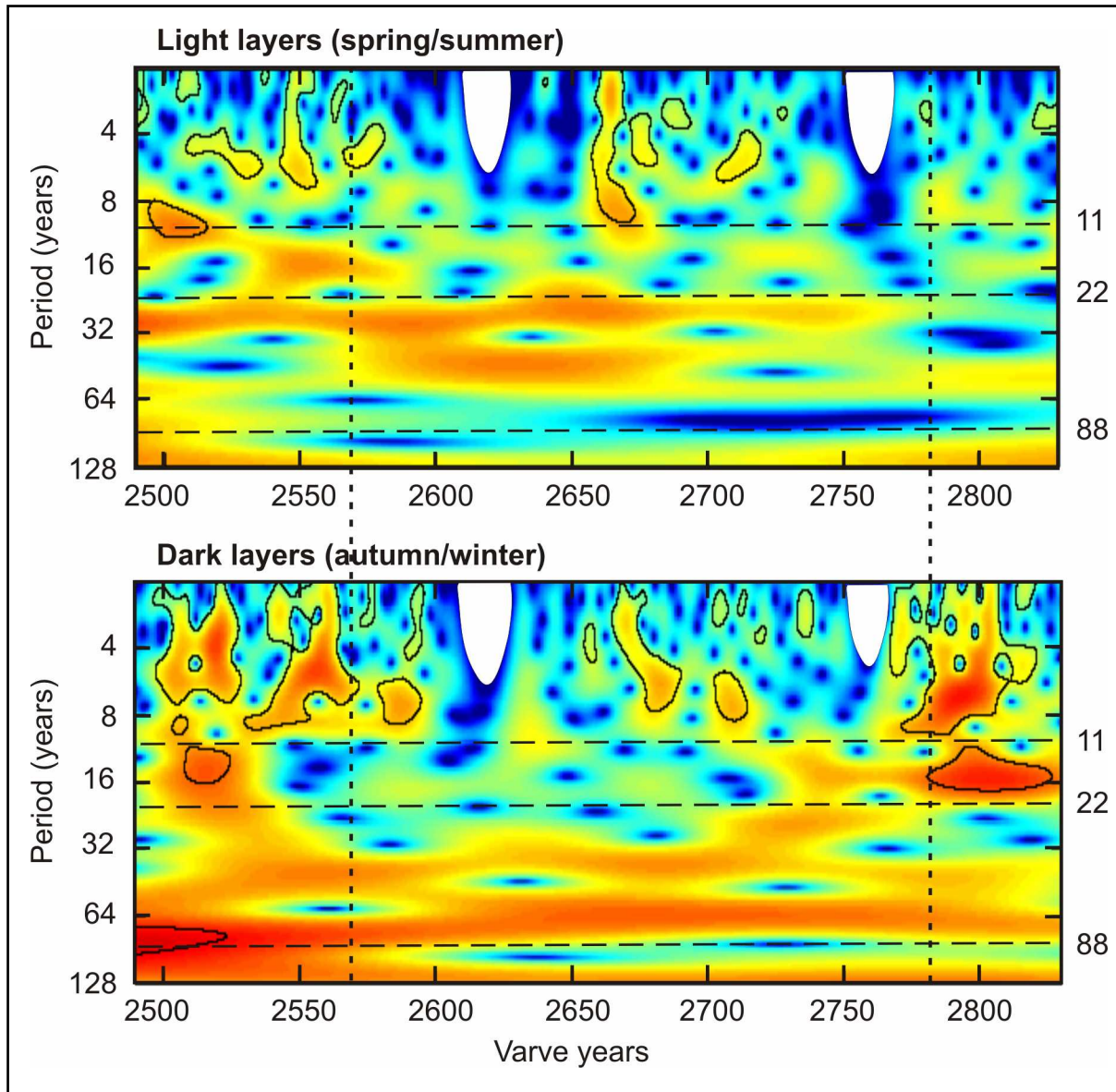
Figure 3.7: *Wavelet spectra of the light and dark layers thickness measurements spanning the OHO interval. Wavelet amplitudes are colour coded from red (high power) to blue (low power). Contoured areas exceed the 95 % confidence levels for a red noise background spectrum. Vertical dashed lines mark the boundaries of the OHO at 2565 and 2782 varve years. Horizontal dashed lines indicate the solar-like periodicities. White cones indicate intervals with no varve-thickness data.*

In particular, the composition of the light layers shifts from *Ulnaria*-dominated to *Stephanodiscus*-dominated layers with the onset of the OHO, suggesting changes in lake productivity (Fig. 3.4). However, the observations from thin sections do not support a scenario of seasonal changes in the dark layers. On top of that, µ-XRF data for the onset of

the OHO (29.16 to 29.05 mbs) do not yield evidence for modifications in the geochemical signal to support changes in the sedimentation processes during autumn/winter (Fig. 3.8). In particular, the intensities of minerogenic-detrital indicator elements (such as Al, Ca, K, Ti) and the Si/Al ratio remain rather constant, suggesting no significant change in terrestrial input. In addition, the constant Fe/Mn ratio does not support any oxygenation changes at the bottom of the lake. We therefore suggest that the absence of cyclical signals in the varves during the OHO points to a weakening of the external forcing. If correct, this implies that both the solar activity and ENSO/NAO-like variability were strongly weakened during this period. It has been suggested that the triggering mechanism of the OHO may be similar to the 8.2 ka BP event, with a cooling caused by a transient slowdown in North Atlantic circulation leading to a turnover in central European vegetation (Koutsodendris et al., 2010, subm.). Based on the Dethlingen time series analysis, it also appears possible that this climate oscillation is related to lower solar irradiation. This may also have modified sub-decadal climate variability, as it has been suggested for prominent climate oscillations of the present interglacial, i.e., the 8.2 ka event (e.g., Muscheler et al., 2004; Rohling and Pälike, 2005) and the Little Ice Age (e.g., Shindell et al., 2001).
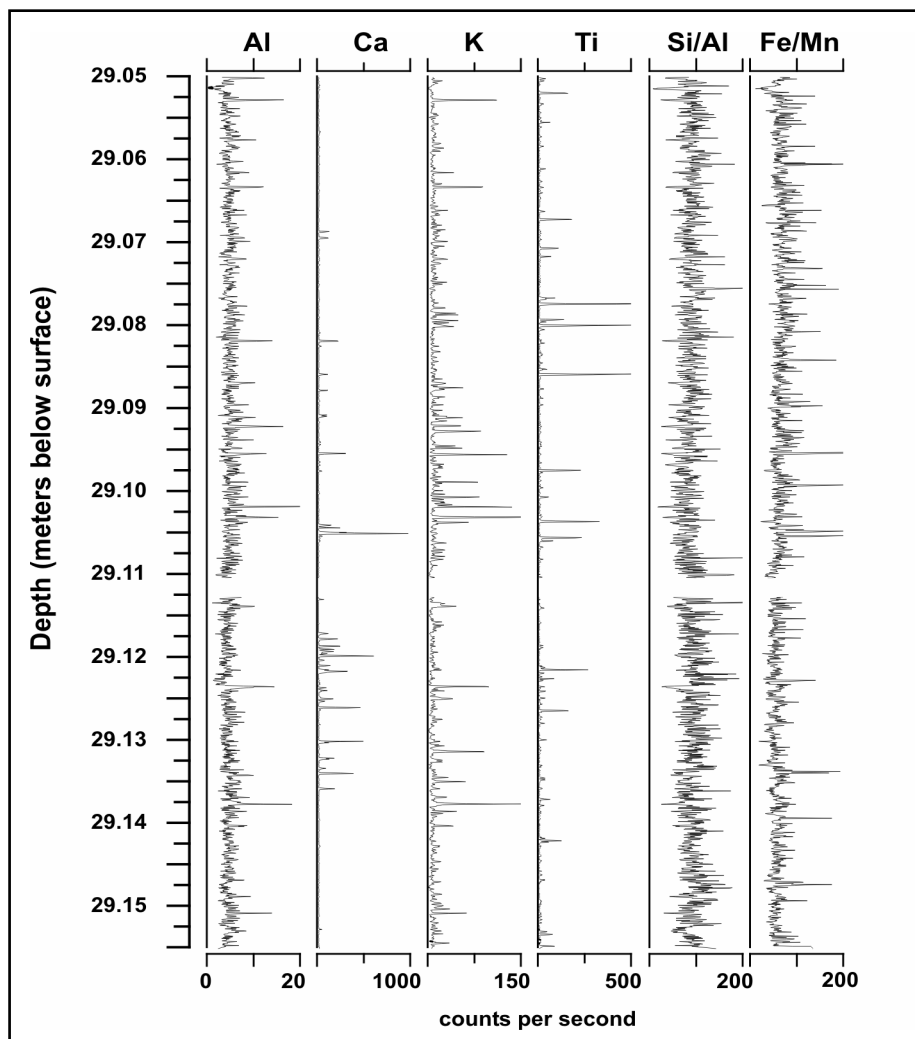
Figure 3.8: *Geochemical results of μ-XRF analyses (step size: 50 μm) spanning the onset of the OHO in the Dethlingen core.*

The two cases of discontinuous short-term climate variability in certain intervals as evidenced in the Dethlingen varve record highlight the need to apply time series analysis on the seasonal thickness measurements. When indications of short-term cyclicities are absent in certain intervals of one of the seasonal layer spectra, but present in the same intervals of the other seasonal layer spectra, the processes involved in varve formation were obviously susceptible to record agents of external forcing only under specific boundary conditions. In contrast, when the cyclic signals are absent from all seasonal layer spectra, the external climate forcing controlling varve formation was altogether weakened and/or ceased completely.

3.4 Conclusions

Microfacies and time series analyses from an annually laminated sedimentary archive of the Holsteinian interglacial (MIS 11) yields a strong signal of natural cyclicity at decadal and sub-decadal time scales. The decadal-scale cyclicity is attributed to solar forcing that may have influenced the sedimentation of the light varve layers (spring/summer) by driving changes in the productivity of the palaeolake. The sub-decadal-scale cyclicity is attributed to ENSO and NAO climate modes, predominantly influencing the dark layer formation (autumn/winter) through changes in atmospheric circulation that affected lake mixing. Our analyses clearly demonstrate that in order to interpret the signals of varve time series analysis and to correlate them with temporal modifications of the external climate forcing, it is essential to (a) understand the sedimentological processes controlling varve formation and to (b) compare the results of individually analyzed seasonal layer-thickness datasets.

The solar- and ENSO/NAO-like natural cyclicity during MIS 11 as recorded in the ~3200-year-long varve time series from Dethlingen is closely comparable with the central European climate cyclicity of the present interglacial. This suggests that the short-term climate cyclicity during the two interglacials is controlled by similar forcing. Taking this observation a step further, we suggest that MIS 11, besides the well-established long-term astronomical analogy, may be regarded as a good analogue for the Holocene with regard to short-term (sub-decadal- to decadal-) timescales. As a result, understanding the short-term climate variability during MIS 11 may potentially contribute to simulate future climate evolution of the present interglacial.

3.5 Acknowledgements

Chapter 4. A short-term climate oscillation during the Holsteinian interglacial (MIS 11c): An analogy to the 8.2 ka climatic event?

Andreas Koutsodendris[1], Jörg Pross[1], Ulrich C. Müller[1], Achim Brauer[2], William J. Fletcher[1,3], André F. Lotter[4]

[1] Paleoenvironmental Dynamics Group, Institute of Geosciences, Goethe University Frankfurt, Altenhöferallee 1, D-60438 Frankfurt, Germany; [2] German Research Centre for Geosciences, Section 5.2 Climate Dynamics and Landscape Evolution, Telegrafenberg, D-14473 Potsdam, Germany; [3] Quaternary Environments and Geoarchaeology, Geography, School of Environment and Development, University of Manchester, Arthur Lewis Building, Oxford Road, Manchester M13 9PL, United Kingdom; [4] Institute of Environmental Biology, Palaeoecology, Laboratory of Palaeobotany and Palynology, Utrecht University, Budapestlaan 4, 3584 CD Utrecht, The Netherlands

Abstract: *To gain insights into the mechanisms of abrupt climate change within interglacial periods, we have examined the characteristics and spatial extent of a prominent, climatically induced vegetation setback during the Holsteinian interglacial (Marine Isotope Stage 11c). Based on pollen analysis and varve counts of lake sediments cored at Dethlingen (northern Germany), this climatic oscillation, here termed the "Older Holsteinian Oscillation" (OHO), lasted 220 years. It can be subdivided into a 90-year-long decline of temperate tree taxa associated with an expansion of* Pinus *and herbs, and a 130-year-long recovery phase marked by the expansion of* Betula *and* Alnus*, and the subsequent recovery of temperate trees. The OHO is widely documented in Europe north of 50º latitude and is characterized by boreal climate conditions with cold winters from the British Isles to Poland, with a gradient of decreasing temperature and moisture availability, and increased continentality towards eastern Europe. This pattern points to a weakened influence of the westerlies and/or a stronger influence of the Siberian High. A comparison of the OHO with the 8.2 ka event of the Holocene reveals close similarities regarding the imprint on terrestrial ecosystems and the interglacial boundary conditions. Hence, in analogy to the 8.2 ka event, a transient, meltwater-induced slowdown of the North Atlantic Deep Water formation appears as a plausible trigger mechanism for the OHO. If correct, meltwater release into the North Atlantic may be a more common agent of abrupt climate change during interglacials than previously thought. We conclude that meltwater-induced climate setbacks during interglacials preferentially occurred when low rates of summer insolation increase during the preceding terminations facilitated the persistence of large-scale continental ice-sheets well into interglacials.*

Key words: *abrupt climate change; Holsteinian interglacial; Marine Isotope Stage 11; 8.2 ka event; meltwater forcing; varve chronology.*

4.1 Introduction

With the increasing manifestation of anthropogenic forcing on the Earth's climate, deciphering the mechanisms and effects of abrupt climate change is crucial in order to extend the lead time for mitigation and adaptation. In this context, the investigation of past interglacials can provide insights into the characteristics of abrupt climate variability, and it can ultimately be instrumental for the prediction of future climate change (e.g., Alley et al., 2003; Tzedakis et al., 2009; Müller et al., 2005; Brauer et al., 2007a). Based on this notion, Marine Isotope Stage (MIS) 11 has received special attention (e.g., Oppo et al., 1998; Bauch et al., 2000; Kukla, 2003; McManus et al., 2003; Desprat et al., 2005; Mangili et al., 2007; Müller and Pross, 2007; Rohling et al., 2010) as it is considered one of the closest palaeoclimatic analogues for the present and future climate (e.g., Loutre and Berger, 2003; Ruddiman, 2005; Tzedakis, 2010).

The absence of sufficiently long terrestrial climate records in northern Europe and the lack of reliable absolute dates have led to controversial views on the terrestrial equivalent of MIS 11 in Europe (e.g., de Beaulieu et al., 2001; Geyh and Müller, 2005; see also Koutsodendris et al., 2010, for a discussion). However, mounting evidence based on a long terrestrial vegetation record from the French Massif Central (Reille et al., 2000) and a direct land-sea correlation off Iberia (Desprat et al., 2005) has led the majority of workers to accept a correlation of the Holsteinian interglacial with MIS 11c (e.g., de Beaulieu et al., 2001; Tzedakis et al., 2001; Kukla, 2003; Nitychoruk et al., 2005; Müller and Pross, 2007; Preece et al., 2007).

In light of this correlation and the close analogy of MIS 11 to the Holocene interglacial with regard to orbital boundary conditions, two pronounced vegetation regressions during Holsteinian interglacial conditions that have been suggested to result from short-term (i.e., centennial-scale) climate oscillations (e.g., Turner, 1970; Müller, 1974; Kukla, 2003; Koutsodendris et al., 2010) merit special attention. The older of these oscillations, here termed "Older Holsteinian Oscillation" (OHO), was rather abrupt, lasted for ~300 years, and occurred ~6000 years after the establishment of interglacial forests in the lowlands of northern Germany (Meyer, 1974; Müller, 1974). There, the OHO is characterized by a marked decline in temperate tree taxa and an increase in pioneer trees and herbs (e.g., Meyer, 1974; Müller, 1974; Kukla, 2003; Koutsodendris et al., 2010). Although the OHO took place within interglacial conditions, a connection to deglaciation processes of the preceding termination, i.e., Termination V, is plausible; this termination was associated with weak insolation changes that prolonged deglaciation processes by ~15 to 20 ka into MIS 11c (Rohling et al., 2010).

Despite a paucity of highly resolved records and the potential shortcomings of biostratigraphic correlation, there is good evidence that this regressive phase in vegetation development is documented in numerous terrestrial climate archives from central and northwestern Europe (e.g., Turner, 1970; Müller, 1974; Krupiński, 2000; Thomas, 2001; Nitychoruk et al., 2006; Geyh and Müller, 2007; see also Section 4.10). However, the spatial extent and pattern of OHO-induced environmental change in Europe and the potential

expression of the OHO in marine records have remained largely unexplored; at the same time, the duration of the climatic forcing of the OHO is insufficiently constrained. These factors have yet precluded insights into the triggering mechanism of the OHO (Kukla, 2003).

Therefore, we studied the timing, duration, and structure of the OHO based on a decadal-scale palynological record from annually-laminated lake sediments of Holsteinian age cored at Dethlingen, northern Germany (Koutsodendris et al., 2010). Based on these findings and the review of available evidence from previously published works, we examined the spatial extent and pattern of the OHO impact across Europe. This allows us to explore the forcing mechanisms of an abrupt climate setback that occurred during an interglacial that, with regard to orbital forcing, bears close similarities with the Holocene.

4.2 Material and Methods

The studied core was recovered from Dethlingen within the lowlands of northern Germany (10º 08.367' E, 52º 57.780' N, 65 m a.s.l.; Table 4.1). Due to the formation of numerous deep lakes after the decay of the Elsterian ice sheet (Ehlers et al., 1984), the region around Dethlingen exhibits partially annually-laminated sedimentary archives of Holsteinian age (Benda and Brandes, 1974), including the classical localities of Munster-Breloh (Müller, 1974) and Hetendorf (Meyer, 1974). The succession cored at Dethlingen comprises organic-rich lake sediments between 37 and 23 m below the present soil surface (mbs; Koutsodendris et al., 2010). Here, we focus on the laminated diatomite between 28.25 and 29.45 mbs that spans the OHO interval. In particular, we present a higher-resolution picture of vegetation dynamics during the OHO at Dethlingen than previously available (Koutsodendris et al., 2010) within the context of a new chronological framework based on varve counting.

Palynological samples of 0.5 cm thickness were taken every 2 cm across the OHO and every 4-8 cm below and above the OHO. Based on varve counting (compare Section 4.3.1), the temporal resolution of the generated pollen record is ~11 years across the OHO and ~30 (min.: 17; max.: 47) years for the adjacent intervals; the individual pollen samples integrate 3-5 years. The palynological preparation followed standard palynological techniques including sediment freeze-drying, weighing, treatment with HCl (10 %), NaOH (10 %), HF (40 %), heavy-liquid separation with Na_2WO_4 x $2H_2O$, acetolysis, and slide preparation using glycerine jelly. *Lycopodium* marker spores were added to each sample to calculate pollen accumulation rates (grains cm^{-2} yr^{-1}). Palynological slides were analysed at 400x magnification. The minimum counting sum was always above 300 pollen grains per sample (average: 390 grains) excluding pollen from aquatic plants, spores, and algae.

Varve counting was performed on thin sections using a petrographic microscope at 100x magnification. The preparation of thin-sections with a dimension of 120 x 35 mm followed standard techniques including freeze-drying, impregnation with Araldite 2020 epoxy resin under vacuum, sawing, and grinding of the sediment (Brauer et al., 1999a; Lotter and Lemcke, 1999). The continuity of observations was secured with an overlap of 2 cm between successive thin sections. This method allows both the investigation of sediment

microstructures and the accurate counting of varves (Brauer et al., 1999a; Lotter and Lemcke, 1999), thereby establishing a floating varve chronology. The chronology was interpolated across small-scale core intervals where varve preservation was poor or sediment had been disturbed during coring and laboratory processing. For each of these intervals, the interpolation was based on the average thickness of 20 varves deposited directly below and above the interval.

Site code	Site name	Country	Latitude/Longitude	OHO present	Reference
-	ODP 646	marine record	58º 12' N / 48º 22' W	?	de Vernal and Hillaire-Marcel, 2008
Ve	Vejlby	Denmark	56º 04' N / 12º 08' E	Yes	Andersen, 1965
Hm	Hummelsbüttel	Germany	53º 38' N / 10º 02' E	Yes	Averdieck, 1992
MB	Munster-Breloh	Germany	53º 01' N / 10º 04' E	Yes	Müller, 1974; Geyh and Müller, 2007
De	Dethlingen	Germany	52º 57' N / 10º 08' E	Yes	this study
OO	Ober-Ohe	Germany	52º 53' N / 10º 10' E	Yes	Gistl, 1928
Ba	Barford	England	52º 37' N / 01º 07' E	Yes	Phillips, 1976
Ne	Nechells	England	52º 30' N / 01º 51' W	Yes	Kelly, 1964
Ho	Hoxne	England	52º 20' N / 01º 12' E	Yes	West, 1956; Turner, 1970
At	Athelington	England	52º 17' N / 01º 14' E	Yes	Coxon, 1985
Ko	Komarno	Poland	52º 09' N / 24º 06' E	Yes	Krupiński, 1995
Os	Ossówka	Poland	52º 07' N / 23º 09' E	Yes	Krupiński, 1995
Ka	Kaliłów	Poland	52º 04' N / 23º 13' E	Yes	Bińka and Nitychoruk, 1996
Wo	Woskrzenice	Poland	52º 03' N / 23º 16' E	Yes	Bińka and Nitychoruk, 1995
MT	Marks Tey	England	51º 52' N / 00º 47' E	Yes	Turner, 1970
GS	Gröbern-Schmerz	Germany	51º 40' N / 12º 28' E	Yes	Eissmann, 2002; Kühl and Litt, 2007
DW	Delitzsch-Wölkau	Germany	51º 31' N / 12º 20' E	Yes	Dassow, 1987
NZ	Nowiny Żukowskie	Poland	51º 04' N / 22º 45' E	Yes	Hrynowiecka-Czmielewska, 2010
Ro	Rossendorf	Germany	51º 03' N / 13º 56' E	Yes	Erd et al., 1987
Dö	Döttingen	Germany	50º 35' N / 07º 12' E	Yes	Diehl and Sirocko, 2007
Sa	Samerberg	Germany	47º 47' N / 12º 13' E	No	Grüger, 1983
HU	Hirschland-Uznach	Switzerland	47º 14' N / 08º 59' E	No	Welten, 1988
Th	Thalgut	Switzerland	46º 57' N / 07º 25' E	No	Welten, 1988; Drescher-Schneider, 2000
Gr	Grandson	Switzerland	46º 49' N / 06º 39' E	No	Welten, 1988
VL	Val-de-Lans	France	45º 05' N / 05º 34' E	No	de Beaulieu et al., 1994; Field et al., 2000
Pr	Praclaux	France	44º 49' N / 03º 50' E	Possibly yes	Reille and de Beaulieu, 1995; Reille et al., 2000
-	MD01-2447	marine record	42º 09' N / 09º 40' E	?	Desprat et al., 2005
TP	Tenaghi Philippon	Greece	40º 58' N / 24º 15' E	?	Wijmstra and Smit, 1976
Io	Ioannina	Greece	39º 39' N / 20º 55' E	?	Tzedakis, 1994
Kp	Kopais	Greece	38º 50' N / 20º 10' E	?	Okuda et al., 2001
-	MD01-2443	marine record	37º 52' N / 10º 10' E	?	Tzedakis, 2010
Hl	Hula	Israel	33º 06' N / 35º 36' E	?	Horowitz, 1989

Table 4.1: *List of sites with Holsteinian pollen records shown in Figure 4.4. Sites are listed from north to south. (?): presence/absence of the OHO uncertain because of yet insufficient temporal resolution of record.*

4.3 The Older Holsteinian Oscillation at Dethlingen

4.3.1 Annual lamination of lake sediments

The laminations of the lake sediments in the Dethlingen core consist of two discrete layers: a light and a dark one (Fig. 4.1A, B). The light layers consist mainly of diatoms of the genera *Stephanodiscus, Ulnaria* and *Aulacoseira*. In most cases, the light layers are dominated by one of these taxa, resulting in an almost monospecific diatomaceous layer. The light layers often contain organic matter that increases in abundance towards the dark layers. The dark sub-layers are composed predominantly of organic matter with fragments of diatom frustules, reworked periphytic diatoms from the littoral zone, and plant remains (Fig. 4.1A, B).The transition from the light diatomaceous layers to the overlaying dark organic-detrital layers is diffuse, whereas the boundary between the dark layer and the following light diatomaceous layer is sharp (Fig. 4.1C). This seasonal layer succession is predominantly controlled by the annual cycle of diatoms blooming in spring and summer; the light layers prove that the lamination couplets are true varves. The regularly and finely laminated sediments from Dethlingen can be characterized as biogenic varves of diatomaceous type (Brauer, 2004).
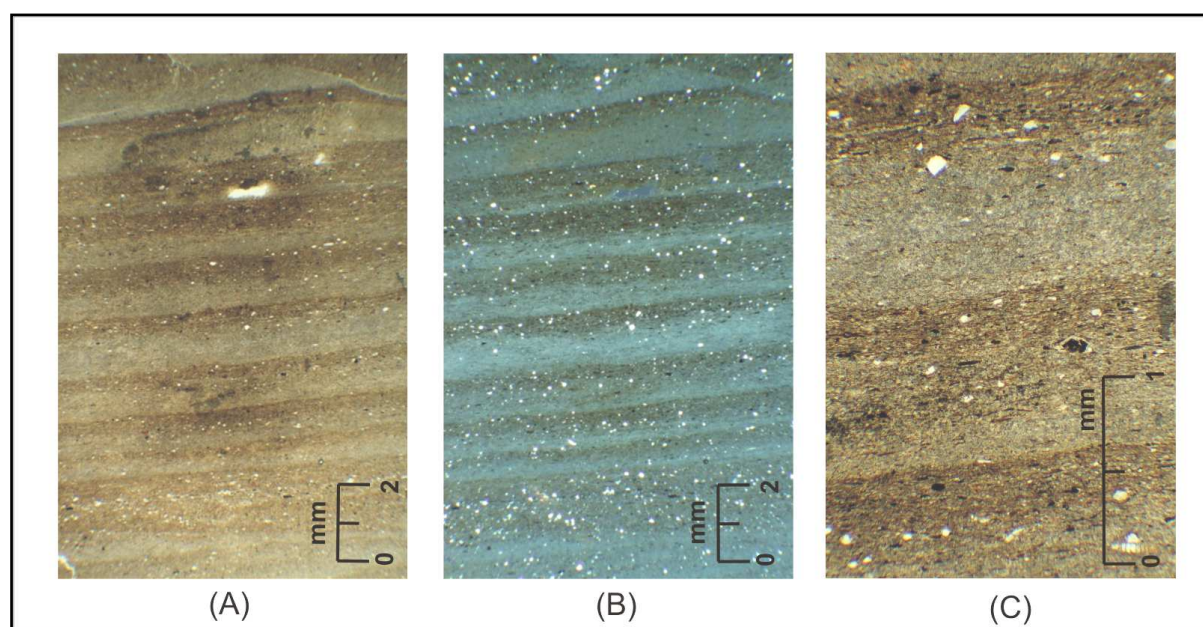
Figure 4.1: *Varve photographs from the Dethlingen core: Light and dark sub-layers (a) under parallel-polarized light and (b) under cross-polarized light; (c) Diffuse and sharp boundaries between successive dark and light sub-layers.*

4.3.2 Characteristics and rates of OHO vegetation change at Dethlingen

In the Dethlingen core, the OHO has been identified between 28.73 and 29.15 mbs (Koutsodendris et al., 2010). The analysis of the OHO interval presented here shows that the oscillation is characterized by a strong short-term decline of pollen from temperate trees and a transient increase in pollen from the pioneer trees *Pinus* and *Betula* (Fig. 4.2). Based on the varve chronology, the overall duration of the OHO, comprising a regressive and a recovery phase, is 220 years (Fig. 4.2).

The regressive phase is marked by the overall decline of temperate taxa from 27 to 4.5 % within 90 years, with more than 80 % of the decline in pollen from temperate trees (from 27 to 8 %) occurring within the first 40 years (Fig. 4.2). Specifically, *Taxus* percentages declined strongly from 9.5 to <1 % within 60 years, whereas *Corylus* declined from 11.5 to 2 % within 90 years and *Quercus* from 4 to 1 % within 50 years (Fig. 4.2). The regressive phase is further characterized by declining percentages of *Alnus* pollen (from 32 to 18 %) and, in the latter part of the regressive phase (i.e., ~60 years after the onset of the OHO), of *Picea* pollen (from 4 to 1 %). In contrast, *Pinus* percentages increased strongly from ~30 to ~60 %, whereas *Betula* percentages remained virtually stable during the regressive phase. The changes in pollen accumulation rates (PAR) during the regressive phase are in agreement with the changes in pollen percentages; the PAR of temperate tree taxa decreased, whereas the PAR of *Pinus* pollen increased towards the upper part of the regressive phase (Fig. 4.2).
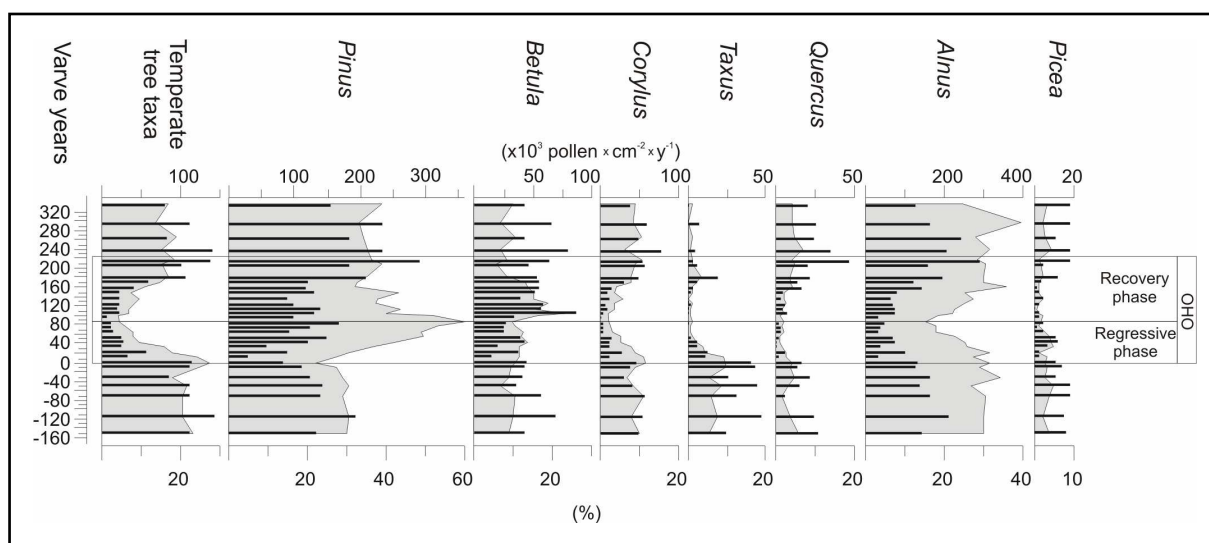
Figure 4.2: *Selected tree taxa and pollen accumulation rates (black bars; grains cm^{-2} yr^{-1}) at Dethlingen plotted against age (based on varve years) for the OHO interval. First varve year indicates the onset of the OHO. Temperate taxa comprise* Abies, Acer, Buxus, Carpinus, Celtis, Corylus, Fagus, Fraxinus, Ilex, Hedera, Ostrya, Pterocarya, Quercus, Taxus, Tilia, *and* Ulmus.

The recovery phase is characterized by the increase in percentages of temperate tree taxa such as *Corylus* and *Quercus*. The onset of the recovery is marked by the sharp rise in the percentages of the pioneer trees *Betula* and *Alnus*, which attained peak values after 20 and 80 years, respectively (Fig. 4.2). The onset of the recovery phase is further marked by a sharp decline in *Pinus* percentages. With the exception of *Taxus*, which did not recover, the temperate tree pollen reached percentages comparable to those prior to the onset of the OHO 130 years after the onset of the recovery phase. With regard to the pollen production, the onset of the recovery phase is marked by the rapid increase in *Betula* PAR that reach peak values after 20 years. The increase in the PAR of temperate taxa and *Alnus* lasted 130 years before the background values of prior to the OHO were attained again (Fig. 4.2).

4.4 Chronological position of the OHO

To constrain the chronological position of the OHO within the Holsteinian interglacial, we have developed a floating chronology by combining the Dethlingen record with two regional sediment archives: Munster-Breloh (Müller, 1974) and Hetendorf (Meyer, 1974) are located within a distance of 5 km to Dethlingen and also comprise varved lake sediments that have previously been subjected to high-resolution palynological analyses. The palynostratigraphic data provide a robust correlation between all three sites such that a varve chronology for most of the Holsteinian can be established (Fig. 4.3). Based on this chronology, the duration of the Holsteinian interglacial as delimited by the prevalence of closed forests in the region can be estimated to 15000 ±1500 years (Fig. 4.3). Varve counting and interpolation using measured average varve thickness revealed that the OHO occurred 6000 ±500 years after the onset of the Holsteinian reforestation (based on 4770 counted varves) and 3100 ±500 years (based on 2664 counted varves) after the expansion of temperate forests (Fig. 4.3).

The phasing between the interglacial conditions of the Holsteinian in central Europe (with a duration of 15-16 ka) and the 28-ka-long MIS 11c (Imbrie et al., 1984) is difficult to establish. Based on insolation-induced seasonality changes (Berger and Loutre, 1991) and the timing of maximum sea-surface temperatures in the eastern North Atlantic during MIS 11c (Kandiano and Bauch, 2007; Helmke et al., 2008), the Holsteinian interglacial forestation in northern Germany most likely coincides with the optimum of MIS 11c, which lasted from ~415 to ~397 ka BP (see discussion in Koutsodendris et al., 2010). Because the OHO occurred 6000 ±500 years after the onset of the Holsteinian reforestation (Koutsodendris et al., 2010), it may be assigned an age of ~408 (±0.5) ka BP.

4.5 Spatial extent and pattern of the OHO impact in Europe

In the following we investigate the spatial extent and pattern of vegetation change in Europe associated with the OHO. Our assessment relies on pollen records that have been confidently assigned to the Holsteinian interglacial based on typical vegetation features such as the immigration pattern of plant taxa and the occurrence of *Pterocarya* late in the interglacial (e.g., Turner, 1970; Müller, 1974; Bińka et al., 1997; Reille et al., 2000; de Beaulieu et al., 2001; Geyh and Müller, 2005; see Section 4.10 for details).

The OHO is widely documented in vegetation records from the British Isles to Poland north of 50⁰ latitude (Table 4.1; see also Section 4.10), where it is marked by pronounced increases in the percentages of pollen from pioneer trees (i.e., *Pinus* and *Betula*) and herbs at the expense of temperate tree taxa (Fig. 4.4A, B). A closer inspection of the pollen signals at the individual sites across the western, central, and eastern part of northern Europe reveals a distinct spatial pattern in the vegetation response to the OHO (Fig. 4.4A-D). In the western part of northern Europe (i.e., the British Isles), the OHO is marked by a decline in temperate tree taxa such as *Corylus* and *Taxus,* and at some localities also in *Alnus* and *Quercus* (Fig. 4.4B, C), whereas the percentages of *Tilia* and *Picea* remain essentially stable (Fig. 4.4D). In the central part of northern Europe (i.e., Germany and Denmark), the percentages of temperate taxa and of *Alnus* decline markedly at all sites (Fig. 4.4B, C). A more complex

picture emerges for *Picea*, which declines at the more continental sites in the lowlands, whereas it increases in more coastal and sub-mountainous settings (Fig. 4.4D). *Tilia* is mostly present, albeit in low percentages. Sites in the eastern part of northern Europe (i.e., Poland) are characterized by similar vegetation dynamics as in the continental settings of central Europe; in addition, an increase in the percentages of *Larix* is observed (Fig. 4.4A-D).
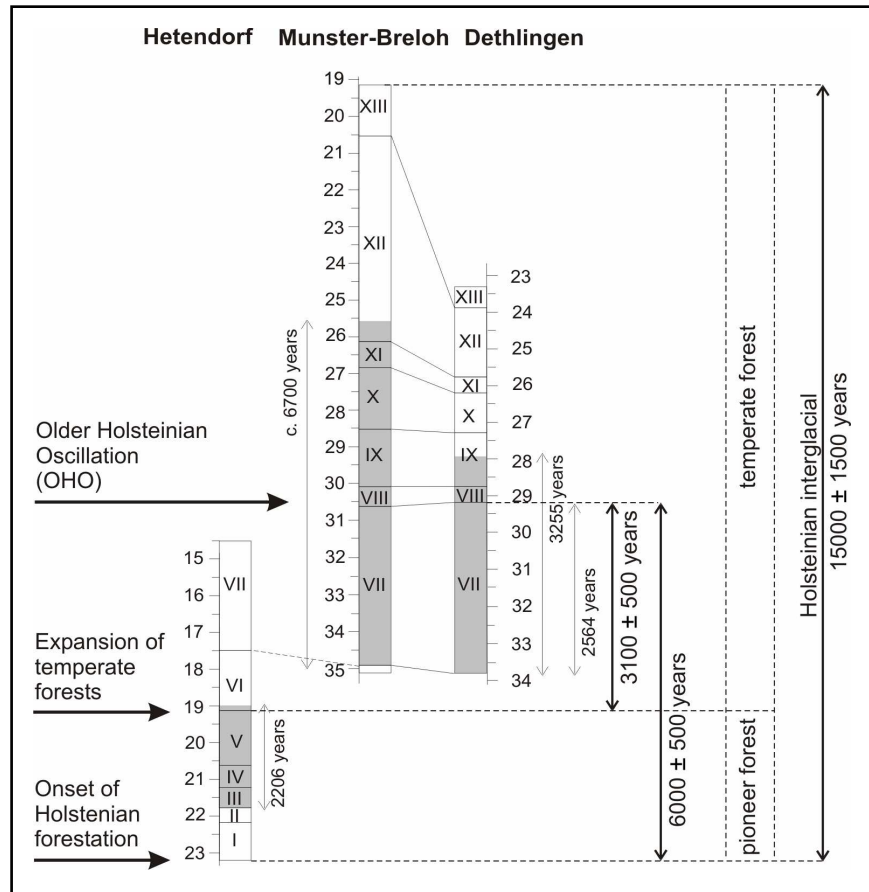
Figure 4.3: *Palynostratigraphic correlation of annually laminated lake sediments from the Holsteinian interglacial in the Lüneburger Heide region, northern Germany, and chronological position of the OHO. Sites: Hetendorf (core KS 430/72), varves counted for pollen zones III-V, and part of VI (Meyer, 1974); Munster-Breloh (core KS 416/71), varves counted for pollen zones VII-XI, and part of XII (Müller, 1974); Dethlingen (this study), varves counted for pollen zones VII-VIII, and part of IX. Interpolations with average varve thickness was made for pollen zones I-II, VI (Meyer, 1974), and XII-XIII (Müller, 1974). Shaded intervals correspond to annually laminated intervals in each sequence. Pollen zones after Müller (1974).*

The nature of climate change associated with the OHO can be inferred from the climatic requirements of the affected tree taxa. *Tilia* and *Quercus* can tolerate cold winters, but require relatively high summer temperatures (Dahl, 1998). *Alnus* is tolerant to cold winters, but very sensitive to cool springs (Frenguelli et al., 1991). *Picea* is also resistant to cold winters and benefits from strong temperature seasonality, but is sensitive to drought (Dahl, 1998). *Larix* is resistant to harsh frosts and less sensitive to drought than *Picea* (Ellenberg, 1988).

In the western part of northern Europe (British Isles), a prevalence of cold conditions during the OHO can be inferred from the decline of temperate tree taxa. The presence of *Tilia* suggests that summer temperatures remained relatively high, which points to a temperature drop in winter. However, the stable percentages of *Picea* exclude an enhancement of temperature seasonality. At the same time, although drier conditions are evidenced by lake level changes during the OHO (e.g., West, 1956; Kelly, 1964), the presence of *Picea* points to a still relatively high moisture availability, probably resulting from the region's proximity to the Atlantic Ocean. In the central part of northern Europe (Germany and Denmark), the strong decline in *Quercus* points to winter temperatures that were lower than on the British Isles. In addition, a prevalence of cold conditions in spring is suggested by the strong decline in *Alnus*, whereas the presence of *Tilia*, albeit in low percentages, suggests warm summers. Based on these vegetation data, the central part of northern Europe experienced a stronger temperature seasonality than the western part. This scenario is corroborated by the increase of *Picea* in coastal settings (Fig. 4.4D) and its decline at more continental lowland sites, which points to a decrease in moisture availability with increasing distance from the sea. For Dethlingen, drier conditions during the OHO are also supported by microfacies and μ-XRF data (Koutsodendris et al., subm.). The eastern part of northern Europe (Poland) experienced a similar temperature drop and enhanced seasonality as the central part. However, the expansion of *Larix* suggests even stronger continentality than in central northern Europe.

Summarizing the above, the climate conditions in Europe north of 50⁰ latitude during the OHO as inferred from vegetation dynamics show a transient prevalence of boreal climate conditions that was primarily associated with a drop in winter temperatures. This scenario is corroborated by quantitative temperature reconstructions suggesting a strong decline in January temperature, but essentially stable July temperature during the OHO (Kühl and Litt, 2007). The temperature decline shows a clear west to east gradient, being weakest in western Europe and strongest in eastern Europe. Moisture availability also exhibits a west-east gradient, with higher moisture availability in westernmost Europe (Fig. 4.4E). This palaeoclimatic pattern reflects a weaker influence of the westerlies towards the east and/or a stronger influence of the Siberian High north of 50⁰ latitude (Fig. 4.4E).

Based on the available data, the OHO appears conspicuously absent in European palaeoclimate records between 45⁰ and 50⁰ latitude. Most Holsteinian pollen records from that region have been analyzed with a sufficient temporal resolution to allow the detection of a centennial-scale oscillation (e.g., Praclaux – Reille and de Beaulieu, 1995; Reille et al., 2000; Thalgut – Drescher-Schneider, 2000). Moreover, a number of mountainous archives from central Europe (e.g., Praclaux, Val-de-Lans, Thalgut) have been cored and analysed repeatedly, which further reduces the probability that any OHO-induced vegetation change may have been simply overlooked. We therefore argue that the vegetation response to the
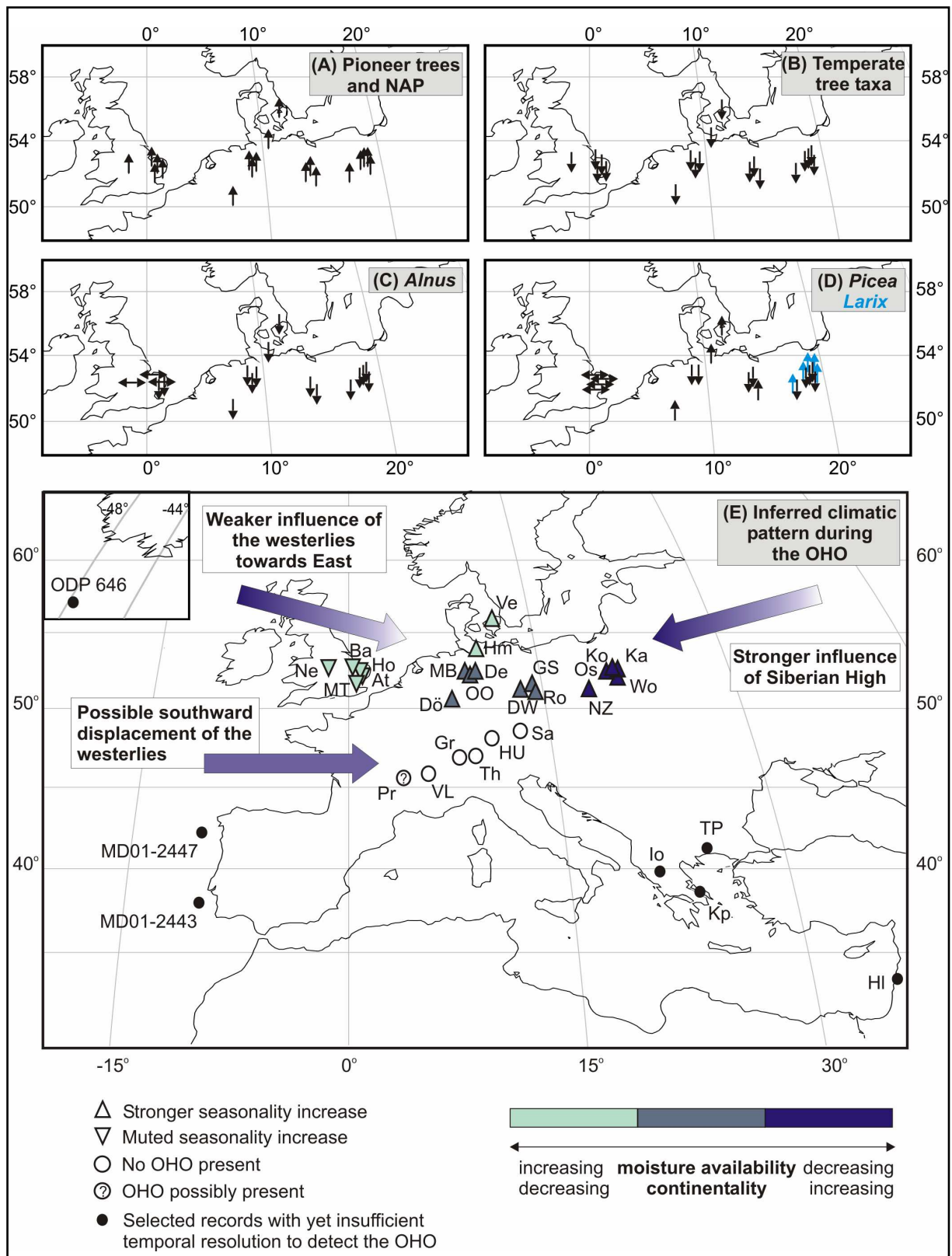
Figure 4.4: *Vegetation dynamics and climate conditions across Europe during the OHO; (a) Temperate tree taxa, including* Abies, Acer, Buxus, Carpinus, Celtis, Corylus, Fagus, Fraxinus, Ilex, Hedera, Ostrya, Pterocarya, Quercus, Taxus, Tilia, *and* Ulmus; *(b) Pioneer trees (*Pinus *and* Betula*) and non-arboreal pollen (NAP); (c)* Alnus; *(d)* Picea *and* Larix; *(e) Presence/absence of OHO in pollen records (see Table 4.1 for list of sites) and inferred climate pattern. Symbols: (↑) increase; (↓) decrease; (↔) stable.*

OHO in the mountainous parts of central Europe was either subdued and/or different in character from the vegetation response in more northerly latitudes of Europe.

A potential explanation for such a subdued expression of the OHO in mountainous vegetation records is based on the notion that the impact of climate change on vegetation communities is determined by the extent to which this change causes the crossing of ecological thresholds (e.g., Smith, 1965; Tzedakis et al., 2004b). In the mountainous parts of central Europe, climate change would strongest affect those taxa that are close to their specific upper altitude limit. The Holsteinian forests in the mountainous regions of central Europe were dominated by trees growing today in the montane and subalpine elevational belt such as *Abies*, *Picea* and *Fagus*. The available Holsteinian pollen records from these regions are from altitudes between 400 and 1200 m (e.g., Grüger, 1983; Welten, 1988; Reille and de Beaulieu, 1995; Drescher-Schneider, 2000). At such altitudes, these tree taxa do not reach their physiological tolerance limits, and none of them is affected by cold winters; consequently, a climatic oscillation such as the OHO is not likely to have a significant effect on this vegetation type. Moreover, despite their large distance to the seaboard, these regions exhibit relatively moist conditions, which prevents a possible drought stress.

Alternatively, the climatic impact of the OHO on vegetation in mountainous settings of central Europe may have strongly differed from that in Europe north of 50º latitude. Such a scenario is supported by climate models for the Holocene suggesting that anomalous cooling in the higher northern latitudes can cause precipitation changes over Europe (Renssen et al., 2002): High pressure over the Nordic Seas leads to a stabilization of the atmosphere in this region, thus blocking depressions and pushing them southwards. Therefore, it appears possible that the OHO-induced cooling as documented for northern Europe was associated with a transient southward displacement of the westerlies over the mountainous regions of central Europe. As a consequence, these regions would have experienced wetter conditions. *Abies*, which is the dominant tree taxon in the alpine Holsteinian (e.g., Reille at al., 2000; de Beaulieu et al., 2001), is particularly competitive when summer precipitation is high and winter temperatures decrease (Ellenberg, 1988). Its expansion during intervals of cool and wet climate has been well documented for the present interglacial across central Europe (Tinner and Lotter, 2006). Following a similar concept as for the present interglacial, the OHO impact on vegetation in the mountainous regions of central Europe would result in an expansion of *Abies* at the expense of other temperate taxa. In fact, a close inspection of the Holsteinian pollen record from Praclaux indicates a rapid expansion of *Abies* well within the younger stage of the temperate forest phase (Reille et al., 2000). Based on this finding, which might indicate an expression of OHO-induced vegetation dynamics in mountainous settings of central Europe, it could be argued that the OHO impact on the Alpine region was associated with cool and wet conditions that supported the expansion of *Abies*.

To date, the OHO has also not been detected in terrestrial vegetation records from the Mediterranean region, notably the classical localities Tenaghi Philippon, Ioannina, and Kopais, or marine cores from the Mediterranean Sea and the North Atlantic (Table 4.1, Fig. 4.4). At present, it cannot be decided whether this is due to the actual absence of an OHO

imprint on these records or whether it results from the relatively low temporal resolution of the data as yet available. Nevertheless, a consistent, spatially differentiated pattern emerges for the climatic change in central and northern Europe connected to the OHO. North of 50⁰ latitude, the OHO was associated with the establishment of colder and drier conditions, and the development of a pronounced west-east temperature and moisture gradient. This pattern is best explained through a climatic driving mechanism associated with a weaker influence of the westerlies towards the east and/or a stronger influence of the Siberian High north of 50° latitude. In the mountainous parts of central Europe, the OHO impact on vegetation has not been unequivocally detected. It is conceivable that a different vegetation response as compared to that in more northerly latitudes resulted from wetter conditions caused by a southward shift of the westerlies; such an increase in moisture availability may have enhanced the growth of certain tree taxa.

4.6 Comparison of the OHO with the 8.2 ka event

To obtain insights into the mechanisms potentially responsible for the OHO, we compare the characteristics and the boundary conditions of the OHO with those of the well-known 8.2 ka event of the Early Holocene. Comprising a high-amplitude abrupt climate anomaly superimposed on a weaker multi-centennial anomaly of the same sign, this event is the most prominent example of abrupt climate change during the Holocene. Its triggering mechanism (i.e., the catastrophic drainage of ice-dammed Laurentide lakes into the North Atlantic, with the resulting surface-water freshening causing a transient slowdown of the North Atlantic Deep Water (NADW) formation (e.g., Barber et al., 1999; Ellison et al., 2006) and impact on terrestrial ecosystems are relatively well understood (see reviews by Alley and Ágústsdóttir, 2005; Rohling and Pälike, 2005; Wiersma and Renssen, 2006).

With regard to the timing of the individual events after the onset of the respective interglacials, the OHO occurred ~6000 (±500) years after the onset of the Holsteinian (Fig. 4.3), whereas the 8.2 ka event occurred ~3500 years after the onset of the Holocene (Lowe et al., 2008). However, if consistent criteria are used for the beginning of both interglacials, such as the expansion of temperate forests in central Europe (Fig. 4.3), the OHO occurred ~3100 (±500) years after the onset of interglacial conditions, which is nearly identical with the timing of the 8.2 ka event. If the reforestation with pioneer trees is taken as the onset of an interglacial, then for the present interglacial the onset of the late-glacial interstadial (corresponding to the onset of Greenland Interstadial 1) at ~14.7 ka BP (Lowe et al., 2008; Lotter et al., 2010) should be considered, because the Younger Dryas represented a meltwater-forced climate deterioration (e.g., McManus et al., 2004; Broecker, 2006) within interglacial conditions. In that case, the timing of the 8.2 ka event would be ~6500 years after the reforestation with pioneer trees, which is again very similar to the timing of the OHO within the Holsteinian (Fig. 4.3). Hence, there is a strikingly close resemblance between the OHO and the 8.2 ka event with regard to the timing after the onset of the interglacial (Table 4.2).

Sea level during the OHO (i.e., at ~408 ka BP) was ~20 m lower than today (Rohling et al., 2010). Similarly, the 8.2 ka event also occurred when the sea level was ~20 m below present (Rohling et al., 2010). Because the contribution of the Antarctic ice sheet to the sea-level lowstand during the last glacial maximum was only minor (Denton and Hughes, 2002), this figure provides a rough measure for the volume of continental ice sheets that were still present in the northern hemisphere. The comparability between both climatic events with regard to sea level suggests that substantial continental ice sheets persisted in the northern hemisphere well into the Holsteinian interglacial and were still present during the OHO. This view is corroborated by ice-core data for MIS 11c, which show peak warmth towards the end of the interglacial (Jouzel et al., 2007). In contrast to the early peak warmth of other interglacials that lead to an early melting of continental ice sheets, such a late climate optimum is likely to have allowed the persistence of substantial ice masses far into the interglacial.

Further similarities emerge when comparing the chronologies of the OHO and the 8.2 ka event. Based on palynological analyses of laminated lake sediments from central and northern Europe (i.e., following the same approach here taken to investigate the OHO), the vegetation regression caused by the 8.2 ka event lasted for less than 150 years, whereas the entire perturbation (i.e., regressive and recovery phases combined) had a duration of ~300 years (Tinner and Lotter, 2001; Veski et al., 2004). Ice-core data from Greenland suggest that the temperature anomaly of the 8.2 ka event had a duration of ~150 years, with the cooling lasting for ~80 years; the latter phase is divided into a 20-year-long temperature drop and a subsequent 60-year-long interval of minimum values (Kobashi et al., 2007). These figures are well in agreement with those found for the OHO (Table 4.2; see also Section 4.3.2).

A systematic comparison of the absolute temperature declines associated with the 8.2 ka event and the OHO is difficult because the available data are based on different reconstruction methods. Pollen-derived temperature reconstructions for the Holsteinian from the Lüneburger Heide region (northern Germany) suggest a mean January temperature decline of ~5 °C during the OHO, whereas the mean July temperature remained essentially stable (Kühl and Litt, 2007). Even if the uncertainty in the absolute temperature values is taken into account, these data suggest unequivocally that the temperature setback of the OHO was characterized by winter cooling, with the effect that seasonality strongly increased. For the 8.2 ka event, proxy evidence generally yields a cooling of up to 2 °C over central Europe both for winter and summer (Klitgaard-Kristensen et al., 1998; von Grafenstein et al., 1998; Magny et al., 2001; Heiri et al., 2003, 2004). However, the seasonal significance of the used proxies, which is strongly skewed towards the summer season, must be taken into account when evaluating these data (Alley and Ágústsdóttir, 2005; Rohling and Pälike, 2005; Lotter et al., 2010). In fact, the event appears to be connected to increased seasonality mainly driven by wintertime cooling (Baldini et al., 2002; Alley and Ágústsdóttir, 2005; Denton et al., 2005; Pross et al., 2009). Hence, both the 8.2 ka event and the OHO were associated with a pronounced seasonality increase mainly caused by a drop in winter temperatures.

A comparison of the vegetation response to the climate change associated with the OHO and the 8.2 ka event is hampered by the fact that data for the OHO are only available for western, central, and eastern Europe north of 50⁰ latitude. Nevertheless, it allows important insights into the similarity of both events. The 8.2 ka event influenced vegetation dynamics across Europe from Scandinavia to the Mediterranean Sea. The magnitude of the impact on vegetation (i.e., the decline of temperate taxa) varies geographically due to differences in the intensity of climate forcing and local environmental factors (e.g., Tinner and Lotter, 2001, 2006; Veski et al., 2004; Seppä et al., 2007; Pross et al., 2009). Vegetation dynamics resulting from the OHO impact in northern Europe exhibit a transient increase in pioneer trees at the expense of temperate trees, *Alnus*, and locally also of *Picea*. During the 8.2 ka event, northern Europe (i.e., Denmark, the Baltic states and Scandinavia) experienced similar vegetation dynamics (Veski et al., 2004; Seppä et al., 2007; Sarmaja-Korjonen and Seppä, 2007; Hede et al., 2009; Paus, 2010).

Reconstructions of the hydrological changes connected to the 8.2 ka event in Europe suggest a tripartite spatial pattern (Magny et al., 2003; Fletcher et al., 2010). In particular, central Europe (between 43⁰ and 50⁰ latitude) experienced wetter conditions, whereas northern Europe and the Mediterranean region became drier. Although the lack of highly resolved Holsteinian climate records from the Mediterranean region does not allow such a differentiation during the OHO, the available data indeed suggest drier conditions associated with the OHO north of 50⁰ latitude. In addition, the absence of the OHO in pollen records from the mountainous regions of central Europe may be attributed to the expansion of tree taxa that are competitive during cooler and wetter conditions such as *Abies*.

Criterion	8.2 ka event	OHO (~408 ±0.5 ka)
Timing after onset of interglacial forestation	~6300 years [1,2]	6000 ±500 years
Sea level below present	~20 m [3]	~20 m [3]
Duration of climate regression	~80 years [4]	90 years
Duration of vegetation regression and recovery	~300 [5,6]	220 years
Temperature decline	T_{winter} and T_{summer}: 1 – 2 ºC [7-10]	T_{Jan} ~5 ºC / T_{Jul} ~0 ºC [11]
Climate pattern in Europe	northern Europe: cold and dry mountainous central Europe: cold and wet [12,13]	northern Europe: cold and increasingly drier towards East mountainous central Europe: possibly wetter

Table 4.2: *Comparison between the OHO and the 8.2 ka BP event with regard to timing, boundary conditions, characteristics and impact. [1] Lowe et al. (2008); [2] Lotter et al. (2010); [3] Rohling et al. (2010); [4] Kobashi et al. (2007); [5] Tinner and Lotter (2001); [6] Veski et al. (2004); [7] Klitgaard-Kristensen et al. (1998); [8] von Grafenstein et al. (1998); [9] Magny et al. (2001); [10] Heiri et al. (2003, 2004); [11] Kühl and Litt (2007); [12] Magny et al. (2003); [13] Wiersma and Renssen (2006).*

Summarizing the above, the available data indicate that the OHO has a strong resemblance to the 8.2 ka event (Table 4.2). Both oscillations took place under similar boundary conditions

with regard to sea level (and thus the volume of continental ice sheets) about 6-6.5 ka after the onset of the reforestation by pioneer trees. The two events also bear strong similarities with respect to vegetation dynamics, notably the duration and intensity of the regressive phase. Moreover, the climate change connected to both events exhibits a similar spatial pattern across central and northern Europe, with a regional differentiation of cooling and moisture availability.

4.7 Trigger mechanism of the OHO

The decline of temperate taxa during the OHO took place within 90 years (Fig. 4.2). Thus, fire (Turner, 1970) or volcanism (Diehl and Sirocko, 2007) can be ruled out as forcing factors because they would have had an immediate and less selective impact on vegetation. Both temporal and spatial vegetation changes associated with the OHO impact suggest a forcing mechanism that caused a winter cooling over northern Europe for several decades. Such cooling points to a short-term decrease of North Atlantic heat transport.

Considering the role of Atlantic heat transport as a key driving mechanism for European climate (e.g., Broecker, 1997; von Grafenstein et al., 1999) and in view of the striking resemblance of the climatic impact of the OHO and the 8.2 ka event, we suggest that the triggering of the OHO may be attributed to a transient slowdown of the NADW formation at ~408 ka BP during the second insolation maximum of MIS 11c. In analogy to the 8.2 ka event, this slowdown may have been caused by freshwater input into the North Atlantic derived from the decay of substantial land-based ice shields that persisted during this interval. Supporting evidence for instabilities in NADW formation during MIS 11c comes from the considerable variability in oxygen isotope values from several marine records in the North Atlantic (Oppo et al., 1998; Poli et al., 2000; Desprat et al., 2005; Martrat et al., 2007). The temporal resolution of these records is, however, too low to allow a reliable correlation with the OHO.

Our results suggest that meltwater-forced slowdown of NADW formation may be a more common agent of climatic forcing during interglacials than previously thought. The occurrence of a probably meltwater-induced climate setback associated with the deglaciation processes during MIS 11 (Termination V) raises the question when and why such events happen. Long oxygen-isotope records from speleothems in China suggest that slower and smaller rises in northern hemisphere summer insolation resulted in prolonged terminations punctuated by stadial events (i.e., Terminations I and III; Cheng et al., 2009). Relatively low summer insolation shifts and rates of northern summer insolation change during Termination V (Berger and Loutre, 1991) have also caused a prolongation of the deglaciation until the second MIS 11c insolation peak (Rohling et al., 2010). Taking these observations a step further, we propose that terminations with low amounts and rates of northern summer insolation increase allowed the remains of continental ice sheets in the Northern Hemisphere (such as the Laurentide and Scandinavian ice sheets) to persist much longer under interglacial conditions than when summer insolation rose strongly and rapidly. Therefore, meltwater-induced climate oscillations during interglacial conditions occurred preferentially

when low shifts and rates of summer insolation increase during glacial terminations facilitated the existence of substantial continental ice sheets well into interglacials.

4.8 Concluding remarks

Our study documents that a short-term climate oscillation during the Holsteinian interglacial caused pronounced vegetation turnover across substantial parts of Europe. Based on a varved pollen record from Dethlingen, northern Germany, this turnover and the subsequent recovery occurred within 220 years. During this "Older Holsteinian Oscillation" (OHO), particularly cold winters occurred in Europe north of 50º latitude, temperature and moisture availability decreased, and continentality was increased towards eastern Europe, all suggesting a weaker influence of the westerlies and/or a stronger influence of the Siberian High towards the East. The absence of the OHO from pollen records from mountainous regions of central Europe suggests that vegetation response to the climate forcing was only weak and/or beneficial for specific tree taxa, thereby resulting in a different expression of the OHO in the pollen spectra. Because the OHO closely resembles the 8.2 ka event with regard to the timing within the respective interglacials, the volume of continental ice sheets present, the spatial pattern of the climatic impact, and the duration, we suggest the forcing mechanisms for the OHO and the 8.2 ka event to be similar. Thus, in analogy to the 8.2 ka event, a meltwater-induced slowdown of North Atlantic Deep Water formation appears as the most likely source for the OHO.

For future research, we suggest that the spatial extent of the OHO should be further constrained. In such an effort, particular emphasis should be placed on high-resolution studies of marine records from the Nordic Seas. In the terrestrial realm, searching for the OHO climate anomaly may be particularly promising in southern Europe (and notably the northeastern Mediterranean region); climate archives from that region have been shown to closely reflect North Atlantic climate dynamics both on decadal (e.g., Rohling et al., 2002; Kotthoff et al., 2008a; Pross et al., 2009) and centennial to millennial (e.g., Wijmstra and Smit, 1976; Fleitmann et al., 2009; Kotthoff et al., 2011; Müller et al., 2011) time scales. A better constrained spatial extent of the OHO will allow deeper insights into the influence of the North Atlantic on, and into latitudinal and longitudinal climate gradients across Europe during MIS 11.

4.9 Acknowledgements

4.10 Supplementary Information

4.10.1 Biostratigraphical correlation and position of the Older Holsteinian Oscillation

Based on a characteristic vegetation succession (i.e., an early *Taxus* phase along with the occurrence of *Picea* and a subsequent *Carpinus-Abies* phase associated with the occurrence of *Buxus*, *Fagus* and *Pterocarya*), a biostratigraphical correlation of the Holsteinian interglacial in Germany with the Hoxnian interglacial on the British Isles and the Mazovian interglacial in Poland is generally well accepted (see discussion in Koutsodendris et al., 2010, and references therein).

The Older Holsteinian Oscillation (OHO) is identified in Holsteinian pollen records predominantly by (i) a sharp decline of *Corylus* and *Taxus* percentages accompanied by a decline of other temperate tree taxa (e.g., *Quercus*, *Carpinus*, *Ulmus*, *Fraxinus*) and partially also of *Alnus* and *Picea*, and (ii) a strong increase of *Pinus*, *Betula* and non-arboreal pollen (NAP) that in some localities is accompanied by an increase of *Larix*, *Juniperus* and *Picea*. Palynostratigraphically, this prominent vegetation turnover occurs before the onset of the *Carpinus-Abies* phase of the Holsteinian interglacial; at the same time, it terminates the expansion of *Taxus* in central Europe. The OHO is known to occur across wide parts of central Europe and has repeatedly been used as a biostratigraphic marker for the internal correlation of Holsteinian pollen records (e.g., Turner, 1970; Müller, 1974; Bińka and Nitychoruk, 1995; Krupiński, 1995, 2000; Thomas, 2001; Kukla, 2003; Geyh and Müller, 2005, 2007; Nitychoruk et al., 2006; Diehl and Sirocko, 2007).

The correlation of the Holsteinian with the Hoxnian and Mazovian interglacials and the identification of the individual positions of the OHO in these interglacials are based on the well-established palynostratigraphic correlations between the classical sites of Munster-Breloh (Müller, 1974) and Hetendorf (Meyer, 1974) from the Lüneburger Heide region, northern Germany, and sites on the British Isles and in Poland (Fig. 4.5). A brief account of the establishment of these correlations is given in the following:

 (a) Geyh and Müller (2007) have provided a detailed correlation of the pollen zones from Munster-Breloh and Hetendorf with those from Hoxne and Marks Tey (West, 1956; Turner, 1970) on the British Isles, and from Woskrzenice, Poland (Bińka and Nitychoruk, 1995). Based on this correlation, the stratigraphic position of the OHO within the individual interglacial sequences can be confidently identified in the pollen records from Barford, Dethlingen, Hoxne, Hummelsbüttel, Kaliłów, Marks Tey, Munster-Breloh, and Woskrzenice.

 (b) Diehl and Sirocko (2007) have correlated the pollen zones from Munster-Breloh and Hetendorf with the zonation scheme of Erd (1970) that has been regionally used for a number of Holsteinian sites in northern Germany over the past 30 years. This correlation allows to determine and compare the stratigraphic position of the OHO in the pollen records from Döttingen, Delitzsch-Wölkau, Gröbern-Schmerz, and Rossendorf.

 (c) Krupiński (1995) has correlated the pollen zones from Komarno and Ossówka (Poland) with those from the Lüneburger Heide region (Meyer, 1974; Müller, 1974), thus allowing

to compare the stratigraphic position of the OHO between Northern Germany and Poland. Based on the work of Krupiński (2000), who correlated c. 70 pollen records of the Mazovian (i.e., Holsteinian) interglacial in Poland, the position of the OHO can be further identified in the pollen record from Nowiny Żukowskie.

(d) Thomas (2001) provided a correlation of Hoxnian pollen records from England. Based on this study, the OHO can be identified in the records from Athelington and Nechells.

(e) Müller (1974) identified the OHO in the pollen record from Ober-Ohe (northern Germany) based on the expansion of *Pinus* and *Betula* at the expense of *Corylus* and from Vejlby (Denmark) based on a strong increase of *Pinus.*

Table 4.3 gives a short description of the OHO characteristics for all sites evaluated in the present study.

	N. Germany	England	Poland	N. Germany	N. Germany	Poland	
Interglacial name	Holsteinian	Hoxnian	Mazovian	Holsteinian	Holsteinian	Mazovian	
Pollen zones by	Müller, 1974; Meyer, 1974	Turner, 1970	Bińka and Nitychoruk, 1995	Diehl and Sirocko, 2007	Erd, 1970	Krupiński, 1995, 2000	
Sites	Munster-Breloh; Hetendorf	Hoxne; Marks Tey	Woskrzenice	Döttingen	Pritzwalk-Prignitz	Ossówka	
Pollen zones		XV	e Gi I		7b	Fuhnian	K	
		XIV	Ho IV b	*Carpinus-Abies* b-e	7a	7	J	M9
		XIII	Ho IV a		5 - 6		H	M8
		XII	Ho III b		4 c-d	5 - 6		
		XI						
		X	Ho III a	*Carpinus-Abies* a	4b	4	G	M7
		IX		*Pinus-Larix* d				
OHO		VIII	Ho II c	*Pinus-Larix* c	4a		F	M6
		VII		*Pinus-Larix* a -b	3 a-b	3	E	M5
		VI	Ho II b	*Taxus*	2	2	D	M4
		V	Ho II a	*Pinus-Alnus*			C	M3
		IV			1b		B	M2
		III	Ho I	*Pinus-Betula*	1a	1	A	M1
		II						
		I	L Lo	*Juniperus - Hippophae*			Ao	

Figure 4.5. *Schematic summary of palynostratigraphic correlation of the Holsteinian, Hoxnian and Mazovian interglacials in central Europe. Position of arrows indicates correlation between individual regions. Grey bar marks the position of the OHO.*

Site code	Site name	Country	Latitude/Longitude	Altitude (m)	OHO at LPZ	decline	increase	Reference
Ve	Vejlby	Denmark	56º 04' N / 12º 08' E	0-50	5	*Alnus*, *Taxus*, *Ulmus*, *Ilex*	*Pinus, Picea, Juniperus, Betula*, NAP	Andersen, 1965
Hm	Hummelsbüttel	Germany	53º 38' N / 10º 02' E	0-50	VIII	*Alnus* (~25%), *Taxus* (>10%), *Corylus* (>5%), *Fraxinus*, *Quercus*	*Pinus* (~30%), *Picea* (>5%), *Betula*, *Juniperus*	Averdieck, 1992
MB	Munster-Breloh	Germany	53º 01' N / 10º 04' E	50-100	VIII	*Alnus* (~20%), *Corylus* (~10%), *Taxus* (~5%), *Quercus*, *Picea*	*Pinus* (up to 60%), *Betula* (~7%), NAP	Müller, 1974; Geyh and Müller, 2007
De	Dethlingen	Germany	52º 57' N / 10º 08' E	50-100	VIII	see Section 4.3.2 for a detailed description		this study
OO	Ober-Ohe	Germany	52º 53' N / 10º 10' E	50-100	-	*Corylus*, *Alnus*, *Quercus*, *Carpinus*,	*Pinus*, *Betula*, NAP	Gistl, 1928 (revised by Müller, 1974)
Ba	Barford	England	52º 37' N / 01º 07' E	0-50	Ho IIc	*Corylus*, *Taxus*, *Quercus*, *Ulmus*	NAP, *Pinus*, *Betula*	Phillips, 1976
Ne	Nechells	England	52º 30' N / 01º 51' W	50-100	IIN.b	*Quercus* (~30%), *Fraxinus*	*Betula* (~30%), NAP (~20%), *Juniperus*	Kelly, 1964
Ho	Hoxne	England	52º 20' N / 01º 12' E	0-50	Ho IIc	*Corylus*, *Quercus*, *Alnus*, *Taxus*, *Ulmus*	*Pinus*, *Betula*, NAP	West, 1956; Turner, 1970
At	Athelington	England	52º 17' N / 01º 14' E	0-50	Ho IIc2	*Corylus*, *Ulmus*	NAP (~18%)	Coxon, 1985
Ko	Komarno	Poland	52º 09' N / 24º 06' E	100-200	F	*Taxus* (>10%), *Alnus* (~10%), *Picea* (~10%), *Corylus*, *Quercus*, *Carpinus*	*Pinus* (~20%), *Betula*, *Larix*, NAP	Krupiński, 1995
Os	Ossówka	Poland	52º 07' N / 23º 09' E	100-200	F	*Taxus* (>10%), *Alnus* (~10%), *Picea* (~7%), *Corylus*, *Quercus*, *Carpinus*	*Pinus* (~25-30%), *Betula* (~10-15%), *Larix*, NAP	Krupiński, 1995
Ka	Kaliłów	Poland	52º 04' N / 23º 13' E	100-200	*Pinus-Larix* c	*Alnus*, *Carpinus*, *Corylus*, *Quercus*, *Picea*	*Pinus*, *Betula*, *Larix*, NAP	Bińka and Nitychoruk, 1996
Wo	Woskrzenice	Poland	52º 03' N / 23º 16' E	100-200	*Pinus-Larix* c	*Alnus*, *Picea*, *Carpinus*, *Corylus*, *Quercus*, *Taxus*	*Pinus*, *Betula*, *Larix*, NAP	Bińka and Nitychoruk, 1995
MT	Marks Tey	England	51º 52' N / 00º 47' E	0-50	Ho IIc	*Corylus* (>30%), *Taxus* (~12%), *Alnus* (~10%), *Quercus* (~5%), *Ulmus* (~4%)	NAP (~20%) *Betula* (~7%), *Pinus* (~4%)	Turner, 1970
GS	Gröbern-Schmerz	Germany	51º 40' N / 12º 28' E	100-150	3 to 4	*Taxus*, *Corylus*, *Fraxinus*, *Picea*	*Pinus*, *Betula*, NAP	Eissmann, 2002; Kühl and Litt, 2007
DW	Delitzsch-Wölkau	Germany	51º 31' N / 12º 20' E	50-100	4	*Alnus*, *Corylus*, *Quercus*, *Taxus*, *Carpinus*, *Fraxinus*, *Picea*	*Pinus* (>25%), *Betula*	Dassow, 1987
NZ	Nowiny Żukowskie	Poland	51º 04' N / 22º 45' E	100-200	NŻ$_{05}$8	*Picea* (~19%), *Alnus*, *Carpinus*, *Corylus*, *Taxus*, *Quercus*, *Fraxinus*	*Betula* (~20%), *Pinus* (~20%), *Larix*	Hrynowiecka-Czmielewska, 2010
Ro	Rossendorf	Germany	51º 03' N / 13º 56' E	300	3 to 4	*Corylus*, *Alnus*, *Quercus*, *Fraxinus*	*Pinus*, *Picea*, *Betula*, NAP	Erd et al., 1987
Dö	Döttingen	Germany	50º 35' N / 07º 12' E	500	4a	*Corylus* (~30%), *Taxus* (~7%), *Alnus* (~5%), *Quercus* (~2.5%), *Carpinus* (~2%)	*Pinus* (~15%), *Betula* (~10%), NAP (~10%), *Picea* (~8%)	Diehl and Sirocko, 2007

Table 4.3. *Major vegetation characteristics during the OHO at individual sites. LPZ: local pollen zone; NAP: non-arboreal pollen.*

Chapter 5. Impact of Lateglacial cold events on the northern Aegean region reconstructed from marine and terrestrial proxy data

Ulrich Kotthoff[1,2], Andreas Koutsodendris[1], Jörg Pross[1], Gerhard Schmiedl[2], André Bornemann[3], Christian Kaul[3], Gianluca Marino[4], Odile Peyron[5], Ralf Schiebel[6,7]

[1] Paleoenvironmental Dynamics Group, Institute of Geosciences, Goethe University Frankfurt, Altenhöferallee 1, D-60438 Frankfurt, Germany; [2] Geological-Palaeontological Institute, University of Hamburg, Bundesstraße 55, D-20146 Hamburg, Germany; [3] Institute of Geophysics and Geology, University of Leipzig, Talstraße 35, D-04103 Leipzig, Germany; [4] Universitat Autònoma de Barcelona (UAB), Institut de Ciència i Tecnologia Ambientals (ICTA), 08193 Bellaterra (Cerdanyola del Vallès), Spain; [5] Laboratoire de Chrono-Environnement, UMR-UFC/CNRS 6249 USC INRA, University of Franche-Comté,16 Route de Gray, F-25030 Besançon, France; [6] National Oceanography Centre, University of Southampton Waterfront Campus, European Way, Southampton SO14 3ZH, United Kingdom; [7] University of Angers, Laboratoire des Bio-Indicateurs Actuels et fossiles, UPRES EA 2644, UFR Sciences, 2 bd Lavoisier, 49045 Angers Cedex 01, France

Abstract: *Marine palynomorph data paired with other indicators of sea-surface hydrography (planktic foraminiferal assemblages and oxygen isotopes) were used to decipher the impact of cold events on the northern Aegean region during the last glacial to interglacial transition. The data, which were derived from marine sediment cores GeoTü SL152 and GeoTü SL148, point to a strong impact of the Heinrich 1 and Younger Dryas cold events on surface-water conditions in the northern Aegean Sea. Shifts in marine palynomorph assemblages correlate with changes in terrestrial vegetation and climate (i.e., precipitation and temperature reconstructions based on pollen assemblages) in the northern borderlands of the Aegean Sea. The climate responses of the Aegean region to the Heinrich 1 (H1, ~17.5 ka to ~15.7 BP) and Younger Dryas (~12.6 to ~11.7 ka BP) events appear similar in magnitude (with mean annual temperatures between ~6 and 10 ºC and mean annual precipitation between ~300 and ~450 mm). However, the annual temperature decline during the H1 event relative to the preceding already cold conditions was minor (<3 ºC). The transition from the relatively warm and humid local equivalent of the Allerød interstadial to the Younger Dryas, on the other hand, witnessed an annual temperature decline of 6 ºC and an annual precipitation decrease of 300 mm, the latter occurring abruptly within only ~150 years. The return to warmer conditions in the northern Aegean region after the Younger Dryas was completed at ~11.6 ka BP.*

Key words: *land-sea correlation; temperature changes; Heinrich event 1; Younger Dryas; Lateglacial; eastern Mediterranean.*

5.1 Introduction

Marking the transition from glacial to present-day interglacial conditions, the late Pleniglacial/Lateglacial interval (coeval with late Marine Isotope Stage 2) was punctuated by a series of millennial-scale climate oscillations that affected the ocean-atmosphere system on an interhemispheric scale (e.g., Waelbroeck et al., 2001; Barker et al., 2009). In the Northern Hemisphere, the last glacial maximum was followed by a severe cold interval (i.e., Heinrich 1 event (H1), ~17 to ~15 ka BP; e.g., Bond et al., 1993), an abrupt shift to warmer conditions connected to the Bølling (~14.5 to ~13.8 ka BP, synonymous with the "Meiendorf interstadial" in central Western Europe; e.g., Litt et al., 2001) and Allerød interstadials (~13.7 to ~11.7 ka BP), and a return to cold conditions during the Younger Dryas (YD, also regarded as event GS 1 in Greenland ice cores; ~12.7 to ~11.7 ka BP; e.g., Björck et al., 1998; Lowe et al., 2008). The latter oscillation precedes the final transition to the interglacial conditions of the early Holocene.

Heinrich 1 and the YD had a significantly stronger impact and lasted much longer than the climate deteriorations punctuating the Holocene (Broecker, 2000). This has been shown by a number of climate records from different archives, such as ice-core data from Greenland (e.g., Björck et al., 1998), lake-sediment records from western Europe (Litt et al., 2001; Brauer et al., 2008b), marine sediment cores from the Atlantic Ocean (e.g., Waelbroeck et al., 2001), the western Mediterranean (e.g., Cacho et al., 1999) and western Africa (Weldeab et al., 2007; Mulitza et al., 2008), and speleothem data from Asia Minor (Fleitmann et al., 2009).

Heinrich 1 and the YD are probably related to a decrease in oceanic heat transport to the northern high latitudes as a result of enhanced freshwater influx to the North Atlantic (e.g., Bond et al., 1993; McManus et al., 2004; Broecker, 2006). Both the H1 and the YD events show durations in the same order of magnitude (~1.2 to ~2.0 ka), which distinguishes them from other, shorter-termed cold events during the late Pleniglacial and Lateglacial (e.g., the Oldest and Older Dryas). However, while the H1 event occurred under glacial boundary conditions, the YD interrupted an interval of near-interglacial climate, pre-dating the last summer insolation maximum of the Northern hemisphere by merely ~1.5 ka (at ~11 ka BP; e.g., Berger and Loutre, 1991).

The eastern Mediterranean region represents an ideal area to study and compare the impacts of these climate events. It has been repeatedly demonstrated that the Aegean region reacts sensitively to short-termed and muted episodes of climate change under the interglacial boundary conditions of the Holocene (e.g., Rohling et al., 2002; Kotthoff et al., 2008a, b; Pross et al., 2009; Marino et al., 2009). Furthermore, the Aegean Sea is an important region for deep-water formation, and climate changes in the Aegean region affect the thermohaline circulation in the entire eastern Mediterranean Sea (e.g., Theocharis et al., 1999; Marino et al., 2007).

To date, several records from the Aegean Sea and its borderlands (e.g., Aksu et al., 1995; Lawson et al., 2005) have allowed analysing the regional expression of the YD to some

degree. However, many of these records lack robust chronologies (see Rossignol-Strick, 1995; Kotthoff et al., 2008b), which hampers the unequivocal identification of the YD. Sedimentological, micropaleontological and palynological records from the northern Aegean Sea indicate that the YD had a strong impact on the marine and terrestrial environments in this area (Aksu et al., 1995; Ehrmann et al., 2007; Kuhnt et al., 2007; Kotthoff et al., 2008a). In the marine realm, the intermediate and deep-water formation was strengthened due to the return to colder conditions (e.g., Kuhnt et al., 2007), while in the terrestrial realm, the YD caused a rapid decline in forest cover and an increase in steppe elements between ~12.7 and ~11.7 ka BP (Kotthoff et al., 2008a).

In contrast, the impact of the H1 event on terrestrial and marine environments of the Aegean region has yet remained poorly constrained; in particular, there is a lack of climate data for the terrestrial realm during the H1 interval. Investigations based on marine sediments have suggested that the H1 did not significantly affect the northern Aegean region (Hamann et al., 2008). This finding appears difficult to reconcile with the evidence that even the relatively low-amplitude climate fluctuations of the Holocene left a clear imprint on terrestrial and marine environments of the Aegean region (e.g., Rohling et al., 2002; Kotthoff et al., 2008a, b; Pross et al., 2009; Marino et al., 2009).

In light of the above, we here present new organic-walled dinoflagellate cyst and oxygen isotope data in combination with previously published pollen data (Kotthoff et al., 2008a) from marine core SL152 (northern Aegean Sea), integrated with new planktic foraminifer census count and previously published oxygen isotope data from neighbouring core SL148. The pollen data from core SL152 have been complemented by previously unpublished quantitative reconstructions for annual precipitation and temperature. Our multi-proxy approach yields a comprehensive view of the impact of late Pleniglacial and Lateglacial climate events, notably the H1 and the YD, on both terrestrial and marine ecosystems in this climatically highly sensitive region.

5.2 Regional setting

The Aegean Sea is semi-isolated from the rest of the Mediterranean Sea and characterized by a complex bathymetry, with large shelf areas in the North and Northeast (Fig. 5.1; Perissoratis and Conispoliatis, 2003). In the South, it is connected to the Levantine and Ionian Seas through several seaways. In the Northeast, there is a connection to the Black Sea via the Dardanelles, the Sea of Marmara and the Bosporus (Fig. 5.1).

The present-day wind field in the Aegean region is characterized by northerly directions, with cold and dry Arctic/polar outbreaks during winter and spring months (Poulos et al., 1997; Fig. 5.1). In comparison to the sediment supply by rivers, aeolian sediment influx is quantitatively negligible (Chester et al., 1977; Ehrmann et al., 2007). Significant suspension loads are carried into the Aegean Sea by several rivers, notably from its northern borderlands (Ehrmann et al., 2007; Kotthoff et al., 2008b; Fig. 5.1); to a lesser extent, riverine input of terrigenous material is derived from western Asia Minor, e.g., via the Kara Menderes and Gediz rivers. Outflow of Black-Sea surface water represents an additional source for

suspended terrigenous material (e.g., Lane-Serff et al., 1997; Çağatay et al., 2000). According to Sperling et al. (2003), the connection of the Aegean Sea and the Sea of Marmara was probably already established at ~14 ka BP, and Verleye et al. (2009) date the establishment of a connection between the Black Sea and Sea of Marmara at ~8.2 ka BP. In any case, it was probably not until ~6.5 ka BP that the marine connection between the Aegean and Black Seas was fully established (Sperling et al., 2003; Ehrmann et al., 2007). The present-day outflow of Black Sea surface water into the Aegean Sea amounts to ~400 km³/yr, with highest values during the late spring and summer months (Aksu et al., 1995). Surface-water temperature and salinity values in the Aegean Sea show a pronounced Northeast-Southwest gradient, with lower values in the North (Aksu et al., 1995).
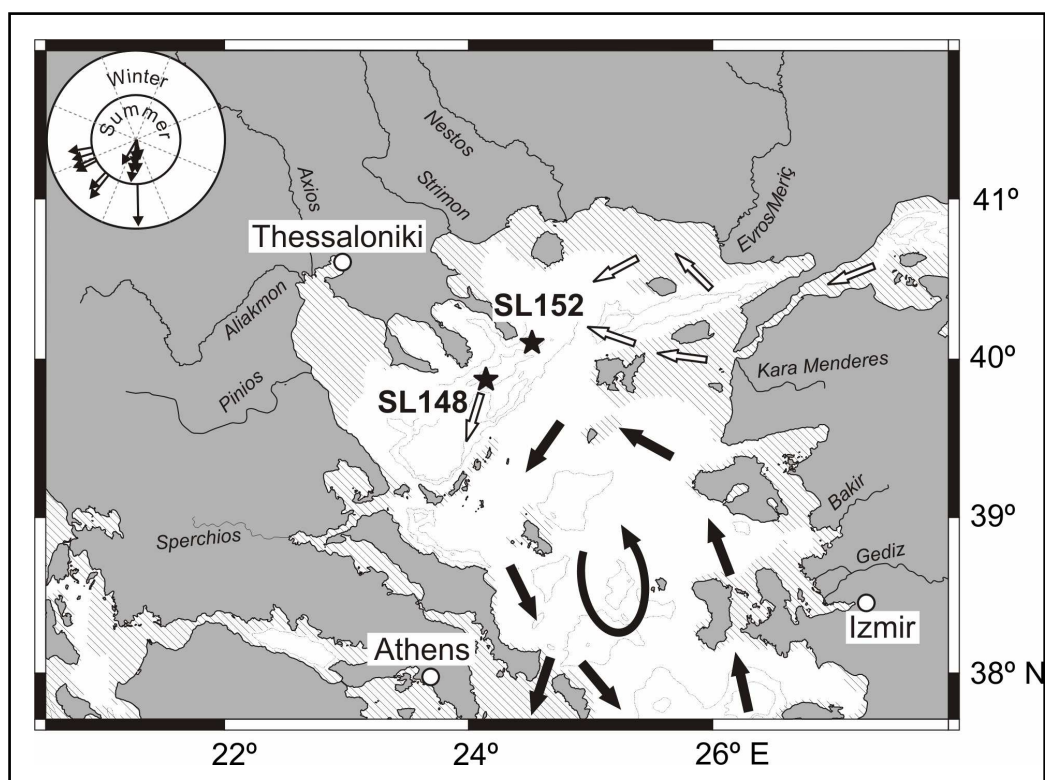
Figure 5.1: *Map of the Aegean region. Black stars mark the locations of cores GeoTü SL152 and SL148. Hatched area indicates shelf exposed between ~19 to ~15 ka BP (after Cramp et al., 1988; Aksu et al., 1995; Perissoratis and Conispoliatis, 2003), isolines show water depths of 600 and 1000 m. White arrows indicate low salinity Black Sea surface water flow, black arrows indicate warm and high salinity surface water circulation, following Aksu et al. (1995), Lykousis et al. (2002) and Ehrmann et al. (2007). Wind directions (following May, 1982; Poulos et al., 1997) over the Aegean region during summer and winter are indicated on the top left.*

5.3 Material and methods

Cores GeoTü SL152 (40º 05.19' N, 24º 36.65' E, water depth 978 m) and GeoTü SL148 (39º 45.23' N, 24º 05.78' E, water depth 1094 m) have been retrieved in 2001 during R.V. *Meteor* cruise M51/3 from the Mount Athos Basin, northern Aegean Sea, ca. 200 km SE of Thessaloniki (Fig. 5.1). The two sites are very close to one another, with the distance amounting to ~50 km. Here we present centennial-scale-resolution (~150 years) dinocyst

and planktic foraminiferal oxygen-isotope data, and quantitative pollen-based terrestrial climate data from core GeoTü SL152 (SL152) comprising the time interval from ~19 to ~9 ka BP. These data are integrated with planktic foraminiferal census counts and oxygen-isotope data from core GeoTü SL148 (temporal resolution: ~300 years). The selected time interval comprises the late Pleniglacial to the earliest Holocene. In-depth information on the terrestrial palynomorph assemblages and sedimentology of core SL152 has been previously provided by Kotthoff et al. (2008a, b). Detailed information on the sedimentary characteristics and benthic foraminiferal assemblages from core SL148 is given by Ehrmann et al. (2007) and Kuhnt et al. (2007).

5.3.1 Age model

The chronology of core SL152 is based on eight ^{14}C accelerator mass spectrometry dates obtained from *Globigerinoides ruber* (white) and, in case that not enough *G. ruber* material was available, from *Globigerina bulloides*, other surface-dwelling foraminifera and pteropods. Detailed information on the age model of core SL152 is given in Kotthoff et al. (2008a, b). Three ^{14}C dates for core SL148 were obtained from *G. ruber*, *G. bulloides*, *Globigerinoides sacculifer*, *Neogloboquadrina incompta*, and *Turborotalita quinqueloba*. Details on the age model of core SL148 are provided by Ehrmann et al. (2007). For both cores, local reservoir-age corrections were applied following Siani et al. (2001; generally 400 yr), and conversions to calendar ages were carried out via the radiocarbon calibration software of Fairbanks et al. (2005). Both age models have been shown to be internally consistent (Kotthoff et al., 2008a, b; Fig. 5.2).
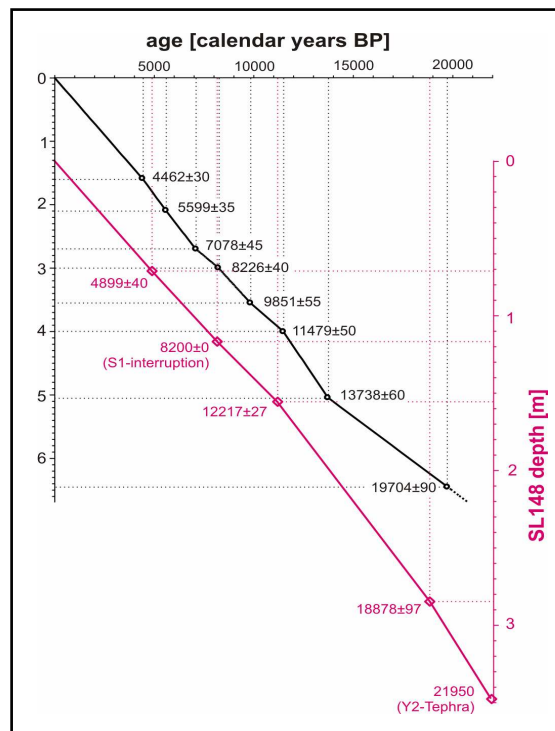
Figure 5.2: *Comparison of the age models of core GeoTü SL152 (Kotthoff et al. 2008a) and core GeoTü SL148 (Kuhnt et al., 2007). In both cases, the ages are reservoir-corrected (following Siani et al., 2001) and converted to calendar ages (via the radiocarbon calibration software of Fairbanks et al., 2005).*

5.3.2 Analyses from core SL152

5.3.2.1 Palynomorphs

For the analysis of terrestrial and marine palynomorph assemblages, samples were taken from the interval between 6.30 and 3.27 m at a resolution of 1 cm within the sapropelic interval of core SL152. Below the interval of sapropel S1 (S1) (equivalent to ~9.6 to ~7 ka BP; see Kotthoff et al., 2008b), the sample spacing was either 5 or 10 cm. For the time interval discussed here (i.e., 19-9 ka BP), an average temporal resolution of 150 years was achieved. Per sample, 1 to 6 g of sediment were processed using standard palynological techniques (e.g., Pross, 2001).

Whenever possible, at least 300 terrestrial palynomorphs (excluding bisaccate pollen and spores) were determined and counted per sample. Since bisaccate pollen is generally overrepresented in marine pollen assemblages due to its particularly good transport properties and high resistance to oxidation (e.g., Rossignol-Strick and Paterne, 1999), it was excluded from the pollen sums. In general, ~200 (at least 150) organic-walled dinoflagellate cysts (dinocysts) were determined per sample (Fig. 5.3).

5.3.2.2 Pollen-based quantitative climate reconstructions

To support the qualitative pollen-derived climate information, the mean annual temperature (MT_{year}) and mean annual precipitation (MP_{year}) were calculated from pollen data using the Modern Analogue Technique (MAT; e.g., Guiot, 1990). Originally developed for continental pollen records, the MAT has been successfully applied to marine pollen assemblages (e.g., Sánchez Goñi et al., 2005; Dormoy et al., 2009, Combourieu-Nebout et al., 2009). The MAT reconstructions are based on a database with 2748 modern pollen spectra from Europe (Bordon et al., 2009), updated to 3530 by the addition of modern spectra from the Mediterranean area (Dormoy et al., 2009). Here we used the ten modern assemblages with smallest chord distances for the reconstructions of the climate parameters. Because of its overrepresentation in marine pollen assemblages, bisaccate pollen was removed from the evaluated samples and the database (see also Section 5.3.2.1).

5.3.2.3 Stable isotopes

Fourty-four samples from core SL 152 were analyzed for planktic foraminiferal oxygen-isotope ratios. In 25 samples, the summer-mixed–layer-dwelling *Globigerinoides ruber* (white) was measured. Due to the low abundance of *G. ruber* in the late Pleniglacial and Lateglacial sediments of core SL152, the sub-thermocline-dwelling *Neogloboquadrina incompta* was additionally used for the time interval from 17 to 12 ka BP.

Samples for planktic foraminifera were wet-sieved over a 63-μm mesh with tap water. *N. incompta* and *G. ruber* were hand-picked from the >150-μm fraction. Specimens were cleaned with de-ionized water and ultrasound for three seconds. Isotope analyses were carried out on batches of 5-10 specimens on a PDZ Europa Geo 20-20 mass spectrometer with individual acid-bath carbonate preparation (orthophosphoric acid reaction at 70 ºC), at the National Oceanography Centre, Southampton. Isotope ratios are expressed relative to

the Vienna PeeDee Belemnite (VPDB). External precision is better than 0.06 ‰ for both δ^{13}C and δ^{18}O. Further samples (*N. incompta*) from the late Pleniglacial and Lateglacial were measured at the Institute of Geosciences, Frankfurt University, using a Flash-EA 1112 connected to the gas-source mass spectrometer MAT 253 (both Thermo-Finnigan). For these results, the external precision is better than 0.06 ‰ for δ^{13}C and 0.08 ‰ for δ^{18}O.

5.3.3 Analyses from core SL 148

5.3.3.1 Planktic foraminiferal assemblages

From core SL148, 35 samples covering the interval between 2.85 and 1.275 m depth have been studied for their content in planktic foraminifera. Samples were usually taken at 5 cm distance, which yields a temporal resolution between ~200 and ~400 yrs. The 4 uppermost samples (1.38 to 1.275 m depth) were taken at 2-2.5 cm distance. Sediment samples were dried, weighed, and washed through a 63 µm screen. The determination of planktic foraminifers was carried out on the size fraction >125 µm. At least 300 specimens were counted per sample.

We distinguished between tropical/subtropical (i.e., warm-water), temperate/transitional, and polar/subpolar (i.e., cold-water) assemblages following Bé and Tolderlund (1971), Hilbrecht (1996) and Kucera (2007). The warm-water assemblage is dominated by *Globigerinoides ruber* (white), *G. sacculifer*, *Globoturborotalita* spp., *Orbulina universa*, and *G. ruber* (pink; in descending order of abundance, Fig. 5.4, Fig. 5.5B). The temperate/transitional assemblage is dominated by *G. bulloides*. The polar/subpolar assemblage comprises mainly *N. incompta* (c.f. Darling et al., 2006), *Turborotalita quinqueloba,* and *N. pachyderma*. Of these forms, *N. pachyderma* prefers the coolest conditions (Hemleben et al., 1989; Hilbrecht, 1996, 1997; Kucera, 2007). *T. quinqueloba* is more frequent at lower sea-surface temperatures than *N. incompta* (Hilbrecht, 1996; Kucera, 2007).

5.4 Results and discussion

5.4.1 Palynomorph preservation

As shown by previous studies, selective degradation affected the palynomorph assemblages from the Aegean Sea, and notably from the Mount Athos Basin, to a much lesser extent than commonly encountered in sediments from the Mediterranean Sea (compare Zonneveld et al., 2001). This is due to the relatively high (>30 cm/ka) sedimentation rates in the Mount Athos basin (Kotthoff et al., 2008a, b).

This view is corroborated by the distribution of dinocysts within core SL152, notably the continuous occurrence of the rather oxidation-resistant taxon *Impagidinium aculeatum* (Sangiorgi et al., 2003) prior to and during S1 deposition. If selective degradation had seriously affected the dinocyst assemblages, *I. aculeatum* should exhibit increased percentages before S1 and during S1 interruptions, as it has been found, e.g., in the Adriatic Sea (Sangiorgi et al., 2003). Instead, changes in *I. aculeatum* percentages do not vary in direct response to the deposition of sapropelic sediments. The determination coefficient

between sediment lightness, which can be used as a total organic carbon (C_{org}) proxy and a means to differentiate between sapropelic and non-sapropelic sediments (see discussion in Kotthoff et al., 2008b), and the percentages of *Impagidinium* is indeed very low (R^2=0.0238, N=66).

Heterotrophic dinocyst taxa (e.g., *Brigantedinium* spp.), often considered particularly sensitive to oxidation (e.g., Zonneveld et al., 2001), show a pronounced abundance increase between ~9.8 and ~9.5 ka BP, which roughly coincides with the onset of S1 (Fig. 5.3). Hence, it could be argued that this abundance pattern reflects the reduced oxidation potential connected to sapropel formation. However, heterotrophic taxa also show almost sapropel-like percentages during the warm phases of the Bølling and Allerød (Fig. 5.3), which to our knowledge have not been featured by reduced bottom water ventilation in the eastern Mediterranean. Thus, the high percentages of heterotrophic taxa during the formation of S1 primarily reflect changes in surface-water conditions such as enhanced nutrient supply rather than enhanced preservation (see Combourieu-Nebout et al., 1998; Sluijs et al., 2005).

5.4.2 Terrestrial palynomorphs and quantitative climate reconstructions

For the interval from ~19 to ~17.5 ka BP, the pollen data from core SL152 suggest cooler and drier conditions in the borderlands of the northern Aegean Sea as compared to present-day conditions. This is qualitatively indicated by relatively high percentages (20-25 %) of steppe element pollen (SEP). Quantitative pollen-based climate reconstructions suggest low annual terrestrial temperatures and precipitation (MT_{year}= ~10 ºC, MP_{year}= ~450 mm). The MT_{year} as reconstructed for the terrestrial realm is in accordance with the results of Hayes et al. (2005), who calculated Aegean Sea surface-water temperatures of ~11 ºC for that time interval by using the artificial neural networks on planktic foraminiferal assemblages.

After 17.5 ka BP, the decrease in NSAP (non-saccate arboreal pollen) percentages is paralleled by a MT_{year} drop of at least 1.5 ºC (Fig. 5.5F). This is followed by an increase in SEP percentages at ~16.5 ka and a decrease in MP_{year} (~100 mm/yr; Fig. 5.5E, G). The MT_{year} remains relatively low until ~15 ka BP. From ~15 to ~12.7 ka BP, NSAP percentages increase to ~40 %. The time interval from ~15 to ~12.7 ka BP is correlative with the tri-partite Bølling/Allerød interval described from Greenland ice cores (compare Björck et al., 1998; Kotthoff et al., 2008a), respectively. Minor relative increases in NSAP (at ~14.5, ~13.7, ~13.5 and ~12.8 ka BP), indicating more humid conditions, correlate well with the Greenland interstadials GI-1e, -1c3, -1c1, and -1a. Our pollen-based quantitative data reveal significantly higher MT_{year} and MP_{year} during that time than during the preceding late Pleniglacial. There are, however, MT_{year} and MP_{year} setbacks.

The following YD is characterized by very high percentages of SEP (up to ~40 %). The reconstructed values for the MT_{year} and MP_{year} are even lower than during the late Pleniglacial (~6 ºC and ~300 mm; Fig. 5.5).

After the YD, the MT_{year} increases rapidly, reaching values typical of the Holocene (~13 ºC) already at ~11.6 ka BP. In the pollen assemblages from core SL152, this warming is paralleled by a rapid decline in SEP percentages. The MP_{year} increases to ~600 mm after the

YD and fluctuates around this level until ~10.5 ka BP. From ~10.5 until ~9.6 ka BP, it increases by another 200 mm. The general trend towards more humid conditions between ~11.7 and ~9.5 ka BP was interrupted by minor setbacks reflected by relatively low NSAP percentages and MP_{year} and MT_{year} decreases at ~11 and ~10.4 ka BP (Fig. 5.5).

5.4.3 Marine proxies

5.4.3.1 Dinocysts

During the late Pleniglacial, particularly between ~18 and ~16 ka BP, *Nematosphaeropsis labyrinthus* dominates the dinocyst assemblages with relative abundances approaching 50 % (Fig. 5.3). Besides being an euryhaline species (Marret & Zonneveld, 2003; Pross et al., 2004), this taxon generally indicates cool surface waters (e.g., Sangiorgi et al., 2002). Similarly, *Spiniferites elongatus* also represents a cool-water indicator (Harland, 1983; Combourieu-Nebout et al., 1998; Marret and Zonneveld, 2003; Marino et al., 2009). Relatively high (>4 %) percentages of *S. elongatus* occur between 17.5 to 16 ka BP (Fig. 5.3), and the combined percentages of the cold-water indicators *N. labyrinthus* and *S. elongatus* are highest at ~16.5 ka BP (Fig. 5.5D). A short-lived peak of *Lingulodinium machaerophorum* and *Operculodinium centrocarpum* precedes the broader maximum of cold-water indicators at ~19 ka BP.

Tectatodinium psilatum and *Spiniferites cruciformis* (results for the latter are not shown here) occur rarely, but consistently since 19 ka BP. This indicates that these species can probably not be used as an indicator for a connection between the Aegean and the Black Sea as previously suggested by Aksu et al. (1995). This is because in light of glacial sea-level dynamics, a linkage of the Aegean Sea and the Black Sea cannot have been established prior to a strong sea-level rise above "glacial" values, probably not earlier than ~10-9 ka BP (Aksu et al., 1995; Major et al., 2006; Bahr et al., 2008) or even later (e.g., Sperling et al., 2003).

After ~16 ka BP, the percentages of cold-water indicators, in particular *N. labyrinthus*, decline, while percentages of the salinity-tolerant taxon *O. centrocarpum* (Combourieu-Nebout et al., 1998; Marret and Zonneveld, 2003) reach peak values at ~15.4 ka BP. During the Bølling and Allerød, between ~14.6 to 12.7 ka BP, *Spiniferites* species dominate the dinocyst assemblages. This interval is furthermore characterized by repeated increases in *S. elongatus* percentages. Heterotrophic taxa (consisting mainly of *Brigantedinium* spp.) show several pronounced peaks at the onset of the Bølling interstadial (~14.5 ka BP), and during the Allerød interstadial (between ~14 to ~13 ka BP).
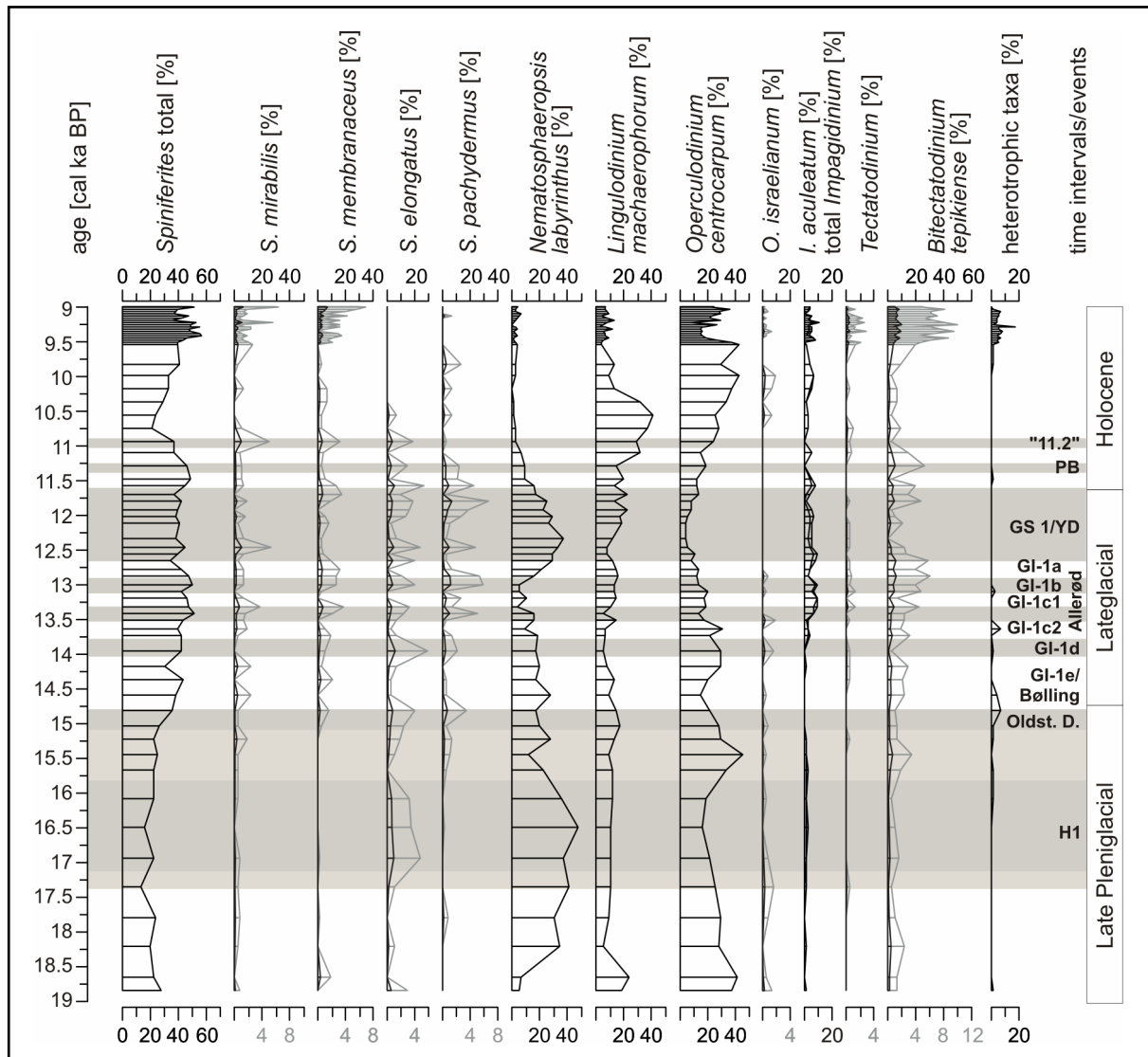
Figure 5.3: *Relative dinocyst abundances in core SL152 vs. age. Grey bars indicate cooling events as indicated in Greenland ice cores and terrestrial proxies from core SL152 (Fig. 5.5, Kotthoff et al., 2008a). 11.2 = 11.2-ka event, PB = preboreal oscillation, GS 1/YD = Greenland stadial 1/Younger Dryas, GI = Greenland interstadial, Oldst. D. = Oldest Dryas, H1 = Heinrich 1 event.*

The YD (~12.6 to ~11.7 ka BP) is characterized by an increase of cold-water indicators at the expense of total *Spiniferites*, *Bitectatodinium tepikiense* and heterotrophic species (Figs. 5.2 and 5.3). Notably, *N. labyrinthus* percentages reach maximum values at ~12.3 ka BP, whereas *S. elongatus* is abundant during the onset (~12.7 to ~12.4 ka BP) and the end of the YD (~12.0 to ~11.8 ka BP).

Between 11.2 and 10.2 ka BP, following a short-term percentage increase of *Spiniferites* species, *L. machaerophorum* dominates the dinocyst assemblages. This taxon indicates estuarine to neritic conditions and occurs under conditions of enhanced sea-surface productivity (e.g., Wall et al., 1977; Combourieu-Nebout et al., 1998; Marret and Zonneveld, 2003). The subsequent phase is characterized by a decrease in *L. machaerophorum* percentages and a coeval dominance of *Operculodinium* spp.

With the onset of S1 formation, percentages of *Operculodinium* ssp. rapidly decrease. A transition from high *N. labyrinthus* percentages over high percentages of *L. machaerophorum* to increased *O. centrocarpum* percentages preceding S1 formation has previously been described from the northern Aegean Sea (Aksu et al., 1995); a rapid increase of *O. centrocarpum* percentages directly preceding S1 formation is also known from the Adriatic Sea (Combourieu-Nebout et al., 1998). Hence, we suggest that this sequence of dominant taxa may be characteristic for the Aegean and Adriatic Seas, and that the last percentage peak of *N. labyrinthus* preceding S1 may be used as a biostratigraphic marker for the YD, similar to high percentages in *Artemisia* and Chenopodiaceae in the terrestrial realm (Rossignol-Strick, 1995; Kotthoff et al., 2008a). After 9.3 ka BP, *O. centrocarpum* percentages recover (>36 %), and *Operculodinium* spp. remain the most abundant cysts apart from *Spiniferites* ssp. during the first phase of S1 (Fig. 5.3). Cysts of heterotrophic taxa reach maximum percentages during S1 deposition (Fig. 5.3).

5.4.3.2 Planktic foraminiferal oxygen isotopes from core SL152

As described above, the $\delta^{18}O$ record of core SL152 is partly based on *G. ruber*, for the interval from ~17 to ~13 ka BP, and supplemented by data from *N. incompta*. Besides a single, very low value at the beginning of the late Pleniglacial, the $\delta^{18}O_{ruber}$ record between the late Pleniglacial and the earliest Holocene shows highly positive values (~2 ‰) indicative of colder and/or more saline summer surface waters (Fig. 5.5C). Between ~11.5 and ~10.5 ka, $\delta^{18}O_{ruber}$ decreases, with the lowest values recorded during S1 deposition. This observation is in agreement with previous studies from the Aegean Sea (Casford et al., 2002, 2003; Marino et al., 2009). The $\delta^{18}O_{pachyderma}$ values for the Lateglacial show even heavier values with a marked decrease (~1 ‰) during the Allerød and Bølling interstadials. The combined curves are generally similar to the planktic $\delta^{18}O$ record from neighbouring core SL148 (Fig. 5.5C; Kuhnt et al., 2007).

5.4.3.3 Planktic foraminiferal assemblages from core SL 148

During most of the study interval, cold-water indicators *N. incompta* and *T. quinqueloba* dominate the planktic foraminiferal fauna, making up to 80 % of the entire assemblage between 19 and 12 ka BP (Fig. 5.5B). *T. quinqueloba* is very abundant during most of the late Pleniglacial between ~19 and ~16.2 ka BP, the YD interval (~12.6 to ~11.7 ka BP) and the onset of S1 formation at ~9.5 ka BP. At the end of the late Pleniglacial, *N. incompta* becomes the dominant faunal element (> 50 %) and remains abundant until the onset of the YD. Percentages of cold indicator *N. pachyderma* > 1 % occur during at ~17.4 ka and ~16.5 ka BP. From ~12 ka BP onwards, warm-water taxa including among others *G. ruber* (pink and white), and *G. sacculifer* show a continuous abundance increase, with a peak at ~10 ka BP, where they make up 50 % of the assemblage. This rise in the abundance of warm-water taxa is also paralleled by an increase of temperate forms (predominantly *Globigerina bulloides*).
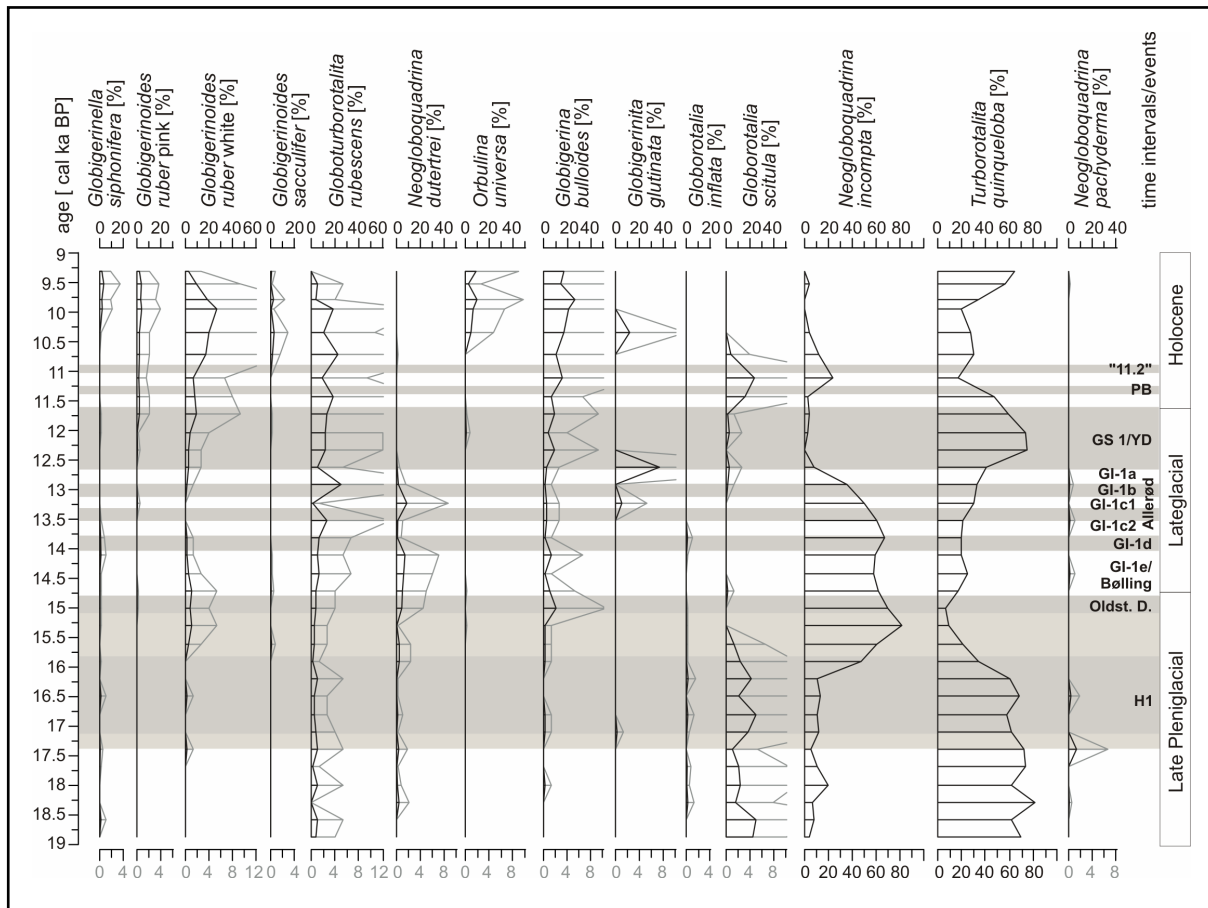
Figure 5.4: *Relative planctic foraminifer abundances in core SL148 vs. age. Grey bars indicate cooling events as indicated in Greenland ice cores and terrestrial proxies from core SL152 (Fig. 5.5, Kotthoff et al., 2008a). 11.2 = 11.2-ka event, PB = preboreal oscillation, GS 1/YD = Greenland stadial 1/Younger Dryas, GI = Greenland interstadial, Oldst. D. = Oldest Dryas, H1 = Heinrich 1 event.*

5.5 Synthesis of marine and terrestrial signals

5.5.1 Late Pleniglacial (~19 to ~14.7 ka BP)

As suggested by the pollen-based climate reconstructions from core SL152, the late Pleniglacial in the northern borderlands of the Aegean Sea is characterized by cold and dry climate conditions. This interval is punctuated by an interlude of particularly dry and cold conditions between ~17.3 and ~16.3 ka BP. The strong percentage increase of dinocyst cold indicators starting at ~19 ka BP (Fig. 5.5D), especially *N. labyrinthus* (Fig. 5.3), suggest decreasing SST during that time, culminating in particularly cold conditions at ~16.5 ka BP. High relative abundances of *T. quinqueloba* and a subordinate peak of *N. pachyderma* in core SL148 also indicate lower SSTs at ~16.5 ka BP (Fig. 5.5B), as do high $\delta^{18}O$ values (Fig. 5.5).

This particularly cold phase around ~16.5 ka BP is coeval with an interval of harsh climate conditions as observed in other sectors along the Southern European margin (e.g., Combourieu-Nebout et al., 1998, 2009; Kageyama et al., 2005; Brauer et al., 2007a; Fletcher and Sánchez Goñi, 2008) and Asia Minor (e.g., Fleitmann et al., 2009). It appears to be

linked to the H1 event in the northern North Atlantic Ocean (e.g., Bond et al., 1993). Hence, the reduction of oceanic heat transport to the high northern latitudes as connected to Heinrich events (e.g., Bond et al., 1993) also led to significantly dryer/colder conditions in the eastern Mediterranean region. A possible link within this teleconnection could be sought in a transient strengthening of the Siberian High during the H1, resulting in harsher conditions during the winter and early spring months. A similar mechanism has already been shown for cold spells in the Aegean region during the Holocene (e.g., Rohling et al. 2002; Kotthoff et al. 2008b), and for changes in Recent climate of the eastern Mediterranean region (Saaroni et al., 1996).

After the particularly cool conditions at ~16.5 ka BP, the decrease of *N. labyrinthus* percentages and the subsequent increases of *O. centrocarpum*, *Lingulodinium machaerophorum* and *Spiniferites* spp. percentages between ~16 and ~14.3 ka BP are probably caused by enhanced freshwater/nutrient influx and increasing surface-water temperatures due to a climatic amelioration. This view is supported by rapid relative abundance increases of benthic foraminiferal high-food/low-O_2 indicators and *N. incompta* in core SL148 (Fig. 5.5). As previously suggested by Rohling et al. (1993) and Casford et al. (2002), an increased abundance of *N. incompta* may indicate prolonged, intensified surface-water stratification and a more pronounced deep chlorophyll maximum in summer.

During the same interval (between ~16 and ~14.5 ka BP), the borderlands of the Aegean Sea witnessed the coeval spreading of broad-leaved trees (indicated by increasing NSAP percentages) and a decrease of steppe vegetation (Fig. 5.5E). Quantitative pollen-based climate reconstructions show a MP_{year} increase in the borderlands of the Aegean Sea between ~16 and ~14.5 ka BP (Fig. 5.5G); MT_{year} became slightly milder between ~15.5 and 15.1 ka BP (Fig. 5.5F). Such a climatic amelioration is compatible with increased melting rates of glaciers in the Rhodope mountains during that time as suggested by Ehrmann et al. (2007).

Our data suggest a further climate setback in the borderlands of the Aegean Sea at ~15 ka BP, which is probably equivalent to the Oldest Dryas (Fig. 5.5F, G). A comparable setback is also reflected in the stalagmite $\delta^{18}O$ records from the Sofular Cave (Turkey; Fleitmann et al., 2009) and from the Hula Cave (Asia; e.g., Wang et al., 2001), and furthermore in the NGRIP $\delta^{18}O$ data (Svensson et al., 2008), and, to a lesser degree, in the GISP2 $\delta^{18}O$ record (Stuiver and Grootes, 2000; Fig. 5.5H). Although H1 is dated between ~16.5 and ~16 ka BP (Bond et al., 1993), several authors imply that this setback may still be related to H1 (e.g., Svensson et al., 2008; Fleitmann et al., 2009).
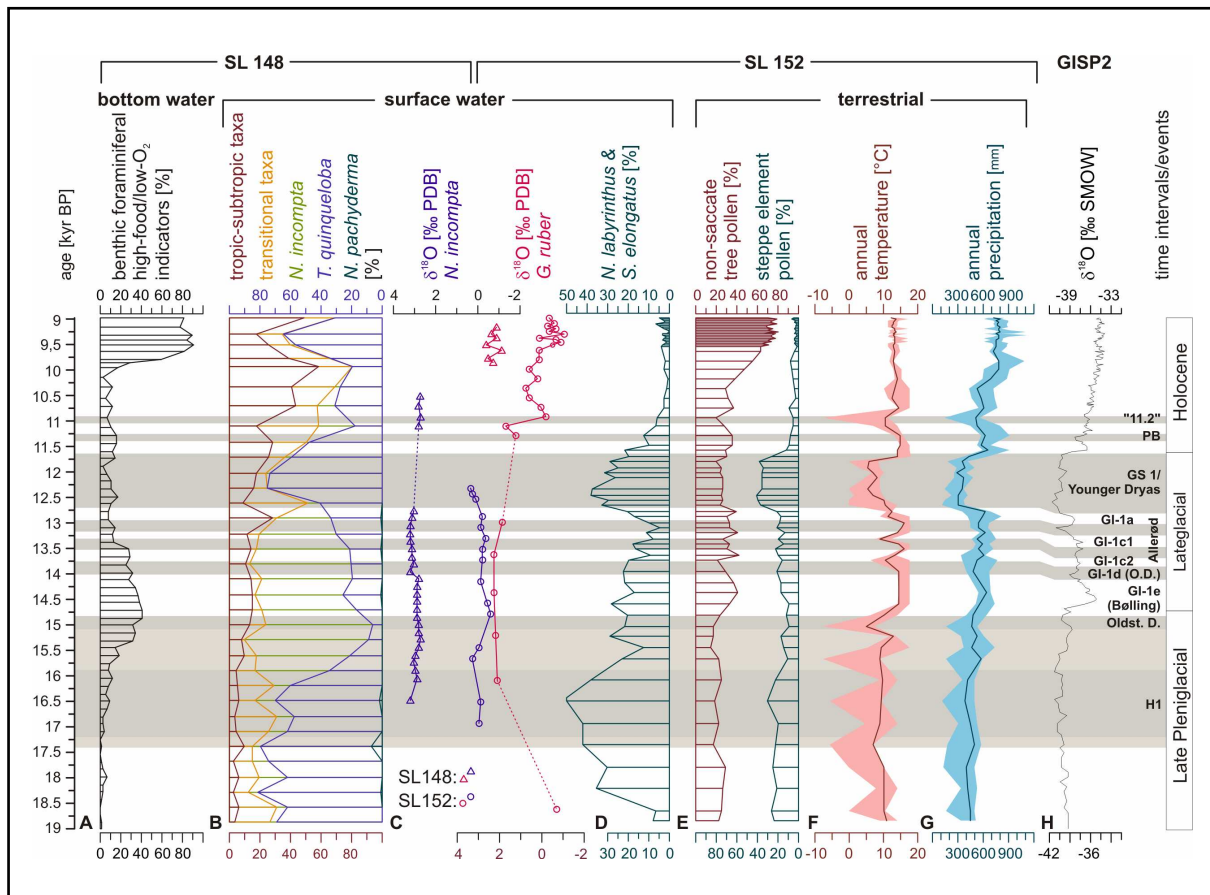
Figure 5.5: *Biological and geochemical proxies in cores SL152 and SL148 compared to Greenland ice-core data. From left to right: benthic (A) and planktic foraminifer abundances (B) and δ¹⁸O record for* Globigerinoides ruber *from core SL148 (C, triangles, Kuhnt et al., 2007); δ¹⁸O records for* Globigerinoides ruber *and* Neogloboquadrina incompta *(C, circles), combined abundances of cold-water indicators* Nematosphaeropsis labyrinthus *and* Spiniferites elongatus *(D), percentages of non-saccate tree pollen vs. percentages of steppe element pollen (E), and reconstructed (pollen-based) annual temperature (F) and annual precipitation (G) from core SL152; δ¹⁸O record from GISP2 ice core (I; http://lnsidc.org). Grey bars indicate cooling events as indicated in Greenland ice cores and terrestrial proxies from core SL152. 11.2 = 11.2-ka event, PB = preboreal oscillation, GS 1/YD = Greenland stadial 1/Younger Dryas, GI = Greenland interstadial, Oldst. D. = Oldest Dryas, H1 = Heinrich 1 event.*

Following this interpretation, the H1 in the Aegean region can be characterized as a ~2.4-ka-long interval (~17.4 to ~15 ka BP) that comprises a particularly dry and cold phase at ~16.5 ka and a milder phase between ~15.7 and ~15.1 ka BP. A comparison with terrestrial H1 signals in the borderlands of the western Mediterranean Sea and in Italy, where the H1 is reflected in strong increases of SEP (e.g., an *Artemisia* pollen percentages increase of >20 %; Brauer et al., 2007a; Fletcher and Sánchez Goñi, 2008; Combourieu-Nebout et al., 2009) and an MT$_{year}$ decline of >5 °C (with temperature of the coldest month decreasing by ~3 °C; Kageyama et al., 2005), shows that the impact of the H1 was less pronounced in the Aegean region compared to preceding climate conditions. In the central Mediterranean region, the impact of the H1 on vegetation dynamics was probably stronger than in the Aegean region, but weaker than in the borderlands of the western Mediterranean Sea (Combourieu-Nebout et al., 1998). This West-East gradient during the H1 can be ascribed to the generally dryer and colder conditions in the eastern Mediterranean region prior to H1 as compared to the

milder conditions in the western Mediterranean region (e.g., Fletcher and Sánchez Goñi, 2008; Combourieu-Nebout et al., 2009; see also Section 5.5.3).

5.5.2 Bølling-Allerød interstadial (~14.7 to ~12.6 ka BP)

Our pollen-based vegetation data and quantitative climate reconstructions for the terrestrial realm as derived from core SL152 suggest relatively mild conditions during Bølling and Allerød in the northern Aegean borderlands, with MT_{year} even reaching Holocene values. However, a pronounced climate setback at ~13.8 ka, which – depending on terminology – represents the local equivalent of the Older Dryas/Greenland stadial 1d (e.g., Lowe et al., 2008, Dormoy et al., 2009) and of the Oldest Dryas in records from western Europe (e.g., Litt et al., 2001; ~13.8 ka BP), separates the relatively stable Bølling (GI-1e) from the more unstable Allerød (GI 1c to 1a). Low sea-surface temperatures during this setback are indicated by high percentages of dinocyst cold indicators (especially *S. elongatus*). In the terrestrial realm, this interval is characterized by decreases in NSAP percentages, MT_{year} and MP_{year} (Fig. 5.5E, F, G).

Rather unstable climate conditions during the following Allerød are indicated for the borderlands of the Aegean Sea by repeated oscillations in the NSAP percentages, and concomitant MT_{year} and MP_{year} setbacks (Fig. 5.5E, F, G). For the marine realm, coeval setbacks are documented by short increases of the cold-water indicator *S. elongatus* (Fig. 5.3), while particularly low values of *N. labyrinthus* and the first consistent occurrences of *Impagidinium* species indicate generally warmer conditions (e.g., Combourieu-Nebout et al., 1998; Sangiorgi et al., 2003) during the Allerød (Fig. 5.3).

Heterotrophic dinocysts occur repeatedly during the Bølling and the more humid phases of the Allerød, with percentages almost comparable with those reached during S1 (Fig. 5.3). They probably indicate an enhanced nutrient supply. This view is supported by a strong percentage increase of intermediate to deep infaunal benthic foraminifers in core SL148, which implies an enhanced nutrient supply to the seafloor (Kuhnt et al., 2007; Fig. 5.5A). The last more humid phase of the Allerød (~13.2 to 12.7 ka BP) is characterized by a decrease in foraminifer high-productivity indicators (Fig. 5.5) and a coeval increase in foraminifer and dinocyst cold indicators, and SEP, reflecting the rapid transition to the YD.

5.5.3 Younger Dryas (~12.6 to ~11.7 ka BP)

Our dinocyst cold-water indicators and the cold-water species *T. quinqueloba* show a marked abundance increase with the onset of the YD (Fig. 5.5B, D). Apart from surface-water cooling, the increase of *T. quinqueloba* may also be ascribed to enhanced input of terrestrial material and a consequent increase in turbidity, since the asymbiotic form of *T. quinqueloba* has been discussed as indicative of turbid water bodies off California, up to 100 km offshore (Ortiz et al., 1995).

Our pollen-based quantitative climate data indicate an abrupt MP_{year} drop between ~12.8 and ~12.7 ka BP, while MT_{year} started declining slightly earlier (~12.9 ka BP), and more gradually; lowest MT_{year} were only reached at 12.5 ka BP (Fig. 5.5F, G). Two particularly dry phases of

the YD are indicated by especially high SEP percentages and low MP_{year} values at ~12.6 and ~11.8 ka BP.

Our results support and complement the findings of Rossignol-Strick (1995), Kuhnt et al. (2007), Kotthoff et al. (2008a), and Dormoy et al., (2009) that the YD is very strongly reflected in the Aegean region, and its impact on both the marine and the terrestrial realm was abrupt, with a decline of annual temperature by 6 °C and an annual precipitation decrease of 300 mm (50 %), the latter occurring abruptly within ~150 years only. This is different from findings from more westerly settings of the Mediterranean region: In the Adriatic Sea, the YD is reflected in a less pronounced, shorter increase in *N. labyrinthus* percentages (Combourieu-Nebout et al., 1998; Sangiorgi et al., 2002) as compared to the northern Aegean Sea. Similarly, a milder YD in terrestrial environments of the central Mediterranean region is indicated by pollen records from Italy (e.g., Magny et al., 2006, Brauer et al., 2007a) and western Greece (e.g., Lawson et al., 2004, 2005). We ascribe this discrepancy to the generally milder temperatures during the YD in that region in comparison to the Aegean region. In terrestrial settings of the western Mediterranean region, the YD is expressed by the spreading of steppe elements, but temperature declines were also weaker than in the Aegean region (Fletcher and Sánchez Goñi, 2008; Combourieu-Nebout et al., 2009; Dormoy et al., 2009).

It cannot be excluded, however, that the abruptness and intensity of the terrestrial, pollen-based YD signal in the northern Aegean region is partly caused by changes in wind direction and intensity (Kotthoff et al., 2008a); such a scenario has been reported from other regions in Europe (e.g., Brauer et al., 2008b) and is also suggested for the northern Aegean region (Ehrmann et al., 2007). Increased storminess during the spring months could have been caused by abrupt changes in intensity and/or direction of the westerlies (Brauer et al., 2008b) and/or by a strengthening of the Siberian High (e.g., Rohling et al., 2002; see also Section 5.5.1).

5.5.4 Early Holocene (~11.7 to ~9.6 ka BP)

Subsequent to the YD, the abundances of tropic-subtropic and transitional planktic foraminifers increase until ~10 ka BP, indicating a rise in sea-surface temperatures (Fig. 5.5B). The planktic $\delta^{18}O$ records of the cores SL152 and SL148 (Fig. 5.5C; Kuhnt et al., 2007) reflect the transition from glacial to interglacial conditions at ~11 ka BP, exemplified by a shift of ~2 ‰ towards lighter values.

For the terrestrial realm, the pollen-based quantitative climate data indicate a return to higher MT_{year} (>13 °C) after the YD within ~150 years, while the MP_{year} appears to have increased more gradually. Both climate parameters underwent several oscillations, the strongest of which is registered at ~11 ka BP (Fig. 5.5). This setback is probably related to the "11.2-ka event" described from Central Europe and the Mediterranean area (Hoek and Bos, 2007; Magny et al., 2007; Dormoy et al., 2009).

Subsequently, at ~10.5 ka BP, *L. machaerophorum* became the most frequent dinocyst taxon (Fig. 5.3). Its abundance increase points either to decreasing salinity or enhanced

nutrient input (e.g., Aksu et al., 1995) and can probably be ascribed to increased meltwater input into the Aegean Sea due to the melting of glaciers in the Rhodope mountains, which resulted from the general temperature increase after the YD (Ehrmann et al., 2007).

The following spreading of *Operculodinium* species between ~10.5 ka to 9.6 ka BP and the almost coeval increase of benthic foraminiferal high food/low-O_2 indicators (Fig. 5.4; Kuhnt et al., 2007) was probably caused by the onset of water-column stratification due to increased precipitation. Such a precipitation increase is reflected by a rise in NSAP and the pollen-based quantitative MP_{year} reconstruction (Fig. 5.5E, H; Kotthoff et al., 2008b). The increased MP_{year} and water stratification finally resulted in the formation of sapropel S1 in the northern Aegean Sea starting at ~9.6 ka BP (Kotthoff et al., 2008b). The increase of *T. quinqueloba* percentages between ~10 and ~9.5 ka BP was probably not caused by decreasing temperature (Ortiz et al., 1995), given that coeval increases in the percentages of dinocyst cold indicators are not observed (Fig. 5.3), and quantitative MT_{year} reconstructions for the terrestrial realm (Fig. 5.5F) suggest rather stable conditions. The onset of the *T. quinqueloba* increase, a taxon considered to be fairly tolerant towards lower salinities (Rohling et al., 1993, 1997), is however, coeval with very high MP_{year} in the borderlands of the Aegean Sea (Fig. 5.5B, G). This observation implies that the *T. quinqueloba* increase was caused by increased freshwater input rather than declining temperatures.

5.6 Conclusions

To elucidate the response of terrestrial and marine ecosystems in the Aegean region to late Pleniglacial and Lateglacial climate perturbations, and to compare the impact of the H1 event with that of the YD, we have analysed and integrated marine and continental proxy data from two northern Aegean sediment cores in centennial-scale (125 to 400 years) resolution.

Our results allow clear identification the impact of the H1 event on surface-water conditions and terrestrial ecosystems. Enhancing the already dry and cold conditions of the regional climate during the late Pleniglacial, the H1 event led to an additional decline in sea-surface temperature in the northern Aegean Sea and a MP_{year} and MT_{year} decrease in the borderlands of the Aegean Sea.

The Bølling and the Allerød were intervals of generally warmer and more humid climate in the northern Aegean region. The humid conditions led to increased runoff and nutrient input into the Aegean Sea. MT_{year} reached almost Holocene levels during both interstadials. However, several short-term climate setbacks (particularly the Older Dryas; ~13.8 ka BP) led to transient temperature decreases in the Aegean Sea and its borderlands; the borderlands further witnessed a decline in MP_{year}.

Climate conditions during the H1 and the YD were almost identical, with only slightly lower temperatures during the YD observed in the terrestrial realm. Similar dinocyst assemblages indicate comparable surface-water conditions in the northern Aegean Sea during both intervals. The YD, however, interrupted a transition to warmer and more humid conditions initiated during the Bølling/Allerød. MT_{year} in the borderlands of the Aegean Sea declined by >6 ºC with the onset of the YD, and MP_{year} dropped by almost 50 % within 150 mm.

Therefore, the YD witnessed strong changes in both marine and terrestrial ecosystems, while only slight ecological changes occurred during the H1, especially concerning the terrestrial realm and the foraminiferal assemblages.

The early Holocene until ~9 ka BP was characterized by relatively stable, high temperatures both in the marine and terrestrial realms, while MP_{year} in the borderlands gradually increased until the deposition of sapropel S1. A major climate setback at ~11 ka BP, probably correlative to a cold event at ~11.2 ka BP known from various European climate archives, strongly affected the terrestrial ecosystems. For the time interval from ~11.6 to ~9.6 ka BP, dinocyst assemblages reflect a transition to a stratified water column, increased nutrient input and higher sea-surface temperatures in the marine realm of the Aegean region.

5.7 Acknowledgements

Chapter 6. Conclusions and outlook

6.1 Conclusions

The integrated palynological, sedimentological and geochemical analyses of predominantly annually laminated lake sediments of Holsteinian age from Dethlingen, northern Germany, has yielded insights into the characteristics of short- and long-term climate change during an interglacial that with respect to astronomical boundary conditions represents a close analogy to the Holocene.

The palynological data from Dethlingen provide evidence for considerable long-term climatic variability during the Holsteinian interglacial. They document a decrease in seasonality and increases in warmth and precipitation towards the younger phases of the interglacial. This observation is in line with a correlation of the Holsteinian interglacial with MIS 11c, which in contrast to MIS 9 shows peak warmth at the end of the warm period. Based on the constellation of orbital parameters, a duration of MIS 11c in the marine realm of ~30-ka and the notion that Atlantic heat transport strongly influences vegetation dynamics in central Europe, an effort is made to place the ~15-16-ka-long expansion of Holsteinian forests in central Europe within MIS 11c. It appears conceivable that the expansion of Holsteinian interglacial forests in central Europe is coeval with the second half of MIS 11c (i.e., between 415 and 397 ka BP). This attribution is based on three main arguments: Firstly, pioneer boreal forests most probably expanded in response to the strengthening of the oceanic heat transport to the North Atlantic after 415 ka BP. Secondly, the prevalence of temperate forests was most likely related with the second Northern Hemisphere summer insolation maximum of MIS 11c (~408 ka BP) in association with the peak in the advection of warm surface waters into the polar North Atlantic during the younger stages of MIS 11c, lowest global ice volume and highest temperatures in Antarctica as reported between 411 and 401 ka BP. Thirdly, the decline of temperate forests in central Europe should have taken place after 401 ka BP following the SST decline in the North Atlantic, whereas the transition towards glacial vegetation was associated with the insolation minimum at ~397 ka BP.

In order to decipher the characteristics of short-term climate variability during MIS 11, time series analyses were carried out on the varve thickness datasets of a ~3200-year-long window of the Holsteinian at Dethlingen. They document a climate cyclicity similar to that known from the Holocene. In particular, the detected decadal-scale cyclicity can be attributed to the 88-yr Gleissberg, the 22-yr Hale and the 11-yr Schwabe sunspot cycles. Sub-decadal cyclicity may reflect an influence of the ENSO and the NAO climate modes on central Europe during the Holsteinian. These results underscore the comparability of climate forcing during MIS 11 and the Holocene on short (sub-decadal- to decadal-) timescales on top of the previously established analogy with regard to the long-term astronomical evolution of both interglacials. Hence, short-term climatic forcing should be considered in any model-based simulations of future climate scenarios that are based on the MIS 11/MIS 1 analogy.

The decadal-scale palynological analysis of the Dethlingen record has also provided insights into two prominent centennial-scale regressive phases in vegetation development. Although

these regressive phases are known since the early 1970's, their trigger mechanisms have yet remained unclear. Both phases are characterised by the supraregional expansion of boreal and sub-temperate forests at the expense of temperate taxa across central and northwestern Europe, suggesting climatic forcing as the underlying cause. However, the marked differences in the pollen signatures of both phases suggest that the vegetation turnovers were caused by climate oscillations with different trigger mechanisms.

Based on the strong resemblance of the older of these oscillations, here termed "Older Holsteinian Oscillation" (OHO), to the 8.2 ka event of the Holocene, the climatic trigger mechanism may be sought in a transient meltwater-induced slowdown of North Atlantic Deep Water (NADW) formation. If correct, meltwater-induced slowdown of NADW formation may be a more common agent of climate forcing during interglacial boundary conditions than previously assumed. Such climate setbacks during interglacials may preferentially occur when low rates in the increase of summer insolation during the preceding terminations facilitate the persistence of large-scale continental ice sheets well into interglacials.

In contrast, the younger centennial-scale climate oscillation that occurred during the Holsteinian, here termed "younger Holsteinian Oscillation" (YHO), is related to a long-term, gradual decline of temperate tree taxa. This decline may reflect the vegetation response to orbital forcing, notably a decline in summer insolation during the younger parts of MIS 11c. Thus, the centennial-scale YHO could have developed when a climatic threshold was crossed under changing orbital boundary conditions. However, the increase of temperate taxa after the YHO is not compatible with the continuously declining summer insolation as it occurred during MIS 11c, suggesting that different mechanisms may be responsible for the long-term decline and recovery of temperate taxa preceding and following the YHO, respectively.

6.2 Outlook

Given the comparability of MIS 11c and the present Holocene interglacial with regard to orbital boundary conditions, the occurrence of centennial-scale climate oscillations and the presence of sub-decadal- to decadal-scale climate cyclicity, this thesis underscores the need to elucidate the causes of abrupt climate oscillations during MIS 11c to better understand the effect of potentially analogous events in the future. Ongoing studies on the Dethlingen record will allow to refine the picture of Holsteinian climate oscillations. In particular, high-resolution (decadal- to centennial-scale) diatom analyses will allow insights in the response of the Dethlingen palaeolake system (e.g., productivity, pH, nutrient availability). Preliminary results show that the diatom assemblages responded quickly to the external forcing during the OHO and the YHO. In addition, the impact of the OHO on the aquatic ecosystem appears to be clearly reflected in $\delta^{18}O_{silica}$ data (A.F. Lotter, unpublished data). Moreover, ongoing organic geochemical analyses have documented the presence of various biomarkers for conifers (tricyclic diterpenoids) and deciduous trees (pentacyclic triterpenoids); their distribution in the Dethlingen record may provide further insights into the forest composition surrounding the

palaeolake, whereas their $\delta_{13}C$ values may yield information on the atmospheric circulation during the Holsteinian (W. Püttmann and J. Regnery, 2011, pers. comm.).

To potentially quantify temperature changes during the OHO and YHO, organic geochemical pilote studies have been performed to determine the TEX_{86}, MBT/CBT and BIT indices. Preliminary results show temperature changes across both intervals; however, the absolute values yet lack reliable calibrations (J. Weijers, 2009, pers. comm.). Another promising avenue towards obtaining additional temperature information on the Holsteinian sequence from Dethlingen may be in quantitative vegetation-based climate reconstructions (e.g., Kühl and Litt, 2007); such efforts appear particularly promising in light of the decadal-scale pollen data available.

A better constrained spatial extent of the OHO will allow deeper insights into the influence of the North Atlantic on, and into latitudinal and longitudinal climate gradients across Europe during MIS 11. In such an effort, particular emphasis should be placed on high-resolution studies of marine records from the Nordic Seas. In the terrestrial realm, the search for the OHO climate anomaly may be particularly promising in southern Europe (and notably the northeastern Mediterranean region) where climate archives have been shown to closely reflect North Atlantic climate dynamics both on decadal and centennial to millennial timescales (e.g., Rohling et al., 2002; Kotthoff et al., 2008a; Fleitmann et al., 2009; Pross et al., 2009; Müller et al., 2011).

The YHO has been recorded only in few pollen records from Germany; hence, its spatial extent is yet insufficiently constrained. It appears well possible that the impact of the YHO on vegetation in northern Europe has yet been overlooked because of the occurrence of frost-sensitive tree taxa across this interval. It may therefore be necessary to re-evaluate available pollen records with a particular focus on (i) overall changes in the abundances of temperate taxa and (ii) changes in summer-warmth-demanding taxa. The YHO is centered within a millennial-scale (~1500-year) decline and subsequent recovery of temperate taxa, which may correlate with long-term declines and subsequent recoveries of temperate taxa percentages and summer SST in marine cores from the North Atlantic (see Figure 1.2; Helmke et al., 2008; Tzedakis, 2010) and oxygen isotope data from Piànico, southern Alps (Mangili et al., 2007) at ~405 ka BP. However, such correlations are notoriously hampered by the lack of robust chronologies. The lack of reliable absolute dates for MIS 11 underlines the need for high-resolution, multi-proxy studies within a well-constrained chronological framework as developed for the Dethlingen record to be established for other varved Holsteinian records from central Europe, e.g., Marks Tey (British Isles) and Ossówka (Poland).

For an improved correlation between individual sites, tephrostratigraphic data may be particularly well suited to complement and possibly refine existing palynostratigraphic correlations. For instance, two tephra layers have been identified in the Holsteinian record from Döttingen in the volcanic field of the Eifel region, Germany (Diehl and Sirocko, 2007). It appears possible that microtephras originating from the same volcanic eruptions are preserved in the Dethlingen record and/or other Holsteinian records from central Europe. Moreover, tephra layers encountered in the MIS 11 record from Piànico, southern Alps

(Brauer et al., 2007b) probably originated from Italy and the Massif Central, France. These tephras may also be preserved in terrestrial records notably from southern Europe. In particular, the new, long and continuous terrestrial record from Tenaghi Philippon, Greece (Pross et al., 2007, 2010) is known for its susceptibility to preserve tephra layers originating from Italy, Greece and Asia Minor (e.g., Seymour et al., 2004; Müller et al., 2011). Hence, the development of a tephrochronological scheme for the Tenaghi Philippon record may potentially yield a baseline frame for biostratigraphic correlations among European terrestrial archives, which along with the further establishment of land-sea correlations will allow to significantly refine our understanding of natural climate variability.

References

Aksu, A.E., Yaşar, D., Mudie, P.J., Gillespie, H., 1995. Late glacial-Holocene paleoclimatic and paleoceanographic evolution of the Aegean Sea: micropaleontological and stable isotopic evidence. Marine Micropaleontology 25, 1-28.

Alley, R.B., Ágústsdóttir, A.M., 2005. The 8k event: cause and consequences of a major Holocene abrupt climate change. Quaternary Science Reviews 24, 1123-1149.

Alley, R.B., Marotzke, J., Nordhaus, W.D., Overpeck, J.T., Peteet, D.M., Pielke, R.A., Jr., Pierrehumbert, R.T., Rhines, P.B., Stocker, T.F., Talley, L.D., Wallace, J.M., 2003. Abrupt climate change. Science 299, 2005-2010.

Andersen, S.T., 1965. Interglacialer og interstadialer I Danmarks kvaertaer. Meddelelser fra Dansk Geologisk Forening 15, 486-506.

Andersen, S.T., 1994. History of the terrestrial environment in the Quaternary of Denmark. Bulletin of the Geological Society of Denmark 41, 219-228.

Anderson, R.Y., 1961. Solar-terrestrial climatic patterns in varved sediments. Annals of the New York Academy of Sciences 95, 424-439.

Anderson, R.Y., 1992. Possible connection between surface winds, solar activity and the Earth's magnetic field. Nature 358, 51-53.

Anderson, R.Y., Koopmans, L.H., 1963. Harmonic analysis of varve time series. Journal of Geophysical Research 68, 877-893.

Appenzeller, C., Stocker, T.F., Anklin, M., 1998. North Atlantic Oscillation dynamics recorded in Greenland ice cores. Science 282, 446-449.

Ashton, N., Lewis, S.G., Parfitt, S.A., Penkman, K.E.H., Coope, R.G., 2008. New evidence for complex climate change in MIS 11 from Hoxne, Suffolk, UK. Quaternary Science Reviews 27, 652-668.

Averdieck, F.R., 1992. Das Holstein-Interglazial von Hamburg-Hummelsbüttel. Meyniana 44, 1-13.

Bahr, A., Lamy, F., Arz, H.W., Major, C., Kwiecien, O., Wefer, G., 2008. Abrupt changes of temperature and water chemistry in the late Pleistocene and early Holocene Black Sea. Geochemistry, Geophysics, Geosystems 9, 1-16.

Baldini, J.U.L., McDermott, F., Fairchild, I.J., 2002. Structure of the 8200-Year cold event revealed by a speleothem trace element record. Science 296, 2203–2206.

Baldwin, M.P., Gray, L.J., Dunkerton, T.J., Hamilton, K., Haynes, P.H., Randel, W.J., Holton, J.R., Alexander, M.J., Hirota, I., Horinouchi, T., Jones, D.B.A., Kinnersley, J.S., Marquardt, C., Sato, K., Takahashi, M., 2001. The Quasi-Biennial Oscillation. Reviews of Geophysics 39, 179-229.

Barber, D.C., Dyke, A., Hillaire-Marcel, C., Jennings, A.E., Andrews, J.T., Kerwin, M.W., Bilodeau, G., McNeely, R., Southon, J., Morehead, M.D., Gagnon, J.-M., 1999. Forcing of the cold event of 8,200 years ago by catastrophic drainage of Laurentide lakes. Nature 400, 344–348.

Barker, S., Diz, P., Vautravers, M.J., Pike, J., Knorr, G., Hall, I.R., Broecker, W.S., 2009. Interhemispheric Atlantic seesaw response during the last deglaciation. Nature 457, 1097-1102.

Bauch, H.A., Erlenkeuser, H., Helmke, J.P., Struck, U., 2000. A paleoclimatic evaluation of marine oxygen isotope stage 11 in the high-northern Atlantic (Nordic Seas). Global and Planetary Change 24, 27-39.

Bé, A.W.H., Tolderlund, D.S., 1971. Distribution and ecology of living planktonic foraminifera in surface waters of the Atlantic and Indian oceans. In: The micropalaeontology of oceans, Funnell, B.W., Riedel, W.R. (Eds), Cambridge University Press, Cambridge, pp. 105-149.

Beer, J., Mende, W., Stellmacher, R., 2000. The role of sun in climate forcing. Quaternary Science Reviews 19, 403-415.

Benda, L., 1974. Neue pollenanalytische Untersuchungen an der Kieselgur von Wiechel. Geologisches Jahrbuch A 21, 141-148.

Benda, L., Brandes, H., 1974. Die Kieselgur-Lagerstätten Niedersachsens. I. Verbreitung, Alter und Genese. Geologisches Jahrbuch A 21, 3-85.

Benda, L., Hofmeister, E., Mielke, K., Müller, H., 1984. Die Kieselgur-Lagerstätten Niedersachsens III. Neue Prospektionsergebnisse (Lagerstätte Dethlingen). Geologisches Jahrbuch A 75, 585-609.

Berger, A., Loutre, M.F., 1991. Insolation values for the climate of the last 10 million years. Quaternary Science Reviews 10, 297-317.

Berger, A.L., Loutre, M.F., 2002. An exceptionally long interglacial ahead? Science 297, 1287-1288.

Bińka, K., Nitychoruk, J., 1995. Mazovian (Holsteinian) lake sediments at Woskrzenice near Biała Podlaska. Geological Quarterly 39, 109-120.

Bińka, K., Nitychoruk, J., 1996. Geological and palaeobotanical setting of interglacial sediments at the Kaliłów site in southern Podlasie. Geological Quarterly 40, 269-282.

Bińka K., Lindner, L., Nitychoruk, J., 1997. Geologic-floristic setting of the Mazovian Interglacial sites in Wilczyn and Lipnica in southern Podlasie (eastern Poland) and their palaeogeographic connections. Geological Quarterly 41, 381-394.

Birks, H.H., Paus, A., 1991. *Osmunda regalis* in the early Holocene of Western Norway. Nordic Journal of Botany 11, 635-640.

Birks, H.J.B., 1986. Late-Quaternary biotic changes in terrestrial and lacustrine environments, with particular reference to north-west Europe. In: Berglund, B.E. (Ed.), Handbook of Holocene Palaeoecology and Palaeohydrology. John Wiley and Sons, UK, pp. 3-65.

Birks, H.J.B., Birks, H.H., 2004. The rise and fall of forests. Science 305, 484-485.

Björck, S., Walker, M.J.C., Cwynar, L.C., Johnsen, S., Knudsen, K.L., Lowe, J.J., Wohlfarth, B., INTIMATE Members, 1998. An event stratigraphy for the Last Termination in the north Atlantic region based on the Greenland ice-core record: a proposal by the INTIMATE group. Journal of Quaternary Science 13, 283-292.

Bond, G., Broecker, W., Johnsen, S., McManus, J., Labeyrie, L., Jouzel, J., Bonami, G., 1993. Correlations between climate records from North Atlantic sediments and Greenland ice. Nature 365, 143-147.

Bond, G., Kromer, B., Beer, J., Muscheler, R., Evans, M.N., Showers, W., Hoffmann, S., Lotti-Bond, R., Hajdas, I., Bonani, G., 2001. Persistent solar influence on North Atlantic climate during the Holocene. Science 294, 2130-2136.

Bordon, A., Peyron, O., Lézine, A.-M., Brewer, S., Fouache, E., 2009. Pollen-inferred Late-Glacial and Holocene climate in southern Balkans (Lake Maliq). Quaternary International 200, 19-30.

Bothwell, M.L., Darren, M.J.S., Pollock, C.M., 1994. Ecosystem response to solar ultraviolet-B radiation: Influence of trophic-level interactions. Science 265, 97-100.

Brauer, A., 2004. Annually laminated lake sediments and their palaeoclimatic relevance. In: Fisher, H., Kumke, T., Lohmann, G., Flöser, G., Miller, H., von Storch, H., Negendank, J.F.W. (Eds.), The climate in historical times. Towards a synthesis of Holocene proxy data and climate models. Springer Verlag, pp. 111-129.

Brauer, A., Endres, C., Negendank, J.F.W., 1999a. Lateglacial calendar year chronology based on annually laminated sediments from Lake Meerfelder Maar, Germany. Quaternary International 61, 17-25.

Brauer, A., Endres, C., Günter, C., Litt, T., Stebich, M., Negendank, J.F.W., 1999b. High resolution sediment and vegetation responses to Younger Dryas climate change in varved lake sediments from Meerfelder Maar, Germany. Quaternary Science Reviews 18, 321-329.

Brauer, A., Allen, J.R.M., Mingram, J., Dulski, P., Wulf, S., Huntley, B., 2007a. Evidence for last interglacial chronology and environmental change from Southern Europe. Proceedings of the National Academy of Sciences of the United States of America 104, 450-455.

Brauer, A., Wulf, S., Mangili, C., Moscariello, A., 2007b. Tephrochronological dating of varved interglacial lake deposits from Piànico-Sèllere (Southern Alps, Italy) to around 400 ka. Journal of Quaternary Science 22, 85-96.

Brauer, A., Mangili, C., Moscariello A., Witt, A., 2008a. Palaeoclimatic implications from micro-facies data of a 5900 varve time series from the Piànico interglacial sediment record, Southern Alps. Palaeogeography, Palaeoclimatology, Palaeoecology 259, 121-135.

Brauer, A., Haug, G.H., Dulski, P., Sigman, D.M., Negendank, J.F.W., 2008b. An abrupt wind shift in Western Europe at the onset of the Younger Dryas cold period. Nature Geoscience 1, 520-523.

Broecker, W.S., 1997. Thermohaline circulation, the Achilles Heel of our climate system: will man-made CO_2 upset the current balance? Science 278, 1582-1588.

Broecker, W.S., 2000. Abrupt climate change: causal constraints provided by paleoclimate record. Earth-Science Reviews 51, 137-154.

Broecker, W.S., 2006. Was the Younger Dryas triggered by a flood? Science 312, 1146-1148.

Brönnimann, S., 2007. Impact of El Niño – Southern Oscillation on European climate. Reviews of Geophysics 45, RG3003.

Brönnimann, S., Xoplaki, E., Casty, C., Pauling, A., Luterbacher, J., 2007. ENSO influence on Europe during the last centuries. Climate Dynamics 28, 181-197.

Cacho, I., Grimalt, J.O., Pelejero, C., Canals, M., Sierro, F.J., Flores, J.A., Shackleton, N., 1999. Dansgaard-Oeschger and Heinrich events imprints in Alboran Sea paleotemperatures. Paleoceanography 14, 698-705.

Çağatay, M.N., Görür N, Algan, O., Eastoe, C., Tchapalyga, A., Ongan, D., Kuhn, T., Kuşcu, L., 2000. Late glacial-Holocene palaeoceanography of the Sea of Marmara; timing of connections with the Mediterranean and the Black seas. Marine Geology 167, 191-206.

Carslaw, K.S., Harrison, R.G., Kirkby, J., 2002. Cosmic rays, clouds, and climate. Science 298, 1732-1737.

Casford, J.S.L., Rohling, E.J., Abu-Zied, R., Cooke, S., Fontainer, C., Leng, M., Lykousis, V., 2002. Circulation changes and nutrient concentrations in the late Quaternary Aegean Sea: A nonsteady state concept for sapropel formation. Paleoceanography 17, PA1024.

Casford, J.S.L., Rohling, E.J., Abu-Zied, R.H., Fontanier, C., Jorissen, F.J., Leng, M.J., Schmiedl, G., Thomson, J., 2003. A dynamic concept for eastern Mediterranean circulation and oxygenation during sapropel formation. Palaeogeography, Palaeoclimatology, Palaeoecology 190, 103-119.

Chapman, M.R., Shackleton, N.J., 2000. Evidence of 550-year and 1000-year cyclicities in North Atlantic circulation patterns during the Holocene. The Holocene 10, 287-291.

Cheng, H., Edwards, R.L., Broecker, W.S., Denton, G.H., Kong, X., Wang, Y., Zhang, R., Wang, X., 2009. Ice age terminations. Science 326, 248-252.

Chester, R., Baxter, G.G., Behairy, A.K.A., Connor, K.A., Cross, D., Elderfield, H., Padgham, R.C., 1977. Soil-sized eolian dusts from the lower troposphere of the Eastern Mediterranean Sea. Marine Geology 24, 201–217.

Cohen, J., 2001. The role of the Siberian High in Northern Hemisphere climate variability. Geophysical Research Letters 28, 299-302.

Combourieu-Nebout, N., Paterne, M., Turon, J.-L., Siani, G., 1998. A high-resolution record of the last deglaciation in the central Mediterranean Sea: palaeovegetation and palaeohydrological evolution. Quaternary Science Reviews 17, 303-317.

Combourieu-Nebout, N., Peyron, O., Dormoy, I., Desprat, S., Beaudouin, C., Kotthoff, U., Marret, F., 2009. Rapid climatic variability in the west Mediterranean during the last 25 000 years from high resolution pollen data. Climate of the Past 5, 503-521.

Cox, E.J., 1993. Freshwater diatom ecology: developing an experimental approach as an aid to interpreting field data. Hydrobiologia 269/270, 44-452.

Coxon, P., 1985. A Hoxnian interglacial site at Athelington, Suffolk. New Phytologist 99, 611-621.

Cramp, A., Collins, M., West, R., 1988. Late Pleistocene-Holocene sedimentation in the NW Aegean Sea: A palaeoclimatic palaeoceanographic reconstruction. Palaeogeography, Palaeoclimatology, Palaeoecology 68, 61-71.

D' Arrigo, R., Cook, E.R., Wilson, R.J., Allan, R., Mann, M.E., 2005. On the variability of ENSO over the past six centuries. Geophysical Research Letters 32, L03711.

Dahl, E., 1998. The phytogeography of northern Europe (British Isles, Fennoscandia and adjacent areas). Cambridge University Press, UK, pp. 297.

Damon, P.E., Peristykh, A.N., 2000. Radiocarbon calibration and application to geophysics, solar physics, and astrophysics. Radiocarbon 42, 137-150.

Darling, K.F., Kucera, M., Kroon, D., Wade, C.M., 2006. A resolution for the coiling direction paradox in *Neogloboquadrina pachyderma*. Paleoceanography 21, PA2011.

Dassow, W., 1987. Neue Holstein-Interglazial-Profile aus dem Quartär im Raum Leipzig. Zeitschrift für geologische Wissenschaften 15, 195-203.

de Abreu, L., Abrantes F.F., Shackleton, N., Tzedakis P.C., McManus J.F., Oppo D.W., Hall, M.A., 2005. Ocean climate variability in the eastern North atlantic during interglacial marine isotope stage 11: A partial analogue to the Holocene? Paleoceanography 20, PA3009.

de Beaulieu, J.-L., Eicher, U., Monjuvent, G., 1994. Reconstruction of Middle Pleistocene palaeoenvironments based on pollen and stable isotope investigations at Val-de-Lans, Isère, France. Vegetation History and Archaeobotany 3, 127-142.

de Beaulieu, J.-L., Andrieu-Ponel, V., Reille, M., Grüger, E., Tzedakis, C., Svobodova, H., 2001. An attempt at correlation between the Velay pollen sequence and the Middle Pleistocene stratigraphy from central Europe. Quaternary Science Reviews 20, 1593-1602.

de Vernal, A., Hillaire-Marcel, C., 2008. Natural variability of Greenland climate, vegetation, and ice volume during the past million years. Science 320, 1622-1625.

Dean, W., Anderson, R., Bradbury, J.P., Anderson, D., 2002. A 1500-year record of climatic and environmental change in Elk Lake, Minnesota I: Varve thickness and gray-scale density. Journal of Paleolimnology 27, 287-299.

Degering, D., Krbetschek, M.R., 2007. Dating of interglacial sediments by luminescence methods. In: Sirocko, F., Claussen, M., Sánchez Goñi, M.F, Litt, T. (Eds.), The Climate of the Past Interglacials, Developments in Quaternary Science. Elsevier, Amsterdam, pp. 157-171.

Denton, G.H., Hughes, T.J., 2002. Reconstructing the Antarctic ice sheet at the Last Glacial Maximum. Quaternary Science Reviews 21, 193-202.

Denton, G.H., Alley, R.B., Comer, G.C., Broecker W.S., 2005. The role of seasonality in abrupt climate change. Quaternary Science Reviews 24, 1159-1182.

Desprat, S., Sanchez-Goni, M.F., Turon, J.-L, McManus J.F., Loutre, M.F., Duprat, J., Malaize, B., Peyron, O., Peypouquet, J.-P., 2005. Is vegetation responsible for glacial inception during periods of muted insolation changes? Quaternary Science Reviews 24, 1361-1374.

Dickson, A.J., Beer, C.J., Dempsey C., Maslin, M.A., Bendle, J.A., McClymont, E.L., Pancost, R.D., 2009. Oceanic forcing of the Marine Isotope Stage 11 interglacial. Nature Geoscience 2, 428-433.

Diehl, M., Sirocko, F., 2007. A new Holsteinian record from the Dry Maar at Döttingen (Eifel). In: Sirocko, F., Claussen, M., Sánchez Goñi, M.F, Litt, T. (Eds.), The Climate of the Past Interglacials, Developments in Quaternary Science. Elsevier, Amsterdam, pp. 397-416.

Dormoy, I., Peyron, O., Combourieu-Nebout, N., Goring, S., Kotthoff, U., Magny, M., Pross, J., 2009. Terrestrial climate variability and seasonality changes in the Mediterranean region between 15000 and 4000 years BP deduced from marine pollen records. Climate of the Past 5, 615-632.

Dowling, L.A., Coxon, P., 2001. Current understanding of Pleistocene temperate stages in Ireland. Quaternary Science Reviews 20, 1631-1642.

Drescher-Schneider, R., 2000. 2. Halt: Kiesgrube Thalgut: Pollen- und großrestanalytische Untersuchungen. In: Kelly, M., Linden, U., Schlüchter, C. (Eds.), Exkursionsführer DEUQUA-Tagung 2000 in Bern, pp. 128-136.

Ehlers, J., Gibbard, P.L., 2004. Quaternary Glaciations – Extent and Chronology Part I: Europe. Elsevier, Amsterdam.

Ehlers, J., Meyer, K.-D., Stephan, H.-J., 1984. The Pre-Weichselian glaciations of North-West Europe. Quaternary Science Reviews 3, 1–40.

Ehrmann, W., Schmiedl, G., Hamann, Y., Kuhnt, T., 2007. Distribution of clay minerals in surface sediments of the Aegean Sea: A compilation. International Journal of Earth Sciences 96, 769-780.

Eissmann, L., 2002. Quaternary geology of eastern Germany (Saxony, Saxon-Anhalt, South Brandenburg, Thüringia), type area of the Elsterian and Saalian stages in Europe. Quaternary Science Reviews 21, 1275–1346.

Ellenberg, H., 1988. Vegetation ecology of central Europe. Cambridge University Press, Cambridge, pp 731.

Ellison, C.R.W., Chapman, M.R., Hall, I.R., 2006. Surface and deep ocean interactions during the cold climate event 8200 years ago. Science 312, 1929-1932.

EPICA community members (Augustin, L., Barbante, C., Barnes, P.R.F., Barnola, J.M., Bigler, M., Castellano, E., Cattani, O., Chappellaz, J., Dahl-Jensen, D., Delmonte, B., Dreyfus, G., Durand, G., Falourd, S., Fisher, H., Flückiger, J., Hansson, M.E., Huybrechts, P., Jugie, G., Johnsen, S.J., Jouzel, J., Kaufmann, P., Kipfstuhl, J., Lambert, F., Lipenkov, V.Y., Littot, G.C., Longinelli, A., Lorrain, R., Maggi, V., Masson-Delmotte, V., Miller, H., Mulvaney, R., Oerlemans, J., Oerter, H., Orombelli, G., Parrenin, F., Peel, D.A., Petit, J.-R., Raynaud, D., Ritz, C., Ruth, U., Schwander, J., Siegenthaler, U., Souchez, R., Stauffer, B., Steffensen, J.P., Stenni, B., Stocker, T.F., Tabacco, I.E., Udisti, R., Van De Wal, R.S.W., Van Den Broeke, M., Weiss, J., Wilhelms, F., Winthers, J.-G., Wolff, E.W., Zucchelli, M.), 2004. Eight glacial cycles from an Antarctic ice core. Nature 429, 623-628.

Erd, K., 1970. Pollen-analytical classification of the Middle Pleistocene in the German Democratic Republic. Palaeogeography, Palaeoclimatology, Palaeoecology 8, 129-145.

Erd, K., Palme, H., Präger, F., 1987. Holsteininterglaziale Ablagerungen von Rossendorf bei Dresden. Zeitschrift für geologische Wissenschaften 15, 281-295.

Fagel, N., Boës, X., Loutre, M.F., 2008. Climate oscillations evidenced by spectral analysis of Southern Chilean lacustrine sediments: the assessment of ENSO over the last 600 years. Journal of Paleolimnology 39, 253-266.

Fairbanks, R.G., Mortlock, R.A., Chiu, T.-C., Cao, L., Kaplan, A., Guilderson, TP., Fairbanks, T.W., Bloom, A.L., Grootes, P.M., Nadeau, M.-J., 2005. Radiocarbon calibration curve spanning 0 to 50,000 years BP based on paired ^{230}Th/^{234}U and ^{14}C dates on pristine corals. Quaternary Science Reviews 24, 1781-1796.

Fedorov, A.V., Philander, S.G., 2000. Is El Niño changing? Science 288, 1997-2002.

Field, M.H., de Beaulieu, J.-L., Guiot, J., Ponel, P., 2000. Middle Pleistocene deposits at La Cote, Val-de-Lans, Isère department, France: plant macrofossil, palynological and fossil insect investigations. Palaeogeography, Palaeoclimatology, Palaeoecology 159, 53-83.

Fleitmann, D., Cheng, H., Badertscher, S., Edwards, R.L., Mudelsee, M., Göktürk, O.M., Fankhauser, A., Pickering, R., Raible, C.C., Matter, A., Kramers, J., Tüysüz, O., 2009. Timing and climatic impact of Greenland interstadials recorded in stalagmites from northern Turkey. Geophysical Research Letters 36, L19707.

Fletcher, W.J., Sánchez Goñi, M.F., 2008. Orbital and sub-orbital-scale climate impacts on vegetation of the western Mediterranean basin over the last 48,000 yr. Quaternary Research 70, 451-464.

Fletcher, W.J., Sanchez Goñi, M.F., Peyron, O., Dormoy, I., 2010. Abrupt climate changes of the last deglaciation detected in a western Mediterranean forest record, Climate of the Past 6, 245-264.

Frenguelli, G., TH, F., Spieksma, M., Bricchi, E., Romano, B., Mincigrucci, G., Nikkels, A. H., Dankaart, W., Ferranti, F., 1991. The influence of air temperature on the starting dates of the pollen season of *alnus* and *populus.* Grana 30, 196-200.

Ganachaud, A., Wunsch, C., 2000. Improved estimates of global ocean circulation, heat transport and mixing from hydrographic data. Nature 408, 453-457.

Geyh, M.A., Müller, H., 2005. Numerical ^{230}Th/U dating and a palynological review of the Holsteinian/Hoxnian interglacial. Quaternary Science Reviews 24, 1861-1872.

Geyh, M.A., Müller, H., 2007. Palynological and geochronological study of the Holsteinian/Hoxnian/Landos interglacial. In: Sirocko, F., Claussen, M., Sánchez Goñi, M.F, Litt, T. (Eds.), The Climate of the Past Interglacials, Developments in Quaternary Science. Elsevier, Amsterdam, pp. 387-396.

Gistl, R., 1928. Die letzte Interglazialzeit der Lüneburger Heide pollenanalytisch betrachtet. Botanisches Archiv 21 (3/4), 648-710.

Gleissbeg, W., 1944. A table of secular variations of the solar cycle. Terrestrial Magnetism and Atmospheric Electricity 49, 243-244.

Graham, L.E., Wilcox, L.W., 2000. Algae. Prentice Hall, USA, 640 pp.

Grüger, E., 1983. Untersuchungen zur Gliederung und Vegetationsgeschichte des Mittelpleistozäns am Samerberg in Oberbayern. Geologica Bavarica 84, 21-40.

Grün, R., Schwarcz, H.P., 2000. Revised open system U-series/ESR age calculations for teeth from Stratum C at the Hoxnian Interglacial type locality, England. Quaternary Science Reviews 19, 1151-1154.

Guiot, J., 1990. Methodology of palaeoclimatic reconstruction from pollen in France. Palaeogeography, Palaeoclimatology, Palaeoecology 80, 49-69.

Haigh, J.D., 1996. The impact of solar variability on climate. Science 272, 981-984.

Hamann, Y., Ehrmann, W., Schmiedl, G., Krüger, S., Stuut, J.-B., Kuhnt, T., 2008. Sedimentation processes in the Eastern Mediterranean Sea during the Late Glacial and Holocene revealed by end-member modelling of the terrigenous fraction in marine sediments. Marine Geology 248, 97-114.

Harland, R., 1983. Distribution map of recent dinoflagellate cysts in bottom sediments from the North Atlantic Ocean and adjacent seas. Palaeontology 16, 321-387.

Hayes, A., Kucera, M., Kallel, N., Sbaffi, L., Rohling, E.J., 2005. Glacial Mediterranean sea surface temperatures based on planktonic foraminiferal assemblages. Quaternary Science Reviews 24, 999-1016.

Hays, J.D., Imbrie, J., Shackleton, N.J., 1976. Variations in the earth's orbit: pacemaker of the ice ages. Science 194, 1121-1132.

Hede, U.M., Rasmussen, P., Noe-Nygaard, N., Clarke, A.L., Vinebrooke, R.D., Olsen, J., 2010. Multiproxy evidence for terrestrial and aquatic ecosystem responses during the 8.2 ka cold event as recorded at Højby Sø, Denmark. Quaternary Research 73, 485-496.

Heiri, O., Lotter, A.F., Hausmann, S., Kienast, F., 2003. A chironomid-based Holocene summer air temperature reconstruction from the Swiss Alps. The Holocene 13, 477-484.

Heiri, O., Tinner, W., Lotter, A.F., 2004. Evidence for cooler European summers during periods of changing meltwater flux to the North Atlantic. Proceedings of the National Academy of Sciences of the United States of America 101, 15285-15288.

Helmke, J.P., Bauch, H.A., 2003. Comparison of glacial and interglacial conditions between the polar and subpolar North Atlantic region over the last five climatic cycles. Paleoceanography 18, PA1036.

Helmke, J.P., Bauch, H.A., Röhl, U., Kandiano, E.S., 2008. Uniform climate development between the subtropical and subpolar Northeast Atlantic across marine isotope stage 11. Climate of the Past 4, 181-190.

Hemleben, C., Spindler, M., Anderson, O.R., 1989. Modern planktonic foraminifera. Springer, Berlin.

Hilbrecht, H., 1996. Extant planktic foraminifera and the physical environment in the Atlantic and Indian Oceans. Mitteilungen aus dem Geologischen Institut der Eidgen. Technischen Hochschule und der Universität Zürich, Neue Folge. No. 300, Zürich.

Hilbrecht, H., 1997. Morphologic gradation and ecology in *Neogloboquadrina pachyderma* and *N. dutertrei* (planktic foraminifera) from core top sediments. Marine Micropaleontology 31, 31-43.

Hoek, W.Z., Bos, J.A.A., 2007. Early Holocene climate oscillations–causes and consequences. Quaternary Science Reviews 26, 1901-1906.

Hopmans, E.C., Weijers, J.W.H., Schefuß, E., Herfort, L., Sinninghe Damsté, J.S., Schouten, S., 2004. A novel proxy for terrestrial organic matter in sediments based on branched and isoprenoid tetraether lipids. Earth and Planetary Science Letters 224, 107-116.

Horowitz, A., 1989. Continuous pollen diagrams for the last 3.5 m.y. from Israel: Vegetation, climate and correlation with the oxygen isotope record. Palaeogeography, Palaeoclimatology, Palaeoecology 72, 63-78.

Hoyt, D.V., Schatten, K.H., 1997. The role of the sun in climate change. Oxford University Press, UK, 279 pp.

Hrynowiecka-Czmielewska, A., 2010. History of vegetation and climate of the Mazovian (Holsteinian) interglacial and the Liviecian (Saalian) glaciation on the basis of pollen analysis of paleolake sediments from Nowiny Żukowskie, SE Poland. Acta Palaeobotanica 50, 17-54.

Hurrell, J.W., 1995. Decadal trends in the North Atlantic oscillation: Regional temperatures and precipitation. Science 269, 676–679.

Hurrell, J.W., van Loon, H., 1997. Decadal variations in climate associated with the North Atlantic Oscillation. Climate Change 36, 301-326.

Imbrie, J., Hays, J.D., Martinson, D.G., Mc Intyre, A., Mix, A.C., Morley, J.J., Pisias, N.G., Prell, W.L., Shackleton, N.J., 1984. The orbital theory of Pleistocene climate: support from a revised chronology of the marine $\delta^{18}O$ record. In: Berger, A.L. et al. (Eds.), Milankovitch and climate, Part I: 269-305.

Ineson, S., Scaife, A.A., 2009. The role of the stratosphere in the European climate response to El Niño. Nature Geoscience 2, 32-36.

IPCC, 2007. IPCC Fourth Assessment Report – Climate Change, The Scientific Basis, Cambridge University Press, Cambridge.

Iversen, J., 1944. *Viscum*, *Hedera* and *Ilex* as climate indicators. Geologiska Föreningens Förhandlingar 66, 463-483.

Jones, P.D., Mann, M.E., 2004. Climate over past millennia. Reviews of Geophysics 42, RG2002.

Jouzel, J., Masson-Delmotte, V., Cattani, O., Dreyfus, G., Falourd, S., Hoffmann, G., Minster, B., Nouet, J., Barnola, J.M., Chappelaz, J., Fischer, H., Gallet, J.C., Johnsen, S., Leuenberger, M., Loulergue, L., Luethi, D., Oerter, H., Parrenin, F., Raisbeck, G., Raynoud, D., Schilt, A., Schwander, J., Selmo, E., Souchez, R., Spahni, R., Stauffer, B., Steffensen, J.P., Stenni, B., Stocker, T.F., Tison, J.L., Werner, M., Wolff, E.W., 2007. Climate variability over the past 800,000 years. Science 317, 793-796.

Kageyama, M., Combourieu Nebout, N., Sepulchre, P., Peyron, O., Krinner, G., Ramstein, G., Cazet, J.P., 2005. The Last Glacial Maximum and Heinrich Event 1 in terms of climate and vegetation around the Alboran Sea: a preliminary model-data comparison. Comptes Rendus Geoscience 337, 983–992.

Kandiano, E.S., Bauch, H.A., 2007. Phase relationship and surface water mass change in the Northeast Atlantic during Marine Isotope Stage 11 (MIS 11). Quaternary Research 68, 445-455.

Kelly, M.R., 1964. The Middle Pleistocene of North Birmingham. Philosophical Transactions of the Royal Society of London B 247, 533-592.

Kilham, P., Kilham, S.S., Hecky, R.E., 1986. Hypothesized resource relationships among African planktonic diatoms. Limnology and Oceanography 31, 1169-1181.

Kobashi, T., Severinghaus, J.P., Brook, E.J., Barnola, J-M., Grachev, A.M., 2007. Precise timing and characterization of abrupt climate change 8200 years ago from air trapped in polar ice. Quaternary Science Reviews 27, 1212-1222.

Kotthoff, U., Pross, J., Müller, U.C., Peyron, O., Schmiedl, G., Schulz, H., Bordon, A., 2008a. Climate dynamics in the borderlands of the Aegean Sea during formation of Sapropel S1 deduced from a marine pollen record. Quaternary Science Reviews 27, 832–845.

Kotthoff, U., Müller, U.C., Pross, J., Schmiedl, G., Lawson, I.T., van de Schootbrugge, B., Schulz, H., 2008b. Late Glacial and Holocene vegetation dynamics in the Aegean region: An integrated view based on pollen data from marine and terrestrial archives. The Holocene 18, 1019-1032.

Kotthoff, U., Koutsodendris, A., Pross, J., Schmiedl, G., Bornemann, A., Kaul, C., Marino, G., Peyron, O., Schiebel, R., 2011. Impact of Lateglacial cold events on the northern Aegean region reconstructed from marine and terrestrial proxy data. Journal of Quaternary Science 26, 86-96.

Koutsodendris, A., Müller, U.C., Pross, J., Brauer, A., Kotthoff, U., Lotter, A.F., 2010. Vegetation dynamics and climate variability during the Holsteinian interglacial based on a pollen record from Dethlingen (northern Germany). Quaternary Science Reviews 29, 3298-3307.

Koutsodendris, A., Pross, J., Müller, U.C., Brauer, A., Fletcher, W.J., Lotter, A.F. A short-term climate oscillation during the Holsteinian interglacial (MIS 11c): An analogy to the 8.2 ka climatic event? Submitted to Global and Planetary Change

Koutsodendris, A., Brauer, A., Pälike, H., Pross, J., Müller, U.C., Lotter, A.F. Sub-decadal- to decadal-scale climate cyclicity during the Holsteinian interglacial (MIS 11) evidenced in annually laminated sediments. Submitted to Climate of the Past

Klitgaard-Kristensen, D., Sejrup, H.P., Haflidason, H., Johnsen, S., Spurk, M., 1998. A regional 8200 cal. yr BP cooling event in northwest Europe, induced by final stages of the Laurentide ice-sheet deglaciation? Journal of Quaternary Science 13, 165-169.

Krupiński, K.M., 1995. Pollen stratigraphy and succession of vegetation during the Mazovian interglacial. Acta Geographica Lodzensis 70, 1-200.

Krupiński, K.M., 2000. Palynostratigraphic correlation of deposits of the Mazovian interglacial of Poland. Prace Państwowego Instytutu Geologicznego 161, 1-61.

Kucera, M., 2007. Planktonic Foraminifera as Tracers of Past Oceanic Environments. In: Proxies in Late Cenozoic Paleoceanography, Hillaire-Marcel. C., de Vernal, A., (Eds). Elsevier, Amsterdam, pp. 213-262.

Kühl, N., Litt, T., 2007. Quantitative time-series reconstructions of Holsteinian and Eemian temperatures using botanical data. In: Sirocko, F., Claussen, M., Sánchez Goñi, M.F, Litt, T. (Eds.), The Climate of the Past Interglacials, Developments in Quaternary Science. Elsevier, Amsterdam, pp. 239-254.

Kuhnt, T., Schmiedl, G., Ehrmann, W., Hamann, Y., Hemleben, C., 2007. Deep-sea ecosystem variability of the Aegean Sea during the past 22 kyr as revealed by benthic foraminifera. Marine Micropaleontology 64, 141-162.

Kukla, G., 2003. Continental records of MIS 11. In: Droxler, A.W., Poore, R.Z., Burckle, L.H. (Eds.): Earth's climate and orbital eccentricity; the marine isotope stage 11 question. AGU Geophysical Monograph Series 137, 207-212.

Kukla, G., 2005. Saalian supercycle, Mindel/Riss interglacial and Milankovitch's dating. Quaternary Science Reviews 24, 1573-1583.

Kukla, G., Berger, A., Lotti, R., Brown, J., 1981. Orbital signature of interglacials. Nature 290, 295-300.

Kukla, G., McManus, J.F., Rousseau, D.-D., Chuine, I., 1997. How long and how stable was the last interglacial? Quaternary Science Reviews 16, 605-612.

Kukla, G.J., Bender, M.L., de Beaulieu, J.-L., Bond, G., Broecker, W.S., Cleveringa, P., Gavin, J.E., Herbert, T.D., Imbrie, J., Jouzel, J., Keigwin, L.D., Knudsen, K.-L., McManus, J.F., Merkt, J., Muhs, D.R., Müller, H., Poore, R.Z., Porter, S.C., Seret, G., Shackleton, N.J., Turner, C., Tzedakis, P.C., Winograd, I.J., 2002. Last interglacial climates. Quaternary Research 58, 2-13.

Landi, M., Angiolini, C., 2008. Habitat characteristics and vegetation context of *Osmunda regalis* L. at the southern edge of its distribution in Europe. Botanica Helvetica 118, 45-57.

Lane-Serff, G.F., Rohling, E.J., Bryden, H.L., Charnock, H., 1997. Postglacial connection of the Black Sea to the Mediterranean and its relation to the timing of sapropel formation. Paleoceanography 12, 169-174.

Lawson, I.T., Frogley, M., Bryant, C., Preece, R., Tzedakis, P.C., 2004. The Lateglacial and Holocene environmental history of the Ioannina basin, north-west Greece. Quaternary Science Reviews 23, 1599-1625.

Lawson, I.T., Al-Omari, S., Tzedakis, P.C., Bryant, C.L., Christanis, K., 2005. Lateglacial and Holocene vegetation history at Nisi Fen and the Boras mountains, northern Greece. The Holocene 15, 873-887.

Lewis, W.M., 1983. A revised classification of lakes based on mixing. Canadian Journal of Fisheries and Aquatic Sciences 40, 1779-1787.

Liedtke, H., Marcinek, J. (Eds.), 2002. Physische Geographie Deutschlands. Klett-Perthes Verlag, Gotha - Stuttgart, 768 p.

Linke, G., Hallik, R., 1993. Die pollenanalytischen Ergebnisse der Bohrungen Hamburg-Dockenhunden (qho 4), Wedel (qho 2) und Hamburg-Billbrook. Geologisches Jahrbuch A 138, 169-184.

Litt, T., Brauer, A., Goslar, T., Merkt, J., Balaga, K., Müller, H., Ralska-Jasiewiczowa, M., Stebich, M., Negendank, J.F.W., 2001. Correlation and synchronisation of Lateglacial continental sequences in northern central Europe based on annually laminated lacustrine sediments. Quaternary Science Reviews 20, 1233-1249.

Livingstone, D.M., Hajdas, I., 2001. Climatically relevant periodicities in the thickness of biogenic carbonate varves in Soppensee, Switzerland (9740-6870 calendar yr BP). Journal of Paleolimnology 25, 17-24.

Lotter, A.F., 1989. Evidence of annual layering in Holocene sediments of Soppensee, Switzerland. Aquatic Sciences 51, 19-30.

Lotter, A.F., Birks, H.J.B., 1997. The separation of the influence of nutrients and climate on the varve time-series of Baldeggersee, Switzerland. Aquatic Sciences 59, 362-375.

Lotter, A.F., Lemcke, G., 1999. Methods for preparing and counting biochemical varves. Boreas 28, 243-252.

Lotter, A.F., Heiri, O., Brooks, S., van Leeuwen, J.F.N., Eicher, U., Ammann, B., 2010. Rapid summer temperature changes during Termination 1a: high-resolution multi-proxy climate reconstructions from Gerzensee (Switzerland). Quaternary Science Reviews, DOI 10.1016/j.quascirev.2010.06.022.

Loutre, M.F., Berger, A., 2003. Marine Isotope Stage 11 as an analogue for the present interglacial. Global and Planetary Change 36, 209-217.

Lowe, J.J., Rasmussen, S.O., Björk, S., Hoek, W.Z., Steffensen J.P., Walker, M.J.C., Yu, Z.C., the INTIMATE group, 2008. Synchronisation of palaeoenvironmental events in the North Atlantic region during the Last Termination: a revised protocol recommended by the INTIMATE group. Quaternary Science Reviews 27, 6-17.

Lykousis, V., Chronis, G., Tselepides, A., Price, N.B., Theocharis, A., Siokou-Frangou, I., van Wambeke, F., Danovaro, R., Stavrakakis, S., Duineveld, G., Georgopoulos, D., Ignatiades, L., Souvermezoglou, A., Voutsinou-Taliadouri, F., 2002. Major outputs of the recent multidisciplinary biogeochemical researches undertaken in the Aegean Sea. Journal of Marine Systems 33/34, 313-334.

Magny, M., Guiot, J., Schoellammer, P., 2001. Quantitative reconstruction of Younger Dryas to Mid-Holocene paleoclimates at Le Locle, Swiss Jura, using pollen and lake-level data. Quaternary Research 56, 170-180.

Magny, M., Bégeot, C., Guiot, J., Peyron, O., 2003. Contrasting patterns of hydrological changes in Europe in response to Holocene climate cooling phases. Quaternary Science Reviews 22, 1589-1596.

Magny, M., de Beaulieu, J.-L., Drescher-Schneider, R., Vannière, B., Walter-Simonnet, A.V., Millet, L., Bossuet, G., Peyron, O., 2006. Climatic oscillations in central Italy during the Last Glacial-Holocene transition: the record from Lake Accesa. Journal of Quaternary Science 21, 311-320.

Magny, M., Vannière, B., de Beaulieu, J.-L., Bégeot, C., Heiri, O., Millet, L., Peyron, O., Walter-Simonnet, A.-V., 2007. Early-Holocene climatic oscillations recorded by lake-level fluctuations in west-central Europe and in central Italy. Quaternary Science Reviews 26, 1951-1964.

Major, C.O., Goldstein, S.L., Ryan, W.B.F., Lericolais, G., Piotroski, A.M., Hajdas, I., 2006. The co-evolution of Black Sea level and composition through the last deglaciation and its paleoclimatic significance. Quaternary Science Reviews 25, 2031-2047.

Mangili, C., Brauer, A., Moscariello, A., Naumann, R., 2005. Microfacies of detrital event layers deposited in Quaternary varved lake sediments of the Piànico-Sèllere Basin (northern Italy). Sedimentology 52, 927-943.

Mangili, C., Brauer, A., Plessen, B., Moscariello, A., 2007. Centennial-scale oscillations in oxygen and carbon isotopes of endogenic calcite from a 15,500 varve year record of the Piànico interglacial. Quaternary Science Reviews 26, 1725-1735.

Mangili, C., Plessen, B., Wolff, C., Brauer, A., 2010. Climatic implications of annual to decadal stable isotope data from calcite varves of the Piànico interglacial lake record, Southern Alps. Global and Planetary Change 71, 168-174.

Mann, M.E., Park, J., 1994. Global-scale modes of surface temperature variability on interannual to century timescales. Journal of Geophysical Research 99, 25.819-25.833.

Mann, M.E., Lees, J.M., 1996. Robust estimation of background noise and signal detection in climatic time series. Climate Change 33, 409-445.

Marino, G., Rohling, E.J., Rijpstra, W.I., Sangiorgi, F., Schouten, S., Sinninghe Damsté, J.S., 2007. Aegean Sea as driver of hydrographic and ecological changes in the eastern Mediterranean. Geology 35, 675-678.

Marino, G., Rohling, E.J., Sangiorgi, F., Hayes, A., Casford, J.L., Lotter, A.F., Kucera, M., Brinkhuis, H., 2009. Early and middle Holocene in the Aegean Sea: interplay between high and low-latitude climate variability. Quaternary Science Reviews 28, 3246-3262.

Marret, F., Zonneveld, K.A.F., 2003. Atlas of modern organic-walled dinoflagellate cyst distribution. Review of Palaeobotany and Palynology 125, 1-200.

Martrat, B., Grimalt, J.O., Shackleton, N.J., de Abreu, L., Hutterli, M.A., Stocker, T.F., 2007. Four climate cycles of recurring deep and surface water destabilizations on the Iberian margin. Science 317, 502-507.

Masson-Delmotte, V., Stenni, B., Pol, K., Braconnot, P., Cattani, O., Falourd, S., Kageyama, M., Jouzel, J., Landais, A., Minster, B., Barnola, J.M., Chappellaz, J., Krinner, G., Johnsen, S., Röthlisberg, R., Hansen, J., Mikolajewicz, U., Otto-Bliesner, B., 2010. EPICA Dome C of glacial and interglacial intensities. Quaternary Science Reviews 29, 113-128.

May, P.W., 1982. Climatological flux estimates in the Mediterranean Sea: Part 1. Winds and Wind Stresses. Naval Ocean Research and Development Activity, Rep. 54, NSTL Station, Mississippi 39529.

McManus, J.F., Oppo, D.W., Cullen, J.L., 1999. A 0.5-million-year record of millennial-scale climate

variability in the North Atlantic. Science 283, 971-975.

McManus, J.F., Oppo, D., Cullen, J., Healey, S., 2003. Marine isotope stage 11 (MIS 11); Analogue for Holocene and future climate? In: Droxler, A.W., Poore, R.Z., Burckle, L.H. (Eds.), Earth's Climate and Orbital Eccentricity; the Marine Isotope Stage 11 Question: AGU Geophysical Monograph Series 137, pp. 69-85.

McManus, J.F., Francois, R., Gherardi, J.-M., Keigwin, L.D., Brown-Leger, S., 2004. Collapse and rapid resumption of Atlantic meridional circulation linked to deglacial climate changes. Nature 428, 834-837.

Meijer, T., Cleveringa, P., 2009. Aminostratigraphy of Middle and Late Pleistocene deposits in the Netherlands and the southern part of the North Sea Basin. Global and Planetary Change 68, 326-345.

Meyer, K.-J., 1974. Pollenanalytische Untersuchungen und Jahresschichtenzählungen an der holstein-zeitlichen Kieselgur von Hetendorf. Geologisches Jahrbuch A 21, 87-105.

Mulitza, S., Prange, M., Stuut, J.-B., Zabel, M., von Dobeneck, T., Itambie, A.C., Nizou, J., Schulz, M., Wefer, G., 2008. Sahel megadroughts triggered by glacial slowdowns of Atlantic meridional overtuning. Paleoceanography 23, PA4206.

Müller, H., 1974. Pollenanalytische Untersuchungen und Jahresschichtenzählungen an der holstein-zeitlichen Kieselgur von Munster-Breloh. Geologisches Jahrbuch A 21, 107-140.

Müller, U.C., Klotz, S., Geyh, M.A., Pross, J., Bond, G.C., 2005. Cyclic climate fluctuations during the last interglacial in central Europe. Geology 33, 449-452.

Müller, U.C., Pross, J., 2007. Lesson from the past: present insolation minimum holds potential for glacial inception. Quaternary Science Reviews 26, 3025-3029.

Müller, U.C., Pross, J., Tzedakis, P.C., Gamble, C., Kotthoff, U., Schmiedl, G., Bowen, S.W., Christanis, K., 2011. The role of climate in the spread of modern humans into Europe. Quaternary Science Reviews 30, 273-279.

Muscheler, R., Beer, J., Vonmoos, M, 2004. Causes and timing of the 8200 yr BP event inferred from the comparison of the GRIP [10]Be and the tree ring Δ^{14}C record. Quaternary Science Reviews 23, 2101-2111.

Muscheler, R., Joos, F., Müller, S.A., Snowball, I., 2005. How unusual is today's solar activity? Nature 436, E3-E4.

Nederbragt, A.J., Thurow, J., 2005. Amplitude of ENSO cycles in the Santa Barbara Basin, off California, during the past 15000 years. Journal of Quaternary Science 20, 447-456.

Nitychoruk, J., Bińka, K., Hoefs, J., Ruppert, H., Schneider, J., 2005. Climate reconstruction for the Holsteinian Interglacial in eastern Poland and its comparison with isotopic data from Marine Isotope Stage 11. Quaternary Science Reviews 24, 631-644.

Nitychoruk, J., Bińka, K., Ruppert, H., Schneider, J., 2006. Holsteinian interglacial = Marine Isotope Stage 11? Quaternary Science Reviews 25, 2678-2681.

O'Sullivan, P.E., 1983. Annually-laminated lake sediments and the study of Quaternary environmental changes – A review. Quaternary Science Reviews 1, 245-313.

O'Sullivan, P.E., Moyeed, R., Cooper, M.C., Nicholson, M.J., 2002. Comparison between instrumental, observational and high resolution proxy sedimentary records of Holocene climatic change – a discussion of possibilities. Quaternary International 88, 27-44.

Okuda, M., Yasuda, Y., Setoguchi, T., 2001. Middle to Late Pleistocene vegetation history and climatic changes at Lake Kopais, Southeast Greece. Boreas 30, 73-82.

Oppo, D.W., McManus, J.F., Cullen, J.L., 1998. Abrupt climate events 500,000 to 340,000 years ago: Evidence from subpolar North Atlantic sediments. Science 279, 1335-1338.

Ortiz, J.D., Mix, A.C., Collier, R.W., 1995. Environmental control of living symbiotic and asymbiotic foraminifera of the California Current. Paleoceanography 10, 987-1009.

Paus, A., 2010. Vegetation and environment of the Rødalen alpine area, Central Norway, with emphasis on the early Holocene. Vegetation History and Archaeobotany 19, 29–51.

Pawley, S.M., Bailey, R.M., Rose, J., Moorlock, B.S.P., Hamblin, R.J.O., Booth, S.J., Lee, J.R., 2009. Age limits on Middle Pleistocene glacial sediments from OSL dating, north Norfolk, UK. Quaternary Science Reviews 27, 1363-1377.

Perissoratis, C., Conispoliatis, N., 2003. The impacts of sea level changes during the latest Pleistocene and Holocene times on the morphology of Ionian and Aegean seas (SE Alpine Europe). Marine Geology 196, 145-156.

Petit, J.R., Jouzel, J., Raynaud, D., Barkov, N.I., Barnola, J.-M., Basile, I., Bender, M., Chappellaz, J., Davis, M., Delaygue, G., Delmotte, M., Kotlyakov, V.M., Legrand, M., Lipenkov, V.Y., Lorius, C., Pepin, L., Ritz, C., Saltzman, E., Stievenard, M., 1999. Climate and atmospheric history of the past 420,000 years from the Vostok ice core, Antarctica. Nature 399, 429-436.

Philips, L., 1976. Pleistocene vegetational history and geology in Norfolk. Philosophical Transactions of the Royal Society of London B 275, 215-286.

Poli, M.S., Thunell, R.C., Rio, D., 2000. Millennial-scale changes in north Atlantic Deep Water circulation during marine isotope stages 11 and 12: Linkage to Antarctic climate. Geology 28, 807-810.

Poulos, S.E., Drakopoulos, P.G., Collins, M.B., 1997. Seasonal variability in sea surface oceanographic conditions in the Aegean Sea (eastern Mediterranean): an overview. Journal of Marine Systems 13, 225-244.

Powers, L.A., Werne, J.P., Johnson, T.C., Hopmans, E.C., Sinninge Damsté, J.S., Schouten, S., 2004. Crenarchaeotal membrane lipids in lake sediments: A new paleotemperature proxy for continental paleoclimate reconstruction? Geology 32, 613-616.

Pozo-Vásquez, D., Esteban-Parra, M.J., Rodrigo, F.S., Castro-Díez, Y., 2000. An analysis of the variability of the North Atlantic Oscillation in the time and frequency domain. International Journal of Climatology 20, 1675-1692.

Prasad, S., Vos, H., Negendank, J.F.W., Waldmann, N., Goldstein, S.L., Stein, M., 2004. Evidence from Lake Lisan of solar influence on decadal- to centennial-scale climate variability during marine oxygen stage 2. Geology 32, 581-584.

Preece, R.C, Parfitt, S.A., Bridgland, D.R., Lewis, S.G., Rowe, P.J., Atkinson, T.C., Candy, I., Debenham, N.C., Penkman, K.E.H., Rhodes, E.J., Schwenningerl, J.-L., Griffiths, H.I., Whittaker,

J.E., Gleed-Owen, C., 2007. Terrestrial environments during MIS 11: evidence from the Palaeolithic site at West Stow, Suffolk, UK. Quaternary Science Reviews 26, 1236-1300.

Pross, J., 2001. Paleo-oxygenation in Tertiary epeiric seas: evidence from dinoflagellate cysts. Palaeogeography, Palaeoclimatology, Palaeoecology 166, 369-381.

Pross, J., Kotthoff, U., Zonneveld, K.A.F., 2004. Die Anwendung organischwandiger Dinoflagellatenzysten zur Rekonstruktion von Paläoumwelt, Paläoklima und Paläozeanographie: Möglichkeiten und Grenzen. Paläontologische Zeitschrift 78, 5-39.

Pross, J., Tzedakis, P.C., Schmiedl, G., Christanis, K., Hooghiemstra, H., Müller, U.C., Kotthoff, U., Kalaitzidis, S., Milner, A., 2007. Tenaghi Philippon re-visited. Drilling a continuous lower-latidude terrestrial climate archive of the last 250,000 years. Scientific Drilling 5, 44-46.

Pross, J., Kotthoff, U., Müller, U.C., Peyron, O., Dormoy, I., Schmiedl, G., Kalaitzidis, S., Smith, A.M., 2009. Massive perturbation in terrestrial ecosystems of the Eastern Mediterranean region associated with the 8.2 kyr B.P. climatic event. Geology 37, 887-890.

Pross, J., Müller, U.C., Koutsodendris, A., 2010. Der Weg ins Eishaus. Natur und Museum 140, 228-231.

Reille, M., de Beaulieu, J.L., 1995. Long Pleistocene pollen record from the Praclaux crater, south-central France. Quaternary Research 44, 205–215.

Reille, M., de Beaulieu, J.L., Svobodova, H., Andrieu-Ponel, V., Goeury, C., 2000. Pollen stratigraphy of the five last climatic cycles in a long continental sequence from Velay (Massif Central, France). Journal of Quaternary Sciences 15, 665–685.

Renssen, H., Goosse, H., Fichefet, T., 2002. Modeling the effect of freshwater pulses on early Holocene climate: The influence of high-frequency climate variability. Paleoceanography 17, PA1020.

Risebrobakken, B., Jansen, E., Andersson, C., Mjelde, E., Hevrøy, K., 2003. A high-resolution study of Holocene paleoclimatic and paleoceanographic changes in the Nordic Seas. Paleoceanography 18, PA1017.

Rittenour, T.M., Brigham-Grette, J., Mann, M.E., 2000. El Niño-like climate teleconnections in New England during the Late Pleistocene. Science 288, 1039-1042.

Rodó, X., Baert, E., Comin, F.A., 1997. Variations in seasonal rainfall in Southern Europe during the present century: relationships with the North Atlantic Oscillation and the El Niño-Southern Oscillation. Climate Dynamics 13, 275-284.

Roe, H.M., Russell Coope, G., Devoy, R.J.N., Harrison, C.J.O., Penkman, K.E.H., Preece, R.C., Schreve, D.C., 2009. Differentiation of MIS 9 and MIS 11 in the continental record: vegetational, faunal, aminostratigraphic and sea-level evidence from coastal sites in Essex, UK. Quaternary Science Reviews 28, 2342-2373.

Rohling, E.J., Pälike, H., 2005. Centennial-scale climate cooling with a sudden cold event around 8,200 years ago. Nature 434, 975-979.

Rohling, E.J., Jorissen, F.J., Vergnaud-Grazzini, C., Zachariasse, W.J., 1993. Northern Levantine and Adriatic Quaternary planktic foraminifera; reconstruction of paleoenvironmental gradients. Marine Micropaleontology 21, 191-218.

Rohling, E.J., Jorissen, F.J., de Stigter, H.C., 1997. A 200 year interruption of Holocene sapropel formation in the Adriatic Sea. Journal of Micropaleontology 16, 97-108.

Rohling, E.J., Mayewski, P.A., Abu-Zied, R.H., Casford, J.S.L., Hayes, A., 2002. Holocene atmosphere-ocean interactions: records from Greenland and the Aegean Sea. Climate Dynamics 18, 587-593.

Rohling, E.J., Braun, K., Grant, K., Kucera, M., Roberts, A.P., Siddall, M., Trommer, G., 2010. Comparison between Holocene and Marine Isotope Stage 11 sea-level histories. Earth and Planetary Science Letters 291, 97-105.

Rossignol-Strick, M., 1995. Sea-land correlation of pollen records in the Eastern Mediterranean for the Glacial-Interglacial transition: Biostratigraphy versus radiometric time-scale. Quaternary Science Reviews 14, 893-915.

Rossignol-Strick, M., Paterne, M., 1999. A synthetic pollen record of the eastern Mediterranean sapropels of the last 1 Ma: implications for the time-scale and formation of sapropels. Marine Geology 153, 221-237.

Rowe, P.J., Richards, D.A., Atkinson, T.C., Bottrell, S.H., Cliff, R.A., 1997. Geochemistry and radiometric dating of a Middle Pleistocene peat. Geochimica et Cosmochimica Acta 61, 4201-4211.

Rowe, P.J., Atkinson, T.C., Turner, C., 1999. U-series dating of Hoxnian interglacial deposits at Marks Tey, Essex, England. Journal of Quaternary Science 14, 693-702.

Ruddiman, W.F., 2005. Cold climate during the closest Stage 11 analog to recent Millennia. Quaternary Science Reviews 24, 1111-1121.

Saaroni, H., Bitan, A., Alpert, P., Ziv, B., 1996. Continental polar outbreaks into the Levant and the Eastern Mediterranean. International Journal of Climatology 16, 1175-1191.

Sánchez Goñi, M.F., Loutre, M.F., Crucifix, M., Peyron, O., Santos, L., Duprat, J., Malaize, B., Turon, J.-L., Peypouquet, J.-P., 2005. Increasing vegetation and climate gradient in Western Europe over the Last Glacial Inception (122–110 ka): model-data comparison. Earth and Planetary Science Letters 231, 111–130.

Sangiorgi, F., Capotondi, L., Brinkhuis, H., 2002. A centennial scale organic-walled dinoflagellate cyst record of the last deglaciation in the South Adriatic Sea (Central Mediterranean). Palaeogeography, Palaeoclimatology, Palaeoecology 186, 199-216.

Sangiorgi, F., Capotondi, L., Combourieu-Nebout, N., Vigliotti, L., Brinkhuis, H., Giunta, S., Lotter, A.F., Morigi, C., Negri, A., Reichart, G.-J., 2003. Holocene seasonal sea-surface temperature variations in the southern Adriatic Sea inferres from a multiproxy approach. Journal of Quaternary Science 18, 723-732.

Sarmaja-Korjonen, K., Seppä, H., 2007. Abrupt and consistent responses of aquatic and terrestrial ecosystems to the 8200 cal. yr cold event: a lacustrine record from Lake Arapisto, Finland. The Holocene 17, 457-467.

Sarnthein, M., van Kreveld, S., Erlenkeuser, H., Grootes, P.M., Kucera, M., Pflaumann, U., Schulz, M., 2003. Centennial-to-millennial-scale periodicities of Holocene climate and sediment injections off the western Barents shelf, 75°N. Boreas 32, 447-461.

Scourse, J.D., 2006. Comment on: Numerical ^{230}Th/U dating and a palynological review of the Holsteinian/Hoxnian interglacial. Quaternary Science Reviews 25, 3070-3071.

Seager, R., Battisti, D.S., Yin, J., Gordon, N., Naik, N., Clement, A.C., Cane, M.A., 2002. Is the Gulf Stream responsible for Europe's mild winters? Quarterly Journal of the Royal Meteorological Society 128, 2563-2586.

Selle, W., 1954. Die Vegetationsentwicklung des Interglazials von Ober-Ohe in der Lüneburger Heide. Abhandlungen des naturwissenschaftlichen Vereins zu Bremen 33, 457-463.

Seppä, H., Birks, H.J.B., Giesecke, T., D. Hammarlund, D., Alenius, T., Antonsson, K., Bjune, A.E., Heikkilä, M., MacDonald, G.M., Ojala, A.E.K., Telford, R. J., Veski, S., 2007. Spatial structure of the 8200 cal yr BP event in northern Europe. Climate of the Past 3, 225-236.

Seymour, St.K.S., Christanis, K., Bouzinos, A., Papazisimou, S., Papatheodorou, G., Moran, E., Dénès, G., 2004. Tephrostratigraphy and tephrochronology in the Philippi peat basin, Macedonia, Northern Hellas (Greece). Quaternary International 121, 53-65.

Shackleton, N.J., 1969. The last interglacial in marine and terrestrial records. Philosophical Transactions of the Royal Society of London B 174, 135-154.

Shindell, D.T., Schmidt, G.A., Mann, M.E., Rind, D., Waple, A., 2001. Solar forcing of regional climate change during the Maunder Minimum. Science 294, 2149-2152.

Siani, G., Paterne, M., Michel, E., Sulpizio, R., Sbrana, A., Arnold, M., Haddad, G., 2001. Mediterranean sea surface radiocarbon reservoir age changes since the Last Glacial Maximum. Science 294, 1917-1920.

Sluijs, A., Pross, J., Brinkhuis, H., 2005. From greenhouse to icehouse; organic-walled dinoflagellate cysts as paleoenvironmental indicators in the Paleogene. Earth-Science Reviews 68, 281-315.

Smith, A.G., 1965. Problems of inertia and threshold related to post-Glacial habitat changes. Philosophical Transactions of the Royal Society of London B 161, 331-342.

Solanki, S.K., Usoskin, I.G., Kromer, B., Schüssler, M., Beer, J., 2004. Unusual activity of the Sun during recent decades compared to the previous 11,000 years. Nature 431, 1084-1087.

Sperling, M., Schmiedl, G., Hemleben, C., Emeis, K.C., Erlenkeuser, H., Grootes, P.M., 2003. Black Sea impact on the formation of eastern Mediterranean sapropel S1? Evidence from the Marmara Sea. Palaeogeography, Palaeoclimatology, Palaeoecology 190, 9-21.

Stenseth, N.C., Ottersen, G., Hurrell, J.W., Mysterud, A., Lima, M., Chan, K.-S., Yoccoz, N.G., Ådlandsvik, B., 2003. Studying climate effects on ecology through the use of climate indices: the North Atlantic Oscillation, El Niño Southern Oscillation and beyond. Proceedings of the Royal Society of London B 270, 2087-2096.

Stuiver, M., Braziunas, T.F., 1993. Sun, ocean, climate and atmospheric $^{14}CO_2$: an evaluation of causal and spectral relationships. The Holocene 3, 289-305.

Stuiver, M., Grootes, P.M., 2000. GISP2 Oxygen Isotope Ratios. Quaternary Research 53, 277-284.

Stuiver, M., Grootes, P.M., Braziunas, T.F., 1995. The GISP2 δ18O climate record of the past 16,500 years and the role of the sun, ocean, and volcanoes. Quaternary Research 44, 341-354.

Svensson, A., Andersen, K.K., Bigler, M., Clausen, H.B., Dahl-Jensen, D., Davies, S.M., Johnsen, S.J., Muscheler, R., Parrenin, F., Rasmussen, S.O., Röthlisberger, R., Seierstad, I., Steffensen, J.P., Vinther, B.M., 2008. A 60 000 year Greenland stratigraphic ice core chronology, Climate of the Past 4, 47-57.

Tallantire, P.A., 2002. The early-Holocene spread of hazel (*Corylus avellana* L.) in Europe north and west of the Alps: an ecological hypothesis. The Holocene 12, 81-96.

Theissen, K.M., Dunbar, R.B., Rowe, H.D, Mucciarone, D.A., 2008. Multidecadal- to century-scale arid episodes on the northern Altiplano during the middle Holocene. Palaeogeography, Palaeoclimatology, Palaeoecology 257, 361–376.

Theocharis, A., Nittis, K., Kontoyiannis, H., Papageorgiou, E., Balapolous, E., 1999. Climatic changes in the Aegean Sea influence the Eastern Mediterranean thermohaline circulation (1986-1997). Geophysical Research Letters 26, 1617-1620.

Thomas, G.N., 2001. Late Middle Pleistocene pollen biostratigraphy in Britain: pitfalls and possibilities in the separation of interglacial sequences. Quaternary Science Reviews 20, 1621-1630.

Thomas, P.A., Polwart, A., 2003. *Taxus baccata* L. Journal of Ecology 93, 489-524.

Tinner, W., Lotter, A.F., 2001. Central European vegetation response to abrupt climate change at 8.2 ka. Geology 29, 551-554.

Tinner, W., Lotter, A.F., 2006. Holocene expansions of *Fagus silvatica* and *Abies alba* in Central Europe: where are we after eight decades of debate? Quaternary Science Reviews 25, 526-549.

Torrence, C., Compo, G.P., 1998. A practical guide to wavelet analysis. Bulletin of the American Meteorological Society 79, 61-78.

Turner, C., 1970. The Middle Pleistocene deposits at Marks Tey, Essex. Philosophical Transactions of the Royal Society of London B 257, 373-440.

Turner, C., 1998. Volcanic maars, long Quaternary sequences and the work of the INQUA Subcommission on European Quaternary Stratigraphy. Quaternary International 47/48, 41-49.

Tzedakis, P.C., 1994. Vegetation change through glacial-interglacial cycles: a long pollen sequence perspective. Philosophical Transactions of the Royal Society of London B 345, 403-432.

Tzedakis, P.C., 2010. The MIS 11 – MIS 1 analogy, southern European vegetation, atmospheric methane and the "early anthropogenic hypothesis". Climate of the Past 6, 131-144.

Tzedakis, P.C., Andrieu, V., de Beaulieu, J.-L., Birks, H.J.B., Crowhurst, S., Follieri, M., Hooghiemstra, H., Magri, D., Reille, M., Sadori, L., Shackleton, N.J., Wijmstra, T.A., 2001. Establishing a terrestrial chronological framework as a basis for biostratigraphical comparisons. Quaternary Science Reviews 20, 1583-1592.

Tzedakis, P.C., Roucoux, K.H., de Abreu, L., Shackleton, N.J., 2004a. The duration of forest stages in Southern Europe and interglacial climate variability. Science 306, 2231-2235.

Tzedakis, P.C., Frogley, M.R., Lawson, I.T., Preece, R.C., Cacho, I., de Abreu, L., 2004b. Ecological thresholds and patterns of millennial-scale climate variability: The response of vegetation in Greece during the last glacial period. Geology 32, 109-112.

Tzedakis, P.C., Raynaud, D., McManus, J.F., Berger, A., Brovkin, V., Kiefer, T., 2009. Interglacial diversity. Nature Geoscience 2, 751-755.

Vautard, R., Yiou, P., Ghil, M., 1992. Singular-spectrum analysis: A toolkit for short, noisy chaotic signals. Physica D 58, 95-126.

Verleye, T.J., Mertens, K.N., Louwye, S., Arz, H.W., 2009. Holocene salinity changes in the southwestern Black Sea: A reconstruction based on dinoflagellate cysts. Palynology 33, 77-100.

Veski, S., Seppä, H., Ojala, A.E.K., 2004. Cold event at 8200 yr B.P. recorded in annually laminated lake sediments in eastern Europe. Geology 32, 681-684.

Visbeck, M.H., Hurrell, J.M., Polvani, L., Cullen, H.M., 2001. The North Atlantic Oscillation: Past, present, and future. Proceedings of the National Academy of Sciences of the United States of America 98, 12876-12877.

von Grafenstein, U., Erlenkeuser, H., Müller, J., Jouzel, J., Johnsen, S., 1998. The cold event 8200 years ago documented in oxygen isotope records of precipitation in Europe and Greenland. Climate Dynamics 14, 73-81.

von Grafenstein, U., Erlenkeuser, H., Brauer, A., Jouzel, J., Johnsen, S.J., 1999. A mid-European decadal isotope-climate record from 15,500 to 5000 years B.P. Science 284, 1654-1657.

Vos, H., Sanchez, A., Zolitschka, B., Brauer, A., Negendank, J.F.W., 1997. Solar activity variations recorded in varved sediments from the crater lake of Holzmaar – a maar lake in the Westeifel volcanic field. Surveys in Geophysics 18, 163-182.

Waelbroeck, C., Duplessy, J.-C., Michel, E., Labeyrie, L., Paillard, D., Duprat, J., 2001. The timing of the last deglaciation in North Atlantic climate records. Nature 412, 724-727.

Wall, D., Dale, B., Lohmann, G.P., Smith, W.K., 1977. The environment and climatic distribution of dinoflagellate cysts in modern marine sediments from regions in the north and south Atlantic oceans and adjacent seas. Marine Micropaleontology 2, 121-200.

Wang, Y.J., Cheng, H., Edwards, R.L., An, Z.S., Wu, J.Y., Shen, C.C., Dorale, J.A., 2001. A high-resolution absolute-dated late Pleistocene monsoon record from Hulu Cave, China. Science 294, 2345-2348.

Wanner, H., Brönnimann, S., Casty, C., Gyalistras, D., Luterbacher, J., Schmutz, C., Stephenson, D.B., Xoplaki, E., 2001. North Atlantic Oscillation – concepts and studies. Surveys in Geophysics 22, 321-382.

Wardle, D.A., Walker, L.R., Bardgett, R.D., 2004. Ecosystem properties and forest decline in contrasting long-term chronosequences. Science 305, 509-510.

Weedon, G., 2003. Time-series analysis and cyclostratigraphy. Cambridge University Press, UK, pp. 259.

Weijers, J.W.H, Schouten, S., Spaargaren, O.C., Sinninghe Damsté, J.S., 2006. Occurrence and distribution of tetraether membrane lipids in soils: Implications for the use of the TEX_{86} proxy and the BIT index. Organic Geochemistry 37, 1680-1693.

Weijers, J.W.H, Schouten, S., van den Donker, J.C., Hopmans, E.C., Sinninghe Damsté, J.S., 2007. Environmental controls on bacterial tetraether membrane lipid distribution in soils. Geochimica et Cosmochimica Acta 71, 703-713.

Weldeab, S., Lea, D.W., Schneider, R.R., Andersen, N., 2007. 155,000 Years of West African Monsoon and Ocean Thermal Evolution. Science 316, 1303-1307.

Welten, M., 1988. Neue pollenanalytische Ergebnisse über das Jüngere Quartär des nördlichen Alpenvorlandes der Schweiz (Mittel- und Jungpleistozän). Beiträge zur geologischen Karte der Schweiz 162, 1-40.

West, R., 1956. The Quaternary deposits at Hoxne, Suffolk. Philosophical Transactions of the Royal Society of London B 239, 265-356.

Wiersma, A.P., Renssen, H., 2006. Model-data comparison for the 8.2 ka BP event: confirmation of a forcing mechanism by catastrophic drainage of Laurentide Lakes. Quaternary Science Reviews 25, 63-88.

Wijmstra, T.A., Smit, A., 1976. Palynology of the middle part (30-78 metres) of the 120 m deep section in Northern Greece (Macedonia). Acta Botanica Neerlandica 25, 297-312.

Winograd, I.J., Landwehr, J.M., Ludwig, K.R., Coplen, T.B., Riggs, A.C., 1997. Duration and structure of the past four interglaciations. Quaternary Research 48, 141-154.

Woillard, G., 1979. Abrupt end of the last interglacial s.s. in north-east France. Nature 281, 558-562.

Zagwijn, W.H., 1996. An analysis of Eemian climate in western and central Europe. Quaternary Science Reviews 15, 451-469.

Zolitschka, B., 1992. Climatic change evidence and lacustrine varves from maar lakes, Germany. Climate Dynamics 6, 229-232.

Zonneveld, K.A.F., Versteegh, G.J.M., de Lange, G.J., 2001. Palaeoproductivity and post-depositional aerobic organic matter decay reflected by dinoflagellate cyst assemblages of the Eastern Mediterranean S1 sapropel. Marine Geology 172, 181-195.

Zusammenfassung

Das marine Isotopenstadium (MIS) 11 stellt eine der besten astronomischen Analogien für das MIS 1 (Holozän) dar, da die Konstellation der orbitalen Parameter (geringe Exzentrizität und reduzierter Einfluss der Präzession) sich während beider Isotopenstadien stark ähnelt. Damit kann die Untersuchung der Klimavariabilität während MIS 11 dazu beitragen, die Klimaentwicklung des gegenwärtigen Holozän-Interglazials ohne eine anthropogene Beeinflussung besser abzuschätzen.

Um tiefere Einblicke in die natürliche Klimavariabilität während MIS 11 zu erhalten, wurden in der vorliegenden Arbeit annual laminierte Seesedimente aus dem Holstein-Interglazial von Dethlingen (Norddeutschland) untersucht. Das Holstein-Interglazial wird allgemein als terrestrisches Äquivalent zu MIS 11c in Mitteleuropa angesehen und kann biostratigraphisch mit dem Hoxnian-Interglazial der Britischen Inseln, dem Masowien-Interglazial Polens und dem Praclaux-Interglazial in Frankreich korreliert werden. Auf der Basis dieser Korrelationen ist ein Vergleich der Vegetations- und Klimadynamik in überregionalem Maßstab möglich. Die vorliegende Arbeit basiert auf einem breiten methodischen Ansatz, der palynologische, mikropaläontologische, sedimentologische und geochemische Analysen sowie Zeitreihenanalysen umfasst. Die Arbeit zielt insbesondere auf (i) die genaue Erfassung der langfristigen (jahrhundert- bis jahrtausend-skaligen) und kurzfristigen (subdekadisch- bis dekadisch-skaligen) Klimavariabilität während des Holstein-Interglazials, (ii) die Ermittlung der Charakteristika und Geschwindigkeit eines abrupten Klimawechsels sowie der ihm zu Grunde liegenden Auslösemechanismen und (iii) das Abschätzen des Einflusses dieses abrupten Klimawechsels auf terrestrische Ökosysteme.

In Bezug auf die langfristige Klimavariabilität erlauben die palynologischen Ergebnisse Einblicke in die holsteinzeitliche Vegetationsabfolge von der mesokratischen bis zur telokratischen Waldphase; die untersuchte Abfolge umfasst ~11,5 ka des 15-16 ka dauernden Holstein-Interglazials. Die palynologischen Befunde belegen die Entwicklung eines gemäßigten Mischwaldes in der Umgebung von Dethlingen. Die älteren Abschnitte des Interglazials werden durch eine starke Präsenz borealer Baumtaxa (z.B. *Picea*) charakterisiert, während die jüngeren Abschnitte durch Expansion subatlantischer bis atlantischer Waldelemente (z.B. *Abies*, *Buxus*, *Ilex*, *Quercus*) gekennzeichnet sind. Diese Vegetationsentwicklung legt einen generellen Erwärmungstrend und eine abnehmende Saisonalität während des Holstein-Interglazials nahe. Die Maximalhäufigkeiten von *Buxus*- und *Quercus*-Pollen während späterer Stadien des Interglazials weisen darauf hin, dass zu dieser Zeit die wärmsten Bedingungen (bei gleichzeitig hoher Humidität) erreicht wurden.

Diese Beobachtung unterstützt eine Korrelation des Holstein-Interglazials mit MIS 11, da während dieses Isotopenstadiums im Gegensatz zu MIS 9 eine maximale Erwärmung im jüngeren Abschnitt des Interglazials auftritt. Basierend auf der Konstellation orbitaler

Parameter und vorhandener Daten zum atlantischen Wärmetransport, welcher die Vegetationsdynamik in Mitteleuropa stark beeinflusst, wird die 15-16 ka andauernde Ausbildung von Wäldern während des Holstein-Interglazials in Mitteleuropa dem ~30 ka langen MIS 11c zugeordnet; dabei fällt die Waldphase in Mitteleuropa sehr wahrscheinlich in die zweite Hälfte von MIS 11c, also zwischen 415 und 397 ka BP. Für diese Einordnung sprechen drei Argumente: Erstens breiteten sich die borealen Pionierwälder höchstwahrscheinlich auf Grund der Verstärkung des ozeanischen Wärmetransports in den Nordatlantik nach 415 ka BP aus. Zweitens besteht mit großer Wahrscheinlichkeit eine Verbindung zwischen der maximalen Ausbreitung gemäßigter Wälder und dem Maximum der Sommer-Insolation in der nördlichen Hemisphäre während MIS 11c bei ~408 ka BP; für diese Zeit zeigen publizierte Daten eine maximale Advektion warmer Meeresoberflächenwässer in den polaren Nordatlantik, ein Minimum im globalen Eisvolumen und zugleich ein Temperatur-Maximum in der Antarktis. Drittens sollte der Rückgang gemäßigter Wälder in Mitteleuropa nach 401 ka BP, d.h. im Anschluss an den Rückgang der Oberflächenwassertemperatur im Nordatlantik stattgefunden haben, während der Übergang zu glazialen Bedingungen mit dem Insolationsminimum bei ~387 ka BP assoziiert war.

Die Waldentwicklung während des Holstein-Interglazials war sowohl durch abrupte als auch durch graduelle Änderungen in den Häufigkeiten gemäßigter Pflanzentaxa gekennzeichnet. Diese Vegetationsänderungen weisen auf eine ausgeprägte Klimavariabilität innerhalb des Interglazials hin. Zwei deutliche Rückgänge gemäßigter Taxa, welche die Entwicklung borealer und subborealer Wälder zur Folge hatten, wurden durch jahrhundertskalige Klima-Oszillationen ausgelöst; sie werden im Folgenden als Ältere („Older") und Jüngere („Younger") Holstein-Oszillation (OHO bzw. YHO) bezeichnet. Diese Oszillationen ereigneten sich ~6000 bzw. ~9000 Jahre nach dem Einsetzen der interglazialen Bewaldung durch Pionier-Baumarten in Mitteleuropa. Basierend auf der Warvenchronologie für das Dethlingen-Profil und der Annahme, dass die Expansion der Wälder des Holstein-Interglazials in Mitteleuropa während der zweiten Hälfte von MIS 11c stattfand, kann der OHO ein Alter von ~408 und der YHO ein Alter von ~405 ka BP zugeordnet werden.

Um den Einfluss der OHO und der YHO auf terrestrische Ökosysteme währen des Holstein-Interglazials zu erfassen und die zu Grunde liegenden Antriebsmechanismen zu entschlüsseln, wurden diese kritischen Intervalle hochauflösend (dekadisch-skalig) palynologisch und sedimentologisch analysiert. Die Ergebnisse zeigen, dass die OHO mit einem ausgeprägten, 90 Jahre andauernden Rückgang gemäßigter Taxa und einer gleichzeitigen Ausbreitung von *Pinus* sowie Gräsern und Kräutern beginnt. Eine darauf folgende, 130 Jahre andauernde Regeneration gemäßigter Taxa wurde durch die Expansion von Pioniergehölzen (*Betula*, *Alnus*) eingeleitet. Auf Grund ihres charakteristischen Einflusses auf die jeweilige Vegetationsdynamik kann die OHO in Pollendatensätzen aus Flachlandgebieten Mitteleuropas nördlich des 50. Breitengrades von den Britischen Inseln bis nach Polen identifiziert werden. Die Auswertung aller verfügbaren palynologischen

Datensätze aus dieser Region zeigt das Vorherrschen kälterer Winter während der OHO, mit graduell abnehmender Temperatur und Humidität und erhöhter Kontinentalität in Richtung Osteuropa. Dieses räumliche Muster deutet auf einen schwächeren Einfluss der Westwinde und/oder einen stärkeren Einfluss des Sibirischen Hochs in Verbindung mit der OHO hin.

In Pollendatensätzen aus den Mittelgebirgen zwischen 45° und 50° nördlicher Breite kann der Einfluss der OHO nicht zweifelsfrei nachgewiesen werden. Die Gründe hierfür bleiben unklar. Möglicher Weise war hier der klimatische Einfluss der OHO auf die Vegetation geringer bzw. blieb innerhalb der klimatischen Toleranz der dortigen Vegetation. Weiter erscheint denkbar, dass eine im Vergleich zum Flachland andersartige Reaktion der Mittelgebirgsvegetation aus höheren Niederschlägen resultierte, die durch eine Südverschiebung der Westwinddrift verursacht wurden. Ein solcher Humiditätsanstieg könnte das Wachstum montaner Baumarten wie z.B. *Abies*, dem dominanten Baumtaxon im alpinen Holstein, gefördert haben; *Abies* besitzt unter Klimabedingungen mit hohen Sommerniederschlägen und niedrigeren Wintertemperaturen einen Wettbewerbsvorteil.

Die Vegetationsdynamik während der YHO wird durch einen Rückgang gemäßigter Taxa (besonders *Carpinus*) und der Ausbreitung von Baumpionieren (vor allem *Betula*) charakterisiert. Im Gegensatz zur OHO treten frostempfindliche Taxa (z.B. *Ilex*, *Buxus* und *Hedera*) auch während der Oszillation, was darauf hin deutet, dass die mittleren Wintertemperaturen während der YHO nicht oder nur wenig unter 0 ºC absanken. Deshalb erscheint es plausibel, dass ein Mangel an Sommerwärme für den Vegetationsrückschlag während der YHO verantwortlich gewesen sein könnte.

Da die YHO bislang nur in wenigen Pollenprofilen nachgewiesen wurde, ist ihre räumliche Ausdehnung bisher nur unzureichend bekannt. Allerdings erscheint es möglich, dass der Einfluss der YHO auf die Vegetation Mitteleuropas bisher auf Grund des Vorherrschens frost-sensitiver Baumtaxa übersehen wurde. Daher erscheint es notwendig, die verfügbaren Pollendatensätze aus Mitteleuropa auf Änderungen in den Häufigkeiten gemäßigter und auf warme Sommer angewiesener Taxa auszuwerten.

Die YHO liegt inmitten eines graduellen, ca. ~1500 Jahre anhaltenden Rückgangs und einer nachfolgender Erholung gemäßigter Taxa. Eventuell korreliert dieser längerfristige Rückgang und Wiederanstieg mit einer in der Literatur dokumentierten längerfristigen Fluktuation der Oberflächenwassertemperaturen im Nordatlantik um ~405 ka BP, wobei diese Korrelationen allerdings durch den Mangel an belastbaren Chronologien erschwert werden.

Da sich die Einflüsse von OHO und YHO auf die Vegetation deutlich voneinander unterscheiden, wurden diese Klima-Oszillationen vermutlich durch unterschiedliche Auslösemechanismen verursacht. Die mit der OHO einher gehende und Jahrzehnte anhaltende Abkühlung der mittleren Wintertemperatur in Mitteleuropa deutet auf einen reduzierten ozeanischen Wärmetransport hin, der mit einem kurzfristigen Rückgang der Bildung des nordatlantischen Tiefenwassers im Zusammenhang stehen könnte. Diese

Hypothese wird durch die starke Ähnlichkeit der OHO mit dem 8.2-ka-Ereignis des Holozäns unterstützt. Weit gehende Übereinstimmungen zwischen beiden Ereignissen bestehen bezüglich der jeweiligen Dauer, der Auswirkung auf terrestrische Ökosysteme, des räumlichen Musters des Klimaeinflusses, des Auftrittszeitpunkts innerhalb des jeweiligen Interglazials und der interglazialen Rahmenbedingungen. Demnach wäre eine durch Schmelzwasser verursachte Abschwächung der Tiefenwasserbildung ein klimatreibender Faktor, der häufiger als bislang angenommen auch unter interglazialen Bedingungen auftritt. Solche Klimarückschläge scheinen unter interglazialen Bedingungen bevorzugt dann aufzutreten, wenn die Zunahme der Sommer-Insolation am Ende des vorherigen Glazials langsam und gering ist und somit einen Fortbestand der großen kontinentalen Eisschilde bis weit in das Interglazial ermöglicht.
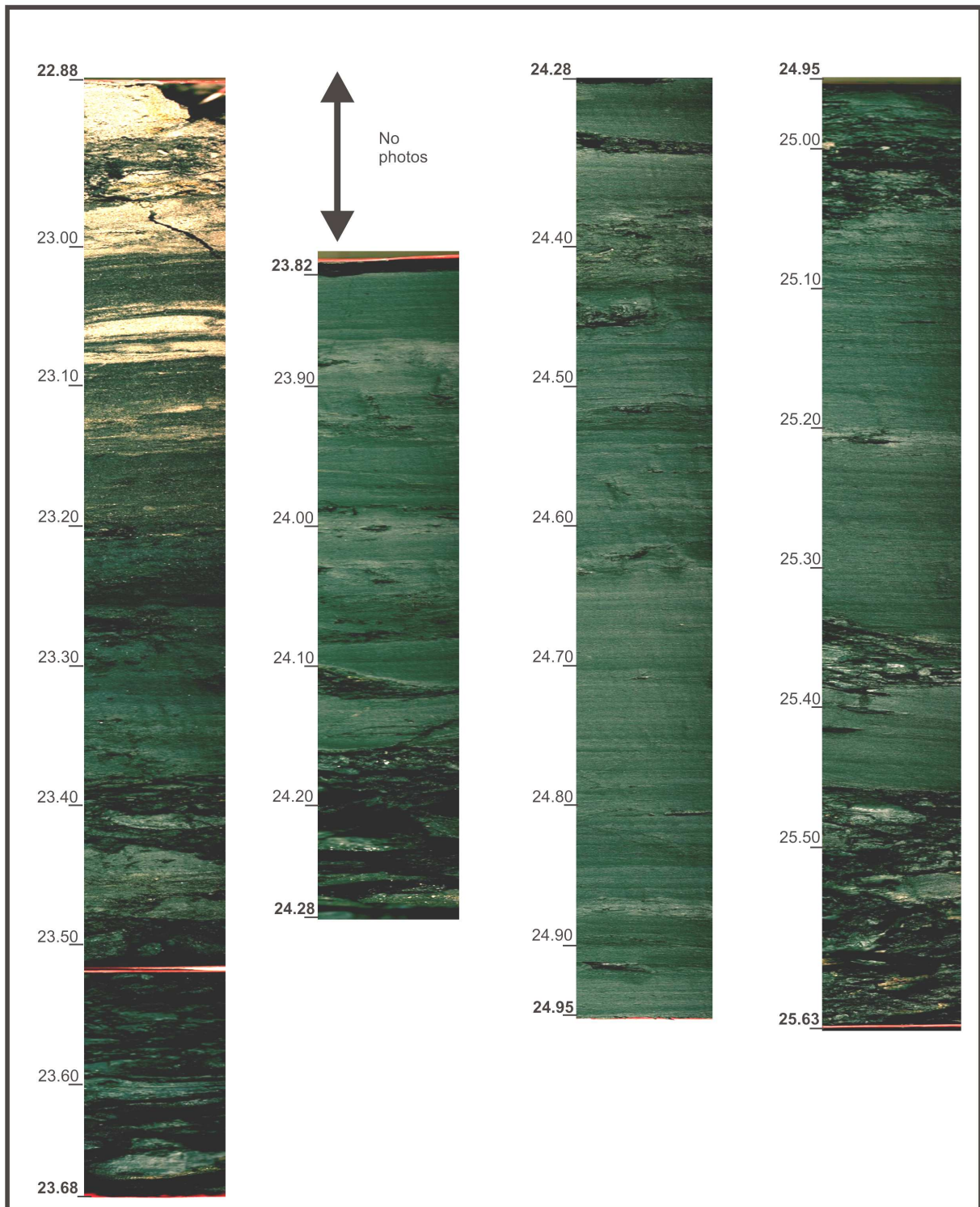
Im Gegensatz dazu widerspricht die Präsenz frostempfindlicher Taxa während der YHO einer vorübergehenden Reduzierung des ozeanischen Wärmetransports, wie er für die OHO postuliert wird. Die YHO liegt am Ende eines langfristigen, graduellen Rückgangs gemäßigter Baumtaxa, der vermutlich die Reaktion der Vegetation auf orbitale Einflüsse widerspiegelt, vor allem auf einen Rückgang der Sommer-Insolation während jüngerer Phasen von MIS 11c. Während des orbital gesteuerten und somit graduellen Rückgangs der Sommer-Insolation wurde vermutlich ein kritischer Schwellenwert überschritten und dadurch die vergleichsweise abrupte YHO ausgelöst. Allerdings ist der Anstieg gemäßigter Taxa nach der YHO nicht mit der weiterhin sinkenden Sommer-Insolation kompatibel. Dies bedeutet, dass unterschiedliche Mechanismen für den langfristigen Rückgang vor und die folgende Erholung gemäßigter Taxa nach der YHO verantwortlich sein dürften.
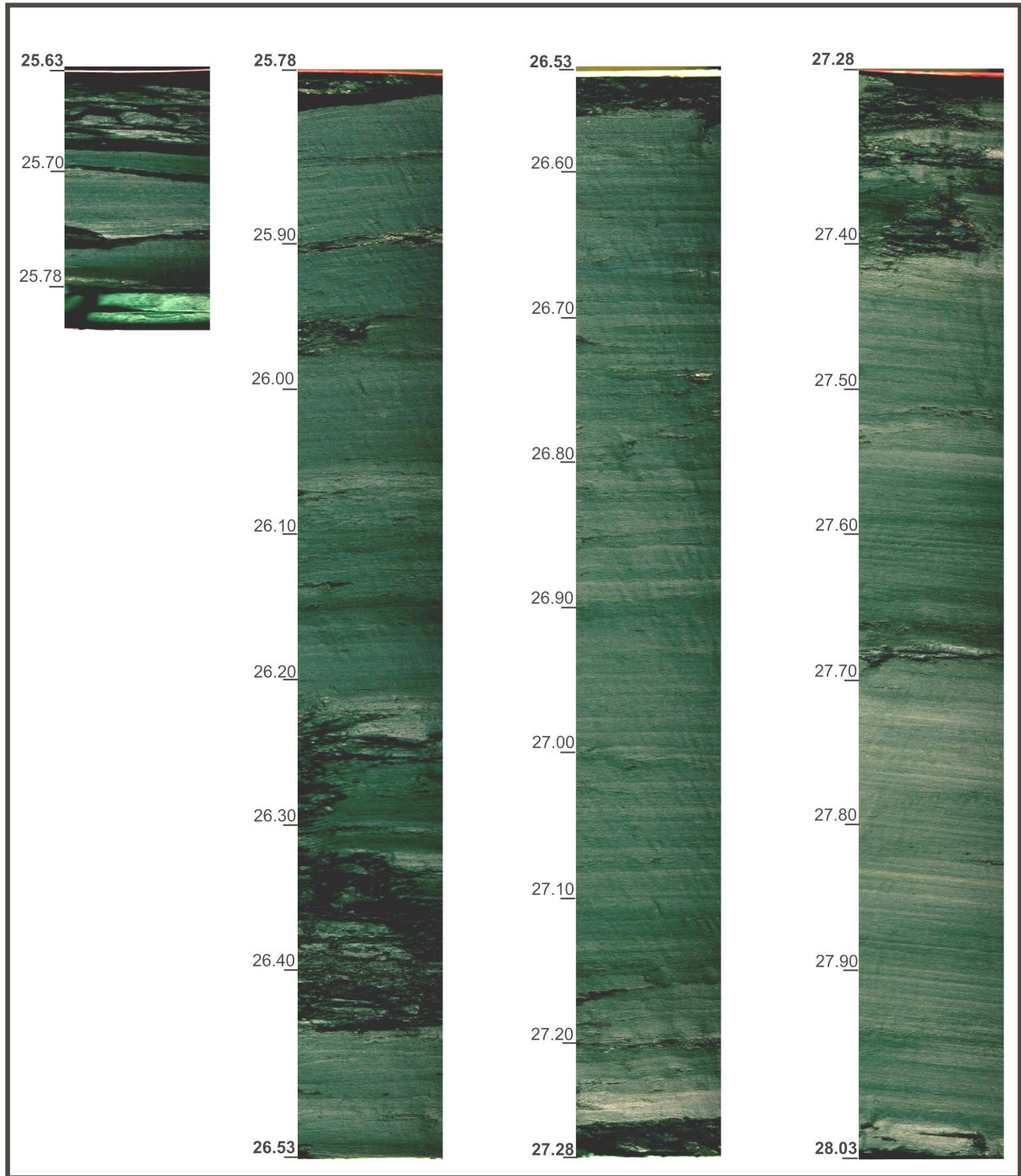
Die Charakteristika kurzfristiger Klimavariabilität wurden an Hand von Mikrofazies- und Zeitreihenanalysen eines ~3200 Jahre umfassenden, jahreszeitlich geschichteten Abschnitts im Profil von Dethlingen untersucht. Die Jahreszeitenschichtung beruht auf biogenen Warven, die aus zwei unterschiedlichen Teillagen bestehen. Die Zusammensetzung und Mächtigkeit der hellen Lagen wird hauptsächlich durch den jährlichen Zyklus der Diatomeenblüte bestimmt. Diese werden durch Taxa der Gattungen *Stephanodiscus*, *Ulnaria* und *Aulacoseira* dominiert. Die dunklen Lagen bestehen primär aus amorphem organischem Material mit Fragmenten von Diatomeen-Frusteln. Aufgearbeitete periphytische Diatomeen, Pflanzenreste, Nadeln von Süßwasserschwämmen der Litoralzone und Goldalgenzysten sind häufig. Die dunklen Lagen enthalten oft geringe Konzentrationen von Tonpartikeln, welche in den hellen Lagen fast völlig fehlen. Die Abfolge und Charakteristika der einzelnen Warvenlagen indizieren, dass die Diatomeenlagen während des Frühlings/Sommers abgelagert wurden und Änderungen in der Produktivität des Paläosees von Dethlingen reflektieren, während die aus organischem Material und Detritus bestehenden dunklen Lagen während des Herbsts/Winters gebildet wurden.

Spektralanalysen der Dicke der hellen und dunklen Lagen zeigen mehrere, die 95%- und 99%-Verlässlichkeitsstufen übersteigende Signale, die mit denjenigen, die aus modernen Messdaten und holozänen Datensätzen bekannt sind, nahezu identisch sind. Dekadisch-skalige Signale mit einer Periodizität von 90, 25 und 10,5 Jahren stehen vermutlich im Zusammenhang mit den 88, 22 und 11 Jahre umfassenden solaren Zyklen; dementsprechend scheint die Sonnenaktivität einer der Auslöser für die Produktivitäts-Änderungen im Paläosee von Dethlingen gewesen zu sein. Subdekadisch-skalige Signale mit einer Periodizität von 3-5 und ~6 Jahren reflektieren vermutlich den Einfluss der „El Niño-Southern Oscillation" (ENSO) und der „Nordatlantischen Oszillation" (NAO) auf die winterliche Lagenbildung.
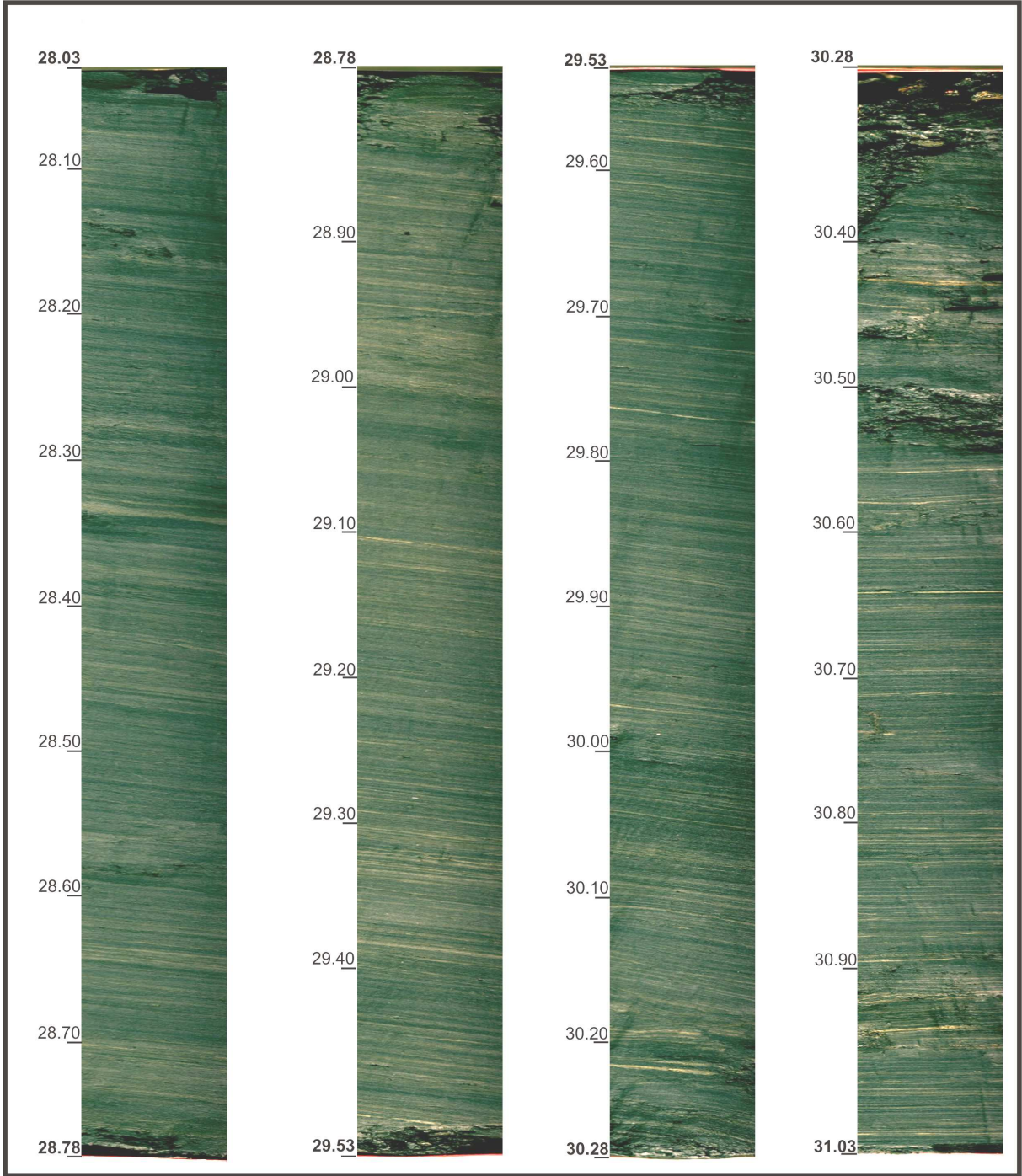
Im Licht dieser Ergebnisse ist die Vergleichbarkeit der klimatreibenden Faktoren während der Holstein- und Holozän-Interglaziale nicht auf die bereits etablierte Analogie bezüglich der langfristigen astronomischen Konstellation beschränkt, sondern erstreckt sich auch auf kurze (subdekadische bis dekadische) Zeitskalen. Somit sollten bei Modellierungen zukünftiger Klimaszenarios, denen die MIS-11/MIS-1-Analogie zugrunde liegt, auch auf kurzfristigen Skalen agierende Klimafaktoren berücksichtigt werden.
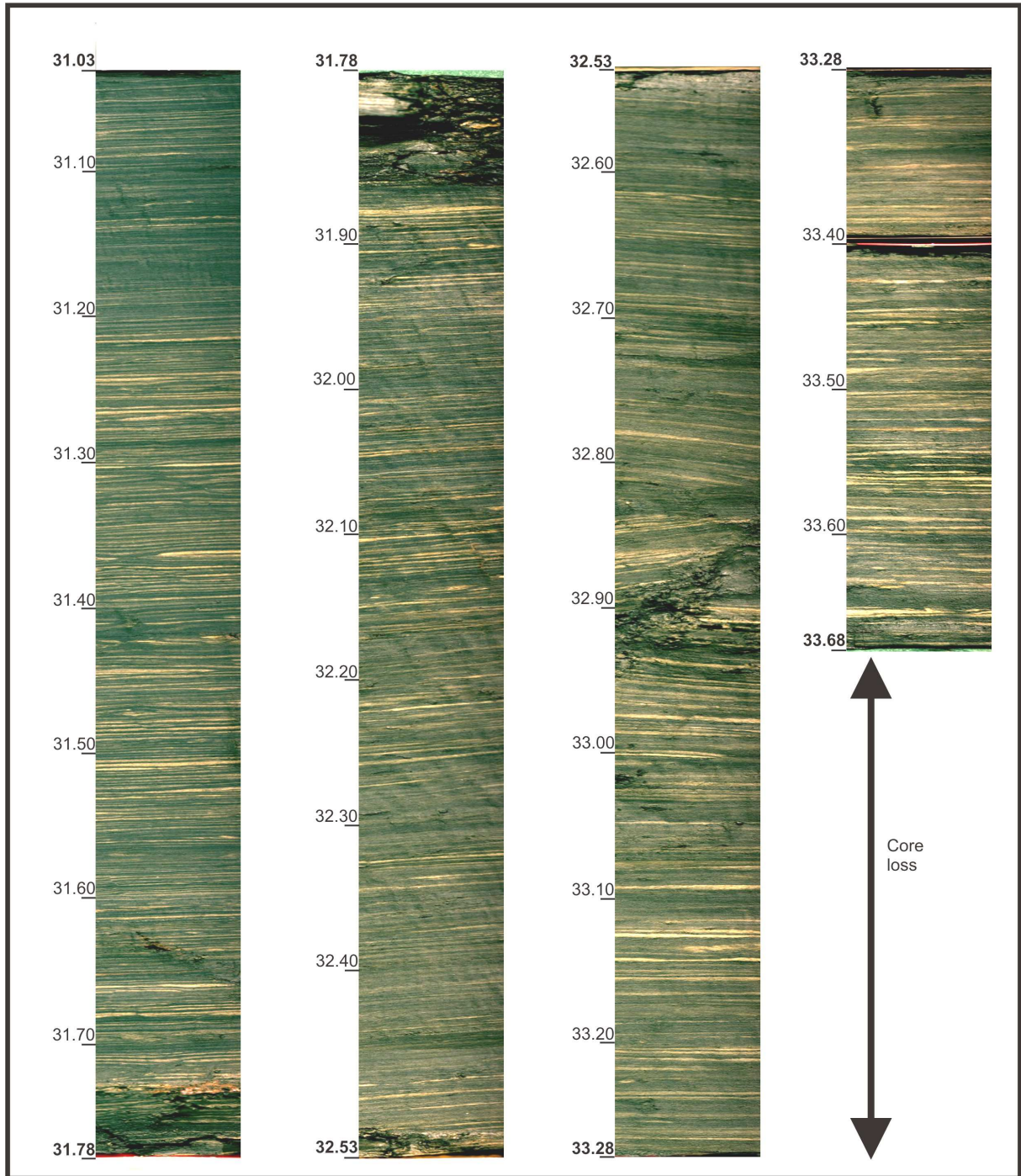
Appendix I: Photographs of the Dethlingen core (depth in meters below surface)
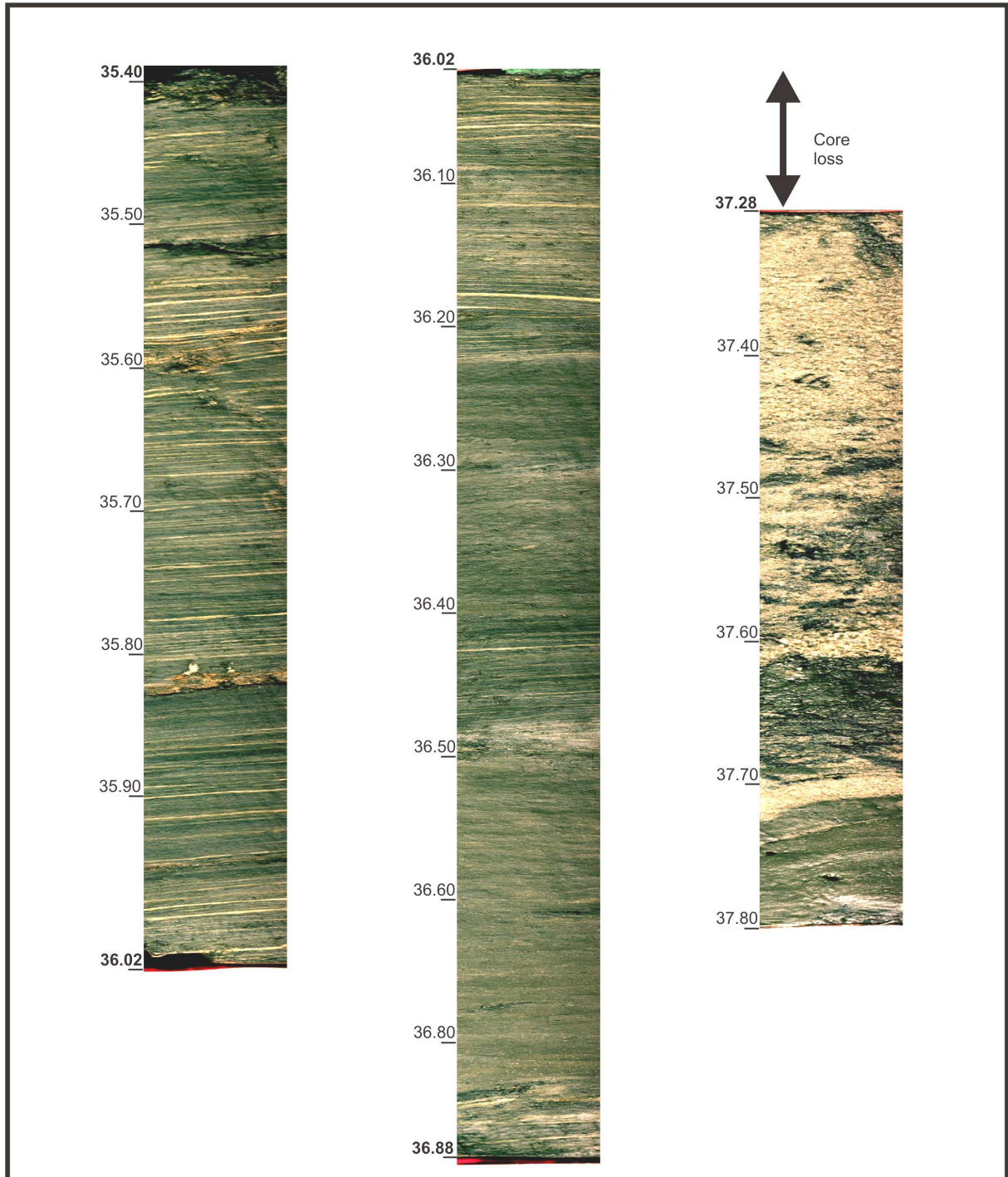
28.03
28.10
28.20
28.30
28.40
28.50
28.60
28.70
28.78

28.78
28.90
29.00
29.10
29.20
29.30
29.40
29.53

29.53
29.60
29.70
29.80
29.90
30.00
30.10
30.20
30.28

30.28
30.40
30.50
30.60
30.70
30.80
30.90
31.03

31.03

31.10

31.20

31.30

31.40

31.50

31.60

31.70

31.78

31.78

31.90

32.00

32.10

32.20

32.30

32.40

32.53

32.53

32.60

32.70

32.80

32.90

33.00

33.10

33.20

33.28

33.28

33.40

33.50

33.60

33.68

Core
loss

35.40

35.50

35.60

35.70

35.80

35.90

36.02

36.02

36.10

36.20

36.30

36.40

36.50

36.60

36.80

36.88

Core
loss

37.28

37.40

37.50

37.60

37.70

37.80

Appendix II: Full list of taxa identified at Dethlingen

Arboreal pollen	Non arboreal pollen	Aquatics
Abies	Apiaceae	*Bottomus*
Acer	*Artemisia*	*Callitriche*
Alnus	Asteraceae	Lemnaceae
Betula	Brassicaceae	*Myriophyllum*
Buxus	Campanulaceae	*Nuphar*
Carpinus	Cannabiaceae	*Nymphaea*
Celtis	Caryophyllaceae	*Potamogeton*
Corylus	*Centaurea jacea* Type	*Typha latifolia*
Fagus	Chenopodiaceae	*T. angustifolia – Sparganium* Type
Fraxinus	*Cicho. crepis* Type	
Hedera	*Cistus salvifolius*	**Spores**
Ilex	*Convolvulus*	*Osmunda*
Juniperus	Cyperaceae	
Ostrya	*Epilobium*	**Algae**
Picea	Ericaceae	*Pediastrum*
Pinus	*Euphrasia*	
Pterocarya	*Filipendula*	
Quercus	*Helianthemum*	
Rhamnus frangula	*Knautia*	
Salix	*Lysimachia*	
Taxus	*Plantago* Type	
Tilia	Poaceae	
Ulmus	*Polygonum*	
Viburnum	*Potentilla* Type	
Viscum	Ranunculaceae	
Vitis	Rubiaceae	
	Rumex	
	Salvia	
	Saxifraga	
	Sedum Type	
	Sorbus	
	Spergularia Type	
	Urticaceae	
	Vicia	

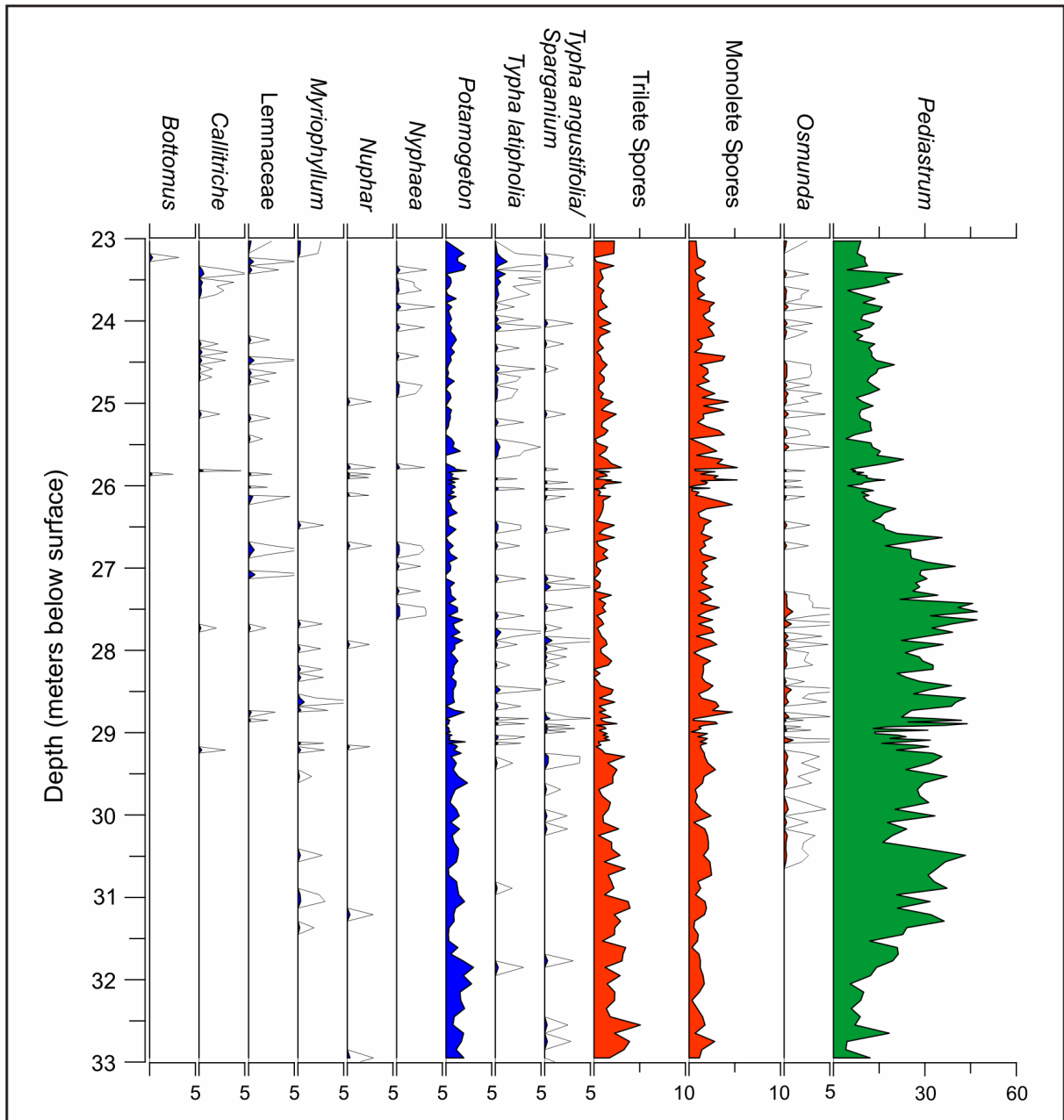## Appendix III: Plots of pollen taxa identified at Dethlingen
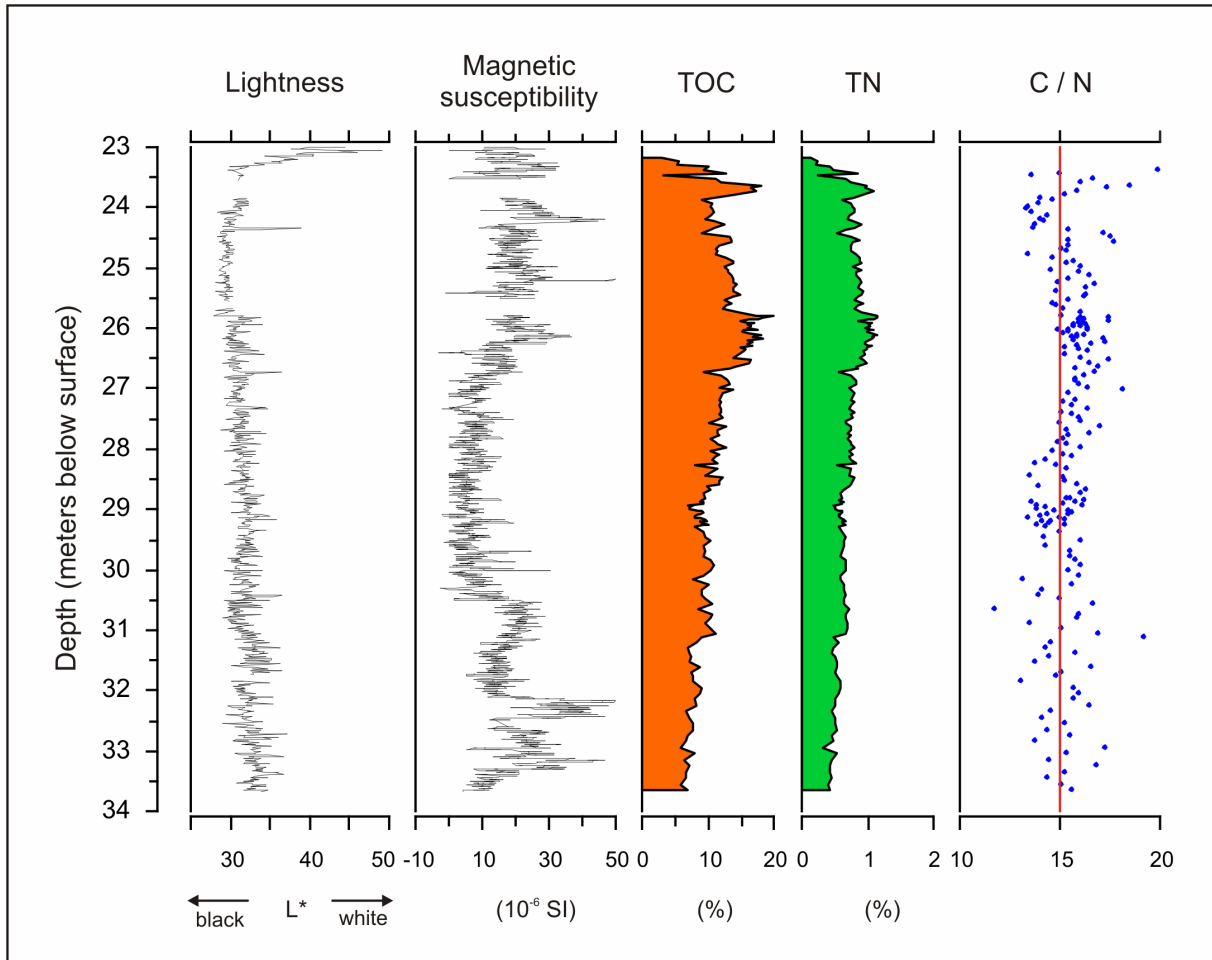
Arboreal pollen (exaggeration line 10x)
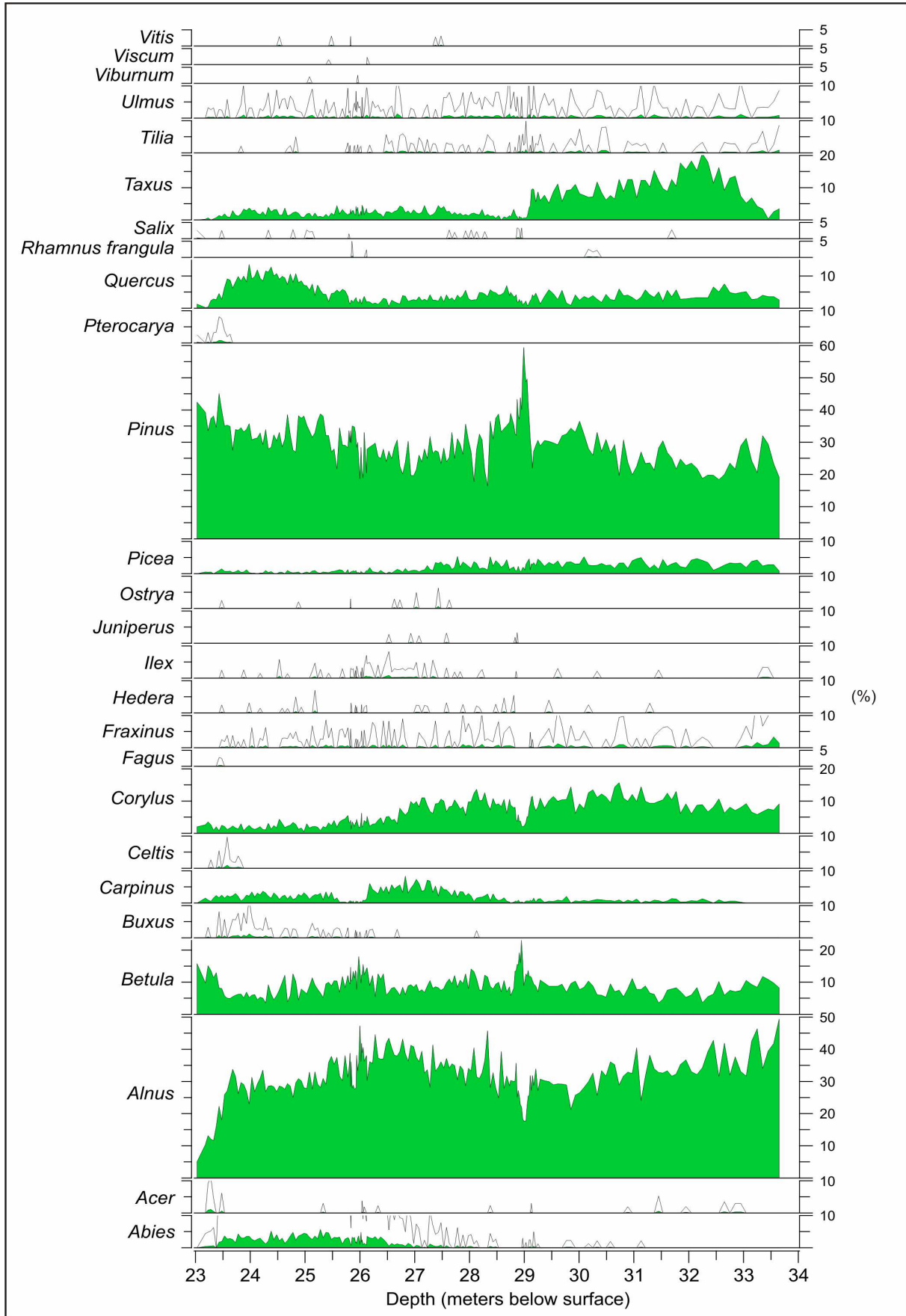
Non arboreal pollen (exaggeration line 10x)
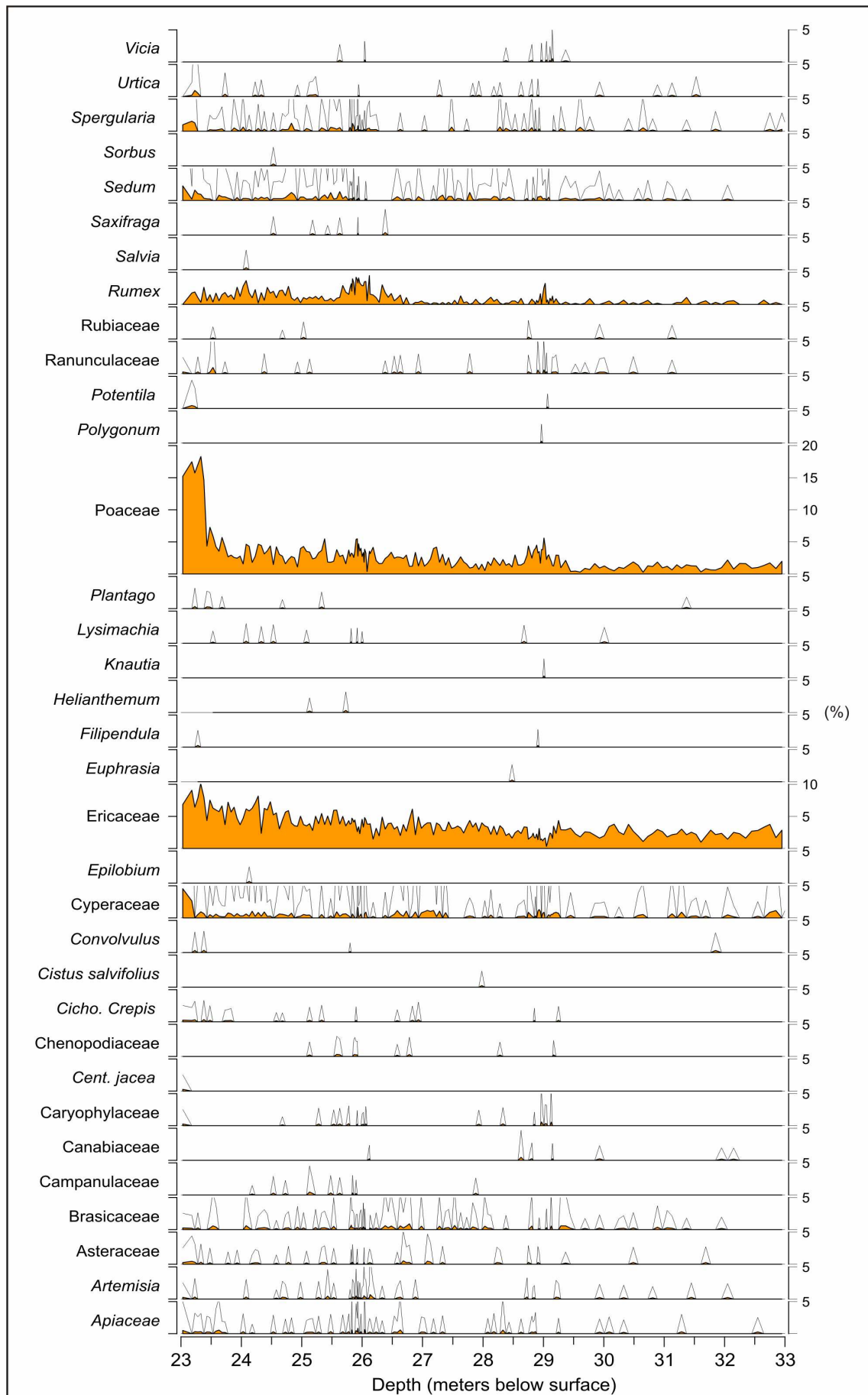
Aquatic plants, spores, and algae (exaggeration line 10x)

Appendix IV: Lightness – magnetic susceptibility – TOC – TN – C/N ratio

Curriculum Vitae

Personal details

Date of birth: 09.08.1978

Place of birth: Athens, Greece

Marital status: Married, one child

Education

2008-2011   PhD at Goethe University Frankfurt (Germany)

Promotor: Prof. Dr. J. Pross
Co-promotors: Prof. Dr. A. Brauer, Prof. Dr. A.F. Lotter, Dr. habil. U.C. Müller

2003-2005   MSc in Environmental Oceanography at University of Patras (Greece)

1997-2003   Degree in Geology at University of Patras (Greece)

Other experience

2010   Urbino Summer School in Paleoclimatology (09-29.07.2010)
 (Best Poster Award)

2008   Two months research visit at GeoforschungsZentrum (GFZ) Potsdam (Host: Prof. Dr. A. Brauer)

2007-2008   Research scholarship at the University of Frankfurt (Germany), Department of Geosciences – Institute of Paleontology, funded by the Deutscher Akademischer Austauschdienst (DAAD) (10.2007 – 02.2008)

2004-2005   Leonardo da Vinci student mobility program to obtain professional experience (Münster, Germany) (11.2004 – 04.2005)

Teaching experience:

2011   Laboratory course assistant: Micropaleontology course, 3rd semester undergraduate studies, Institute of Geosciences, Goethe University Frankfurt

2010   Field assistant: Field trip to the Dolomites, Italy, 30.08-06.09.2010

2010   Short course on lake sediments: German Scientific Earth Probing Consortium (GESEP), Frankfurt/Main, 11-12.03.2010

2006-2007   Laboratory course assistant: Ocean Engineering course, 1st semester undergraduate studies, Department of Geology, University of Patras

List of publications (* citation index journals)

Submitted

1. * **Koutsodendris, A.,** Müller, U.C., Pross, J., Brauer, A., Fletcher, W.J, Lotter, A.F. A short-term climate oscillation during the Holsteinian interglacial (MIS 11c): An analogy to the 8.2 ka climatic event? Submitted to Global and Planetary Change

2. * **Koutsodendris, A.,** Brauer, A., Pälike, H., Pross, J., Müller, U.C., Lotter, A.F. Sub-decadal- to decadal-scale climate cyclicity during the Holsteinian interglacial (MIS 11) evidenced in annually laminated sediments. Submitted to Climate of the Past

Published

3. * Kotthoff, U., **Koutsodendris, A.,** Pross, J., Schmiedl, G., Bornemann, A., Kaul, C., Marino, G., Peyron, O., Schiebel, R., 2011. Impact of Lateglacial cold events on the Northern Aegean region reconstructed from marine and terrestrial proxy data. Journal of Quaternary Science 26, 86-96.

4. * **Koutsodendris, A.,** Müller, U.C., Pross, J., Brauer, A., Kotthoff, U., Lotter, A.F., 2010. Vegetation dynamics and climate variability during the Holsteinian interglacial based on a pollen record from Dethlingen (northern Germany). Quaternary Science Reviews 29, 3298-3307.

5. Pross, J., Müller, U.C., **Koutsodendris, A.,** 2010. Der Weg ins Eishaus. Natur und Museum 140, 126-129.

6. * **Koutsodendris, A.,** Papatheodorou G., Kougiourouki O., Georgiadis M., 2008. Benthic marine litter in four Gulfs in Greece, Eastern Mediterranean; Abundance, composition and source identification. Estuarine, Coastal and Shelf Science 77, 501-512.

7. Margaritoulis, D., **Koutsodendris, A.,** Panagopoulou, A., 2007. Fisheries interactions with marine turtles. In: State of Hellenic Fisheries. Papacostantinou C., Zenetos A., Vassilopoulou V., Tserpes G. (Eds.), Hellenic Center of Marine Research (HCMR) Publications., p. 279-286.

8. Papatheodorou, G., Papaefthymiou, H., Florou, H., **Koutsodendris, A.,** Moustakli, K., 2007. Natural radionuclides and ^{137}Cs in marine sediments from two gulfs of Greece. Rapp. Comm. Int. Mer Medit., 38, 300.

Abstracts in the fields of paleontology - sedimentology

1. **Koutsodendris, A.,** Pross, J., Müller, U.C., Brauer, A., Fletcher, W.J., Lotter, A.F., 2011. A short-term climate oscillation during the Holsteinian interglacial (MIS 11c): Characteristics, spatial extent and potential triggering mechanisms. 18th INQUA (International Union for Quaternary Research) Congress, Bern, Switzerland.

2. **Koutsodendris, A.,** Brauer, A., Pälike, H., Pross, J., Müller, U.C., Lotter, A.F., 2011. Sub-decadal- to decadal-scale climate variability during the Holsteinian interglacial (MIS 11) evidenced in varves from northern Germany. Geophysical Research Abstracts, Vol. 13.

3. **Koutsodendris, A.,** Müller, U.C., Pross, J., Brauer, A., Lotter, A.F., 2010. Intra-Holsteinian (MIS 11) climate variability reconstructed from microfacies and micropaleontological analyses of the Dethlingen core (northern Germany). 18th International Sedimentological Congress (ISC), Mendoza, Argentina.

4. **Koutsodendris, A.,** Müller, U.C., Pross, J., Brauer, A., Fletcher, W.F., Lotter, A.F., 2010. A climatically driven abrupt vegetation setback during the Holsteinian interglacial (MIS 11). Cioppino workshop "Transient changes in past warm climates", Urbino, Italy.

5. Verhagen, F.T.M., **Koutsodendris, A.,** Lotter, A.F., 2010. Trophic state shifts within the Holsteinian interglacial (Middle Pleistocene) as recorded in an annually-laminated diatomite from Dethlingen (Northern Germany). 10th Nederlands Aarwetenschappelijk Congres (NAC), Veldhoven, The Netherlands.

6. **Koutsodendris, A.,** Müller, U.C., Brauer, A., Pross, J., 2009. Vegetation setbacks within the Holsteinian interglacial (MIS 11) as recorded in an annually-laminated core from Dethlingen paleolake, Northern Germany. Geophysical Research Abstracts, Vol. 11.

7. Papatheodorou, G., Fakiris, E., Geraga, M., Patsourakis, M., **Koutsodendris, A.,** Ferentinos, G., Kiparissis, S., Kapareliotis, A., Kornaros, M., Zafiri, C., Rallatos, D., 2008. Mapping of *Posidonia Oceanica* meadows using side scan sonar and ground trouthing techniques. 33rd International Geological Congress (IGC), Oslo, Norway.

8. Geraga, M., Tsaila-Monopoli, S., **Koutsodendris, A.,** Papatheodorou G., Ferentinos G., 2007. Planktonic foraminifera zonation in the Eastern Cretan Basin, Greece: Preliminary results. 25th International Association of Sedimentologists (IAS) Meeting, Patras, Greece.

9. **Koutsodendris, A.,** Papatheodorou, G., Papaefthymiou, E., 2006. Vertical distribution of ^{137}Cs in the sediments of Patras Gulf. 8th Greek Symposium of Oceanography and Fisheries, Thessaloniki, Greece.

Abstracts in other fields

10. Panagopoulou, A., **Koutsodendris, A.,** Margaritoulis, D., 2008. Interactions with small scale fisheries in Greece: An important factor for the reduction of turtle mortality at sea. In: Rees A.F., Frick, M., Panagopoulou, A., Williams K. (compilers), Proceedings of the 27th Annual Symposium on Sea Turtle Biology and Conservation. NOAA Technical Memorandum NMFS-SEFSC-569, 262 pp.

11. **Koutsodendris, A.,** Papadopoulou, S., Margaritoulis, D., 2006. Distribution of sea turtles (*Caretta caretta* and *Chelonia mydas*) based on 15 years of strandings (1990-2005). 10th

International Congress on the Zoogeography and Ecology of Greece and Adjacent Regions, Patras, Greece.

12. **Koutsodendris, A.,** Papadopoulou, S., Kardakari, N., Margaritoulis, D., 2006. Pilot sand dune restoration at Kotychi-Strofylia loggerhead nesting beach, Northwestern Peloponnesus, Greece. In: Frick, M., Panagopoulou, A., Rees, A.F., Williams, K., (compilers), Book of abstracts, 26th International Symposium on Sea Turtle Biology and Conservation. International Sea Turtle Society, Athens, Greece, 376 pp.

13. Papadopoulou, S., **Koutsodendris, A**., Margaritoulis, D., 2006. Implementation of GIS in sea turtle strandings along the Greek coastline: A modern management tool. In Frick, M., Panagopoulou, A., Rees, A.F., Williams, K., (compilers), Book of abstracts, 26th International Symposium on Sea Turtle Biology and Conservation. International Sea Turtle Society, Athens, Greece, 376 pp.

14. **Koutsodendris, A.**, Teneketzis, K., 2003. Environmental educational activities at the Educational Center of Evrotas – ARCHELON. In: Proceedings of the Hellenic Symposium "Design and production of educational material for the environmental education", Piraeus, Greece.